

Sex differences in perivascular adipose tissue-dependent vascular control in the porcine coronary artery

Abdulla A Ahmad, MSc. Medical Physiology

School of Life Sciences

Faculty of Medicine and Health Sciences

University of Nottingham

Thesis submitted to the University of Nottingham

for the degree of Doctor of Philosophy

July 2018

Abstract

Research during the past decade has highlighted the functional role of perivascular adipose tissue (PVAT) in regulating the contractility of the underlying vascular smooth muscle cell layer. However, the mechanisms underlying these observations are poorly understood. As a sexual dimorphism has been identified in the regulation of vascular tone, the aim of this thesis was to determine whether there are sex differences in PVAT-mediated regulation of the porcine coronary arterial (PCA) tone.

In the presence of adherent PVAT, which was stored overnight at 4C^{o}, contractions to the thromboxane mimetic U46619 and endothelin-1 were significantly reduced in PCAs from females, but not PCAs from males. In PCAs pre-contracted with U46619, re-addition of PVAT caused relaxation in PCAs from females, but not PCAs from males. This relaxant response in coronary arteries derived from females was inhibited by a combination of both NO synthase inhibitor (L-NAME) and the cyclooxygenase inhibitor indomethacin. Pre-incubation with an anti-adiponectin antibody abolished the relaxant effects of PVAT, indicating that adiponectin is likely to be the mediator released from the fat. There was no difference in either expression or release of adiponectin from PVAT between sexes. On the other hand, the adiponectin receptor agonist adipoRon produced greater relaxation in PCAs from females compared to PCAs derived from males. No adiponectin receptor 1 expression was detected in PCAs whilst adiponectin receptor 2 and adiponectin binding protein (APPL1) were expressed equally in PCAs from both sexes. Pre-incubation with the hydrogen sulphide enzyme inhibitors 4-propargylglycine (PPG) and 2-(aminooxy)-acetic acid (AOAA) did not reduce the anticontractile responses to PVAT. Cystathionine β-synthase (CBS) and 3-mercaptopyruvate sulfurtransferase (3MPST) are expressed in PVAT from both sexes equally, with a relatively low activity, whilst no cystathionine γ-lyase (CSE) expression has been identified in PVAT from both sexes. These data indicate a clear sex difference in the regulation of coronary artery tone in response to adiponectin receptor stimulation, which may underlie the anticontractile effects of PVAT in females. Although H_2S synthesizing enzymes are expressed in PVAT, they have no functional role in PVAT-induced vasorelaxation.

In arteries from both male and female pigs, addition of fresh PVAT caused a contraction, which was partially inhibited by the cyclooxygenase inhibitors indomethacin and flurbiprofen. The $PGF_{2\alpha}$ receptor (FP) antagonist AL8810 attenuated the PVAT-induced contractions in arteries from males, whereas the TXA_2 receptor (TP) antagonist GR32191B inhibited the PVAT-induced contractions in arteries from females. Although there was no difference in $PGF_{2\alpha}$ levels in PVAT between females and males, $PGF_{2\alpha}$ produced a larger contraction in arteries from males, correlating with a higher FP receptor expression detected by immunoblotting. In contrast, the release of TXB_2 from PVAT from females was greater than the release from males PVAT, but there was no difference in the contraction by the TXA_2 agonist U46619. Furthermore, there was no difference in the role of extracellular Ca^{2+} and Rho kinase pathway (intracellular Ca^{2+}) in the action of U46619, or TP receptor expression in arteries from different sexes.

Pre-incubation with the reactive oxygen species (ROS) scavenger N-acetyl-L-cysteine (NAC), a non-selective NADPH oxidase (Nox) inhibitor (DPI), a selective Nox1 inhibitor (ML171), a selective Nox2 inhibitor Phox-I2 and selective Nox1 and Nox4 inhibitor (GKT137831) significantly reduced PVAT-induced vasoconstriction in PCAs from both females and males. Nox1, Nox2 and Nox4 were expressed equally in PVAT from male and females. However, in PCAs, Nox1 expression was greater in females whilst Nox4 was higher in males. Nox2 was expressed equally in PCAs from different sexes. ML171 and phox-I2 reduced superoxide anion (O_2^-) production in PVAT and PCAs from both sexes. GKT137831 inhibited H_2O_2 production in PCAs, but not PVAT, from both sexes. Both U46619 and $PGF_{2\alpha}$ had similar effects on ROS production in that they did not increase O_2^- production in PVAT while they enhanced O_2^- production in PCA from females only. Functional studies showed that Nox inhibitors could inhibit the PCAs response to both U46619 and $PGF_{2\alpha}$ in females only.

The adipose-derived compound chemerin-9 caused a significantly higher vasoconstriction in PCAs from females in comparison with males PCAs. Similarly, chemerin-9 enhanced Nox activity in females PCAs but not in males PCAs. Chemerin mRNA was expressed in the PVAT, and the chemerin receptor

ChemR23 was expressed in PCAs, although there were no sex differences. The anti-chemerin antibody can abolish the PVAT-induced contractions in both sexes. The sexual dimorphism in the contraction to chemerin could be explained by differences in the signalling downstream of the chemerin receptor in PCAs rather than the expression of chemerin or its receptor in PVAT and PCA, respectively.

In conclusion, this thesis has demonstrated clear sex differences in the regulation of coronary artery tone by PVAT, with a dual effect of PVAT on the contractility of the PCA. PVAT stored overnight enhanced vasorelaxation in PCAs from females only due to the increased adiponectin activity compared to the males PCAs. In contrast, fresh PVAT augments vasoconstriction in PCAs from both sexes. Prostanoids have an important role in PVAT-induced vasoconstriction in which $PGF_{2\alpha}$ and TXA_2 are responsible for vasoconstriction in male and female PCAs, respectively. In addition, chemerin may have a role as a PVAT-derived contractile agent in female PCA only, while Nox-derived ROS regulates PVAT-induced contraction in the PCAs from both sexes. This study highlighted the importance of considering potential sex differences in the responses to PVAT and that sex-specific drug treatment may represent a potential strategy in the treatment of cardiovascular diseases.

Publications

Papers

1- **Ahmad, A. A.**, Randall, M. D. & Roberts, R. E. 2017. Sex differences in the regulation of porcine coronary artery tone by perivascular adipose tissue: a role of adiponectin? *Br. J. Pharmacol.*, **174,** 2773-2783.

2- **Ahmad, A. A.**, Randall, M. D. & Roberts, R. E. 2017. Sex differences in the role of phospholipase A2 -dependent arachidonic acid pathway in the perivascular adipose tissue function in pigs. *J. Physiol.*, **595,** 6623-6634.

Abstracts for conferences

1- **Ahmad A**, Roberts R, Randall M (2015). Gender differences in the role of phospholipase A2-dependent arachidonic acid pathway in the perivascular adipose tissue function in pigs. *Pharmacology 2015*. Queen Elizabeth II conference centre, London, UK.

2- **Ahmad A**, Randall M, Roberts R (2016). Role of reactive oxygen species in perivascular adipose tissue induced vasoconstriction: Impact of sex. *Physiology 2016*. Convention centre Dublin, Ireland.

3- **Ahmad A**, Roberts R, Randall M (2016). Sex differences in the regulation of porcine coronary artery tone by perivascular adipose tissue: role of adiponectin. *Pharmacological aspects of microvascular cell-cell signalling and CVS disease meeting*. Oxford, UK.

4- **Ahmad A**, Roberts R, Randall M (2017). Effect of sexual dimorphism on the role of perivascular adipose tissue -derived chemerin in regulation of vascular tone of porcine coronary artery. *FEPS 2017,* Vienna, Austria.

5- **Ahmad A**, Roberts R, Randall M (2017). No role for hydrogen sulphide in the anticontractile effect of perivascular adipose tissue in porcine coronary artery. *Pharmacology 2017*. Queen Elizabeth II conference centre, London, UK.

6- **Ahmad A**, Roberts R, Randall M (2017). Effect of sex differences on the coupling between reactive oxygen species and prostanoids in perivascular adipose tissue-induced vasoconstriction of porcine coronary artery. *Pharmacology 2017*. Queen Elizabeth II conference centre, London, UK.

Dedication

To my beloved late father,

Aqeel Ahmad Altayar,

whose prayers and support had been instrumental in achieving my goals,

yet never had the opportunity to see his dream comes true.

May his soul rest in peace.

Acknowledgements

First and above all, I praise ALLAH for providing me with the opportunity and the capability to complete this doctoral thesis, and being with me all the time during the hard moments that I faced throughout my research.

I would like to express my sincere gratitude to my supervisors Prof. Michael Randall and Dr Richard Roberts for their excellent supervision throughout my PhD study, for their patience, expertise, motivation, and immense knowledge. It has been an honour to be their PhD student. Their guidance helped me all the time of research and developed me academically and personally. I could not have imagined having better supervisors for my PhD study.

My profound thanks and appreciation to Dr Michael Garle for being very helpful and for his great advice. I would like to acknowledge all friends and colleagues in E floor for their company and help around the laboratory. I also would like to thank all staff and members in the University of Nottingham, School of Life Sciences who have given any technical, administrative or educational help during the course of my research. My special gratitude to the Iraqi Ministry of Higher Education and Scientific Research for funding this PhD and making my dream real.

I wish to thank my beloved mother, sister and brothers for their continuous encouragement and help who were all patient during our long absence abroad. I will never be able to pay my debt of gratitude in full. My sincere thanks and love go to my wife and my little two princes. Thanks for being in my life. Without your support this work would have been impossible.

Table of Contents

Abstract i

Publications iv

Papers iv

Abstracts for conferences iv

Acknowledgements vii

Abbreviations xii

Chapter one 1

General Introduction 1

1.1. Introduction: 2

Adipose tissue 2

1.2. Adipokines 3

1.3. Effects of vasoactive adipokines 4

1.4. Sex differences in physiology and pathology 5

1.4.2. Sex differences in adipose tissue 7

1.5. Perivascular adipose tissue 9

1.5.1. Overview 9

1.5.2. PVAT functions 11

1.5.3. PVAT effect in regulation of vascular tone 13

1.5.4. PVAT pathology 26

1.6. Aims 28

Chapter Two 29

Sex differences in the perivascular adipose tissue-derived vasorelaxation: the role of adiponectin 29

2.1 Introduction 30

2.2 Materials and Methods 32

2.2.1 Tissue preparation 32

2.2.2 Functional responses in the isolated porcine coronary arteries 32

2.2.3 Histological analysis 33

2.2.4 Immunoblotting 34

2.2.5 Determination of adiponectin levels released from PVAT 36

2.2.6 Estimation of CBS and 3-MPST activity using SF7 36

2.2.7 Statistical analysis 36

2.2.8 Materials 37

2.3 Results 38

2.3.1 The effects of PVAT on U46619-induced vasoconstriction in PCAs from female and male pigs. 38
2.3.2 Acute effects of added PVAT on rings pre-contracted with U46619. 40
2.3.3 Expression of UCP1 41
2.3.4 The effects of L-NAME and indomethacin on the anti-contractile effects of PVAT in female PCAs. 43
2.3.5 Role of adiponectin in PVAT-mediated vasorelaxation in females 45
2.3.6 Adiponectin expression and release from PVAT 46
2.3.7 Responsiveness of porcine coronary arteries to adipoRon 48
2.3.8 Expression of Adiponectin receptors in PCAs 50
2.3.9 Expression of APPL1 in PCAs 52
2.3.10 Functional effects of H_2S synthesizing enzymes on the relaxant response to PVAT in female PCAs. 52
2.3.11 Functional effects of PVAT-derived H_2S on responses to 5HT in female PCAs. 53
2.3.12 Identification of CSE, CBS and 3-MPST expression in porcine PVAT 54
2.3.13 Identification of CBS and 3-MPST activity in porcine PVAT 57
2.4 Discussion 58
Chapter Three 65
Sex differences in the role of phospholipase A_2-dependent arachidonic acid pathway in the perivascular adipose tissue function 65
3.1 Introduction 66
3.2 Materials and Methods 68
3.2.1 Tissue preparation 68
3.2.2 Characterization of vascular effects of the porcine isolated coronary artery 68
3.2.3 Determination of levels of TXB_2 and $PGF_{2\alpha}$ by ELISA. 69
3.2.4 Assessment of the PVAT-released TXB_2 by ELISA. 69
3.2.5 Estimation of TP and FP receptor expression in coronary arteries by immunoblotting 69
3.2.6 Statistical analysis 70
3.2.7 Materials 70
3.3 Results 71
3.3.1 Effects of addition of PVAT on vascular tone of female and male PCAs. . 71
3.3.2 Role of prostanoids in PVAT-induced contraction 72
3.3.3 Determination of the level of TXB_2 and $PGF_{2\alpha}$ in PVAT by ELISA 74
3.3.4 Assessment of the responsiveness of PCAs to TXA_2 and $PGF_{2\alpha}$ 75
3.3.5 Determination of the level of TP and FP receptor expression in PCAs 75

3.3.6 Role of extracellular Ca^{2+} in TXA_2 action 78
3.3.7 Role of Rho-kinase pathway in TXA_2 action 78
3.3.8 Determination of the release of TXA_2 from PVAT 79
3.3.9 Effects of phospholipase A_2 stimulation on PVAT-induced contractions 80
3.3.10 Effect of phospholipase A_2 stimulation on TXB_2 release from PVAT 83
3.4 Discussion 83
Chapter Four 88
Role of reactive oxygen species in perivascular adipose tissue-induced vasoconstriction: influence of sex 88
4.1 Introduction 89
4.2 Materials and Methods 91
4.2.1 Tissue preparation 91
4.2.2 Functional responses in the isolated porcine coronary arteries 91
4.2.3 Protein Expression of Nox Subunits 91
4.2.4 Quantification of superoxide anion production by lucigenin chemiluminescence assay 92
4.2.5. Quantification of hydrogen peroxide production using luciferin-enhanced chemiluminescence assay and Amplex Red 93
4.2.6 Materials 94
4.2.7 Statistical analysis 94
4.3 Results 95
4.3.1 Role of reactive oxygen species in PVAT-induced vasoconstriction 95
4.3.2 The effects of Nox inhibitors on PVAT-induced vasoconstriction in PCAs from female and male pigs 95
4.3.3 Measurement of superoxide anion production in coronary artery PVAT 97
4.3.4 Measurement of hydrogen peroxide production 100
4.3.5 Measurement of superoxide anion production in coronary artery 100
4.3.6 Measurement of hydrogen peroxide production in coronary artery 102
4.3.7 Expression of Nox isoforms in PVAT 104
4.3.8 Expression of Nox isoforms in coronary artery 108
4.3.9 Effects of Prostanoids on the ROS productions 110
4.3.10 Effect of LPS on PVAT function 114
4.4 Discussion 116
Chapter Five 123
Effects of sexual dimorphism on the role of perivascular adipose tissue-derived chemerin in the regulation of vascular tone of porcine coronary artery 123
5.1 Introduction 124

5.2 Materials and Methods 125
5.2.1 Tissue preparation 125
5.2.2 Functional responses in the isolated porcine coronary arteries 125
5.2.3 Determination of levels of mRNA expression of chemerin and ChemR23 by RT-PCR. 126
5.2.4 Quantification of NADPH oxidase activity by lucigenin chemiluminescence assay 126
5.2.5 Statistical analysis 126
5.2.6 Materials 127
5.3 Results 128
5.3.1 Responsiveness of PCAs to chemerin-9 128
5.3.2 ROS production by chemerin-9 128
5.3.3 The effects of Nox antagonist on chemerin9-induced vasoconstriction in PCAs 129
5.3.4 mRNA expression of chemerin and ChemR23 130
5.3.5 Role of chemerin in PVAT-mediated vasoconstriction 131
5.3.6 Role of chemerin in U46619-induced vasoconstriction 132
5.4 Discussion 133
Chapter six 138
General Discussion 138
6.1 Dual effect of PVAT on the vascular tone of PCA 139
6.2 Vasomotor effects of PVAT in different conditions 145
6.3 Conclusions 148
Appendices 149
A. List of buffers and chemicals used for immunoblotting 150
Table 1. Lysis buffer 150
Table 3. Tris-buffered saline containing 0.1% Tween 20 (TBS-T) 150
Table 4. 6x solubilisation buffer 150
Table 5. Protease Inhibitor Cocktail Set I (Calbiochem) 151
Table 6. 10X electrophoresis buffer 151
Table 7. Transfer buffer 151
B. Immunoblots 152
C. LPS effect on PVAT-induced contractions of PCAs (Pilot study) 157
D. Effect of overnight continuous oxygenation on the vasomotor effect of PVAT in PCAs 157
E. Sequence of primers 158
References 159

Abbreviations

3-MPST	3-mercaptopyruvate sulfurtransferase
5-HT	5-Hydroxytryptamine (serotonin)
AA	Arachidonic acid
AdipoR	Adiponectin receptor
ADRF	Adipose-derived relaxing factor
ADCF	Adipose-derived constricting factor
Ang II	Angiotensin II
AOAA	aminooxyacetic acid
APPL1	Adaptor protein, phosphotyrosine interacting with PH domain and leucine zipper 1
AT	Adipose tissue
CVD	Cardiovascular disease
BAT	Brown adipose tissue
BMI	Body mass index
BP	Blood pressure
CBS	Cystathionine β-synthase
COX	Cyclooxygenase
CSE	Cystathionine γ-lyase
DMSO	Dimethyl sulfoxide
DPI	Diphenyliodonium chloride
EDH	Endothelium-derived hyperpolarization
ET-1	Endothelin-1
FP	$PGF_{2\alpha}$ receptor
GAPDH	Glyceraldehyde-3-phosphate dehydrogenase
H_2O_2	Hydrogen peroxide
H_2S	Hydrogen sulphide
HDL-C	High-density lipoprotein cholesterol
IL	Interleukin
Kv	Voltage-gated K^+ channel
L-NAME	NG-nitro-L-arginine methyl ester
MCP-1	Monocyte chemoattractant protein–1
Min	Minutes

ML-171	2-acetylphenothiazine
MLC	Myosin light chain
NA	Noradrenaline
NO	Nitric oxide
NOS	Nitric oxide synthase
Nox	NADPH oxidase enzyme
O_2^-	Superoxide anion
PCA	Porcine coronary artery
$PGF_{2\alpha}$	Prostaglandin $F_{2\alpha}$
PGI_2	Prostacyclin
PLA_2	Phospholipase A_2
PPG	D,L-propargylglycine
PVAT	Perivascular adipose tissue
ROS	Reactive oxygen species
SAT	Subcutaneous adipose tissue
SOD	Superoxide dismutase
TNF-α	Tumour necrosis factor-alpha
TP	TXA_2 receptor
TXA_2	Thromboxane A_2
TXB_2	Thromboxane B_2
VSM	Vascular smooth muscle
VSMC	Vascular smooth muscle cell
U46619	9,11-dideoxy-11α,9α-epoxymethanoprostaglandin $F_{2\alpha}$
UCP1	Uncoupling protein 1
VAT	Visceral adipose tissue
WAT	White adipose tissue

Chapter one

General Introduction

1.1. Introduction:

Adipose tissue

Adipose tissue (AT) is composed of a heterogeneous mixture of cellular structures (that is, adipocytes, preadipocytes, precursor cells, T-lymphocytes, macrophages, fibroblasts and endothelial cells) and tissue structures (blood vessels and nerves). Collectively, these non-adipose cells comprise the stromal-vascular fraction of adipose tissue. AT has been classified into white adipose tissue (WAT) and brown adipose tissue (BAT) according to the type of the constituent adipocytes (Ramsay, 1996; Lowell, 1998; Avram *et al.*, 2005). Fat cells in WAT are small with large unilocular lipid droplets, few numbers of mitochondria and lacking uncoupling protein 1 (UCP1) (Cinti, 2005; Nedergaard *et al.*, 2007). Adipocytes in BAT are larger in size with multilocular small fat droplets, abundant in mitochondria and expressing UCP1 (Cinti, 2005; Nedergaard *et al.*, 2007). UCP1 enables the BAT to exert a thermogenic effect by increasing the permeability of the inner mitochondrial membrane and allowing leakage of protons via uncoupling the respiratory chain (Cannon and Nedergaard, 2004; Sidossis and Kajimura, 2015).

In contrast to WAT, BAT is described as more vascularised, metabolically active and with noradrenergic innervations (Cannon and Nedergaard, 2004; Cinti, 2011). White adipose tissue, which comprises up to 20% to 25% of total body weight (Mariman and Wang, 2010), acts primarily as an energy store, mainly lipid storage depot, and to a lesser extent, thermal insulator and body support against mechanical shocks (such as, skin or kidney) (Mariman and Wang, 2010). On the other hand, BAT is considered as a site of non-shivering thermogenesis that aids in the regulation of body temperature by enhancing lipid metabolism. While WAT is distributed throughout the whole body, BAT is located in dedicated local depots, for instance, interscapular region in human infants and rodents (Wankhade *et al.*, 2016). Although interscapular BAT in human infants is known to regress with age and is almost absent in adults (Aherne and Hull, 1966; Heaton, 1972) recent research has identified the presence of classical BAT in supraclavicular fat in adult human as well (Cypess *et al.*, 2009; Virtanen *et al.*, 2009).

In addition to the well-recognized WAT and BAT, "beige" or "brite" adipose tissue has been recently identified as a third type of AT. It is composed of beige adipocytes that exhibit BAT-like characteristics and reside with white adipocytes (Vitali *et al.*, 2012). It occurs in response to environmental and pharmacological stimuli such as exercise, chronic cold exposure, β-adrenoceptor agonists and long-term treatment with peroxisome proliferator-activated receptor gamma (PPARγ) agonists (e.g., pioglitazone), a process often called as "browning" of white adipose tissue (Harms and Seale, 2013; Wu *et al.*, 2013; Kajimura and Saito, 2014).

According to its location and origin, AT can be classified as either visceral adipose tissue (VAT) present in the abdominal cavity or subcutaneous adipose tissue (SAT) present in subcutaneous areas. There are substantial differences between two types including morphological, physiological, clinical and prognostic differences (Ibrahim, 2010). VAT accounts for 6-20% of total body fat while SAT stores ~80-90% of total body fat and exhibits sex-specific variations in size and function (Karastergiou *et al.*, 2012). In general, VAT is linked with a greater prediction of cardiovascular disease risk than SAT (Ibrahim, 2010). Excess VAT has the potential to trigger hypercoagulability, coronary heart disease and peripheral arterial disease (Lemieux *et al.*, 2000; Planas *et al.*, 2001; Tanko *et al.*, 2005). Moreover, only obese individuals characterized by elevated VAT establish the predictive complications of type 2 diabetes and cardiovascular disease (McFarlane *et al.*, 2001).

1.2. Adipokines

As mentioned earlier, adipose tissue (AT) has traditionally been viewed as being simply connective tissue supporting the adjacent structures, with additional fat storage facility (WAT) and regulation of body temperature (BAT). However, compelling evidence in recent years has led to the view that adipose tissue is far more than a fat reservoir and thermoregulator but is indeed an active secretory organ of numerous bioactive signaling molecules, which are important in both health and disease.

Indeed, adipocytes and stromal cells of the AT are regarded as a source of an ever growing list of bioactive mediators that are collectively termed adipokines. These molecules include hormones (such as adiponectin, leptin and sex steroids),

inflammatory cytokines (for example, interleukin-1, interleukin-6, tumour necrosis factor-α (TNF-α)), other proteins (as angiotensinogen, plasminogen activator protein (PAI-1) and vascular endothelial growth factor (VEGF)) and reactive oxygen species (Fortuno *et al.*, 2003; Havel, 2004; Thalmann and Meier, 2007; Yamawaki *et al.*, 2010). In addition to the autocrine role of these biological active substances in the regulation of adipocyte metabolism, these mediators that are produced *in situ* affect the neighbouring tissue cells through paracrine mechanisms or could be secreted into the bloodstream to play an endocrine role in the control of different physiological processes (Gollasch, 2012). Therefore, adipose tissue affects the normal function of many organs such as brain, liver, muscle and vasculature as well as it has essential role in overall metabolism.

1.3. Effects of vasoactive adipokines

The tone of vascular smooth muscle (VSM) determines both regional blood flow and systemic blood pressure (BP). In addition to myogenic mechanisms, vasoactive molecules released by nerves or by paracrine and endocrine tissues are responsible for regulation of vascular tone. In recent decades, the pivotal role of the endothelium in the homeostasis of the underlying smooth muscle cell layer has become clear. More recently, studies suggested the concept of endocrine and paracrine role for adipocytes in vasoregulation (Yiannikouris *et al.*, 2010; Maenhaut and Van de Voorde, 2011). More than 100 adipokines have since been identified and described to have the ability to elicit haemodynamic, metabolic and immunological effects. Close associations between adipocytes and immune cells are increasingly clear, and pre-adipocytes have been described to act as 'macrophage-like' cells (Cousin *et al.*, 1999). Furthermore, the adipose tissue in obese individuals has been identified to be extensively infiltrated by macrophages (Weisberg *et al.*, 2003). As adipose tissue expands, the expression and secretion of inflammation-related adipokines mostly enhances (Trayhurn, 2005). Moreover, obesity has been attributed to a low-grade chronic inflammation and this inflammatory state seems to link causally to the progression of the metabolic syndrome (Trayhurn and Wood, 2005). The extent of the adipokines' endocrine effect is still obscure and they seem to have both

advantageous and deleterious impact on vascular biology and pathophysiology (Mattu and Randeva, 2013).

One of the most important adipocyte-derived substances is the peptide leptin. Leptin aids in blood pressure regulation by different mechanisms, such as induction of direct vasorelaxation via stimulation of nitric oxide and endothelium-derived hyperpolarizing factor (EDHF) (Lembo *et al.*, 2000) whilst ATP-sensitive (K_{ATP}) and tetraethylammonium chloride (TEA)-sensitive potassium channels are not involved in modifying the anticontractile effects (Kimura *et al.*, 2000; Sahin and Bariskaner, 2007). On the other hand, indirect vasocontraction is elicited via central stimulation of the sympathetic nervous system (Fruhbeck, 1999). TNF-α also has both a vasodilator (Brian and Faraci, 1998; Johns and Webb, 1998) and a vasoconstrictor effect (Zhang *et al.*, 2002). Additionally, TNF-α has a role in endothelial dysfunction via downregulation of nitric oxide synthase and impairing endothelium-dependent vasorelaxation (Wimalasundera *et al.*, 2003; Yang *et al.*, 2009; Park *et al.*, 2011). Notably, a complete renin–angiotensin system (RAS) has been recognized in adipose tissue (Engeli *et al.*, 2003; Galvez-Prieto *et al.*, 2008). Thus, adipose cells can play a more significant role in modulating cellular processes than previously illustrated. Nevertheless, the majority of the research has been focused on the recognition of the humoral vasoactive effects of the adipokines but not on a possible paracrine action for AT in the adjustment of arterial tone and peripheral vascular resistance.

1.4. Sex differences in physiology and pathology

1.4.1. Sex differences in cardiovascular system

The heart supplies the myocardium with oxygen-rich blood through two main coronary arteries (left coronary artery and right coronary artery) which originate at the base of the aorta and support the coronary circulation. The heart has the highest oxygen consumption per tissue mass of all human organs. The resting coronary blood flow is ~250 ml min^{-1} which represents 5% of cardiac output (Guyton and Hall, 1996). Coronary flow is controlled mainly by physical factors, including transmural pressure during systole, vasodilator metabolites like

adenosine, and autonomic, mainly sympathetic, innervation (Rang and Dale, 2012).

Vascular tone is regulated by contraction of the smooth muscle cells, the major constituent of the blood vessel wall. The free intracellular Ca^{2+} and Ca^{2+} sensitivity of contractile proteins determine the vascular smooth muscle contractility. The elevation of intracellular Ca^{2+}, either by entry from the extracellular space or release from intracellular stores, initiates contractile activity by a Ca^{2+}-calmodulin interaction, stimulating myosin light chain (MLC) kinase with subsequent phosphorylation of the myosin light chains (Dabrowska *et al.*, 1977). This latter enables cross-bridge formation with actin and is considered as a key event in smooth muscle contraction (Gabella, 1984).

Studies have reported a greater incidence of cardiovascular diseases (CVD) in men and postmenopausal women compared to premenopausal women (Lerner and Kannel, 1986; Barrett-Connor, 1997). Sex differences have been identified in the changes of cardiovascular risks during the transition from childhood to adolescence. In females, insulin resistance and triglycerides are significantly decreased and HDL-C (high-density lipoprotein cholesterol) is significantly increased, whilst opposite changes have been found in males (Moran *et al.*, 2008). Sex differences in vascular function have been suggested as a causative factor to the variation in cardiovascular risks (Reckelhoff, 2005). There is a growing body of evidence that sex variation may be evoked by sex hormones, particularly oestrogen, which can modulate endothelial function as well as the platelet function, recruitment of circulating cells like leukocytes, endothelial progenitor cells and platelets, and several other processes in vascular inflammation and development of CVD (Villar *et al.*, 2008). In addition, sex differences have been identified in the changes of cardiovascular risks during the transition from childhood to adolescence. In females, insulin resistance and triglycerides are significantly decreased and HDL-C (high-density lipoprotein cholesterol) is significantly increased, whilst opposite changes have been found in males (Moran *et al.*, 2008). The protective effects of oestrogen have been studied extensively in numerous studies and a number of targets/pathways/mediators have been identified (Orshal and Khalil, 2004; Villar *et al.*, 2006). Much attention has been applied to the role of sex differences in

the incidence of coronary artery diseases (CAD) showing a potential effect of oestrogen in upregulating nitric oxide synthase (NOS) and enhancing endothelium-derived nitric oxide (NO)-dependent vasodilation (Mendelsohn and Karas, 1999). In addition, the endothelial function in the coronary circulation has been significantly improved after an acute administration of oestrogen to postmenopausal women (Gilligan *et al.*, 1994).

Moreover, elimination of H_2O_2 by polyethylene glycol-catalase significantly attenuated the bradykinin-induced vasorelaxation in the absence, but not in the presence of N^G-nitro-L-arginine methyl ester (L-NAME) and COX inhibitor (indomethacin) in females, but not in males (Wong *et al.*, 2014b). The same authors found that non-selective inhibition of NADPH oxidase (Nox) reduced the potency of the bradykinin-induced vasorelaxation in porcine coronary artery from males whereas no effect was seen in females (Wong *et al.*, 2015a). Furthermore, the impact of sex differences was further confirmed by another study from Wong *et al.*, in which the authors this time showed a variation in the transient receptor potential (TRP) channels where TRPC3 isoform has a role in the NO- and EDH-type response in male PCAs, whereas TRPV4 isoform plays a role in the NO-induced response in female PCAs (Wong *et al.*, 2015b).

1.4.2. Sex differences in adipose tissue

Sexual dimorphism in adipose tissue has been extensively studied and clarified in many reviews (Fuente-Martin *et al.*, 2013; White and Tchoukalova, 2014; Greenhill, 2016). Sex differences in adipose tissue distribution can be observed before and after puberty, although they become much more pronounced after pubertal onset (He *et al.*, 2002; Taylor *et al.*, 2010). Females predominantly characterized by accumulating more SAT and less VAT, whereas males have a significantly more central or abdominal fat which is considered, as mentioned earlier, a greater risk factor in metabolic disorders (Kotani *et al.*, 1994; Demerath *et al.*, 2007). However, this sexual variation in fat distribution is reduced at older ages as women reach postmenopausal stage (Goodman-Gruen and Barrett-Connor, 1996; Camhi *et al.*, 2011), highlighting the role of sex hormones in this phenomenon.

Adipose tissue expresses both nuclear receptors of oestrogen, ERα and ERβ, with greater ERα expression compared to ERβ (Ribas *et al.*, 2010; Gorres *et al.*, 2011). In addition, oestrogen has been suggested as a potential regulator of cell metabolism after identification of its two receptors in the mitochondria of WAT (Chen *et al.*, 2009). Moreover, a recent study by Davis *et al.*, (2013) complemented these findings by showing that ERα signalling in adipose tissue is important for the protection against adiposity, adipose tissue inflammation and fibrosis (Davis *et al.*, 2013). Noteworthy, apart from oestrogen, other gonadal sex hormones have a potential effect on adipose tissue function. For instance, androgens have adipogenic effects and are capable of enhancing insulin sensitivity in male AT, whilst testosterone attenuates insulin sensitivity in female AT (Corbould, 2007; Varlamov *et al.*, 2012). Furthermore, progesterone administration to female rats enhanced production of leptin, resistin and adiponectin with males having no response to the same pharmacological dose (Stelmanska *et al.*, 2012).

Sexual dimorphism has been identified even in the metabolic rate of AT. A recent study reported a higher resting metabolic rate in women than in men which is explained by 5-fold higher expression of the brown adipocyte marker (UCP1) gene in female adipocytes (Nookaew *et al.*, 2013). Rates of lipolysis and mobilization of AT triglyceride stores (Nielsen *et al.*, 2003) is greater in women compared to men, and simultaneously women are more efficient in managing free fatty acids, retaining their insulin sensitivity (Karastergiou *et al.*, 2012). Multiple studies have found that the circulating adiponectin levels are higher in women than men in spite of their superior adiposity, which is concomitant in both sexes with reduced adiponectin levels (Nishizawa *et al.*, 2002; Cnop *et al.*, 2003; Arita *et al.*, 2012). Women also have a higher leptin levels, even after adjusting for differences in body mass index (BMI) and body fat content (Considine *et al.*, 1996), a finding that is reproduced in *ex vivo* AT cultures (Hellstrom *et al.*, 2000). Furthermore, other factors could modulate AT development and, adipokine and cytokine production such as prolactin and thyrotropin stimulating hormone (TSH) (Bell *et al.*, 2002; Menendez *et al.*, 2003; Flint *et al.*, 2006). Noteworthy, many of these anterior pituitary hormones

are also sexually dimorphic (Tong *et al.*, 1989; Chowen *et al.*, 1996), proposing a possible sex differences in their impact on AT.

1.5. Perivascular adipose tissue

1.5.1. Overview

Perivascular adipose tissue (PVAT) is positioned around blood vessels and is regarded distinct from the adventitia in spite of absence of a barrier between them (Figure 1.1). PVAT is distributed with various proportions throughout the body according to the anatomical origin and vessel calibre ranging from more abundant (such as aorta), somewhat detached from the surrounded adipose tissue (as with the coronary perivascular adipose tissue inside epicardial fat) or absent (e.g. cerebral and microcirculation) (Szasz *et al.*, 2013). Indeed, in addition to the well-recognized three layers of the blood vessel (tunica adventitia, tunica media and tunica intima), tunica adiposa (or perivascular adipose tissue PVAT) has been recently described as a new fourth layer (Chaldakov *et al.*, 2007; Chaldakov *et al.*, 2012; Brown *et al.*, 2014) (Figure 1.1).

PVAT is composed mainly of adipocytes (white or brown) as well as a stromal vascular fraction, like other AT, which includes pre-adipocytes, macrophages, lymphocytes, fibroblasts, vasa vasorum endothelial cells, mesenchymal stem cells and nerve endings (Szasz *et al.*, 2013). Noteworthy, the crosstalk between adipocytes and the stromal vascular fraction is critical for PVAT function, and more importantly, in disease conditions (Weisberg *et al.*, 2003; Tilg and Moschen, 2006).

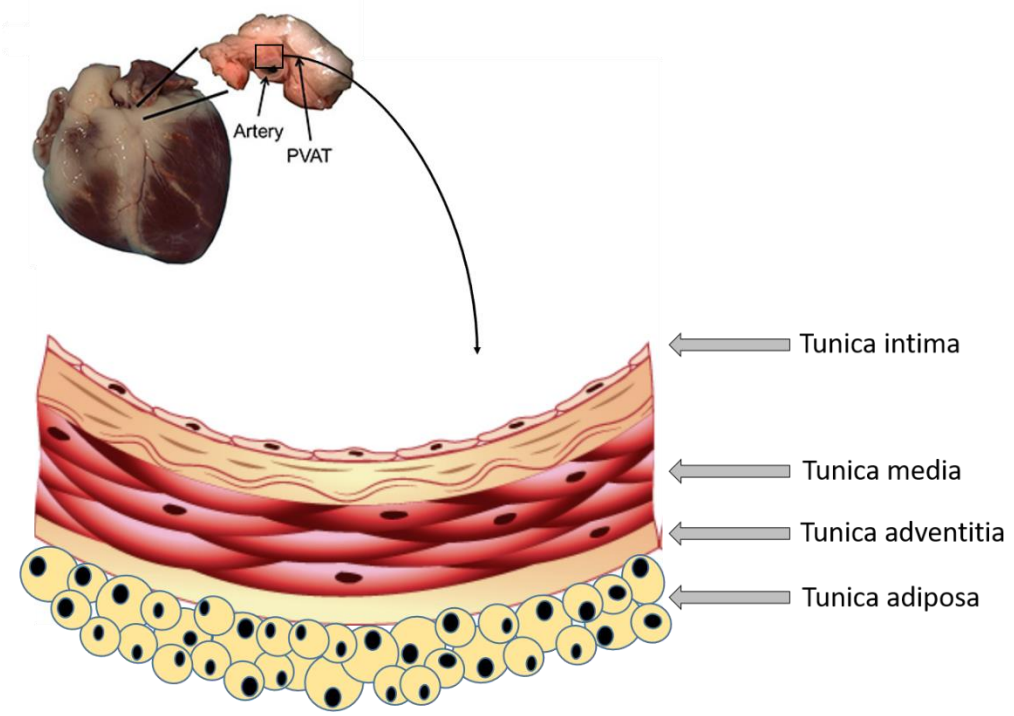


Figure 1.1: Structure and composition of a blood vessel. The innermost layer is tunica intima (endothelium), followed by the tunica media (VSM), tunica adventitia and then tunica adiposa (PVAT). Figure adapted from (Payne *et al.*, 2010).

Both white and brown PVAT are encountered, with different ratios depending on the anatomical location (Cinti, 2011). In Sv129 mice, the mediastinal depot (coronary artery and thoracic aorta) is composed mainly of BAT, the abdominal-pelvic depot (iliofemoral blood vessels) has an equal amount of both types, while the retroperitoneal and mesenteric depots (abdominal aorta and mesenteric arteries) consist mostly of WAT (Frontini and Cinti, 2010). Correspondingly, Wang *et al.* (2009) reported that PVAT surrounding thoracic aorta of Sprague-Dawley rats is mainly BAT (Wang *et al.*, 2009). In humans, PVAT around the aorta and its main branches including the carotid, subclavian, intercostal and renal arteries is mostly brown adipose tissue corresponding to the necessity to distribute generated heat by BAT to the body via the circulation (Frontini and Cinti, 2010). However, the findings from human coronary arteries have been conflicting, with one study reported that PVAT dissected from the base of human right coronary arteries expressing greater level of brown adipocyte-related genes in comparison with substernal, and subcutaneous thoracic, abdominal, and leg fat (Sacks *et al.*, 2009), while another

study has showed gene expression in perivascular adipocytes surround human coronary arteries to be related to white, rather than brown, adipocytes (Chatterjee *et al.*, 2009). Moreover, the concept of the presence of strictly defined adipocytes as either white or brown has been rejected due to identifying brown-like adipocytes in the midst of a WAT, the finding that supports the concept of adipocyte transdifferentiation.

In terms of its classification as either subcutaneous (SAT) or visceral (VAT), a study clarified that PVAT around the aorta is generally considered as VAT, notably linked with cardiovascular diseases (Schlett *et al.*, 2009). However, the secretory profile of PVAT is significantly different from other fat depots. Some evidence suggests that murine aortic PVAT produces less leptin, adiponectin and resistin, reverse expression profile of adipose-related lipid synthesis and storage genes, with decreased expression of lipid-oxidation genes in comparison with VAT and SAT (Chatterjee *et al.*, 2009; Fitzgibbons *et al.*, 2011). In addition, there is relatively less expression of adipocyte differentiation and maturation markers in PVAT compared with SAT and VAT (Chatterjee *et al.*, 2009). The nerve supply in PVAT is mostly sympathetic. Vasa vasorum may be present in PVAT in some of the vascular bed (Lafontan and Berlan, 1993; Szasz *et al.*, 2013). The function of the vasa vasorum, which is present in the adventitia of the blood vessel, is promoting neovascularization following vascular injury and inflammation. This facilitates conveyance of vasoactive substances secreted by PVAT to the inner vasculature (Gossl *et al.*, 2009).

1.5.2. PVAT functions

The recent attention concerning perivascular adipose tissue as a paracrine organ has led to several studies investigating the characteristics of various fat depots in the body. A complex world of physiology resides in PVAT, including the presence of many chemokines, adipokines and other bioactive signalling molecules that are released and affect the adjacent vessels (Nava and Llorens, 2016; Gollasch, 2017).

As both rodent and human thoracic PVAT comprise UCP1-positive brown adipocytes, which is associated with non-shivering thermogenesis, PVAT could have significant physiological and pathophysiological thermogenesis properties. This hypothesis is supported by a recent study which showed that intravascular

temperature is regulated by PVAT (Chang *et al.*, 2012a). Noteworthy, a temperature gradient is recognized in the vasculature, with a blood temperatures getting higher in the vessels closest to the heart (Robinson, 1952) and it is possible that PVAT has a potential role in maintaining this temperature gradient.

Several adipocyte products are expressed and released from PVAT affecting the inflammatory state including adipokines (e.g leptin, adiponectin, resistin, visfatin, adrenomedullin) and classical chemokines/ cytokines (e.g. TNF-α, interleukin-1, interleukin-6, interleukin-8, monocyte chemoattractant protein–1 (MCP-1) and plasminogen activator inhibitor-1) (Rajsheker *et al.*, 2010). Obviously, the majority of these substances are normally produced and released in inflammatory conditions. Moreover, Chatterjee *et al.* (2009) showed that PVAT exhibits a rather proinflammatory phenotype compared to the subcutaneous and visceral depots (Chatterjee *et al.*, 2009). The authors found that both human coronary perivascular adipose tissue and adipocytes secrete higher proinflammatory cytokines levels compared to subcutaneous or visceral depots. Furthermore, they showed that feeding mice with high fat diet caused a further increase in proinflammatory gene expression in PVAT which was much more robust than that observed in the other adipocyte depots.

PVAT of the human aorta has the ability to induce chemotaxis of peripheral blood granulocytes and monocytes, which is mostly mediated by IL-8 and MCP-1 (Henrichot *et al.*, 2005). Balloon overstretch injury induces accumulation of neutrophils and macrophages in PVAT of porcine coronary arteries, possibly through the release of reactive oxygen species and/or cytokines (Okamoto *et al.*, 2001). In fact, the inflammatory cells (such as macrophages and T-lymphocytes) which are either infiltrating the PVAT or recruited in response to released cytokines are essential to secrete inflammatory mediators, maintain a balance of theses mediators and modulate the inflammatory response to external stimuli. Noteworthy, other reports have emphasized that although PVAT has a basal adipokine-releasing ability, this does not mean an essential deleterious effect is expected from PVAT. For instance, Rittig *et al.*, (2008) found that PVAT does not cause endothelial dysfunction in human brachial artery (Rittig *et al.*, 2008) and several studies have showed that the PVAT attached to the vessels does not

impede the endothelium-dependent relaxations in comparison with PVAT-free vessels (Ketonen *et al.*, 2010; Mendizabal *et al.*, 2013).

Several growth factors have been identified in PVAT which play an important role in the regulation of structural remodelling of the vascular wall (Barandier *et al.*, 2005; Engeli, 2005). Visfatin can promote vascular smooth muscle cell (VSMC) growth via activation of ERK1/2 and p38 MAP kinase pathways. It has been shown that PVAT secretes a higher visfatin level compared to subcutaneous or visceral fat depots (Wang *et al.*, 2009). Leptin and resistin are capable of stimulating proliferation and migration of VSMC via MAPK and/or PI3K pathways (Tilg and Moschen, 2006; Shyu *et al.*, 2016). Examples of other VSMC growth and migration promoters includes free fatty acids (FFA) (Lamers *et al.*, 2011), angiotensin II (Schling *et al.*, 1999), TNF-α, fibroblast growth factor, insulin-like growth factor, and heparin-binding epidermal growth factor-like growth factor (Matsumoto *et al.*, 2002; Schling and Loffler, 2002). On the other hand, adiponectin can act as a VSMC growth inhibitor thus enhancing a beneficial antiangiogenic effect (Lamers *et al.*, 2011) which could be reduced in the pathophysiological conditions in which the adiponectin level is diminished. However, it is for future study to evaluate the proliferative signalling substances that are released from PVAT and contribute to the vascular remodelling in both physiological and pathological conditions.

1.5.3. PVAT effect in regulation of vascular tone

PVAT is routinely removed in vascular functional studies based largely on the assumption that it is an extraneous tissue which even could impede the diffusion of exogenous molecules into the vascular tissue. The claim of the PVAT as a mere supportive structure without any role in modulating vascular function was widely accepted until Soltis and Cassis (1991) first described that PVAT significantly attenuated vascular responsiveness of Sprague-Dawley rat aorta to noradrenaline. The authors demonstrated that sympathetic nervous system innervation to the periaortic adipose tissue manipulates aortic vascular responsiveness. They proposed that the uptake of noradrenaline by AT was responsible for this anti-contractile effect (Soltis and Cassis, 1991).

The results of Soltis and Cassis's study were confirmed by Löhn *et al.*, (2002), who re-examined the concept of periadventitial vasoregulation. The

latter study afforded additional proof that PVAT could inhibit vasoconstriction, which was induced by a number of agonists such as serotonin, phenylephrine and angiotensin II (Lohn *et al.*, 2002). The advantage of using these various agonists is that it excludes the initial assumption that PVAT would increase the uptake of noradrenaline, since the other agonists could not be taken up, inactivated or cleaved (Lohn *et al.*, 2002). So the claim that the physical presence of PVAT could mechanically impede the diffusion of vasoactive substances, and subsequently the anti-contractile effect, was questioned. In the Lohn *et al.*, (2002) study, the supernatant from incubated PVAT or cultured adipocytes relaxed pre-contracted rat aorta after complete removal of the adherent adipose tissue which confirms the existence of a diffusible vasoactive "adventitium-derived relaxing factor (ADRF)" derived from PVAT. The same group demonstrated that ADRF could hyperpolarize smooth muscle cells via K_v channel activation in mesenteric artery rings from Sprague-Dawley rats. Additionally, the authors decided that "A" in ADRF should stand for adipocyte rather than adventitium (Verlohren *et al.*, 2004). Since then, the same acronym (ADRF) is used to describe both adventitium and adipocyte interchangeably.

Noteworthy, Gao *et al*. have presented novel findings that highlight the potential role of PVAT in regulating homeostasis. The existence of PVAT-derived transferable relaxing molecule in human vessels was first reported by Gao *et al.*, (2005b) who found that this ADRF acts through the activation of calcium-dependent potassium channels (Gao *et al.*, 2005b). In addition, the first study on PVAT in obesity was by Gao *et al.*, (2005a) who showed that prenatal exposure to nicotine is associated with increased adiposity along with the loss of modulatory function of PVAT on the response of thoracic aorta of female Wistar rats (Gao *et al.*, 2005a). The same group also published the first report which described the presence of a pro-contractile diffusible molecule in PVAT, highlighting the role of superoxide anion in PVAT-induced vasoconstriction in mesenteric artery of male Wistar rats (Gao *et al.*, 2006). Subsequently, the term perivascular contractile factor (PVCF) was firstly introduced in the literature in 2007 (Gao, 2007). In fact, what makes PVAT's role in body homeostasis unique is the close proximity with the vessels. Although the exact mechanism of different adipose-derived relaxing and constricting factors (ADRFs and ADCFs)

is yet to be identified, a number of potential PVAT-derived bioactive substances have been suggested to affect the vascular contractility, for instance, NO, H_2S, angiotensin 1-7, methyl palmitate, ROS and angiotensin II (Nava and Llorens, 2016) (Figure 1.2 and 1.3). Below are the details of some of these factors.

1.5.3.1. PVAT-mediated vasorelaxtion

1.5.3.1.1. Nitric Oxide

The identification of nitric oxide as a novel gaseous molecule and endothelium-derived relaxing factor (EDRF) had a major impact on vascular research. However, the involvement of NO in PVAT-dependent vasoregulation has yet to be defined clearly (Lohn *et al.*, 2002; Verlohren *et al.*, 2004; Gao *et al.*, 2007). In aortic rings from Wistar rats, NO released from PVAT could induce endothelium-dependent vasodilatation via activation of smooth muscle K^+ channels (Gao *et al.*, 2007). In contrast, blocking NO synthesis in the aorta of Sprague-Dawley rats by L-NNA does not influence the effects of PVAT (Lohn *et al.*, 2002). Although Dashwood *et al.*, (2007) proposed that NO could be released by adipocytes and endothelium of the vasa vasorum, the exact cell type responsible for production of NO is still a matter of debate (Dashwood *et al.*, 2007; Malinowski *et al.*, 2008; Gil-Ortega *et al.*, 2010).

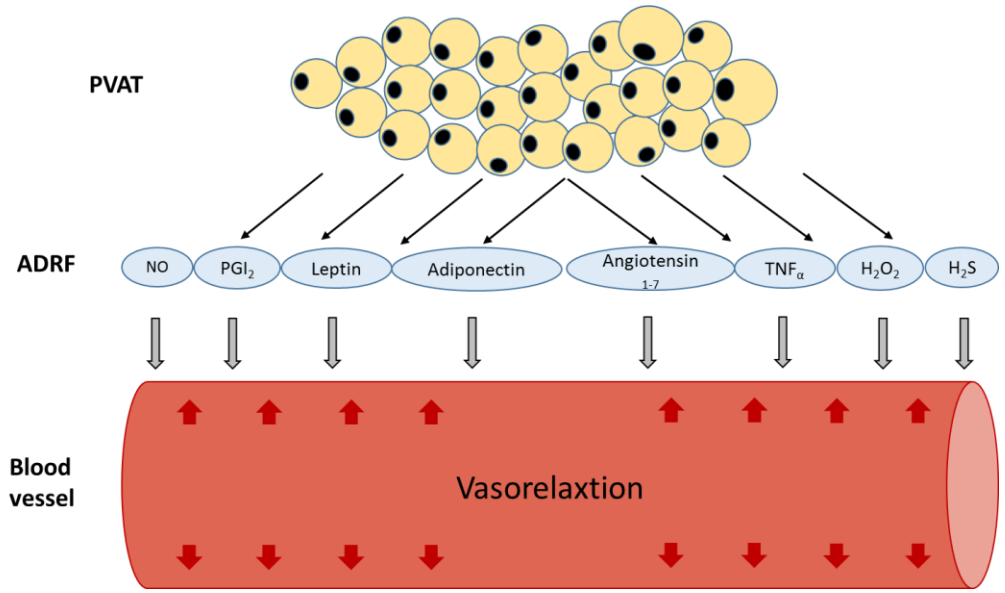


Figure 1.2: The vasodilator effects of PVAT. Several adipocyte-derived relaxing factors are secreted from PVAT that reduce the contractility state of the

blood vessels, such as nitric oxide (NO), prostacyclin (PGI_2), leptin, adiponectin, angiotensin 1-7, TNF-α, H_2O_2 and H_2S.

1.5.3.1.2. Prostacyclin

Prostacyclin (PGI_2) is a potent vasorelaxant synthesized primarily in the endothelium and by the action of PGI_2 synthase. PGI_2 binds to prostacyclin receptors on the vascular smooth muscle to provide atheroprotection by restraining both oxidative stress and platelet activation that contribute to atherogenesis (Egan *et al.*, 2004). Decreased prostacyclin secretion has been reported in age-related studies and hypertensive conditions. The diminished relaxant effects of PGI_2 in older subjects may be associated with a diminution in the contribution of endothelial-derived NO when compared with younger individuals (Nicholson *et al.*, 2009). Recent studies have demonstrated that prostacyclin released by PVAT exerts vasorelaxant effects and protects against endothelial dysfunction (Virtanen *et al.*, 2009). However, Chang and co-workers suggested that PVAT-derived prostacyclin may have a role as a secondary source of this vasorelaxant once the endothelium is dysfunctional in diseases such as atherosclerosis (Chang *et al.*, 2010). Conversely, cyclooxygenase inhibition with indomethacin failed to inhibit the anti-contractile effect of PVAT of human internal thoracic artery (Malinowski *et al.*, 2008).

1.5.3.1.3. Adiponectin

Adiponectin was first recognized in 1995 (Scherer *et al.*, 1995) and is the most abundant adipokine in the circulation (Japp and Newby, 2008). The endothelium-dependent vasorelaxation is proportional to the level of plasma adiponectin in humans. It was found that a significant increase in NO production was caused by adiponectin and both isoforms of adiponectin receptors, AdipoR1 and AdipoR2, were expressed in aortic endothelial cells (Tan *et al.*, 2004). Furthermore, 5-HT-mediated contraction of rat aorta has been attenuated by recombinant adiponectin (Fesus *et al.*, 2007). Moreover, a fragment of the adiponectin receptor impeded the PVAT-induced vasodilatation in human small arteries taken from subcutaneous gluteal fat biopsy samples (Greenstein *et al.*, 2009).

Contrasting with the above results, Fesus *et al.*, (2007) ruled out that adiponectin is an ADRF in visceral arteries via studies using adiponectin gene knockout mice. They reported that proven humoral vasodilator characteristics of adiponectin maybe through stimulation of 4-AP-sensitive K_v channels. Despite the latter findings, adiponectin still has important vasoregulatory effects (Fesus *et al.*, 2007). In addition, many studies reported that adiponectin is a beneficial adipokine playing a role as anti-inflammatory, anti-atherogenic and antidiabetic mediator (Matsuzawa, 2010). A recent study suggested PVAT-derived adiponectin as a local protective signalling substance which prevents vascular oxidative stress (Antonopoulos *et al.*, 2015).

1.5.3.1.4. Tumour necrosis factor-α

As the TNF-α gene was identified to be expressed in adipose tissue in 1993 (Hotamisligil *et al.*, 1993), TNF-α has been suggested as a vital adipokine. TNF-α exhibits both time-dependent vasoconstrictor (Wagner, 2000; Zhang *et al.*, 2002) and vasodilator (Brian and Faraci, 1998; Johns and Webb, 1998) effects. This adipokine-induced vasoregulation can occur via both endothelium-dependent (Brian and Faraci, 1998) and endothelium-independent mechanisms (Johns and Webb, 1998). In obese subjects undergoing bypass surgery, epicardial fat shows a higher TNF-α level than subcutaneous fat (Mazurek *et al.*, 2003). In addition, the anticontractile effects of PVAT are diminished significantly after incubation with TNF-α in mesenteric arteries from Wistar rats (Greenstein *et al.*, 2009). Moreover, PVAT-derived TNF-α has a critical role in progression of inflammation and atherosclerosis (Chang *et al.*, 2013).

1.5.3.1.5. Interleukin-6

Acute exposure of IL-6 *in vitro* induces relaxation of the rings isolated from Sprague-Dawley rat aorta. The latter effect can be endothelium-independent through an increase of prostacyclin in VSMC (Ohkawa *et al.*, 1994). In contrast, incubation with IL-6, but not IL-1, reduced the PVAT-mediated anticontractile effect in mesenteric arteries from Wistar rats (Greenstein *et al.*, 2009). In obesity, IL-6 is markedly increased at the mRNA levels in PVAT in Zucker rats (Hamlat-Khennaf *et al.*, 2017). Furthermore, human perivascular adipocytes *in vitro* expressed higher levels of IL-6 compared with SAT (Chatterjee *et al.*, 2009). Significant associations have been found between a sustained elevation in IL-6

plasma level and high BP (Lee *et al.*, 2006). Moreover, a study by Ridker *et al.*, (2000) postulated that IL-6 could be regarded as a predictor of future myocardial infarction (Ridker *et al.*, 2000) whereas other study found a correlation of IL-6 with cardiovascular mortality (Langenberg *et al.*, 2006).

1.5.3.1.6. Angiotensin [1-7]

A possible candidate as a new ADRF is the peptide angiotensin [1-7], which is expressed and secreted from PVAT, and is responsible for a vasorelaxant action via opening of large-conductance, Ca^{2+} activated K^+ (BK_{Ca}) channels (Lee *et al.*, 2009). Blocking of this particular peptide reduces partly the anti-contractile effect of PVAT surrounding rat aorta (Lee *et al.*, 2009) and rat vena cava (Lu *et al.*, 2011), effects supported by another study performed with angiotensin [1-7] receptor knockout mice (Lee *et al.*, 2011).

1.5.3.1.7. H_2S

Hydrogen sulphide has received attention, particularly due to its vasorelaxant effects and has described as a novel candidate of ADRF (Fang *et al.*, 2009; Schleifenbaum *et al.*, 2010; Wojcicka *et al.*, 2011). Although it is demonstrated that in the body H_2S is synthesised through cystathionine-ß-synthase (CBS), cystathionine γ-lyase (CSE) and 3-mercaptopyruvate sulfurtransferase (3-MPST) (Cheng *et al.*, 2004; Kuo *et al.*, 2016; Donovan *et al.*, 2017), studies on PVAT focused on CSE and suggested it as the main source of H_2S synthesis. In rats, CSE is expressed in PVAT and endogenously produces H_2S (Feng *et al.*, 2009). In addition, inhibitors of CSE inhibited the anti-contractile effects of PVAT in mouse mesenteric arteries and rat aorta (Fang *et al.*, 2009; Schleifenbaum *et al.*, 2010). Furthermore, Schleifenbaum *et al.*, (2010) reported that H_2S-mediated vasodilatation of rat aorta was attenuated by a particular ADRF-related K^+ -channel (KCNQ) blocker XE991 (Schleifenbaum *et al.*, 2010). In addition, the same authors have found that the effects of ADRF can be augmented by KCNQ channel openers (VRX0621688, retigabine, VRX0621238 and VRX0530727) in situations of low H_2S release from perivascular fat, by inhibition of CSE by b-cyano-L-alanine.

Fang *et al.*, (2009) illustrated that in ageing normotensive rats, endogenous H_2S generation in aorta and isolated PVAT was suppressed,

whereas CSE protein expression levels rose (Fang *et al.*, 2009). On the other hand, a study on spontaneously hypertensive rats showed decreased level of both plasma H_2S and its precursor enzyme expression in thoracic aorta (Yan *et al.*, 2004), a finding that raises the notion that malfunctioning CSE/H_2S may be considered as a new candidate that is involved in the pathogenesis of hypertension.

1.5.3.2. PVAT-mediated vasoconstriction

Interestingly, some studies showed opposing effects of PVAT on vascular tone (Figure 1.3). A study of Soltis and Cassis (1991) demonstrated that the contraction of the rat aorta to electrical field stimulation was induced only in the presence of PVAT. This response was blocked by using non-selective α-adrenoceptor antagonist phentolamine and diminished by angiotensin II receptor antagonist SarI-Ile8-AII, suggesting that PVAT could release angiotensin II (Soltis and Cassis, 1991). A study of canine coronary arteries demonstrated that perivascular adipose tissue reduced endothelium-dependent dilatation by impairing NO production (Payne *et al.*, 2009).

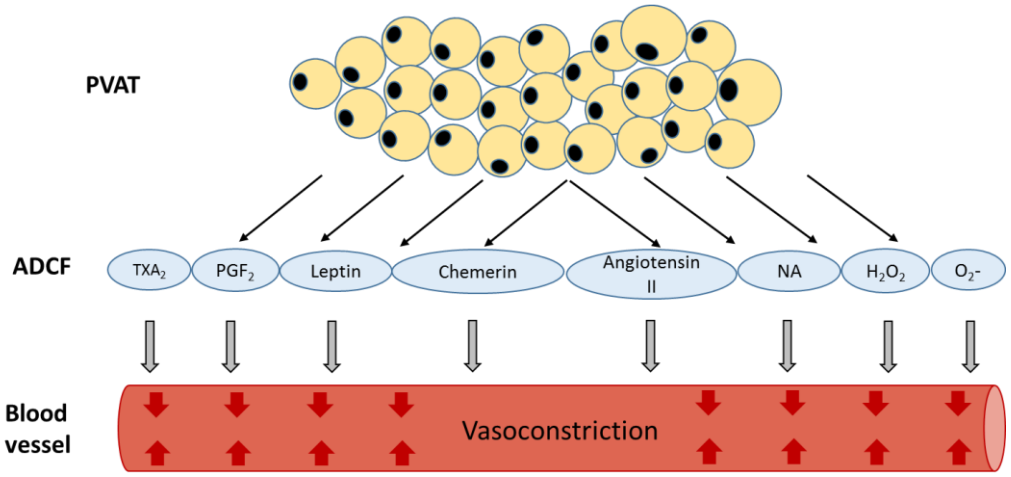


Figure 1.3: The vasoconstrictor effects of PVAT. Several adipocyte derived constricting factors are secreted from PVAT that enhance the contractility state of the blood vessels, such as thromboxane A_2 (TXA_2), prostaglandin $F_{2\alpha}$, leptin, chemerin, angiotensin II, noradrenaline (NA), H_2O_2 and O_2^-.

1.5.3.2.1. Prostanoids

Prostanoids, including prostaglandins and thromboxane, are autacoids produced in response to various physiological and pathological stimuli. Firstly, cell

membrane phospholipid is cleaved by phospholipase A_2 to generate arachidonic acid (AA), the step which is considered as a rate-limiting step in prostanoid synthesis. Then, AA can be metabolized by the enzymatic reaction of COX to the prostanoid precursor PGG_2, which is subsequently peroxidized to PGH_2 (Morita *et al.*, 1995). This latter short-lived but biologically active PG is metabolized rapidly by a set of cell-specific synthases namely thromboxane, PGF, PGE, PGD, PGI synthases, producing corresponding various biologically active prostanoids. There are mainly five prostanoids that affect vascular tone, TXA_2, $PGF_{2\alpha}$, PGE_2, PGD_2 and PGI_2. These prostanoids are released and interact with their specific seven transmembrane domain receptors, which belong to the G-protein-coupled receptor (TXA_2 with TP, $PGF_{2\alpha}$ with FP, PGE_2 with EP_1, EP_2, EP_3, and EP_4, PGD_2 with DP and PGI_2 with IP) (Narumiya *et al.*, 1999; Bos *et al.*, 2004).

Although it is already known that prostanoids have a role in the vasomotor control of the endothelium, particularly in obesity, (Jones *et al.*, 1993; Traupe *et al.*, 2002a; Traupe *et al.*, 2002b; Feletou *et al.*, 2009; Meyer *et al.*, 2012), less is known about the vasomotor effects of PVAT-derived prostanoids. Among the first evidence that suggest prostanoids as an ADCF is the confirmation of COX expression in adipocytes (Xu *et al.*, 2007) as well as other cell types in PVAT, such as endothelial cells, immune cells and fibroblasts (Simmons *et al.*, 2004). Thereafter, a study by Meyer et al., 2013 has showed that PVAT could augment arterial vasoconstriction via the release of COX-derived ADCF. In this study, non-selective COX inhibition prevented adipocyte-derived vasoconstriction of the aorta of obese mice whilst selective COX1 or COX2 inhibition resulted in a partial antagonism of ADCF. Additionally, TXA_2 formation is detected in PVAT of lean control mice and to a greater extent in PVAT of obese mice (Meyer *et al.*, 2013). COX-derived vasoconstrictor prostanoids have also been suggested to attribute to endothelial dysfunction of visceral adipose arterioles in human obesity (Farb *et al.*, 2014). Disruption of TP receptor in mice resulted in lowering systolic BP compared to wild-type mice (Thomas *et al.*, 1998). Lack of the effect of PVAT-derived TXA_2 could be, at least partly, the reason for this reduced BP. Furthermore, several studies have demonstrated a link between COX-derived prostanoids and atherosclerosis

progression (Bailey *et al.*, 1979; Pratico *et al.*, 2001). Thus, the recent observation of provoking atherosclerosis by PVAT (Ohman *et al.*, 2011) highlights the importance of ADCF-dependent mechanisms and consequently, the importance of inhibition of prostanoid formation as a novel therapeutic strategies to reduce the cardiovascular disease risk.

1.5.3.2.2. Reactive oxygen species

Reactive oxygen species (ROS) are small molecules produced at low levels during normal physiological conditions (Holmstrom and Finkel, 2014; Panieri and Santoro, 2015), affecting cell homeostasis and survival (Filomeni *et al.*, 2015). However, excessive increase in production of ROS leads to oxidative stress which causes toxic cellular effects and tissue dysfunction (Yue *et al.*, 2015). ROS are produced due to partial reduction of molecular O_2 and leads to production of different kinds of ROS including superoxide anion (O_2^-), hydroxyl radical (OH•), hydrogen peroxide (H_2O_2), and singlet oxygen ($^1O_2$). ROS can be generated by different mitochondrial and non-mitochondrial enzymes either primarily as NADPH oxidases (Nox) (Babior *et al.*, 2002; Lambeth, 2004) or as a part of other reactions such as xanthine oxidase, lipoxygenase and cyclooxygenase (Droge, 2002; Huang *et al.*, 2013). There are different isoforms of Nox, all utilize NADPH as an electron donor to produce ROS (Katsuyama, 2010). Nox1, Nox2 and Nox4 are expressed in VSM and linked to several cardiovascular dysfunctions, such as hypertension and atherosclerosis (Cave *et al.*, 2006; Streeter *et al.*, 2013).

The interaction between ROS and vascular tone is quite complex. Superoxide anion is produced from reduction of O_2 molecule and is a precursor of many ROS. Superoxide has a complex biphasic effect on the vascular tone, inducing both direct vasoconstriction and vasorelaxtion depending on the model and circumstances (Didion and Faraci, 2002; Snetkov *et al.*, 2011). In addition, O_2^- can affect the vascular tone indirectly by interacting with the potent vasodilator, nitric oxide. The reaction between NO and O_2^- is three times faster than the dismutation of superoxide by superoxide dismutases (SODs) (Faraci and Didion, 2004). This characteristic confers O_2^- the ability to act as a key determinant of the biological half-life of nitric oxide. Dismutation of O_2^- produces hydrogen peroxide, a molecule with low reactivity and high stability

that can readily penetrate the cell membrane and generate the most active form of ROS, hydroxyl radical. Several studies have consistently identified a vasodilator effect of H_2O_2 in different arteries (Burke and Wolin, 1987; Fujimoto *et al.*, 2001; Sato *et al.*, 2003). However, high concentration of H_2O_2 can cause vasoconstriction followed by vasorelaxtion. In addition to the acute regulation of vascular tone mentioned above, ROS have much more chronic effects within the vascular wall including, for instance, vascular structure (Birukov, 2009), vascular permeability (Abbott, 2000) and gene expression and inflammation (Faraci, 2005). Furthermore, excessive Nox-derived ROS have been suggested to be detrimental to vascular function as mice lacking components of Nox subunits showed a higher level of protection against hypertension which attributed to a reduced vascular ROS production and increased NO bioavailability (Barry-Lane *et al.*, 2001; Judkins *et al.*, 2010).

Recent studies on PVAT have identified the existence of a complete reactive oxygen species/reactive nitrogen species machinery including Nox, superoxide dismutase (SOD) isoforms and eNOS (Szasz and Webb, 2012). Gao *et al*. (2006) proposed for the first time that PVAT could augment vasoconstriction induced by perivascular nerve stimulation of rat superior mesenteric artery. They reported that superoxide production from NAD(P)H oxidase is involved in PVAT-induced potentiation of perivascular nerve stimulation-elicited contraction (Gao *et al.*, 2006). Moreover, ROS has been suggested as a possible mechanism of resistin, an adipokine which is derived from PVAT and induced vascular contraction (Guzik *et al.*, 2007; Cho *et al.*, 2011). In contrast to the clarified vasoconstrictor effect of PVAT-derived superoxide anion, hydrogen peroxide (H_2O_2) could elicit anti-contractile effects by stimulation of soluble guanylyl cyclase in Wistar rats aortic rings (Gao *et al.*, 2007). However, H_2O_2-mediated vasorelaxation is attenuated by PVAT in coronary arteries from Ossabaw swine (Owen *et al.*, 2013).

PVAT removal or treatment with ROS scavengers restored the endothelium-dependent vasorelaxation in diet-induced obese mice. This finding suggested a potential role for PVAT-derived ROS in the obesity-associated endothelial dysfunction (Ketonen *et al.*, 2010). In addition, another study by da Costa *et al.*, (2016) tested the effect of induced obesity on the mitochondrial function in

PVAT (da Costa *et al.*, 2016). The authors found that obesity can cause impairment of the mitochondrial function, augmentation of O_2^- and H_2O_2 production, and loss of the anti-contractile effects of PVAT. TNF-α-induced oxidative stress was proposed to be a key mechanism for the loss of this anti-contractile effect of PVAT.

1.5.3.2.3. Chemerin

Chemerin (tazarotene induced gene 2 or TIG2) is a protein discovered in 1997 (Nagpal *et al.*, 1997) and expressed as a pre-prochemerin which is composed of 163 amino acids. Several proteases are responsible for activation and processing of this chemerin precursor to produce different isoforms of chemerin (Zabel *et al.*, 2005; Guillabert *et al.*, 2008; Yoshimura and Oppenheim, 2008) whilst other proteases are responsible for its inactivation (John *et al.*, 2007). Chemerin and its receptors (CMKLR1/ChemR23, G protein-coupled receptor 1 (GPR1) and C-C chemokine receptor-like 2 (CCRL2)) have been recently found to be attributed to various physiological and pathological conditions (Mattern *et al.*, 2014).

Chemerin is secreted mainly from liver and visceral fat (Ernst and Sinal, 2010; Iannone and Lapadula, 2011) and considered as a biomarker for adiposity since its increased level is strongly attributed to high BMI and metabolic syndrome (Bozaoglu *et al.*, 2007; Jialal *et al.*, 2013) whereas weight loss causes a reduction in chemerin level (Sell *et al.*, 2010; Ernst *et al.*, 2012). Additionally, genetic knockout of ChemR23 diminished adiposity and body weight (Ernst *et al.*, 2012). Adipocyte differentiation is modulated by chemerin (Goralski *et al.*, 2007; Roh *et al.*, 2007; Muruganandan *et al.*, 2011). Chemerin is capable of attracting monocytes and macrophages, through activation of their ChemR23 receptor, and stimulating inflammation (Goralski *et al.*, 2007; Hart and Greaves, 2010). This inflammation induced by chemerin could have an essential role in obesity, particularly because of the ability of chemerin to elicit production of a number of proinflammatory cytokines as well. Furthermore, the link between chemerin and inflammation is further supported by the idea of that TNF-α could stimulate chemerin production from adipocytes (Parlee *et al.*, 2012).

Chemerin can act as an adipokine and growth factor, affecting the cardiovascular system via autocrine/paracrine manners (Ferland and Watts,

2015). Intracellular signalling of chemerin involves Ca^{2+}-mobilization, inhibition of cAMP accumulation, (Wittamer *et al.*, 2003), p38 MAPK and ERK-1/2 (Zhang *et al.*, 2014). In addition to ERK signalling, the protein kinase C pathway has a role in the chemerin receptor internalization (Zhou *et al.*, 2014). Furthermore, chemerin could attenuate nitric oxide signalling in the rat aorta (Neves *et al.*, 2014) and enhance generation of mitochondrial ROS in cultured endothelial cells (Shen *et al.*, 2013).

The link between PVAT and chemerin has been established as chemerin expression is detected in epicardial and aortic adipose tissue (Spiroglou *et al.*, 2010). In addition, a ChemR23 agonist caused a dose-dependent vasoconstriction, via a proposed elevation of intracellular calcium, whereas a ChemR23 antagonist caused inhibition of PVAT-derived vasoconstriction in isolated rat thoracic aorta, superior mesenteric artery, and mesenteric resistance artery (Watts *et al.*, 2013). This is supported by Kostopoulos *et al.* (2014) who confirmed the expression of chemerin and its receptor CMKLR1 in human aorta and coronary artery, and PVAT. In addition, they found that coronary atherosclerosis is positively correlated with chemerin (Kostopoulos *et al.*, 2014). These findings are noteworthy since it describes a new possible mechanism of how chemerin can regulate BP and affect cardiovascular pathophysiology. In fact, these recent researches also raise our attention to the importance of PVAT and expands our view of chemerin's role in BP regulation. It is important to mention that other adipokines in PVAT could balance or enhance the vasoconstrictor effects of chemerin, for instance, the chemerin:adiponectin ratio is regarded as a predictor of metabolic syndrome (Rourke *et al.*, 2013). Although it is clear that PVAT is not the only source of chemerin, PVAT with its location in close proximity to the blood vessels should be regarded as a potential source of the chemerin-induced vascular tone.

1.5.3.2.4. Angiotensin II

A complete machinery of renin-angiotensin-aldosterone system (apart from renin) has also been found in adipocytes (Galvez-Prieto *et al.*, 2008), indicating adipocytes as another source of Ang II. This is supported by another study which showed the existence of all the components of the renin-angiotensin system in PVAT as well as angiotensin receptors (angiotensin (1a) and angiotensin (1b)

receptors) (Galvez-Prieto *et al.*, 2008). In addition, PVAT-derived Ang II could increase electrical field stimulation-evoked contraction in rat mesenteric arteries. Moreover, this *in vivo* study showed that chronic treatment with an ACE inhibitor quinapril diminished the potentiating effects of PVAT on EFS-induced contraction (Lu *et al.*, 2010). Furthermore, an angiotensin 1 receptor antagonist (losartan) had the ability to improve the PVAT-associated vascular regulation in fructose-induced hypertensive rats (Huang *et al.*, 2010).

1.5.3.2.5. Noradrenaline

A complete "adrenergic system" resides in PVAT which includes releasing, taking up and metabolism of noradrenaline (NA) (Ayala-Lopez and Watts, 2016). Adipocytes and stromal vascular fraction contain components that constitute this adrenergic system. A study of (Lafontan and Berlan, 1993) found that 5 adrenoceptors (α_1, α_2, β_1, β_2 and β_3) are expressed on adipocytes with variation in their existence and distribution in different types of AT depots. Furthermore, α and β adrenoceptors are found on mouse mesenteric artery PVAT, but without identifying the subtypes (Bulloch and Daly, 2014). A significantly higher level of NA has been found in aortic and superior mesenteric arterial PVAT compared with retroperitoneal WAT of male Sprague-Dawley rats. Noteworthy, there was approximately no adrenaline in either PVAT or adipose tissue (Ayala-Lopez *et al.*, 2014). The same authors found that tyramine could cause a concentration-dependent vasoconstriction in aorta with PVAT but not with PVAT-free vessel. In addition, adipose tissue can affect the adrenergic system via secretion of three adipokines which are resistin, leptin and angiotensin II (Soltis and Cassis, 1991; Rayner and Trayhurn, 2001; Brunetti *et al.*, 2004).

On the other hand, NA has a role in the vasomotor effects of PVAT through augmentation of mitochondrial superoxide (O_2^-) generation and its rapid dismutation of superoxide into H_2O_2 (Costa *et al.*, 2016). In fact, the adrenergic system within PVAT has been suggested as an integral connection linking obesity with vascular dysfunction that includes a substantial augmentation of sympathetic nervous stimulation such as obesity-associated hypertension (Ayala-Lopez and Watts, 2016). Obviously, as considering PVAT an important integral part of the blood vessel supplied with a complete adrenergic system, it

is recommended for future studies to focus on its role in understanding obesity-associated hypertension.

1.5.4. PVAT pathology

It has been reported that PVAT dysfunction, just like endothelial dysfunction, plays an important role in many cardio-metabolic diseases, such as hypertension and obesity (Greenstein *et al.*, 2009; Zou *et al.*, 2016) (Figure 1.4). The anti-contractile characteristics of PVAT are reduced due to local inflammation and hypoxia of PVAT in obese patients (Greenstein *et al.*, 2009). Another study showed a reduction in the vasorelaxant properties of PVAT in obese rats and the diminished bioavailability of NO from PVAT has been suggested as a reason for this obesity-associated PVAT dysfunction (Bussey *et al.*, 2016). PVAT dysfunction could contribute to uncoupling of endothelial nitric oxide synthase (eNOS) and enhanced O_2^- production in obese mice (Xia *et al.*, 2016). In addition, the prostanoids could be regarded as another mechanism of obesity-induced PVAT dysfunction. A study by Lobato *et al.* (2011) showed an increased level of TXA_2 and decreased level of PGI_2 in obese rats which is explained by inflammation-enhanced COX2 activity and, subsequently, increased production of prostaglandins from arachidonic acid (Lobato *et al.*, 2011). This finding is supported by another study which described increased COX2 activity and TXA_2 production in PVAT of mice aorta as a causative factor to obesity-induced PVAT dysfunction (Meyer *et al.*, 2013). PVAT has also been proposed to be responsible for enhanced vasoconstriction of porcine coronary arteries in obesity (Owen *et al.*, 2013).

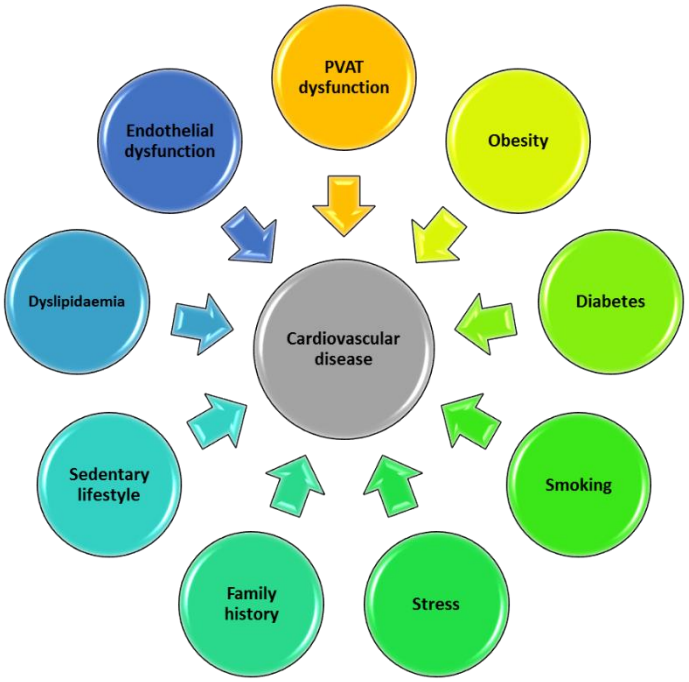


Figure 1.4: PVAT dysfunction and other traditional risk factors for cardiovascular disease.

Some of the adipokines derived from PVAT have a considerable impact on cardiovascular pathophysiology. For instance, leptin, a pro-inflammatory adipokine, can act as a direct pro-atherogenic factor through its ability to induce C-reactive protein expression in human artery endothelial cells which provokes atherosclerosis (Martin *et al.*, 2012). Moreover, a cross-sectional study showed that high leptin concentrations contribute to arterial thrombosis (Petrini *et al.*, 2016). Additionally, increased risk of atherosclerosis is associated with stimulation of the renin–angiotensin system in PVAT in uni-nephrectomized mice (Kawahito *et al.*, 2013). In human atherosclerosis, PVAT is infiltrated by various inflammatory cells which are linked to the vascular inflammatory response in atherosclerosis (Henrichot *et al.*, 2005; Chaldakov *et al.*, 2014). Moreover, as adiponectin has anti-atherosclerotic characteristics via reduction of several atherogenic growth factors (Okamoto *et al.*, 2008), a recent study demonstrated that atherosclerosis could be augmented in adiponectin deficiency state in mice (van Stijn *et al.*, 2014). To conclude, although endothelial dysfunction is regarded as a well-known predictor of cardiovascular pathology, more recently, PVAT seems to have a crucial role as well.

1.6. Aims

Although previous studies have identified a sexual dimorphism in the modulation of vascular tone, to date, no study has investigated whether there are sex differences in the regulation of blood vessel tone by PVAT. So the principal aim of this study was to identify any sex differences in PVAT-regulation of vascular tone of the porcine coronary artery in physiological and pathophysiological conditions, which could explain the contradictory findings between previous studies. The specific aims of the present study were the following:

- As there are sex differences in the release of adipokines from adipose tissue in general, the aim was to identify whether there are sex differences in PVAT-induced vasorelaxation, especially the role of adiponectin and H_2S.
- To determine whether phospholipase A_2 (PLA_2)-dependent arachidonic acid pathway plays a role in PVAT-induced contractile responses and to investigate whether there are sex differences in these responses of the coronary artery to PVAT.
- Given that sex differences in oxidative stress have been reported in the vasculature, another objective of the present study was to determine whether there are sex differences in production of ROS from NADPH oxidase in PVAT and its effect on vasomotor function of isolated PCAs.
- As chemerin has been identified as a potential vasoconstrictor, a further objective of this study was to determine the impact of PVAT-derived chemerin on the vascular tone of the PCAs and to identify any sex differences in this adipose-vascular coupling.
- The aims were also to examine the effect of PVAT-derived prostanoids and ROS on the vascular tone of PCAs in non-physiological conditions and to identify any sexual dimorphism in these signalling pathways.

Chapter Two

Sex differences in the perivascular adipose tissue-derived vasorelaxation: the role of adiponectin

2.1 Introduction

Adipose tissue has traditionally been described as being simply a structural support, with additional lipid storage (white adipose tissue) and thermoregulator (brown adipose tissue) roles (Cannon and Nedergaard, 2004; Mariman and Wang, 2010). However, compelling evidence in recent years has led to the view that adipose tissue is in fact an active secretory organ which releases several bioactive signalling molecules, collectively termed adipokines, which are important in both health and disease (Fortuno *et al.*, 2003; Havel, 2004; Thalmann and Meier, 2007; Yamawaki *et al.*, 2010). Multiple studies have established that there are variations in the function of adipose tissue in different sexes where, for instance, women have higher circulating adiponectin levels compared to men (Nishizawa *et al.*, 2002; Cnop *et al.*, 2003; Arita *et al.*, 2012).

The recent interest in perivascular adipose tissue as an endocrine and paracrine organ has led to a number of studies investigating the characteristics of various fat depots in the body. Soltis and Cassis (1991) firstly described that perivascular adipose tissue significantly attenuated vascular responsiveness of Sprague-Dawley rat aortae to noradrenaline (Soltis and Cassis, 1991). This result was confirmed by Löhn *et al*., (2002) who re-examined the concept of periadventitial vasoregulation. Their study provided additional proof that PVAT-inhibited vasoconstriction induced by a number of additional agonists such as angiotensin II, serotonin and phenylephrine (Lohn *et al.*, 2002). Adiponectin is a major factor secreted by adipocytes (Scherer *et al.*, 1995) and exerts its action by binding to its receptors (AdipoR1 and AdipoR2) (Kadowaki and Yamauchi, 2005). Although downstream regulation of signalling of these receptors has yet to be fully identified, overexpression of APPL1 (adaptor protein, phosphotyrosine interacting with PH domain and leucine zipper 1) enhances, and suppression of APPL1 level attenuates, adiponectin signalling and its downstream events (Mao *et al.*, 2006).

Functional studies have found that adiponectin relaxes murine mesenteric arteries by opening Kv channels (Fesus *et al.*, 2007), and Greenstein *et al.*, (2009) concluded that adiponectin was the anti-contractile adipokine released from rat mesenteric arterial PVAT (Greenstein *et al.*, 2009). Moreover, a fragment of the adiponectin receptor abolished the PVAT-induced

vasorelaxation in human small arteries taken from subcutaneous gluteal fat biopsy samples, which further suggests that adiponectin is a predominant mediator of the relaxation (Greenstein *et al.*, 2009).

In rats and mice, hydrogen sulphide has been described as a novel candidate for an adipose-derived relaxing factor (ADRF), or at least as a mediator in the action of ADRF (Fang *et al.*, 2009; Schleifenbaum *et al.*, 2010). However, this area is still a matter of debate because of the controversial findings in the expression and function of H_2S synthesizing enzymes in different species. For instance, Kohn *et al.*, (2012) found that CSE and CBS inhibition in mouse aorta did not influence the ADRF effect, which is in contrast to their findings on rat aorta (Kohn *et al.*, 2012). In addition, species differences are obviously present in the CSE expression in the vasculature (Yang *et al.*, 2008; Fang *et al.*, 2009; Kohn *et al.*, 2012). Noteworthy, there are accumulating data about the potential effect of PVAT in regulating the vascular tone where PVAT could induce both vasorelaxation and vasoconstriction depending on the anatomical position, species and condition (Verlohren *et al.*, 2004; Yudkin *et al.*, 2005; Owen *et al.*, 2013; Szasz *et al.*, 2013; Nava and Llorens, 2016).

A recent study in our laboratory has demonstrated that there are sex differences in the regulation of tone in the porcine coronary artery (Wong *et al.*, 2014b). As there are also sex differences in the release of adipokines from adipose tissue in general, this study aimed to investigate whether there are sex differences in the regulation of vascular tone by PVAT in the porcine coronary artery.

2.2 Materials and Methods

2.2.1 Tissue preparation

Hearts from male and female pigs (large white hybrid pigs, 4-6 months old, weighing ~ 50 kg) were obtained from a local abattoir, G Woods & Sons, Clipstone, Nottinghamshire, and transported back to the laboratory in ice-cold modified Krebs'-Henseleit solution (118 mM NaCl, 4.8 mM KCl, 1.1 mM $MgSO_4$, 25 mM $NaHCO_3$, 1.2 mM KH_2PO_4, 12 mM D-glucose, 1.25 mM $CaCl_2$). The anterior proximal part of the left coronary artery was then dissected and placed in Krebs'-Henseleit solution pre-gassed with 5% CO_2 and 95% O_2 and kept overnight in the refrigerator. On the second day, fine dissection was performed to prepare paired PCAs rings from each artery ensuring vessels were not stretched or damaged. PCAs were then cut into rings of approximately 5 mm in length and suspended in a multichannel 5 ml organ bath. Each bath was filled with 5 ml of Krebs'-Henseleit solution and maintained at 37^{o}C and constantly gassed with carbogen (95% O_2, 5% CO_2). Tension was measured and recorded using a Powerlab data acquisition system (ADInstruments) via an amplifier.

2.2.2 Functional responses in the isolated porcine coronary arteries

Arteries were initially pre-tensioned to 8 g, determined from preliminary studies, and then left to equilibrate for approximately 30-45 minutes. Once a stable baseline was obtained, two consecutive responses to 60 mM KCl were obtained for standardization. After about 20 min the KCl was washed out with fresh Krebs'-Henseleit solution. Following the return to a stable baseline and, after a further 15-30 minutes, exposure to KCl was repeated. Once again, the tissue was washed out with Krebs'-Henseleit solution, to allow the segment to re-stabilize to baseline. The data were calculated and expressed as a percentage of the contraction in response to 60 mM KCl. The KCl response is considered as a reference to the viability and activity of each segment in order to avoid the individual variation in the response of the coronary artery. There was inter-individual variation in the size of the contractile response to PVAT, therefore, adjacent coronary arterial segments from the same animal were always used as controls. Thereafter, relevant test compounds were added and allowed 60 minutes incubation time. The following test compounds were used: L-NAME

(300 µM) to inhibit NO synthase (Wong *et al.*, 2014b), and indomethacin (10 µM) (Malinowski *et al.*, 2008) to inhibit cyclooxygenase. Pre-incubation with an anti-adiponectin antibody (1:100; ABIN1857924, Antibodies-online Inc., Atlanta, USA) was performed to determine the role of adiponectin in PVAT-induced vasorelaxation in females. To study the role of H_2S, 4-propargylglycine (PPG) (10 µM) (Cheng *et al.*, 2004; Kohn *et al.*, 2012) and 2-(aminooxy)-acetic acid (AOAA) (100 µM) were used as inhibitors of cystathionine γ-lyase (CSE) or cystathionine-ß-synthase (CBS), respectively. U46619 (9,11-Dideoxy-11α,9α-epoxymethano-prostaglandin F2α) was added cumulatively (1 nM-300 nM) to induce contraction in the arterial rings, which was calculated as a percentage of the contraction in response to 60 mM KCl. In some experiments, endothelin-1 (ET-1) (1 nM-300 nM) was used as a contractile agent. In another set of experiments, PVAT, which was stored overnight with the blood vessel, was dissected, cleaned of myocardium and stored in cold Krebs' Henseleit solution for later use at the same day of experiment. Known quantities of PVAT (0.3 g) were then added to the vessels in which the PVAT had previously been removed and PCAs pre-contracted with U46619 to a level of 40-60% of the maximum KCl response. Of note, there was no obvious difference in the amount of PVAT per unit length of coronary artery between female and male. In a further set of experiments, cumulative concentration-response curves to the adiponectin receptor agonist, adipoRon (1-100 µM) (Okada-Iwabu *et al.*, 2013) were performed in PCAs pre-contracted with U46619. In some tissues, the endothelial layer was removed by rubbing the lumen with a fine pair of forceps before attaching the vessels to the setup (Rayment *et al.*, 2007) and successful removal of endothelium confirmed by lack of response to 0.1 µM substance P.

2.2.3 Histological analysis

Coronary arterial segments with their adherent PVAT from both females and males were fixed overnight by immersion in 4% (w/v) paraformaldehyde at room temperature. Then, samples were embedded using optimal cutting temperature compound (OCT) and the frozen tissue sections were sectioned at 20 µm using a cryostat. After defrosting the fixed tissue, the slides were washed with (0.1M) phosphate buffer solution (PBS). The slides were initially stained using haematoxylin and eosin staining (Sigma-Aldrich, UK) to assess general

adipocyte morphology. Secondly, staining with Oil Red O (Sigma-Aldrich, UK) was performed to detect the localization of lipids in the tissues. A stock solution of oil red O (0.25 g in 40 ml of isopropanol) was prepared with shaking for 2 hr while a working solution was prepared by diluting 18 ml of stock solution in 12 ml of distilled water, and filtered through a 0.2 µm filter before use. Thirdly, slides were permeabilized with 0.5% IGEPAL® CA-630 (Sigma-Aldrich, UK) for 5 min. After washing twice with PBS, hydrogen peroxide was added as a quenching step for 10 min.

Immunohistochemical staining was made using rabbit specific HRP/DAB detection kit (ab64261, Abcam, Cambridge, UK), following the manufacturer's instructions. Briefly, non-specific binding was blocked with Protein Block solution. The blocking solution was then removed and replaced with the primary antibody anti-UCP1 antibody (ab10983, Abcam, Cambridge, UK) 1:500 in 1% (w/v) bovine serum albumin (BSA), and incubated overnight in a humidifier at 4°C. The following day, the primary antibody was removed and samples washed in PBS. After washes, slides were incubated with the secondary anti-rabbit antibody at 37°C for 10 min. Slides were then developed with streptavidin–biotin complex/HRP and DAB substrate, according to the manufacturer's instructions. Slides were rinsed, air dried,mounted for microscopy (DM4000B light microscope, Leica) and visualized using an objective magnification of x10. Images were acquired using a Micropublisher 3.3 RTV digital camera (Q-Imaging, British Columbia, Canada) with OpenLab software (Perkin Elmer). Negative controls were performed by omitting the primary antibody.

2.2.4 Immunoblotting

Polyacrylamide gel electrophoresis followed by immunoblotting was performed to determine the expression of adiponectin levels in PVAT, and the adiponectin receptors (AdipoR1 and AdipoR2) and APPL1 in PCAs from different pigs from each sex. PVAT or PCA samples were finely dissected and homogenized on ice using Tris-EDTA buffer (pH 7.4) and protease inhibitor cocktail (Calbiochem, VWR International Ltd, Lutterworth, Leicestershire, UK) (Appendix A). Estimation of the protein content of each sample was performed using a Lowry

protein assay, which is based on measuring the amount of proteins with Folin phenol reagent in the presence of alkaline copper conditions (Lowry *et al.*, 1951). Then, Laemmli solubilisation buffer (Appendix A) was added. Samples were then heated at 100^{o}C for 5 min and centrifuged at 13,000×g for 1 min. PVAT (20 μg), except for CBS blot in which 10 μg was added, and PCA (20 μg) samples were separated using a 4–20% gradient SDS-polyacrylamide gradient gel (Bio-Rad, Hemel Hempstead, Hertfordshire, UK) and then transferred onto nitrocellulose membrane (GE Healthcare, Little Chalfont, Buckinghamshire, UK) by immunoblotting. Porcine skeletal muscle and rat liver tissues were used as a positive control for AdipoR1 and AdipoR2, respectively (Ding *et al.*, 2009).

Membranes were then blocked with 5% (w/v) non-fat milk, or 5% (w/v) BSA in the case of APPL1, in Tris-buffered saline containing 0.1% (v/v) Tween 20 (TBST) (Appendix A) at room temperature for 1 h. The blot was then incubated with rabbit polyclonal anti-UCP1 antibody (ab10983 Abcam®, Cambridge, UK) (1:1000), rabbit anti-adiponectin antibody (1:400 dilution; ABIN1857924, Antibodies-online Inc., Atlanta, USA), rabbit anti-AdipoR1 antibody (1:500; 250476, Abbiotec, USA), rabbit anti-AdipoR2 antibody (1:250 dilution; orb10047, Biorbyt, Cambridge, UK), rabbit anti-CBS (clone 3E1; Abnova, London, UK) (1:1000), rabbit anti-CSE (ab80643, Abcam, Cambridge, UK) (1:1000), rabbit anti-MPST (HPA001240; Atlas antibodies, Stockholm, Sweden) (1:1000) or rabbit anti-APPL1 antibody (1:2000; mAb 3858, Cell Signaling Technology, UK) in 5% (w/v) milk, or in 5% (w/v) BSA in the case of APPL1 antibody, in Tris-buffer overnight at 4°C. Membranes were also incubated with a mouse anti-β-actin antibody (1:50,000 in 5% (w/v) milk; Sigma-Aldrich, Poole, Dorset, UK) or a mouse anti-myosin light chains (MLC) antibody (1:1000 in 5% (w/v) milk; Sigma-Aldrich, Poole, Dorset, UK) as a loading control. On the second day, the blot was washed in TBST followed by incubation with IRDye 800CW goat anti-rabbit and IRDye 680CW goat anti-mouse secondary antibodies (both 1:10,000 dilution; IRDye, Licor, Cambridge, UK). The immunoblot was then visualized using an Odyssey system from Licor and intensity of the bands measured using Odyssey Image Studio (Licor).

2.2.5 Determination of adiponectin levels released from PVAT

PVAT (0.15g) was incubated in 1ml of Krebs'-Henseleit solution at 37°C. Adiponectin levels in the buffer were then determined using a pig adiponectin ELISA Kit (abx255420; Abbexa, Cambridge, UK) following the manufacturer's protocol. The range of standard curve was 31.25 ng/ml - 1000 ng/ml, sensitivity: < 18.75 ng/ml.

2.2.6 Estimation of CBS and 3-MPST activity using SF7

SF7 fluorescence recording production of intracellular H_2S was estimated using SF7-AM (sulfide fluor-7- acetoxymethyl ester). PVAT homogenate was centrifuged at 1000g for 20 min followed by 30000g for 1 hr, to get the cytosol. Rat liver was used as a positive control. For CBS activity measurement, cytosol of female and male PVAT was incubated in the presence and absence of 100 µM AOAA for 15 min at 37°C. This was followed by incubation of the samples with 10 mM L-Cysteine, 100 µM pyridoxal 5-phosphate (PLP) and 5 µM SF7-AM probe for 90 min at 37°C in a 96-well plate. For 3-MPST activity measurement, cytosol of PVAT homogenate from both sexes was incubated with 5 µM SF7-AM probe and 10 mM 3-mercaptopyruvate for 90 min at 37°C. Fluorescence was then read in a fluorimeter using 485 nm and 538 nm as excitation and emission wavelengths, respectively.

2.2.7 Statistical analysis

Data are expressed as mean ± S.E.M. where *n* = the number of different animals. The concentration-response curves were fitted to a sigmoidal curve with a variable slope using four parameters logistic equation using GraphPad Prism software:

$$\mathrm{R} = \frac{\mathrm{R_{max}} \times \mathrm{A}^{n\mathrm{H}}}{\mathrm{EC_{50}}^{n\mathrm{H}} + A^{n\mathrm{H}}}$$

The maximum percentage contraction (R_{max}) and the negative log of concentration required to produce half the maximal contraction of the induced tone (pEC_{50}) were calculated from the fitted curves. R_{max} and pEC_{50} values were

analysed using a 2-tailed, paired or unpaired Student's *t*-test to compare differences between 2 groups, as appropriate. Differences between 3 or more groups were assessed using a one-way ANOVA or two-way ANOVA in conjunction with the Sidak's *post hoc* test to assess possible difference at individual concentrations. $P < 0.05$ was considered statistically significant. Statistical analysis was performed by GraphPad Prism (Version 6, GraphPad Software, La Jolla, California, USA).

2.2.8 Materials

All drugs were purchased from Sigma-Aldrich except for endothelin-1 which came from Tocris Bioscience and adiponectin from Antibodies-online Inc. Stock solutions of L-NAME, PPG, AOAA and adiponectin were dissolved in distilled water. Stock solution of indomethacin was dissolved in absolute ethanol. Stock solutions of U46619 were made to 10 mM in ethanol whilst DMSO was used as a solvent to make 10 mM of adipoRon. All further dilutions of the stock solutions were made using distilled water. All stocks were kept frozen at -20^{o}C apart from KCl which kept at room temperature.

2.3 Results

2.3.1 The effects of PVAT on U46619-induced vasoconstriction in PCAs from female and male pigs.

In order to determine the effects of perivascular fat on vascular contraction, concentration-response curves to the thromboxane mimetic U46619 were determined in coronary artery segments from female and male pigs (Figure 2.1 A, B), with and without adherent PVAT. The presence of fat reduced the maximum contraction to U46619 in coronary arteries from females. There was also a rightward shift in the concentration-response curve. At a maximum concentration of U46619 (300 nM), the percentage of contractile response of intact rings to KCl contraction in females (R_{max} = 82 ± 4.8%) was significantly lower than that of vessels lacking PVAT (R_{max} = 106 ± 8%). Similarly the log EC_{50} was also significantly reduced in the rings with fat attached (pEC_{50} = 7.88 ± 0.06) compared to control (pEC_{50} =8.21 ± 0.04) (Figure 2.1 A). On the other hand, the presence of PVAT had no effect on the U46619 induced-contraction in coronary arteries from male pigs (Figure 2.1 B). The maximal response equalled 81.3 ± 8.8%, pEC_{50} =7.81 ± 0.02% versus 81.5 ± 5.1%, pEC_{50} =7.85± 0.04; PVAT versus no PVAT attached, respectively. Similarly, the endothelin-1 (ET-1)-induced vasoconstriction was significantly reduced in coronary arteries from female pigs in the presence of fat with no significant change in pEC_{50} (with PVAT, R_{max} = 76.5 ± 10.2%, pEC_{50} = 7.5 ± 0.2, compared to controls, R_{max} = 114 ± 18.3%, pEC_{50} = 7.2 ± 0.3) (Figure 2.1 C). Conversely, PVAT did not affect the ET-1-mediated vasoconstriction in PCAs from male (R_{max} = 88.2 ± 15.4%, pEC_{50} =7.6 ± 0.11) compared to maximum contraction of 93.3 ± 13.3%, pEC_{50} =7.68 ± 0.12 under control conditions (Figure 2.1 D). Noteworthy, there was no significant difference in the size of the contractile response to 60 mM KCl with PVAT compared to without PVAT (females, control = 8 ± 0.8 g without PVAT compared to 6.4 ± 0.6 g with PVAT; males, control =9.4 ± 1.2 without PVAT compared to 7.7 ± 0.9 g with PVAT) (Figure 2.1 E,F).

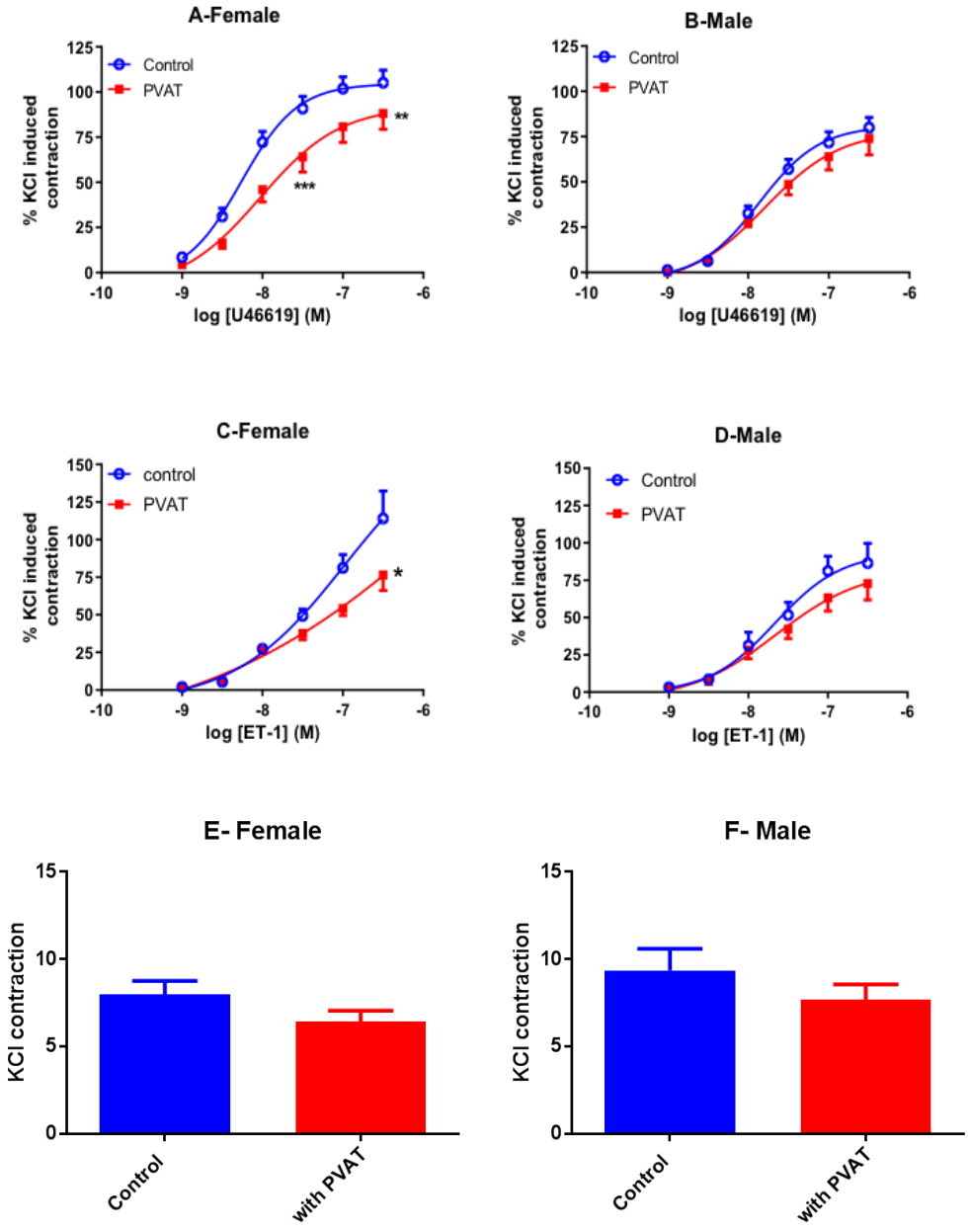


Figure 2.1: Log concentration-response curves for the vasoconstrictor effects of U46619 (**A & B**) or ET-1 (**C & D**) in the absence (Control) or presence of PVAT (PVAT) in coronary arteries from female (A & C) and male pigs (B & D). Data are expressed as a percentage of the contraction to 60 mM KCl and are mean ± S.E.M. of n=12(A), n=6(B), n=8(C), n=7(D). R_{max} and pEC_{50} values were compared. **(E & F)** Effect of PVAT on KCl-induced arterial contraction. Data are expressed as mean ± S.E.M. of n=13(E), n=6(F). * indicates P<0.05, ** indicates P<0.01, *** indicates P<0.001, 2-tailed, paired Student's *t*-test vs control values.

2.3.2 Acute effects of added PVAT on rings pre-contracted with U46619.

To confirm the previous results using separated PVAT, coronary arterial segments from female pigs with fat removed were pre-contracted submaximally with U46619. Once stable tone was obtained, 0.3 g PVAT was then added (Figure 2.2 C). PVAT from female animals caused immediate relaxation (PVAT(-): R_{max}= 5.8 ± 1.4%; PVAT(+): R_{max}= 25.3 ± 5.12% (Figure 2.2 A, C). On the other hand, PVAT from male animals had no significant effect on the U46619-induced vasoconstriction compared to time control (PVAT(-): R_{max}= 4.41 ± 0.6%; PVAT(+): R_{max}= 10.12 ± 4.6% (Figure 2.2 B). Furthermore, a crossover study showed no vasorelaxant effect of the addition of PVAT from females on PCAs from males (Figure 2.2 D).

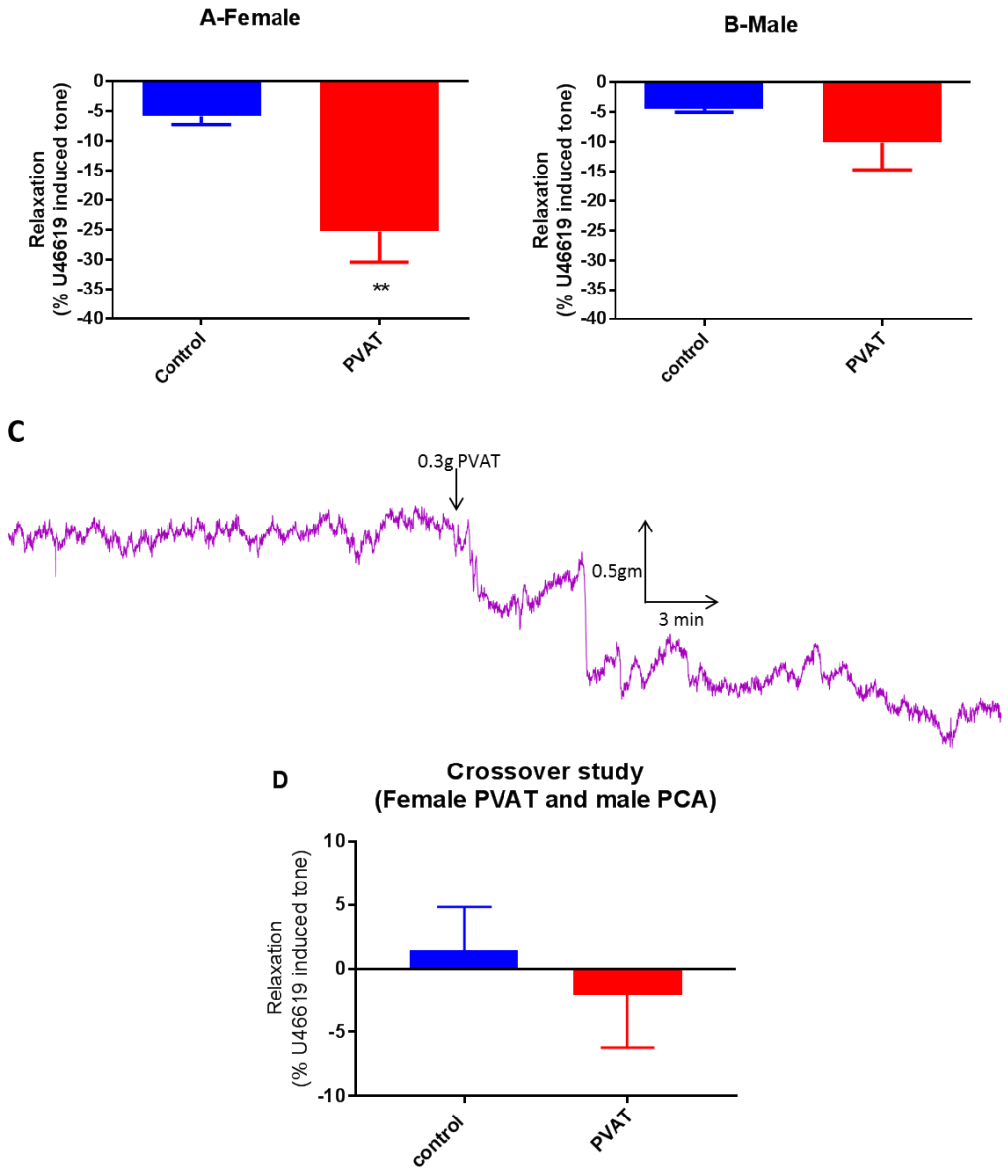


Figure 2.2: Effects of PVAT (0.3 g) in female **(A)** and male **(B)** PCAs. Original trace of recording showing the response of female PCA to addition of PVAT **(C)**. Effects of addition of PVAT (0.3 g) from female animals on coronary arteries from male animals **(D)**. Data are expressed as a percentage relaxation from the U46619-induced tone and are expressed as mean ± S.E.M. of n=8(A), n=8(B), n=6(D). **indicates P<0.01, 2-tailed, paired Student's *t*-test vs control values.

2.3.3 Expression of UCP1

Staining with oil red O confirmed the typical adipocytic morphology in the fixed samples (Figure 2.3 B). Uncoupling protein 1 (UCP1) was used as a biomarker characteristic to brown adipocytes

to identify the type of coronary PVAT in both female and male animals. Immunostaining showed that both female and male PVAT have the same low level of expression of UCP1 (Figure 2.3 E, F). Expression of UCP1 was almost undetectable in rat epididymis white adipose tissue in comparison with heavy staining of rat interscapular brown adipose tissue (Figure 2.3 D, C).

To confirm these results, immunoblotting was performed to quantify the expression of UCP1 in PVAT from females and males. Again there is similar low level of UCP1 expression in both sexes compared to positive control (Figure 2.4). In the thesis, the whole blots are presented in the appendices.

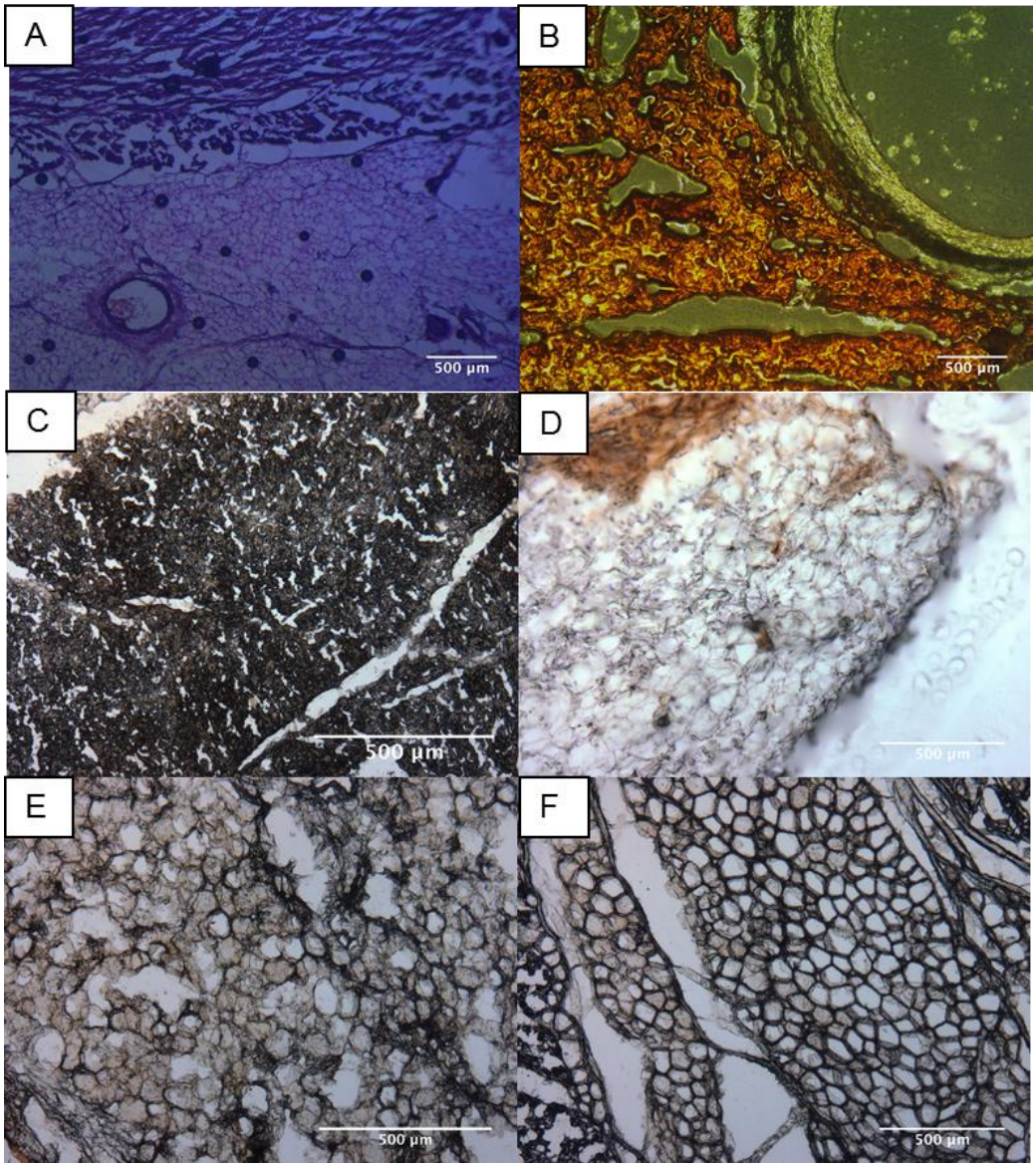


Figure 2.3: Representative histological sections of adipose tissue and PVAT. Hematoxylin-and-eosin staining of PVAT **(A);** Lipid content of PVAT as determined by Oil Red O extraction technique **(B);** Immunohistochemical staining of uncoupling protein 1 (UCP1) expression in different adipose tissue depots. Rat interscapular brown adipose tissue **(C);** Rat epididymis white adipose tissue **(D);** Female porcine coronary PVAT **(E);** Male porcine coronary PVAT **(F)**. Scale bar = 500 µm, magnification power 10X.

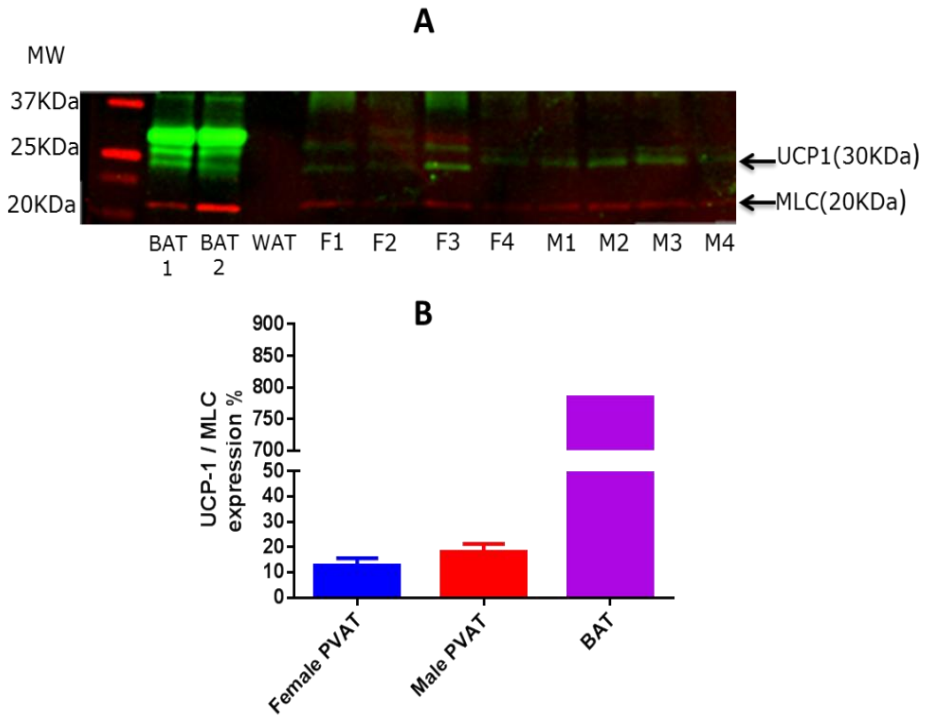


Figure 2.4: Representative immunoblotting showing protein expression of the uncoupling protein1 (UCP1) in PVAT from female (F1-F4) and male (M1-M4) pigs compared to interscapular brown adipose tissue (BAT1), aortic brown adipose tissue (BAT2) and epididymal white adipose tissue (WAT) **(A)**. Percentage of the expression levels of UCP1 to myosin light chain (MLC) in male and female PVAT, and aortic brown adipose tissue (BAT) based on the intensities of their bands **(B)**. Values are expressed as the percentage of UCP1 to MLC intensities bands and are mean ± SEM of 4 females-4 males pigs.

2.3.4 The effects of L-NAME and indomethacin on the anti-contractile effects of PVAT in female PCAs.

To investigate the involvement of NO and COX metabolites in the PVAT response, coronary arteries are preincubated with and without NOS and COX inhibitors before adding cumulative concentrations of U46619. The maximum response of PCAs to U46619 was significantly inhibited in the presence of PVAT, as before (with PVAT, R_{max}= 84.6 ± 9.3%, pEC_{50} = 7.2 ± 0.18) compared to their respective control responses (R_{max}= 121 ± 6.9%, pEC_{50} = 7.7 ± 0.07) (Figure 2.5 A). A combination of L-NAME and indomethacin had no effect on the concentration-response curve to U46619 in the absence of PVAT, but this combination prevented the inhibitory effects of PVAT on the U46619 response

(R_{max}= 104 ± 7%, pEC_{50} = 7.4 ± 0.12) (Figure 2.5 A, B). In another set of experiments, incubation with either L-NAME or indomethacin alone had no effect on the anti-contractile response of PVAT (Figure 2.5 B).

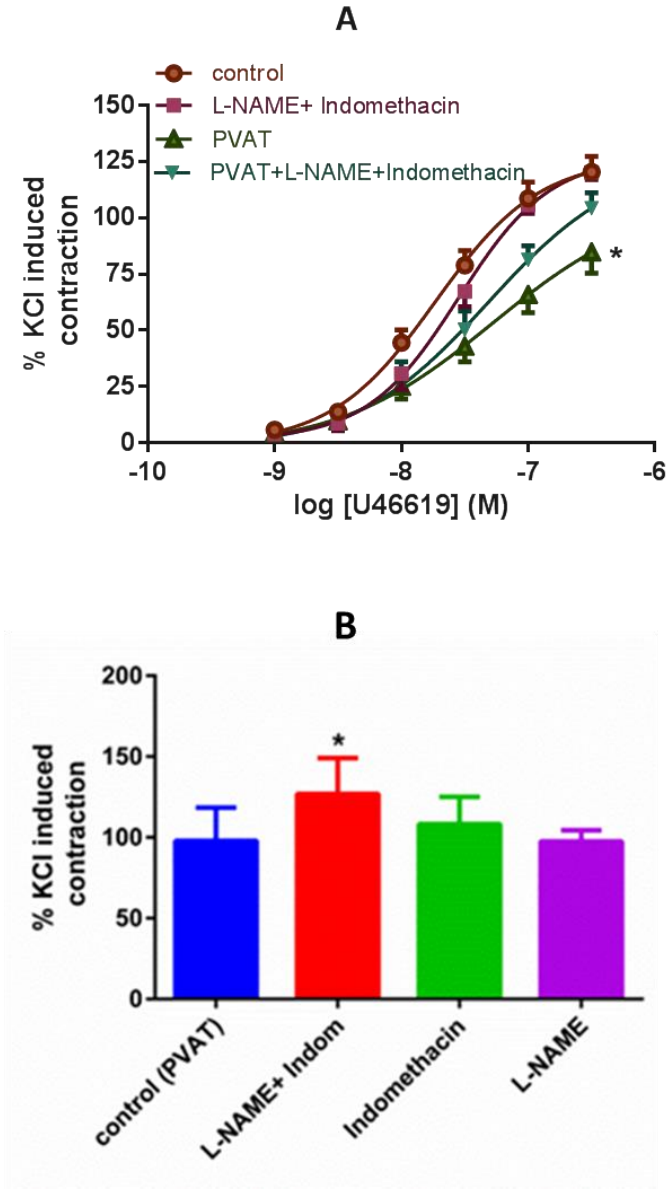


Figure 2.5: Role of NOS and COX in PVAT-induced vasorelaxation. **(A)** Log concentration-response curves for the vasoconstrictor effects of U46619 in the absence (control) or presence of PVAT (PVAT) in female PCAs with and without pre-incubation with L-NAME (300 µM) and indomethacin (10 µM). **(B)** Maximum responses to the vasoconstrictor effects of U46619 in female PCAs with fat attached and either absence or presence of pre-incubation with L-NAME (300 µM) and/or indomethacin (10 µM). Data are expressed as a percentage of the contraction to 60 mM KCl and are mean ± S.E.M. of 11 (A) - 6 (B)

experiments. * indicates P<0.05, one-way ANOVA followed by a Sidak's *post hoc* test vs control values.

2.3.5 Role of adiponectin in PVAT-mediated vasorelaxation in females

Previous studies have indicated that adiponectin acts through nitric oxide synthase and cyclooxygenase-dependent pathways. Therefore the role of adiponectin in the relaxation effect was examined in the presence of PVAT. Segments of coronary arteries from females were pre-treated with an anti-adiponectin antibody, in order to bind any released adiponectin. In the presence of the anti-adiponectin antibody, the PVAT-induced relaxation was abolished (Figure 2.6).

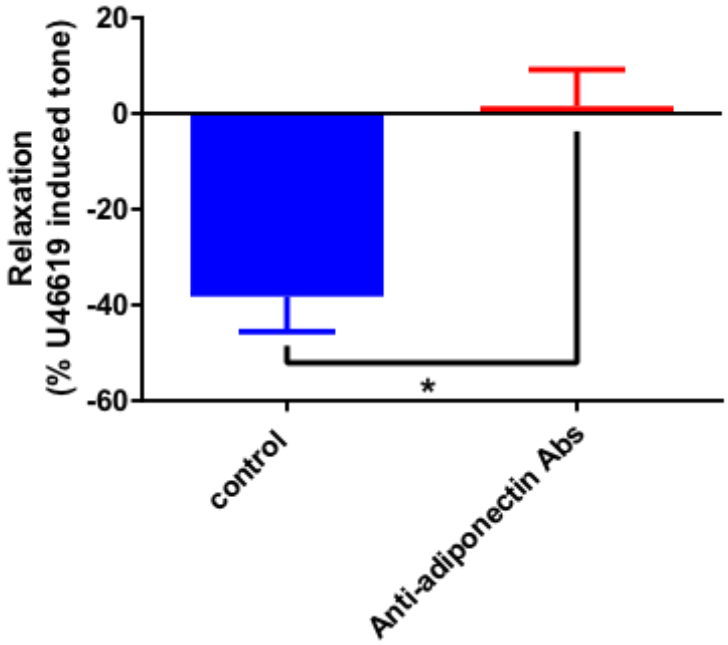


Figure 2.6: Effects of pre-incubation with an anti-adiponectin antibody on PVAT vasomotor function. PVAT (0.3 g) –induced vasorelaxation in the absence (control) or the presence of anti-adiponectin antibody in female PCAs. Data are expressed as a percentage change from the U46619-induced tone and are mean ± S.E.M. of 4 experiments. * indicates P<0.05, 2-tailed, Student's paired *t*-test vs control values.

2.3.6 Adiponectin expression and release from PVAT

The results indicated that PVAT from females, but not males, causes relaxation of coronary arteries through the release of adiponectin. In order to determine whether the differences in the role of PVAT in arteries from male and female animals was due to differences in the amount of adiponectin in PVAT, the expression of adiponectin in PVAT was determined by immunoblotting. There was no significant difference in the expression of adiponectin in coronary arterial PVAT from female and male animals (Figure 2.7 A, B).

As there was no difference in the level of expression of adiponectin in PVAT between male and female animals, the release of adiponectin from PVAT was determined. Although adiponectin could be detected in the buffer that the PVAT was incubated in, there was no significant difference in the level of released adiponectin between PVAT from male and female animals (Figure 2.7 C).

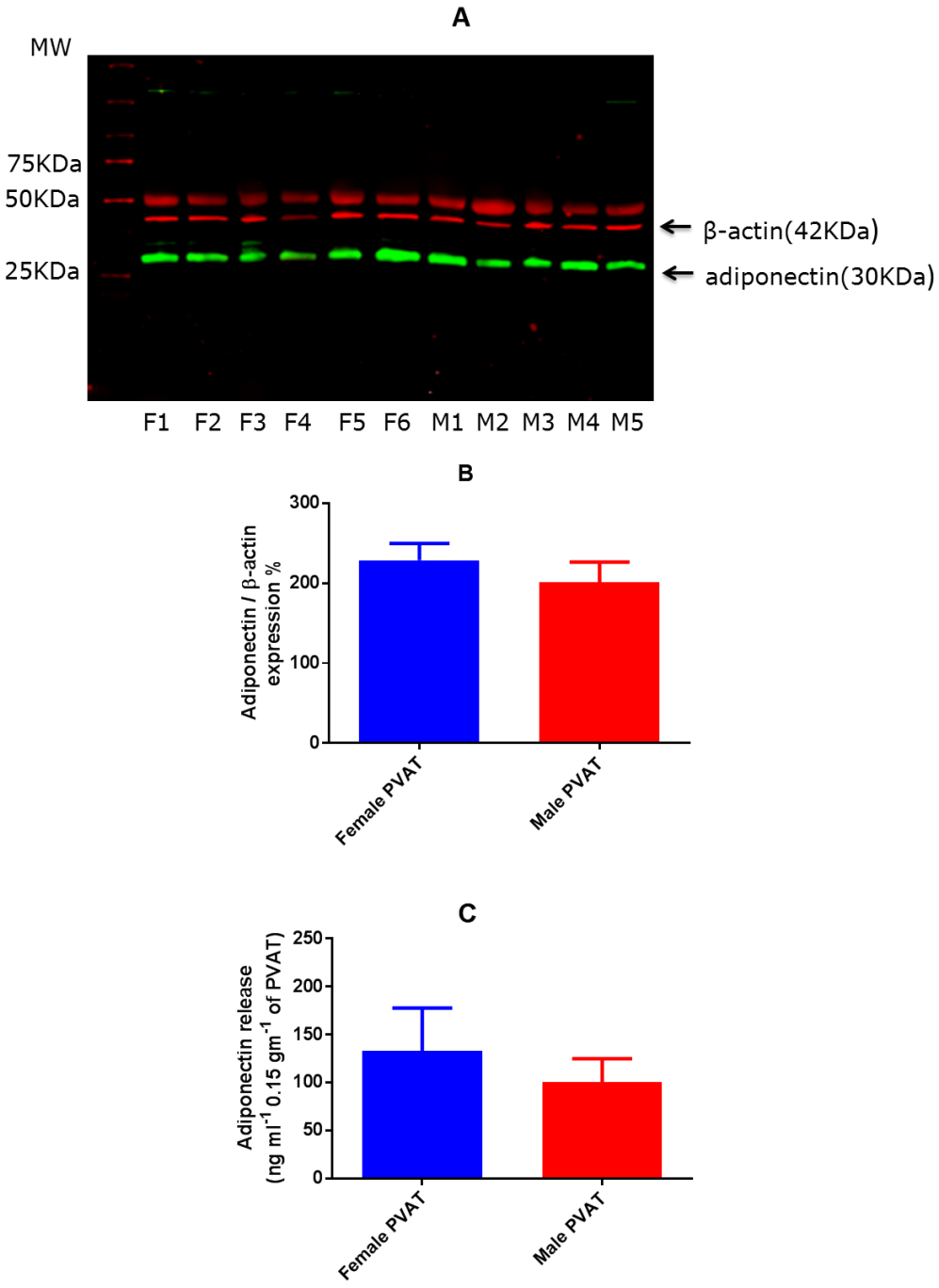


Figure 2.7: (A) Representative immunoblot showing expression of adiponectin (30 kDa) and β-actin (42 kDa) levels in 20 µg of PVAT from female (F1-F6) and male (M1-M5) pigs. **(B)** Bar chart showing density of adiponectin bands normalised to β-actin levels, in PVAT from female and male animals. Data are expressed as mean ± SEM. **(C)** Comparison of the levels of adiponectin in the buffer after incubation with PVAT from female or male pigs for 1 hour. Data are expressed as a ratio of adiponectin released to whole weight of PVAT (0.15 g) and are mean ± S.E.M. of 6 female and 6 male PVAT samples.

2.3.7 Responsiveness of porcine coronary arteries to adipoRon

As there was no difference in either the expression of adiponectin or release of adiponectin from PVAT, the sensitivity to adiponectin receptor activation was compared between male and female animals. AdipoRon, an adiponectin receptor agonist, produced a concentration-dependent relaxation of coronary arteries from both female and male pigs. However, there was a greater relaxation in arteries from female pigs compared to male (at 100 µM, females: 106 ± 8 % relaxation, n=6; males: 78 ± 6 % relaxation). AdipoRon also appeared to be more potent in arteries from females compared to males, based on the observation that adipoRon produced a relaxation at lower concentrations (Figure 2.8 A). The adipoRon-induced vasorelaxation was endothelium-independent as denudation of endothelium did not affect the responses of coronary arteries to adipoRon (Figure 2.8 B).

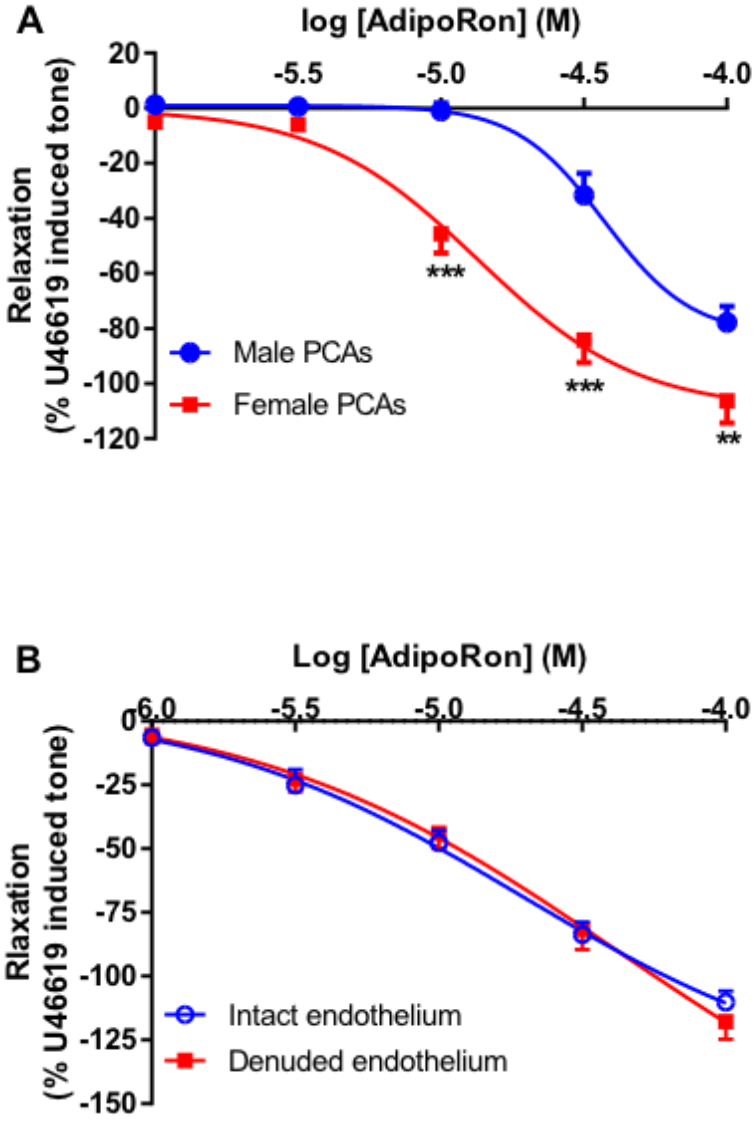


Figure 2.8: (A) Log concentration-response curves to adipoRon in coronary arteries from female and male pigs. Data are expressed as a percentage change from U46619-induced tone and are mean ± S.E.M. of 6 female and 8 male experiments. **(B)** Log concentration-response curves to adipoRon in intact (control) or endothelium-denuded coronary arteries from female and male pigs. Data are expressed as a percentage change from U46619-induced tone and are mean ± S.E.M. of 8 experiments. ** indicates P<0.01, *** indicates P<0.001 (two-way ANOVA followed by a Sidak's *post hoc* test).

2.3.8 Expression of Adiponectin receptors in PCAs

To clarify the difference in the responsiveness of PCAs in different sexes, the level of expression of two different isoforms of adiponectin receptors (AdipoR1 and AdipoR2) was measured in PCAs from both sexes, using immunoblotting. Numerous bands were detected with the anti-AdipoR1 antibody, but none lined up with the band in the porcine skeletal muscle positive control at the predicted molecular weight of 40 kDa, suggesting there is no detectable expression of AdipoR1 in PCAs from either females or males (Figure 2.9 A). Similarly, numerous bands were obtained with the anti-AdipoR2 antibody (Figure 2.9 B). A band at the predicted molecular weight of 42 kDa lined up with a band at the same molecular weight in the rat liver positive control was taken to be AdipoR2. This band was expressed in PCAs from both sexes. However, there was no apparent difference in the expression of AdipoR2 in PCAs from females compared to males (Figure 2.9 B, C).

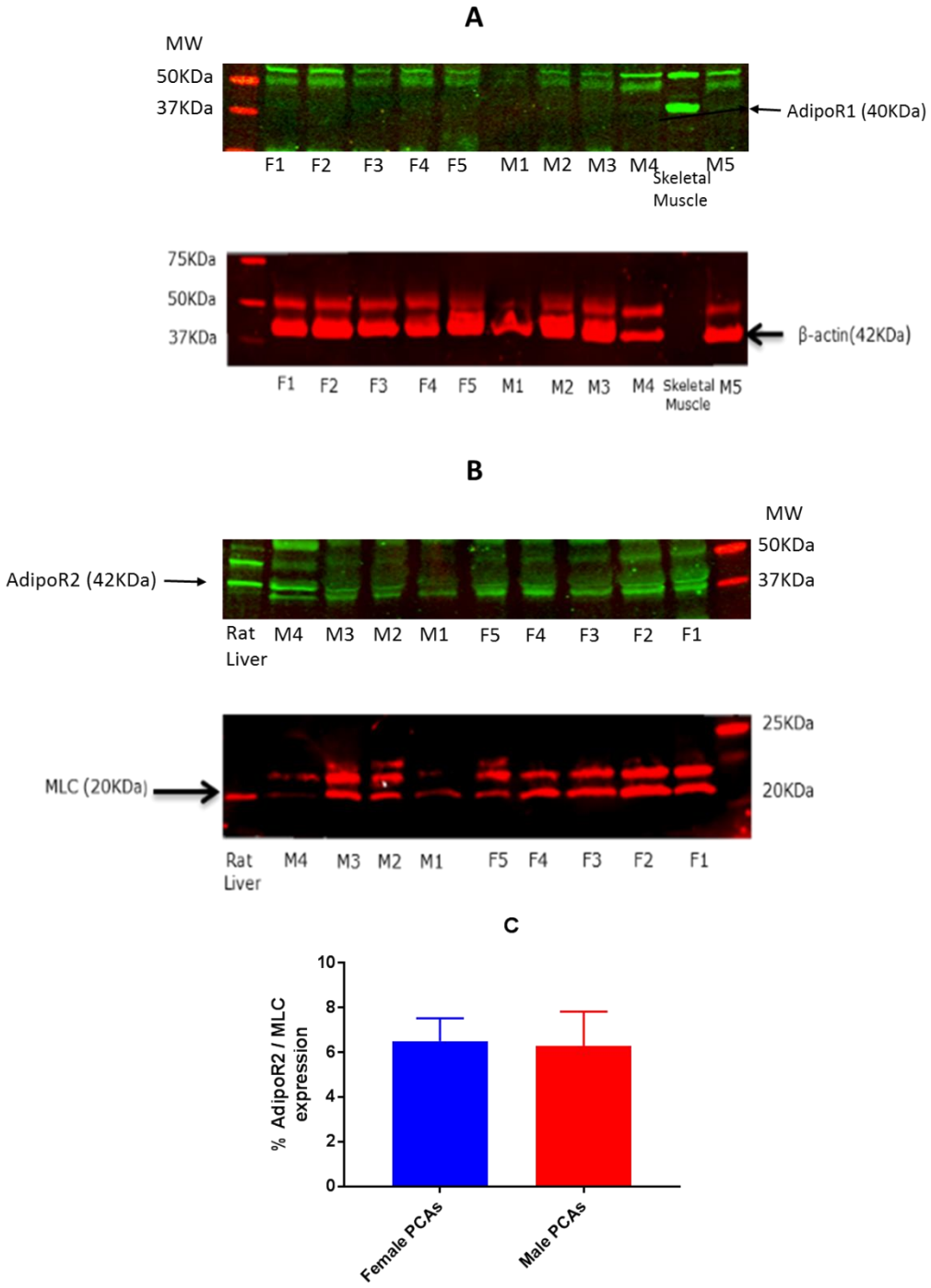


Figure 2.9: (A) Expression of AdipoR1 (40 kDa) and β-actin (42 kDa) levels in 20 µg of PCA from female (F1-F6) and male (M1-M5) pigs. Porcine skeletal muscle is used as a positive control. **(B)** Expression of AdipoR2 (42 kDa) and myosin light chain (MLC) (20 kDa) levels in 20 µg of PCA from female (F1-F5) and male (M1-M4) pigs. Rat liver was used as a positive control. **(C)** Bar chart showing density of AdipoR2 band normalised to MLC levels, in PCA from female and male animals. Data are expressed as mean ± SEM.

2.3.9 Expression of APPL1 in PCAs

As there was no difference in the expression of adiponectin receptors between females and males PCAs, the expression of the adiponectin binding protein APPL1 in PCAs was then investigated by immunoblotting. A band for APPL1 was detected at the predicted molecular weight of 82 kDa. However, there was no significant difference in APPL1 expression between PCAs from both sexes (Figure 2.10 A,B).

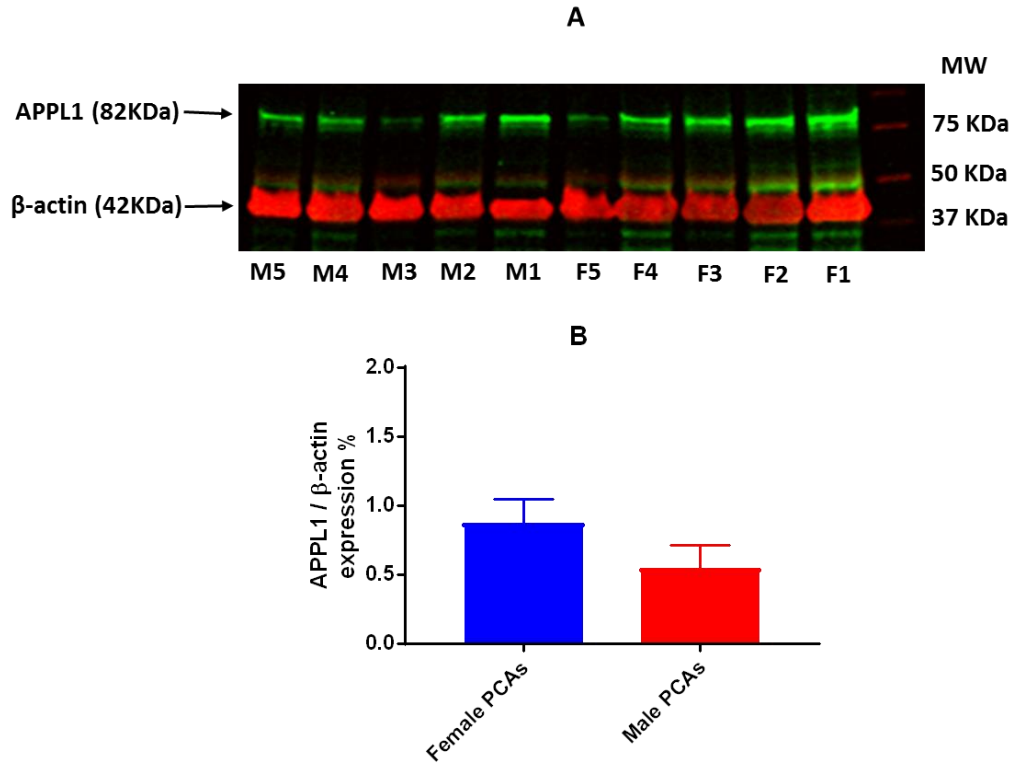


Figure 2.10: (A) Expression of adiponectin binding protein APPL1 (82 kDa) and β-actin (42 kDa) levels in 20 µg of PCA from female (F1-F5) and male (M1-M5) pigs. **(B)** Bar chart showing density of APPL1 band normalised to β-actin levels, in PCA from female and male animals. Data are expressed as mean ± SEM.

2.3.10 Functional effects of H_2S synthesizing enzymes on the relaxant response to PVAT in female PCAs.

Previous studies have indicated that PVAT can release H_2S to produce a vasorelaxation. Therefore, the effects of PVAT on coronary rings after cumulative contraction with U46619 were evaluated in the presence of 4-

propargylglycine (PPG) (10 µM) and 2-(aminooxy)-acetic acid (AOAA) (100 µM) as inhibitors of CSE and CBS, respectively. As shown in Figure 2.11, PPG and AOAA had no effect on the inhibition of U46619-induced contraction in fat-attached vessels.

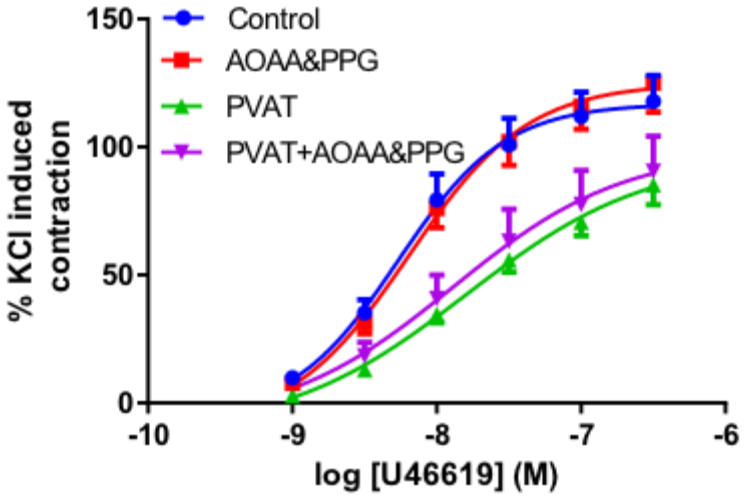


Figure 2.11: Log concentration-response curves for the vasoconstrictor effects of U46619 in the absence or presence of PVAT in female PCAs with and without pre-incubation with 4-propargylglycine (PPG) (10 µM, 1hr) and 2-(aminooxy)-acetic acid (AOAA) (100 µM, 1hr). Data are expressed as a percentage change from 60 mM KCl and are mean ± S.E.M. of 6 experiments.

2.3.11 Functional effects of PVAT-derived H_2S on responses to 5HT in female PCAs.

Previous studies have demonstrated that H_2S released from PVAT inhibited the contraction to 5-HT (Kohn *et al.*, 2012). Therefore, in order to test whether inhibition of H_2S synthesis prevents the reduction in contraction to 5-HT in the coronary artery, tissues were pre-treated with (PPG) (10 µM) and (AOAA) (100 µM) prior to addition of a single concentration of 5-HT (10 µM). AOAA and PPG inhibited the contraction to 5-HT regardless of the presence of PVAT (Figure 2.12).

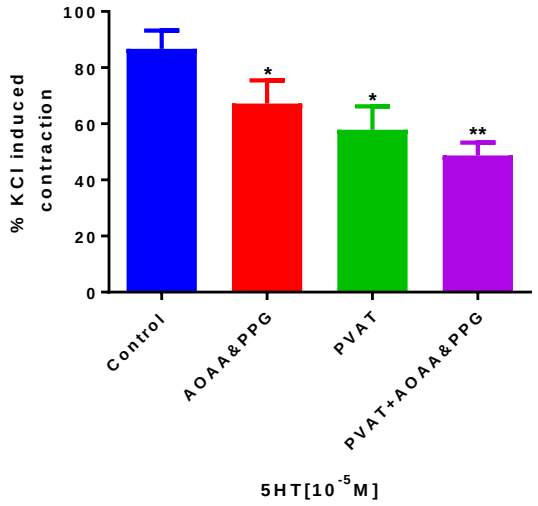


Figure 2.12: Effects of pre-incubation with 4-propargylglycine (PPG) (10 µM, 1hr) and 2-(aminooxy)-acetic acid (AOAA) (100 µM, 1hr) with and without PVAT on response to 5HT (10 µM) in female PCAs based on the percentage change from 60 mM KCl response and expressed as mean ± S.E.M. of 9 experiments, * indicates P<0.05, ** indicates P<0.01, one-way ANOVA followed by a Sidak's *post hoc* test vs control values.

2.3.12 Identification of CSE, CBS and 3-MPST expression in porcine PVAT

Although there is no functional role of H_2S in the PVAT response, expression of H_2S synthesizing enzymes was determined by immunoblotting in both female and male PVAT. Both CBS and 3-MPST were expressed in PVAT from both sexes (Figure 2.13 A, 2.14 A). Conversely, CSE expression was not identified in PVAT. Furthermore, there was no significant variation in the ratio of the enzyme band intensities to their respective loading control between PVAT from males and females (for CBS:β-actin, 1.8 ± 0.3, females and 3.16 ± 1.0, males (Figure 2.13 B); for 3-MPST: β-actin, 1.4 ± 0.17, females and 2.4 ± 0.6, males (Figure 2.14 B)). For CSE, no bands were observed at 45 KDa (Figure 2.15).

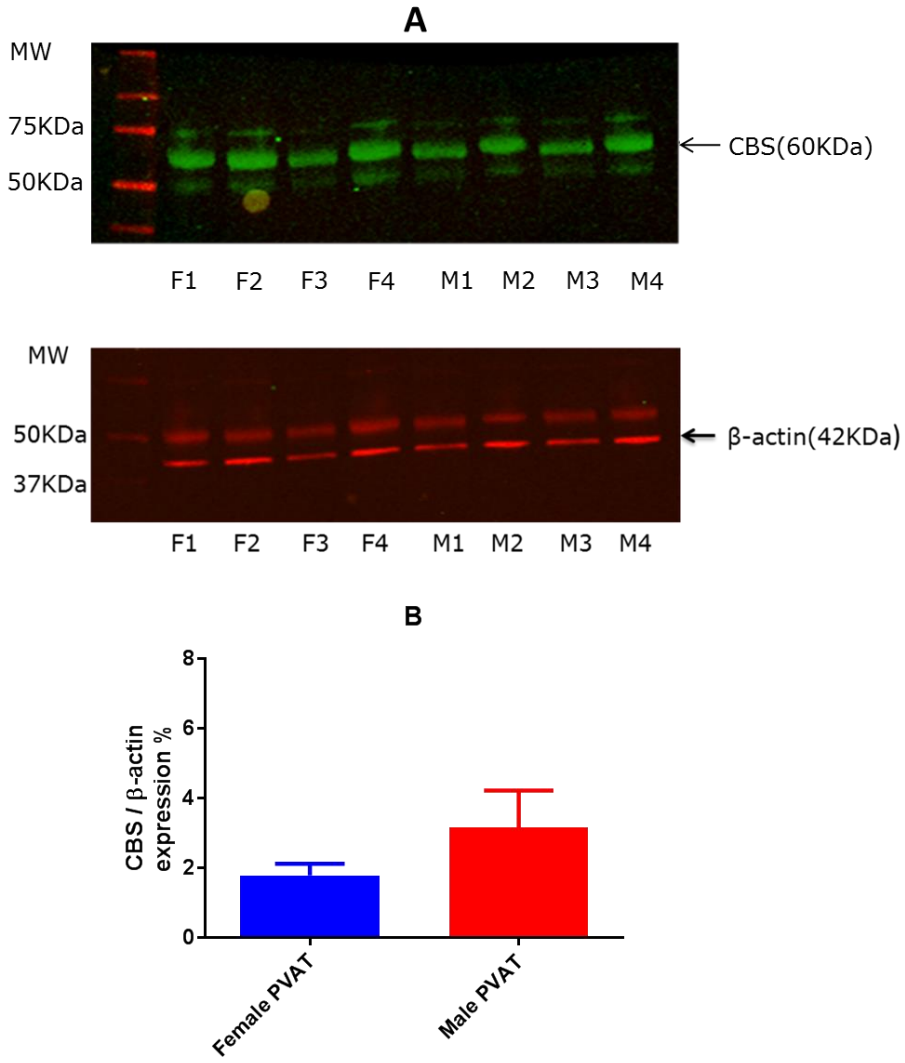


Figure 2.13: Representative immunoblot showing expression of CBS (61 kDa) and β-actin (42 kDa) levels in 10 µg of female (F1-4) and male PVAT (M1-4) **(A)**. Percentage of the expression levels of CBS to β-actin in male and female PVAT based on the intensities of their bands **(B)**. Data are expressed as mean ± SEM, n=8.

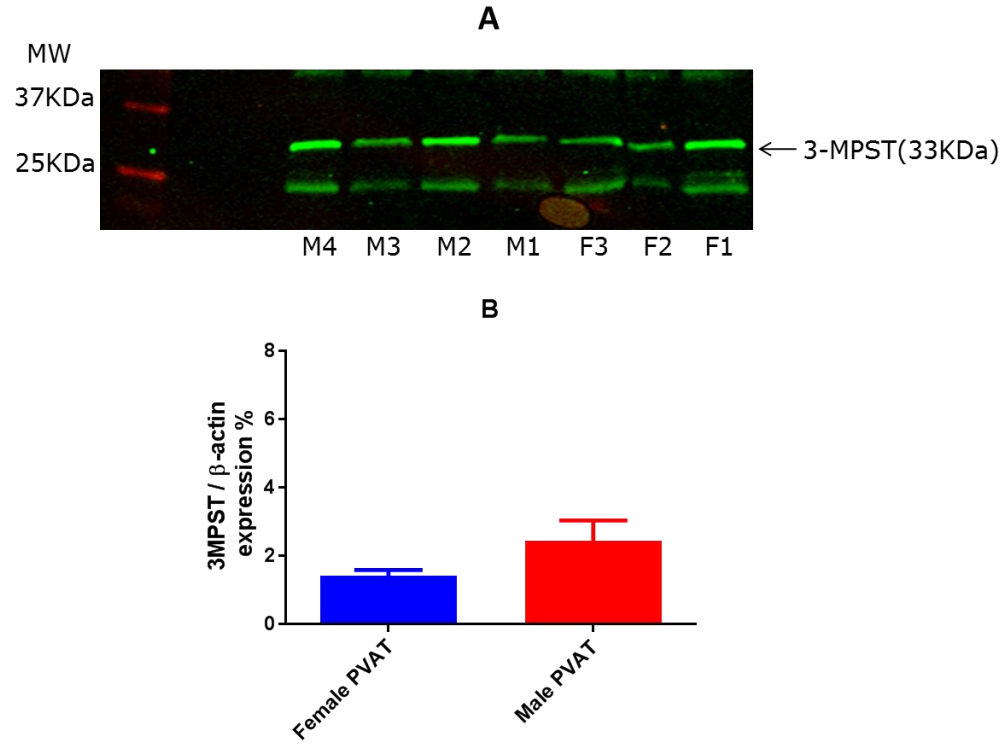


Figure 2.14: Representative immunoblot showing expression of 3-MPST (33 kDa) levels in 20 µg of female (F1-F4)) and male PVAT (M1-M4) **(A)**. Percentage of the expression levels of 3-MPST to β-actin in male and female PVAT based on the intensities of their bands **(B)**. Data are expressed as mean ± SEM, n=8.

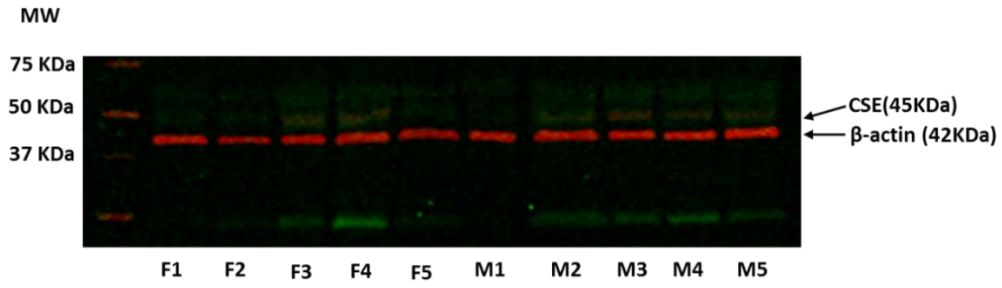


Figure 2.15: Representative immunoblot showing expression of CSE (45 kDa) and β-actin (42 kDa) levels in 20 µg of female (F1-F5) and male PVAT (M1-M5).

2.3.13 Identification of CBS and 3-MPST activity in porcine PVAT

As both CBS and CSE are expressed in porcine PVAT, the activity of these H_2S synthesizing enzymes was measured using SF7 fluorescence assay. The SF7 assay showed an activity for CBS enzyme, which was inhibited by AOAA, and 3-MPST enzyme in PVAT from both females and males. However, the activities of these enzymes in PVAT were much lower than the activities of the enzymes in rat liver (Figure 2.16).

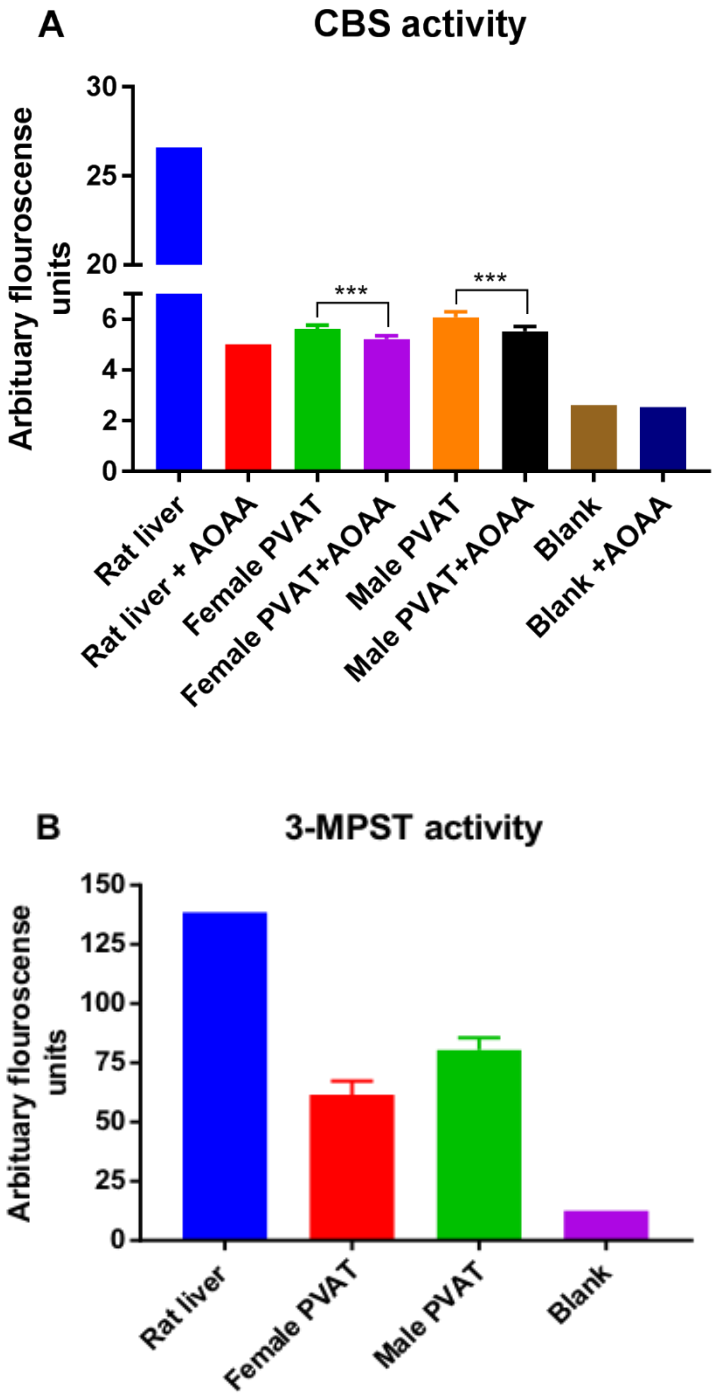


Figure 2.16: (A) Bar charts showing measurement of CBS activity in PVAT homogenates using the SF7 assay in the absence or presence of 100μM AOAA in PVAT from female or male pigs. **(B)** Bar charts showing measurement of 3-MPST activity in PVAT homogenates using SF7 assay in PVAT from females or male pigs. Data are expressed as arbitrary fluorescence units and are mean ± S.E.M. of 5 experiments. *** indicates P<0.001, one-way ANOVA followed by a Sidak's *post hoc* test vs control values.

2.4 Discussion

The recognition that perivascular adipose tissue is not simply a reservoir for lipid storage, but is also a complex endocrine organ has led to substantial research efforts to establish the mechanistic links between the PVAT and vascular tone regulation. The majority of research in this area has been carried out on blood vessels from male animals and has concentrated mostly on the murine aorta and mesenteric vessels. A few studies have determined the role of PVAT in the regulation of coronary arterial tone, but this is the first study to compare the effects of PVAT from male and female animals. Clear sex differences have been identified in the regulation of coronary artery tone by PVAT, with PVAT from female animals producing an anti-contractile, relaxant response, which was not seen in PVAT from male animals.

Localization of uncoupling protein-1 (UCP1) in PVAT has been investigated by immunohistochemical staining. Several studies have clarified different histological features of the coronary PVAT (Chatterjee *et al.*, 2009; Sacks *et al.*, 2009; Frontini and Cinti, 2010). The histological analysis has showed low expression of UCP1 in the PVAT, suggesting a mixed, white and brown, nature of porcine coronary PVAT in comparison with white (epididymal) and brown (interscapular) adipose tissue (Figure 2.3). In addition, there are no sex differences in the histological appearance of PVAT. These findings are confirmed quantitatively by Westen blotting. However, the band of the positive control (from rat) does not align exactly with the PVAT bands (from pigs) which can be explained by the species difference (Figure 2.4). Noteworthy, to overcome this issue, porcine interscapular and epididymal adipose tissue should be used, which was not available, or the rodent positive control should be used along with rodent coronary PVAT. However, this latter solution is not possible

because there is no PVAT around the rodent coronary arteries. To the best of our knowledge, this is the first report showing the exact histological character of porcine coronary PVAT from different sexes.

In the presence of fat, contractile responses to both the thromboxane receptor agonist (U46619) and ET-1 were reduced in coronary arteries from female pigs, but not from male pigs, indicating the release of an anti-contractile compound from the PVAT surrounding the coronary arteries in females (Figure 2.1). Re-addition of fat removed from the coronary arteries into the tissue baths produced a relaxant response in arteries from females, but not males. In order to confirm this finding, a crossover study was performed in which PVAT from females was added to male arteries. Although PVAT from females induced a relaxation in coronary arteries from females, the PVAT from females did not produce a relaxation in coronary arteries from males (Figure 2.2). Taken together, these data suggest that the PVAT surrounding coronary arteries from female animals may release a compound that has a protective, anti-contractile role, which may contribute to the reduced incidence of coronary artery disease in females.

The present results are consistent with the studies by Gao *et al.*, (2007) and Malinowski *et al.*, (2008) which have shown that PVAT reduces vascular tone in the rat aorta and human internal thoracic arteries, respectively, although sex differences in these responses were not determined (Gao *et al.*, 2007; Malinowski *et al.*, 2008). In contrast, previous studies in porcine coronary artery have indicated the release of a contractile agent from PVAT, although again sex differences in the responses were not examined (Owen *et al.*, 2013).

In mouse mesenteric arteries, the anti-contractile effects of PVAT are mediated through either NO or COX-dependent pathways (Lynch *et al.*, 2013). Similarly, this study has demonstrated that the anti-contractile effect of PVAT in coronary arteries from female pigs was sensitive to inhibition with a combination of the nitric oxide synthase inhibitor L-NAME and the cyclooxygenase inhibitor indomethacin, whereas inhibition of each enzyme separately had no significant effect (Figure 2.5). These data indicate the involvement of both NO and COX metabolites in the PVAT response. Dual

inhibition is probably necessary because of compensatory activation of the other pathway. In general, this observation is in line with a previous study on aorta from Wistar rats which found that PVAT exerted its anti-contractile effects by secreting a relaxant factor which mediates endothelium-dependent vasorelaxation through NO release (Gao *et al.*, 2007). On the other hand, these findings differ from a previous study by Malinowski *et al.*, (2008) which demonstrated that blocking NOS and COX could not restore the vascular response in intact rings of the human internal thoracic artery (Malinowski *et al.*, 2008). In fact, these differences may reflect changes in vascular responses in cardiovascular disease as the human vessels used were from patients with severe coronary artery disease. In addition, the inconsistency of findings for the role of NO and COX in all previous studies could probably be due to the undefined sex used.

In order to identify the mechanism underlying the sex difference in the anti-contractile effects of PVAT in the porcine coronary artery, the role of adiponectin was investigated. Adiponectin is the most abundant adipokine in the circulation and has been shown to activate both NO and COX-dependent pathways (Tan *et al.*, 2004; Shibata *et al.*, 2005; Lee *et al.*, 2010). As there is no selective adiponectin receptor antagonist available, an anti-adiponectin antibody was used to bind any adiponectin released from the PVAT and prevent it from activating the receptor on the artery. To this end, the effects of the antibody on the relaxation due to addition of PVAT, rather than using fat-attached arteries were determined. This is because the close proximity of the fat to the blood vessel in fat-attached preparations may not allow the antibody access to bind released adiponectin. Under these conditions, the presence of the anti-adiponectin antibody prevented the PVAT-induced relaxation, indicating that adiponectin is likely to be the mediator released from the fat (Figure 2.6). Although it is not used, pure IgG could be added as a control for optimal comparison. Therefore, whether the sex differences in the relaxation were due to differences in adiponectin expression, release or function were investigated. Using immunoblotting, the presence of adiponectin in PVAT from the coronary artery was identified, although there was no difference between males and females. Furthermore, there was no difference in the level of adiponectin

released from PVAT, indicating that the difference in the relaxant response is not due to a difference in either expression or release of adiponectin (Figure 2.7). On the other hand, using an adiponectin receptor agonist, adipoRon, it was found that activation of the adiponectin receptor produces a greater relaxation and that the agonist is more potent in coronary arteries from females compared to males (Figure 2.8A). These data indicate that the sex difference in the anti-contractile effect of PVAT is likely to be due to a difference in the responsiveness of the arteries to adiponectin. Noteworthy, responses to adiponectin receptor activation are independent of the endothelium in that denudation of the endothelium did not alter the relaxation to adipoRon in the coronary artery (Figure 2.8B).

In an attempt to identify the reason for the differences in adiponectin responses, the expression of the adiponectin receptors in the coronary artery was determined. Using immunoblotting, expression of AdipoR2 receptors was identified but not AdipoR1 receptors in PCAs from both sexes (Figure 2.9). To the best of our knowledge, this is the first study to identify expression of adiponectin receptor in the coronary artery. However, there was no apparent difference in the expression of AdipoR2 between male and female PCAs.

Since no sex difference was identified in adiponectin receptors expression, the expression of APPL1 was investigated. APPL1 has been identified as an AdipoR1 and AdipoR2 binding protein (Buechler *et al.*, 2010) and considered as a downstream regulator of adiponectin signalling (Mao *et al.*, 2006; Cheng *et al.*, 2007). Although expression of this adaptor protein APPL1 in PCAs was identified, there was no significant difference between sexes (Figure 2.10). The limitation in the present investigation is that the expression of different proteins studied were examined in total homogenate rather than vascular smooth muscle only. In addition, total AdipoRs expression was measured rather than the expression of just surface receptors. As adiponectin receptors are distributed in the cytoplasm (Ding *et al.*, 2009) and on the cell membrane (Yamauchi *et al.*, 2003), differences in either cellular or subcellular distribution could underlie the sex differences. Further experiments are required to measure the level of expression of AdipoRs in the surface of vascular myocytes by, for instance, immunocytochemistry (ICC).

Sex differences were previously demonstrated in intracellular signaling pathways involved in vasorelaxation. In particular, there are sex differences in the relative contributions of the NO and endothelium derived hyperpolarization (EDH) signalling pathways in the porcine coronary artery, as well as differences in the mechanisms underlying the EDH-type responses (Wong *et al.*, 2015a; Wong *et al.*, 2015b). Therefore, differences in signalling may contribute to the sex differences in adiponectin relaxation seen in this study. In addition, malfunction and resistance to adiponectin have been identified in different conditions such as obesity (Bruce *et al.*, 2005; Chen *et al.*, 2005), animals fed a high fat diet (Mullen *et al.*, 2009) and cardiovascular diseases including atherosclerosis, endothelial dysfunction, and cardiac injury (Lau *et al.*, 2011). Therefore, the possibility of adiponectin resistance in the coronary arteries from males cannot be excluded.

Although there was reduced relaxation to AdipoRon in porcine coronary arteries from males, there was still a relaxation and not the complete absence of relaxation seen with the addition of PVAT. The lack of relaxation to PVAT in males could be because the amount of adiponectin released from PVAT is insufficient to induce a relaxation in males. Alternatively, other studies have indicated that several contractile factors are released from porcine coronary arterial PVAT (see Chapters 3,4,5,6). This may counteract the relaxant response to adiponectin in males.

A previous study has indicated that H_2S is released from PVAT to induce vasorelaxation in rat aorta (Wojcicka *et al.*, 2011). Immunoblot analysis has identified CBS and 3-MPST expression in PVAT from the PCA (Figure 2.13 and 2.14 respectively), while no CSE expression was recognized (Figure 2.15). However, there was no significant difference in the expression of CBS and 3-MPST in PVAT from male and female pigs. Noteworthy, Donovan *et al.*, (2017) have identified the expression of CSE in coronary arteries from pigs (Donovan *et al.*, 2017) whilst the same authors found no expression of CSE in PVAT (unpublished data) by using the same antibody that is used in this study. Of note, species differences are obviously present in the CSE expression in the vasculature. In rat aorta, CSE expression has been observed in PVAT and vascular smooth muscle but not in the endothelium (Fang *et al.*, 2009) while

CSE expression has been identified in the endothelium but not in VSM of mouse aorta (Yang *et al.*, 2008). In addition, Kohn *et al*., (2012) found that CSE is expressed in PVAT from mouse aorta, but less than PVAT from rat aorta (Kohn *et al.*, 2012). Although bands have been found in the predicted positions in the blots investigated in this study, nonspecific bands are also encountered which suggests further studying using more selective antibodies. Next, the activity of CBS and 3-MPST was investigated using SF7 fluorescence assay. The data have showed that PVAT from the PCA has the ability to produce H_2S, although there was low activity of these enzymes in porcine PVAT in comparison with a high level of activity of the same enzymes in rat liver (Figure 2.16). Inhibition of CSE and CBS did not affect the inhibition of the U46619-induced contraction in the presence of PVAT in PCAs from female pigs (Figure 2.11). In addition, using serotonin as another contractile agent has confirmed that there is no functional role of H_2S synthesizing enzymes in PVAT-induced vasorelaxation, at least in these conditions of experiments, since AOAA and PPG inhibited the contraction to 5-HT regardless of the presence of PVAT (Figure 2.12). The present findings are consistent with the study by Kohn *et al.*, (2012) which found that CSE and CBS inhibition in mouse aorta did not influence the ADRF effect, which is in contrast to their findings on rat aorta (Kohn *et al.*, 2012), indicating species differences.

In summary, the present study illustrates that there are clear sex differences in PVAT function, where PVAT exhibits anti-contractile responses in PCAs from female pigs, but not male pigs, which appears to be due to increased adiponectin activity. The sex difference in the PVAT response is not explained by a difference in the expression or release of adiponectin, but may be explained by a greater sensitivity of coronary arteries from females to adiponectin receptor activation. In contrast, H_2S has no obvious role in this effect despite the identified expression of its synthesizing enzymes (CBS and 3-MPST). This is the first study to demonstrate that PVAT may have a protective effect on coronary arteries in females, which is not present in males. This protective effect could contribute to the cardiovascular protective effects observed in females.

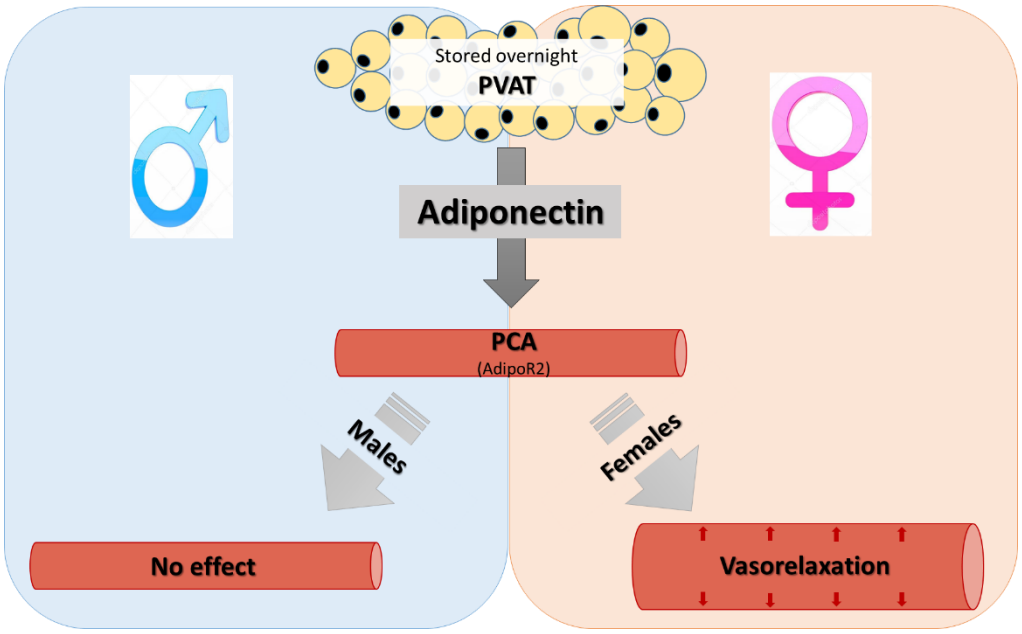


Figure 2.17 Hypothesized schematic diagram of sex differences in the contractile response of PCA to PVAT. Present study demonstrated clear sex differences in PVAT function where PVAT can mediate vasorelaxation in PCAs from females only with the PVAT-derived adiponectin as a bioactive signalling molecule that induces this vasorelaxant effect.

Chapter Three

Sex differences in the role of phospholipase A_2-dependent arachidonic acid pathway in the perivascular adipose tissue function

3.1 Introduction

Prostanoids are cyclooxygenase metabolites of arachidonic acid that exert diverse physiological and pathological effects in different systems, including relaxation and contraction of vascular smooth muscle (Wright *et al.*, 2001). According to their selectivity for the prostanoids, prostaglandins (PG) PGI_2, PGD_2, PGE_2, PGF_2 and thromboxane A_2 (TXA_2), there are five main types of prostanoids receptors IP, DP, EP, FP and TP, respectively. Of these receptors, TP, and FP have the ability to mediate vasoconstriction, IP and DP generally mediate vasorelaxation while depending on receptor subtype, EP has the ability to induce both contraction (EP_1 and EP_3) and relaxation (EP_2 and EP_4) (Coleman *et al.*, 1994). Prostanoids released from PVAT have been shown to regulate vascular tone. For example, PGE_2 and PGI_2 released from PVAT surrounding human saphenous vein attenuates noradrenaline-induced contraction (Ozen *et al.*, 2013). Similarly, prostacyclin released from the mouse carotid artery PVAT exerts vasorelaxant effects and protects against endothelial dysfunction (Chang *et al.*, 2012a). In contrast, another study showed that aortic PVAT from mice releases cyclooxygenase (COX)-derived adipocyte derived contracting factor (ADCF) that becomes functionally of greater activity in obesity (Meyer *et al.*, 2013).

Extensive epidemiological data have revealed the existence of a prominent sexual dimorphism in the incidences of primary vascular diseases that involve excessive vasoconstriction. Thus, among the strongest risk factors for coronary artery disease is male sex and a male to female ratio of approximately 2:1 is consistently observed (Nettleship *et al.*, 2009). In contrast, migraine headache (Bartelink *et al.*, 1993) and Raynaud's Disease (Voulgari *et al.*, 2000) all occur in premenopausal women at rates as much as fourfold higher than in men. Furthermore, a previous study has found that oestrogen could upregulate the expression of COX-2 and thromboxane synthase in both endothelium and vascular smooth muscle, and upregulate the expression of TP receptors in smooth muscle of female rat aorta, leading to enhanced vasoconstrictor prostanoid function (Li *et al.*, 2008). However, to date, no study has determined whether there are sex differences in the regulation of vascular tone by PVAT-derived prostanoids.

In the porcine coronary artery, PVAT induces a contraction and enhances agonist and electrical field-stimulated contractile responses (Owen *et al.*, 2013). However, the contractile agents involved in these responses are unknown. PVAT is a potential therapeutic target for controlling coronary artery tone. Therefore, in this present study, the role of cyclooxygenase-derived vasoconstrictor prostanoids in PVAT-induced vasoconstriction was investigated and whether there are sex differences in the response of the coronary artery to PVAT was determined.

3.2 Materials and Methods

3.2.1 Tissue preparation

Tissues were set up as previously described in Chapter 2.2.1. However, in this chapter, fine dissection of PVAT was performed directly upon arrival from abattoir and 0.3 g of this 'fresh' PVAT was used in the experiments.

3.2.2 Characterization of vascular effects of the porcine isolated coronary artery

As previously described in Chapter 2, tissues were initially pre-tensioned to 8 g and then left to equilibrate for approximately 30-45 minutes. Once a stable baseline was attained, two consecutive responses to 60 mM KCl were obtained for standardization. Relevant test compounds were then added with 60 minutes incubation time. The following test compounds were used: melittin (10 µM) to stimulate phospholipase A_2 (PLA_2) activity (Koumanov *et al.*, 2003); indomethacin (10 µM) (Malinowski *et al.*, 2008) and flurbiprofen (10 µM) (Stanley and O'Sullivan, 2014) to determine the role of cyclooxygenase. To study the role of specific prostanoids, GR32191B (3 µM) (He and Yang, 1999) and AL8810 (10 µM) (Ramos-Alves *et al.*, 2012) were used as antagonists of TP and FP receptors, respectively. Rho kinase inhibitor (Y27632) (0.1-3 µM) (Zhu *et al.*, 2011) was used for further determine the actions of TXA_2 in both sexes. To study the role of extracellular Ca^{+2} in the contractile response to TXA_2, cumulative response curves of U46619 have been constructed in both Ca^{+2} free and Ca^{+2} containing Krebs' Henseleit solution. Ethanol or DMSO (0.1% v/v) were used as vehicle controls, as appropriate. After incubation of the coronary arterial segments with test compounds, PVAT was added to the organ baths and contractile responses measured. In some tissues, the endothelial layer was removed by rubbing the lumen using the same protocol described in (section 2.2.2).

In a separate series of experiments, cumulative concentration-response curves to U46619 (1 nM-300 nM) or $PGF_{2\alpha}$ (0.1-100 µM) were constructed in coronary artery segments from male and female pigs.

3.2.3 Determination of levels of TXB_2 and $PGF_{2\alpha}$ by ELISA.

Levels of TXB_2, a stable metabolite of TXA_2, and $PGF_{2\alpha}$ in PVAT were determined by ELISA. For TXB_2 estimation, PVAT was homogenised in (0.1M) potassium phosphate buffer (pH 7.4) and for $PGF_{2\alpha}$ estimation, PVAT was homogenised in Tris-buffered saline containing 0.1% (v/v) Tween 20, along with protease inhibitor cocktail (Calbiochem) (Appendix A) and indomethacin (10 µM). The amount of TXB_2 and $PGF_{2\alpha}$ in PVAT samples from male and female animals was analysed by ELISA (ab133022; ab133041, Abcam, Cambridge, UK), according to the instructions of the manufacturer. TXB_2 and $PGF_{2\alpha}$ were detected colourimetrically using an alkaline phosphatase (AP) conjugated-secondary antibody with para-Nitrophenylphosphate (pNpp) as substrate. Colour intensity produced was determined by reading at 405 nm using a SpectraMAX 340 PC microplate reader (Molecular Devices, 50 Wokingham, Berkshire, UK). The results were expressed as pg ml^{-1} μg^{-1} of total protein.

3.2.4 Assessment of the PVAT-released TXB_2 by ELISA.

Porcine coronary arterial PVAT from each sex was dissected, weighed and placed in an Eppendorf tube containing 1ml pre-gassed Krebs'-Henseleit solution, at 37^{o}C. For consistency with the functional studies, PVAT from both sexes was incubated for 2½ hr without and with melittin (10 µM). The level of TXB_2 in the Krebs'-Henseleit solution was then determined using ELISA (as described above) and the data normalized for weight of PVAT.

3.2.5 Estimation of TP and FP receptor expression in coronary arteries by immunoblotting.

Immunoblotting was performed to determine the expression of TP and FP receptors in segments of coronary arteries from female and male pigs. Arteries were finely dissected from the adherent PVAT and connective tissue and homogenized on ice using Tris buffer (pH 7.4) with protease inhibitor cocktail (Calbiochem, VWR International Ltd, Lutterworth, Leicestershire, UK) (Appendix A). After estimation of the protein content of each sample using the Lowry method (Lowry *et al.*, 1951), 6x Laemmli sample buffer (Appendix A)

was added to the samples. Samples were subsequently boiled at 100°C for 5 min and centrifuged at 13000×g for 1 min. Protein samples (20 µg) were run on 4–20% gradient polyacrylamide gradient gels (Bio-Rad, Hemel Hempstead, Hertfordshire, UK). Proteins were then transferred onto nitrocellulose membrane (GE Healthcare, Little Chalfont, Buckinghamshire, UK) by immunoblotting, and then the membrane blocked with 5% (w/v) non-fat milk in Tris-buffered saline containing 0.1% Tween 20 (TBST) (Appendix A) at room temp for 1 h. The blot was then incubated with either rabbit anti-TXA_2 receptor antibody (1:250 dilution; ab188897, Abcam, Cambridge, UK) or rabbit anti-$PGF_{2\alpha}$ receptor antibody (1:250 dilution; orb185891, Biorbyt, Cambridge, UK) in 5% milk in TBST overnight at 4°C with shaking. An anti-mouse myosin light chain (MLC) antibody was also included as a loading control (1:1000 dilution; M4401, Sigma-Aldrich, Poole, Dorset, UK). The following day, the blot was washed in TBST followed by incubation for 1 hour with IRDye 800CW goat anti rabbit (1:10,000) and IRDye 680CW goat anti-mouse (1:10,000) secondary antibodies (IRDye, Licor, Cambridge, UK). Immunoblot was then visualized using an Odyssey system from Licor.

3.2.6 Statistical analysis

Data are presented and were analysed as described in Chapter 2.

3.2.7 Materials

All drugs were purchased from Sigma-Aldrich except for AL8810 from Santa Cruz Biotechnology and $PGF_{2\alpha}$ from Cayman Chemicals. Stock solutions of flurbiprofen, $PGF_{2\alpha}$ and GR32191B were dissolved in dimethyl sulfoxide (DMSO). Stock solution of indomethacin and AL8810 were dissolved in absolute ethanol whereas melittin and Y27632 were dissolved in distilled water. Stock solutions of U46619 were made to 10 mM in ethanol. All further dilutions of the stock solutions were made using distilled water.

3.3 Results

3.3.1 Effects of addition of PVAT on vascular tone of female and male PCAs.

In order to investigate the effect of fresh PVAT on vascular contraction, PVAT was added to PCAs from both sexes. Addition of PVAT caused a time-dependent increase in tone compared to time controls in coronary arterial segments from both female and male PCAs (Figure 3.1). To investigate the role of endothelium in the contractile response of coronary arteries to PVAT, PVAT added to both intact and endothelium-denuded arterial segments. Responses to PVAT were independent of the endothelium because denudation of the endothelium did not alter the contraction to PVAT in the coronary artery (Figure 3.1 C).

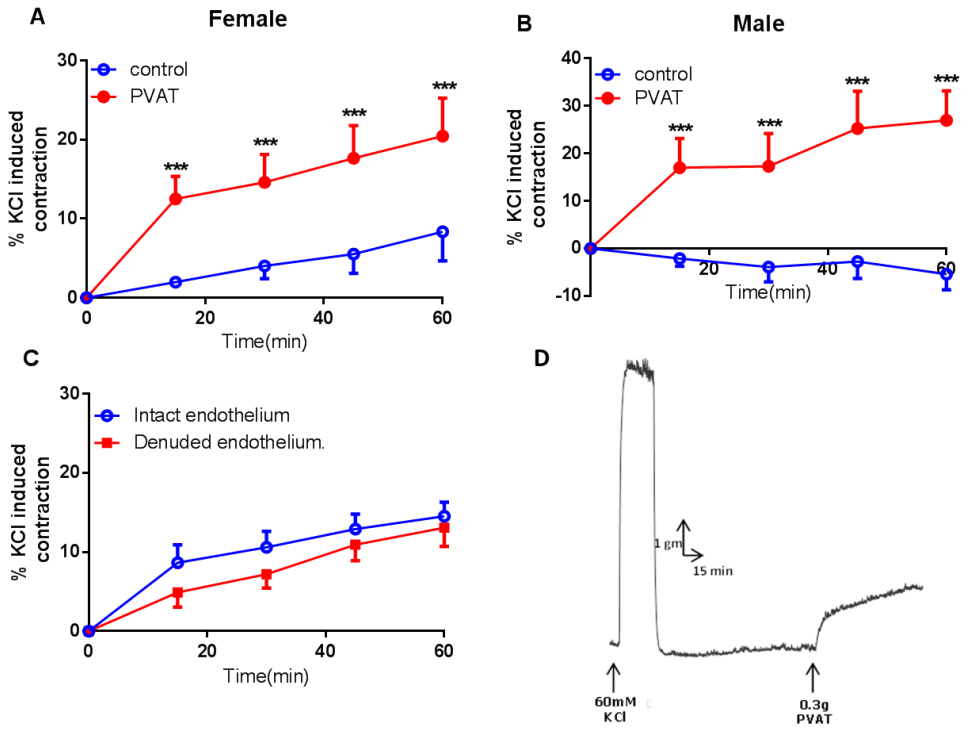


Figure 3.1: Increases in vascular tone following addition of fresh PVAT (0.3g) in female **(A)** and male **(B)** PCAs. Effects of endothelial denudation on the PVAT-induced vasoconstriction in PCAs from both females and males **(C)**. Data are expressed as a percentage change from 60 mM KCl and are mean ± SEM of arteries from 7(A), 4(B), 5(C) different animals. Original trace of recording showing the response of female PCA to addition of PVAT **(D)**. ***$P < 0.001$, two-way ANOVA followed by a Sidak's *post hoc* test vs control values.

3.3.2 Role of prostanoids in PVAT-induced contraction

Coronary arteries were pre-treated with and without cyclooxygenase inhibitors before addition of PVAT to investigate the role of contractile prostanoids in the PVAT contractile response. The COX inhibitors indomethacin and flurbiprofen (both 10 µM) caused significant inhibition of the contraction to PVAT compared to control in both sexes (Figure 3.2). The thromboxane receptor antagonist GR32191B (3 µM) caused a partial reduction in the PVAT-induced contraction in coronary arteries from female animals (Figure 3.3A), whereas the responses of coronary arteries from male animals to PVAT were unaffected by the TP receptor antagonist, GR32191B (Figure 3.3B). As GR32191B had no effect on the PVAT-induced contraction in males, the effect of a FP receptor antagonist was examined. In contrast to the effects of TP receptor antagonism, the FP receptor antagonist AL8810 had no effect on the PVAT-induced contraction in coronary arteries from female animals, but reduced the contraction in coronary arteries from male animals (Figure 3.3 C , D).

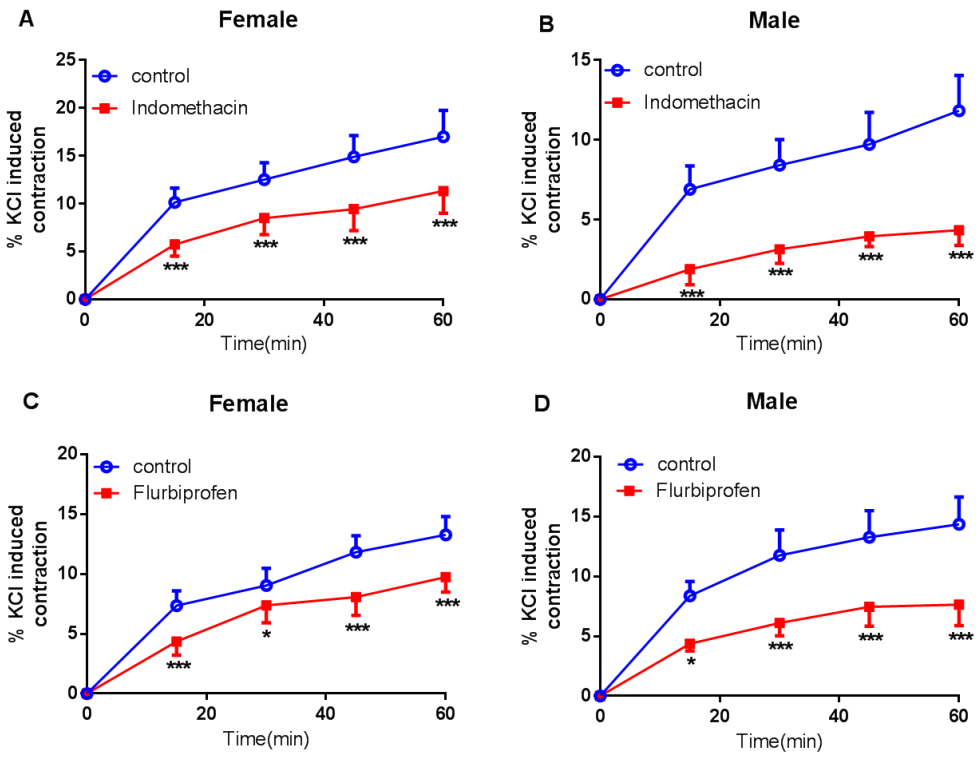


Figure 3.2: Contractile responses of the PCAs to fresh PVAT (0.3g) in the absence (control) or presence of indomethacin (10 µM) (**A & B**) or flurbiprofen (10 µM) (**C & D**). Data are expressed as a percentage of the contraction to 60 mM KCl and are mean ± SEM from arteries from 15 female (A & C) and 8 male (B & D) animals . * indicates $P < 0.05$, *** indicates $P < 0.001$, two-way ANOVA followed by a Sidak's *post hoc* test vs control values.

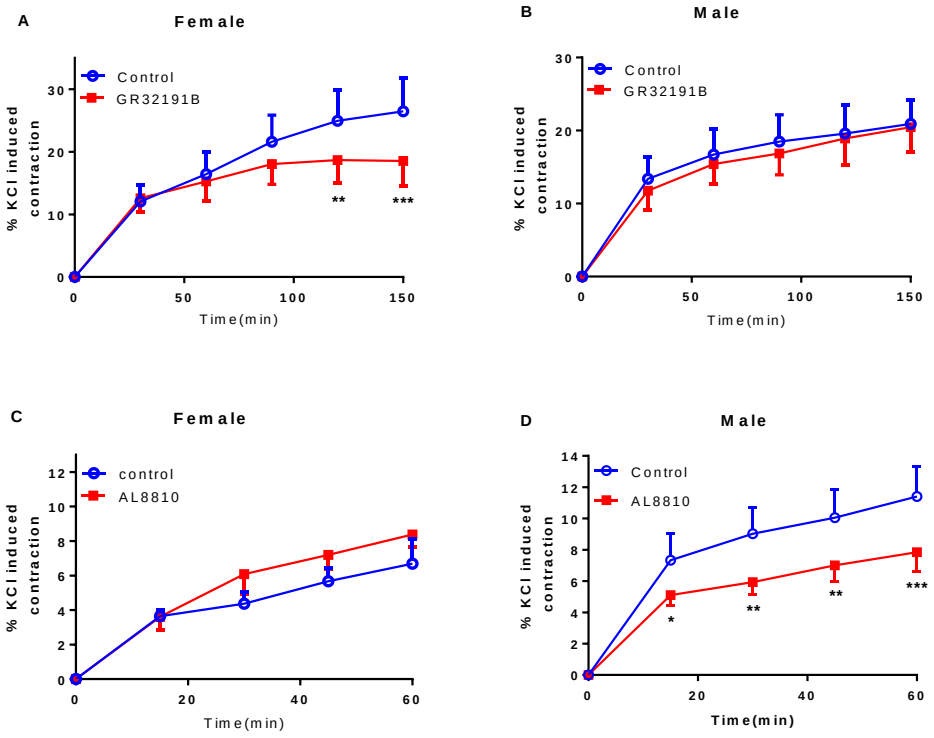


Figure 3.3: Effects of pre-incubation with GR32191B (3 µM) on the responses of porcine coronary arteries to PVAT (0.3 g) in female (**A**) and male (**B**) pigs. Effects of pre-incubation with AL8810 (10 µM) on PVAT-induced vasoconstriction in female (**C**) and male (**D**) pigs. Data are expressed as a percentage of the contraction to 60 mM KCl and are mean ± S.E.M. of arteries from 5-6 female (A & C) and 6-7 male (B & D) animals. * indicates P<0.05, ** indicates P<0.01 and *** indicates P<0.001, two-way ANOVA followed by a Sidak's *post hoc* test vs control values.

3.3.3 Determination of the level of TXB_2 and $PGF_{2\alpha}$ in PVAT by ELISA

In order to determine whether the differences in the role of TP and FP receptors in arteries from male and female animals could be due to differences in the content of thromboxane and $PGF_{2\alpha}$ in the PVAT, levels of the stable thromboxane metabolite TXB_2, and $PGF_{2\alpha}$ in PVAT were determined by ELISA. Although both prostanoids are expressed in PVAT homogenates compared to blank (no tissue), there was no significant difference in the level of TXB_2 or $PGF_{2\alpha}$ in coronary artery PVAT from female and male animals (Figure 3.4).

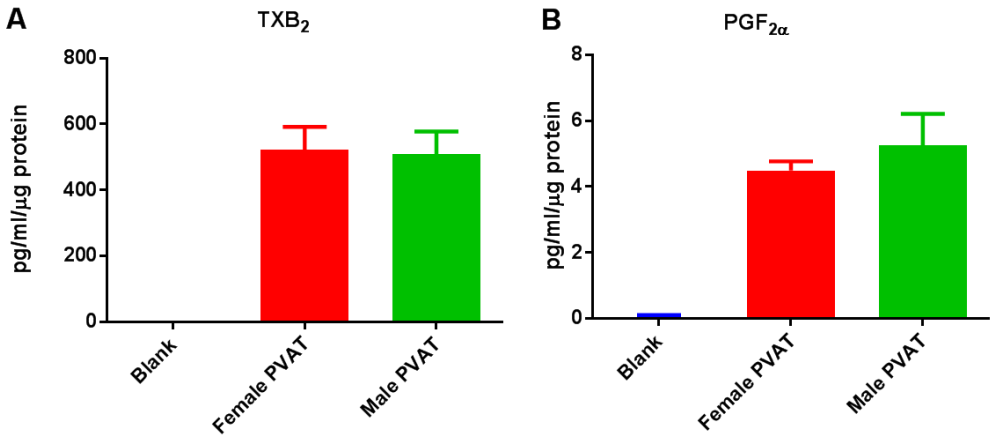


Figure 3.4: Comparison of the levels of the TXB_2 and $PGF_{2\alpha}$ between PVAT from female and male pigs. Data are expressed as pg per ml per µg protein concentration and are mean ± S.E.M. of PVAT from 5(A) - 7(B) female and 5(A) – 8(B) male animals.

3.3.4 Assessment of the responsiveness of PCAs to TXA_2 and $PGF_{2\alpha}$

As the data indicate differences in the role of TP and FP receptors in the PVAT-induced contractions in coronary arteries from male and female animals, which cannot be explained by differences in the content of thromboxane and $PGF_{2\alpha}$ in the fat, it was determined whether there are differences in the contractions in response to TP or FP receptor activation, in the absence of PVAT. There were no differences in the response of PCAs to the TXA_2 mimetic U46619 between female and male pigs (females: R_{max} =84 ± 4.3%, pEC_{50}=7.9 ± 0.1; males: R_{max} = 92.4 ± 10.1%, pEC_{50}=7.7 ± 0.1) (Figure 3.5A). On the other hand, contractile responses to $PGF_{2\alpha}$ (0.1-100 µM) were significantly greater in arteries from male (pEC_{50}=5.43 ± 0.08) compared to female animals (pEC_{50}=5.29 ± 0.1) (Figure. 3.6A).

3.3.5 Determination of the level of TP and FP receptor expression in PCAs

As there were no differences in the levels of TXB_2 or $PGF_{2\alpha}$ in PVAT from male and female animals, it was determined whether there were differences in the expression of the receptors on the coronary artery, which might explain the differences in the role of these prostanoids. Immunoblotting for the TP receptor identified a band at the predicted molecular weight of 40 kDa. When expressed as a ratio to myosin light chains, used as a loading control, there was no difference in the level of expression of TP receptor between coronary arteries

from male and female animals (Figure 3.5 B, C). Immunoblotting also detected a band at 50 kDa for the FP receptor. In this case, there was a significantly higher level of expression of the FP receptor in coronary arteries from male animals compared to female animals (Figure 3.6 B, C).

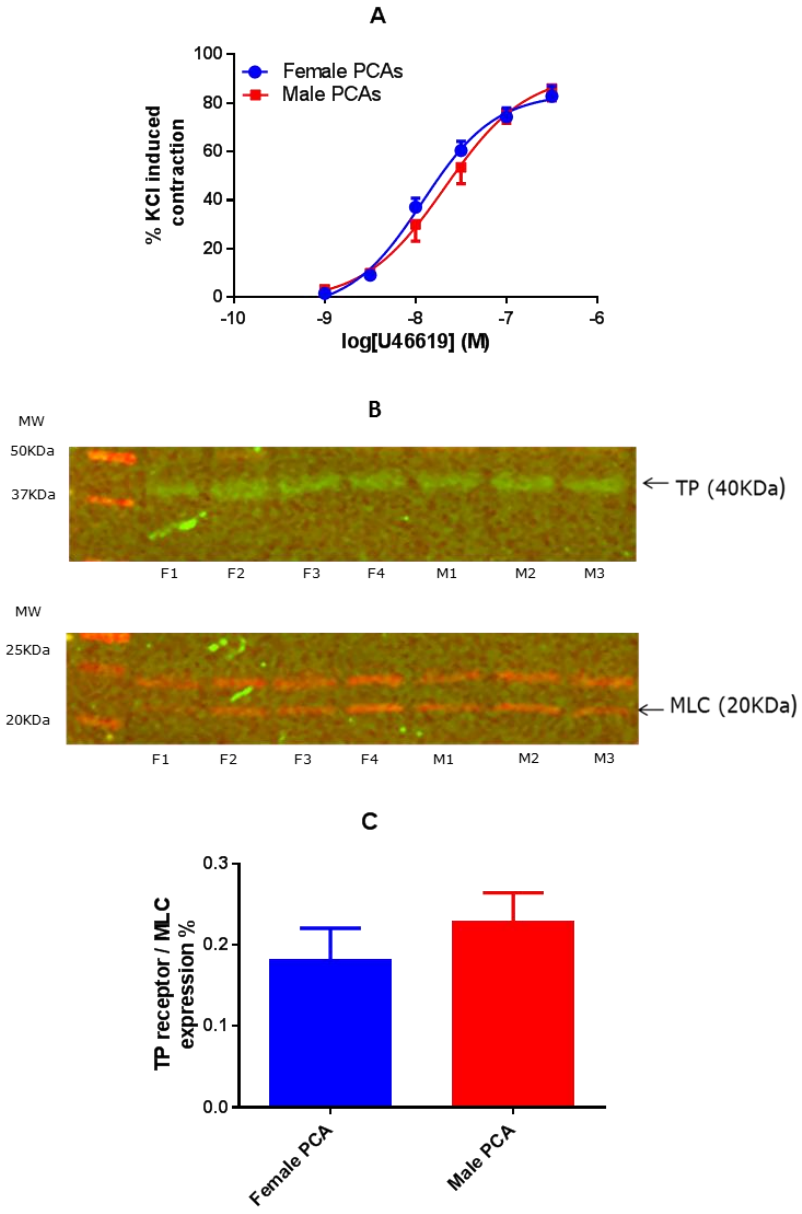


Figure 3.5: Comparison of the responsiveness of PCAs to TXA_2 and the expression of TP receptor in PCAs from both sexes **(A)** Log concentration-response curves to the thromboxane receptor agonist U46619 in female and male porcine coronary artery segments. Data are expressed as a percentage of the response to 60 mM KCl and are mean ± S.E.M. of 12 female and 9 male arteries. **(B)** Representative immunoblot showing expression of TP receptor (40 kDa) and

MLC (20 kDa) levels in 20 µg of female (F1-F4) and male (M1-M3) PCAs. **(C)** Percentage of the expression levels of TP receptor to MLC in male and female PCAs based on the intensities of their bands (6 female and 8 male PCAs).

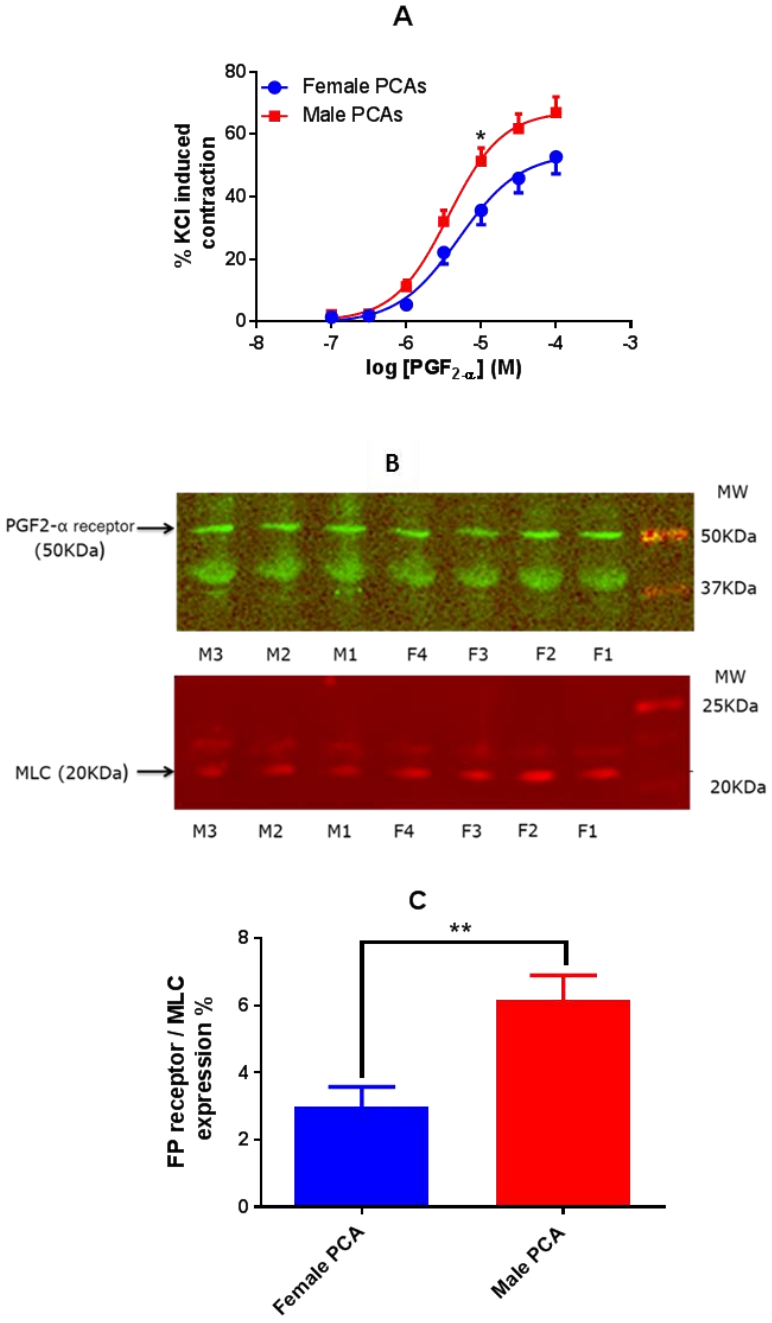


Figure 3.6: Comparison of the responsiveness of PCAs to $PGF_{2\alpha}$ and the expression of FP receptors in PCAs from both sexes. **(A)** Contractile response to serial concentrations of $PGF_{2\alpha}$ (0.1-100 µM). Data are expressed as a percentage of the response to 60 mM KCl and are means ± SEM of 10 Female and 7 male coronary arteries. Data are expressed as mean ± SEM, * indicates $P<0.05$, **

indicates P<0.01, two-tailed, unpaired Student's *t*-test. **(B)** Representative immunoblots showing the expression of FP receptor (50 kDa) and MLC (20 kDa) levels in 20 µg of female (F1-F4) and male (M1-M3). **(C)** Percentage of the expression levels of $PGF_{2\alpha}$ receptor to MLC in male and female PCAs based on the intensities of their bands (7 female and 8 male PCAs).

3.3.6 Role of extracellular Ca^{2+} in TXA_2 action

For further clarification of the mechanism of action of TXA_2, role of extracellular Ca^{+2} was identified in PCAs from both sexes. U46619-induced contractions were inhibited by pre-incubation of PCAs in Ca^{2+}-free Krebs' solution containing 2 mM ethylene glycoltetraacetic acid (EGTA) in both females and males. Vascular response was significantly reduced: Females, control R_{max} = 85.5 ± 5 % compared to 23.5 ± 1.7 % in Ca^{2+}-free condition; Males, control R_{max} = 77.5 ± 4.1 % compared to 20.3 ± 2.16% in Ca^{2+}-free condition (Figure 3.7).

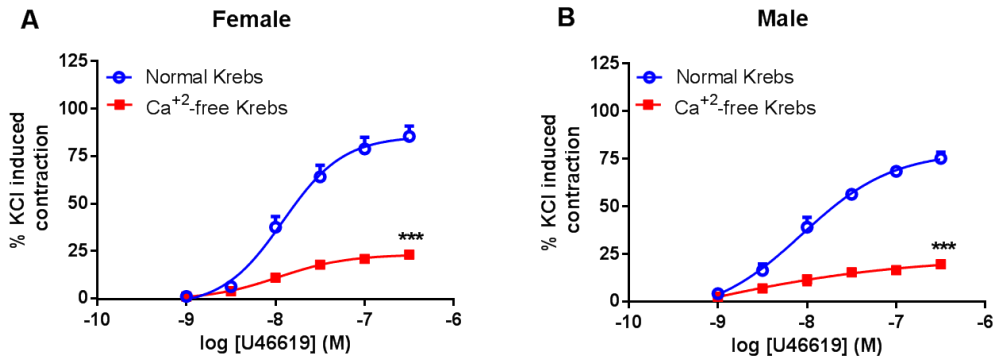


Figure 3.7: Log concentration-response curves for the vasoconstrictor effects of U46619 in the absence or presence of Ca^{2+} in female **(A)** and male PCAs **(B)**. Data are expressed as a percentage of the contraction to 60 mM KCl and are mean ± S.E.M. of 8(A) - 7(B) experiments. *** indicates P<0.001, 2-tailed, paired Student's *t*-test vs control values.

3.3.7 Role of Rho-kinase pathway in TXA_2 action

To determine the role of intracellular Ca^{+2} in the contractile effect of TXA_2, coronary arteries are preincubated with and without Rho kinase inhibitor. The Rho kinase inhibitor Y27632 (10 µM) induced a significant vasorelaxation of PCAs pre-contracted with U46619 in both sexes compared to controls (Figure 3.8).

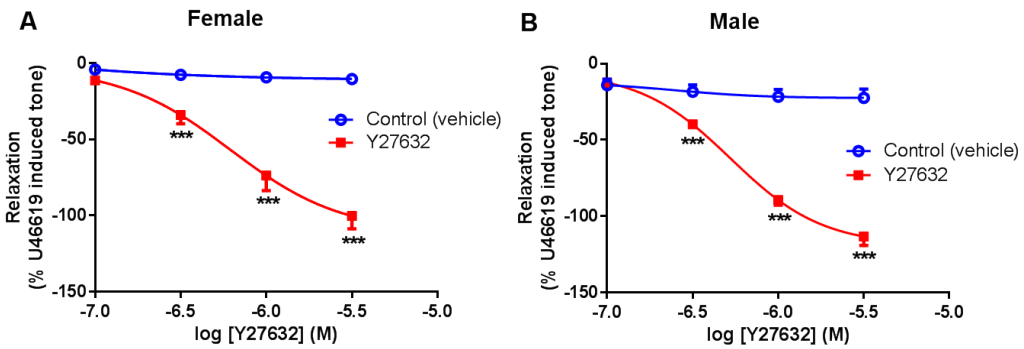


Figure 3.8: Log concentration-response curves for the vasorelaxant effects of Y27632 in female **(A)** and male PCAs **(B)** vs no Y27632 (control). Data are expressed as a percentage change from U46619-induced tone and are mean ± S.E.M. of arteries from 5(A) - 6(B) different animals. *** indicates P<0.001, two-way ANOVA followed by a Sidak's *post hoc* test vs control values.

3.3.8 Determination of the release of TXA_2 from PVAT

Although there was no difference in the levels of TXB_2 in the PVAT from male and female animals, the possibility that there are differences in the release of thromboxane from PVAT was explored. Therefore, the levels of TXB_2 in the buffer after incubation with PVAT were determined. In these experiments it was found that the concentration of TXB_2 was higher in the buffer after incubation with PVAT from female animals compared to PVAT from male animals (Figure 3.9).

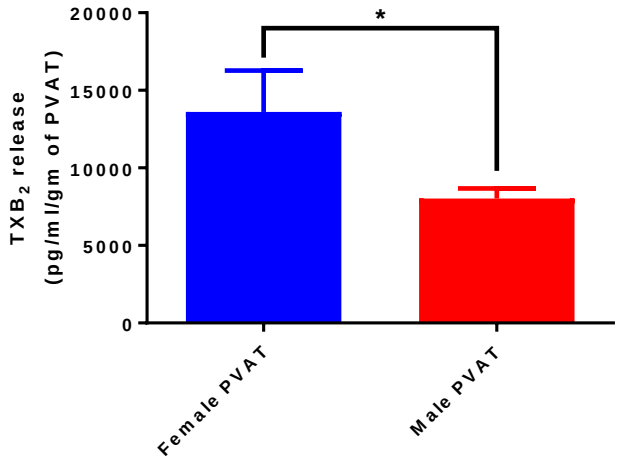


Figure 3.9: Comparison of the levels of TXB_2 in the buffer after incubation with PVAT from female or male pigs for 2.5 hours. Data are expressed as a pg of TXB_2 released per ml per gm of PVAT and are mean ± S.E.M. of PVAT from 10 female and 9 male animals. * indicates $P<0.05$, 2-tailed, unpaired Student's *t*-test.

3.3.9 Effects of phospholipase A_2 stimulation on PVAT-induced contractions

The data indicated that cyclooxygenase produced prostanoids play a role in the PVAT-induced contraction in the porcine coronary artery. In order to support these data further, the effects of the phospholipase A_2 (PLA_2) stimulator melittin was investigated. Pre-treatment with melittin (10 µM) significantly enhanced PVAT-dependent vasoconstriction compared with that of PVAT alone in coronary artery segments from both sexes (Figure 3.10). The TP antagonist GR32191B caused complete inhibition of the PVAT-induced contraction in the presence of melittin in arteries from female animals and partial inhibition in arteries from male animals (Figure 3.10 C, D). The FP receptor antagonist AL8810 had no effects on the PVAT-induced contractions in arteries from male or female animals (Figure 3.10 E, F). However, in subsequent experiments, it was demonstrated that pre-incubation with melittin resulted in desensitization of the FP receptor, but not TP receptor-mediated contraction (Figure 3.11).

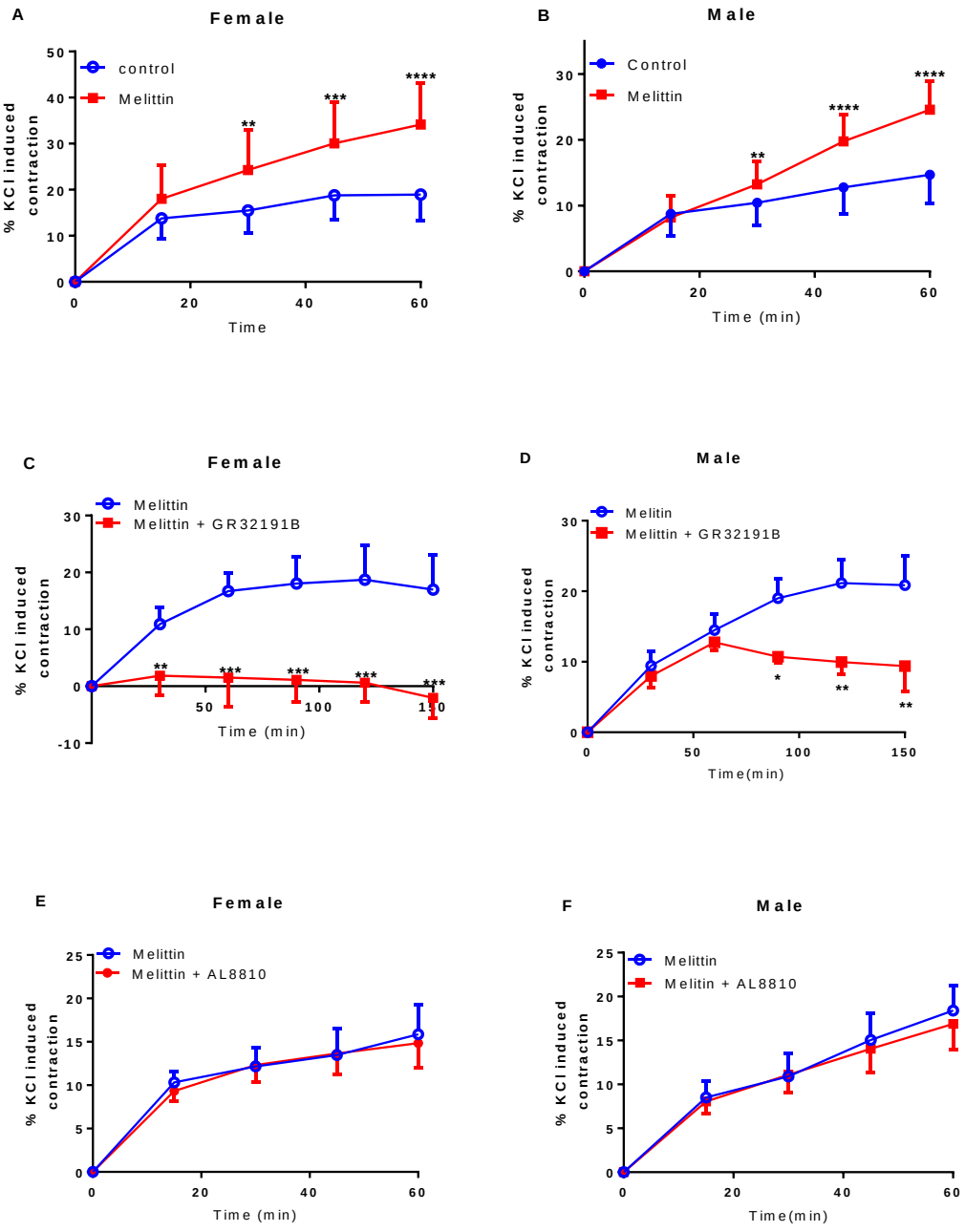


Figure 3.10: (A & B) Contractile responses of the PCAs to fresh PVAT (0.3g) in the absence (control) or presence of melittin (10µM). Data are expressed as a percentage of the contraction to 60 mM KCl and are mean ± SEM from arteries from 5 female (A) and 8 male (B) animals. **(C & D)** Effect of pre-incubation with the TP receptor antagonist GR32191B (3 µM) on the PVAT-induced contraction, in the absence or presence of melittin (10 µM). Data are expressed as a percentage of the contraction to 60 mM KCl response and are means ± S.E.M. of 5 female (C) and 5 male (D) animals. **(E & F)** Effect of pre-incubation

with the FP receptor antagonist AL8810 (10 µM) on the PVAT-induced contraction, in the absence or presence of melittin (10 µM). Data are expressed as a percentage of the contraction to 60 mM KCl response and are means ± S.E.M. of 4 female (E) and 5 male (F) animals. * indicates P<0.05, ** indicates P<0.01 and ***indicates P<0.001, two-way ANOVA followed by a Sidak's *post hoc* test vs control values.

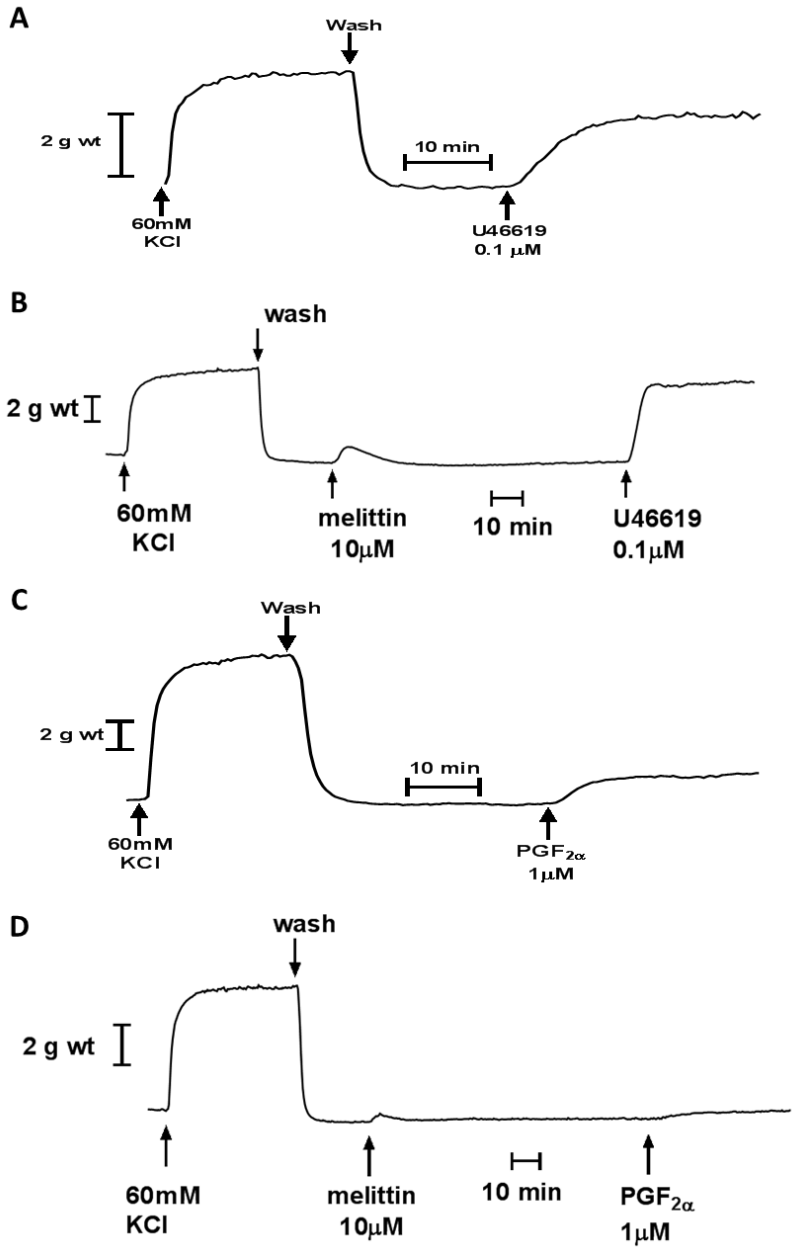


Figure 3.11: Original traces of recording showing the vasomotor responses of PCA to U46619 and $PGF_{2\alpha}$ in the presence and absence of melittin. (A & B) Original traces of recording showing the response of female PCA to addition of 0.1 µM U46619 in the absence and presence of 10 µM melittin (A and B,

respectively). (C & D) Original traces of recording showing the response of PCA to addition of 1 µM $PGF_{2\alpha}$ in the absence and presence of 10 µM melittin (C and D, respectively).

3.3.10 Effect of phospholipase A_2 stimulation on TXB_2 release from PVAT

To confirm the previous functional effect of melittin in the PVAT from both sexes, the levels of TXB_2 released from PVAT was measured in the presence and absence of melittin. The level of TXB_2 released was significantly potentiated after addition of the PLA_2 stimulator (melittin) in both females and males (Figure 3.12 A, B).

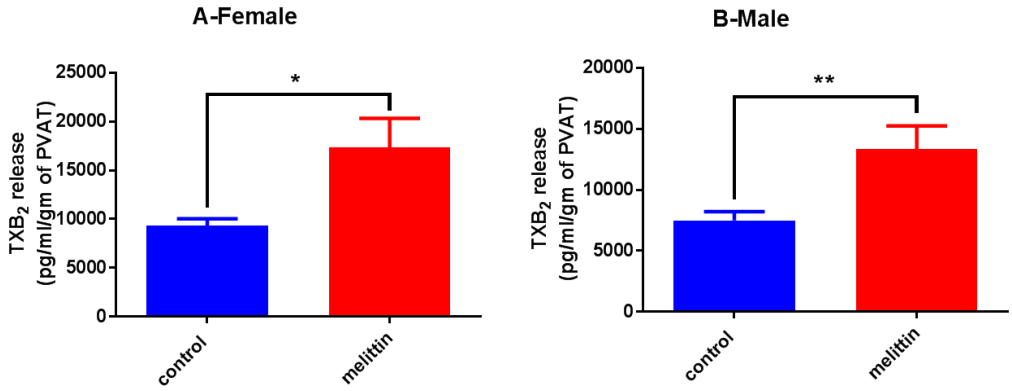


Figure 3.12: Comparison of the levels of TXB_2 in the buffer after a 2.5 hr incubation with PVAT without (control)or with melittin (10 µM) from female (A) or male (B) pigs. Data are expressed as pg of TXB_2 released per ml per gm of PVAT and are mean ± S.E.M. of 6 female and 7 male PVAT samples. * indicates P<0.05, ** indicates P<0.01, 2-tailed, paired Student's *t*-test vs paired controls.

3.4 Discussion

The data presented in this chapter demonstrate that fresh PVAT added to segments of porcine coronary artery produced a contractile response (Figure 3.1), which is in line with previous studies, indicating that the coronary artery PVAT releases adipose-derived contractile factors (ADCFs) (Owen *et al.*, 2013). Endothelial denudation did not affect the responses of PCA to applied PVAT (Figure 3.1C). This contractile response was inhibited by cyclooxygenase inhibitors, indicating a role for contractile prostanoids in this contractile

response (Figure 3.2). Interestingly, the contractile response to coronary artery PVAT from female animals was inhibited by a TP receptor antagonist, whereas the contractile response to coronary artery PVAT from male arteries was inhibited by a FP receptor antagonist (Figure 3.3). These data suggest sex differences in the prostanoids mediating the contractile response.

The role of cyclooxygenase products in the PVAT-induced contraction is similar to that seen in mouse aorta, although in this previous study, only thromboxane levels were measured (Meyer *et al.*, 2013). In the present study the presence of both thromboxane and $PGF_{2\alpha}$ was clearly detected in the PVAT of the porcine coronary artery, although there were no differences in the levels of these prostanoids between male and female animals (Figure 3.4). In addition, a concentration-response curve with a TXA_2 agonist (U46619) was determined to assess the responsiveness of PCAs to TXA_2 in both sexes and showed no difference in the responses of coronary rings from different sexes to TXA_2. Moreover, immunoblotting analysis found no difference in TP expression between female and male coronary arteries (Figure 3.5). These data indicate that the sex differences in the role of thromboxane in the PVAT-induced contraction cannot be attributable to either differences in receptor expression or coupling of the receptor to intracellular signalling pathways mediating contraction. Therefore, it was determined whether there are differences in the release of thromboxane from the PVAT by measuring the levels of TXB_2 in the buffer. Of note, TXB_2 has been measured instead of TXA_2 because TXA_2 has a half-life of only 37 seconds under physiological conditions, and the production of TXA_2 *in vivo* is typically monitored by measurement of TXB_2. Thromboxane B_2 (TXB_2) is produced by the non-enzymatic hydration of TXA_2, and has been shown to be stable. Interestingly, there was a greater amount of TXB_2 in the buffer containing PVAT from female animals compared to males (Figure 3.9), suggesting that, although levels of thromboxane are the same in PVAT from both sexes, a greater amount of thromboxane is actually released from the PVAT in females. Although the exact reason for the difference in release of TXB_2 has not been addressed in this study, many reasons could be speculated such as the difference of the expression or function of TXB_2 transporters. For example, multidrug resistance protein 4 or other prostaglandin transporters which act as a prostanoid

efflux pumps (Schuster, 2002; Reid *et al.*, 2003; Rius *et al.*, 2005), or differences in the turnover of released TXB_2. However, the data explain why the PVAT-induced contraction in coronary arteries from female animals is inhibited by the TP receptor antagonist.

The present study indicates that $PGF_{2\alpha}$ is involved in the PVAT-dependent contraction in male pigs as FP receptor antagonism by AL8810 significantly reduced the resultant vasocontraction. In addition, $PGF_{2\alpha}$ was detected in PVAT indicating that $PGF_{2\alpha}$ has a role as a PVAT-derived contractile agent. Although there was no difference in the level of $PGF_{2\alpha}$ in the PVAT from male and female pigs, $PGF_{2\alpha}$ itself produced a greater contractile response in coronary arteries from male animals compared to females. This corresponds with a greater expression of the FP receptor in coronary arteries from male animals (Figure 3.6). Therefore, this could be the explanation underlying the sex differences in the role of the FP receptor in the PVAT-induced contraction in the coronary artery. However, $PGF_{2\alpha}$ release has not been measured because FP receptor expression in the vessels is already different.

In order to confirm the role of prostanoids in the PVAT-induced contraction in the coronary artery, the effects of the PLA_2 stimulator melittin were examined. Melittin enhanced the PVAT-induced contraction in coronary arteries from both sexes, which correlates with the role of the PLA_2-arachidonic acid-cyclooxygenase pathway (Figure 3.10 A,B). Furthermore, melittin enhanced the production of thromboxane within PVAT and the level of thromboxane released from the PVAT (Figure 3.12). Antagonism of TP receptors inhibited the contraction to PVAT in coronary arteries from both male and female animals, although there was greater inhibition of the contraction in PCAs from females (Figure 3.10 C,D), which correlates with the fact that TP antagonism inhibits the PVAT-induced contraction under non-PLA_2-stimulated conditions. Interestingly, the FP antagonist no longer inhibited the PVAT-induced contractions in either male or female arteries (Figure 3.10 E,F). However, it was found that melittin could cause desensitization of the $PGF_{2\alpha}$ contraction but not the TXA_2,-induced contraction (Figure 3.11), which would explain the lack of effect of the FP antagonist. It is hypothesized that this desensitization is caused by release of $PGF_{2\alpha}$ from the coronary artery in

response to melittin. Although the hypothesis in the present study focuses on the PVAT as a source of the PLA_2- dependent arachidonic acid pathway that affects the vascular smooth muscle cells, other potential sources of prostanoids could not be excluded such as adventitia, endothelial cells and VSMC itself (Stemme *et al.*, 2000; Tang *et al.*, 2014). In addition, the present study showed the effect of whole PVAT on the vascular tone of PCA but did not investigate which cell is responsible for this vasomotor effect as different cells in PVAT express COX and can produce prostanoids (Stemme *et al.*, 2000; Simmons *et al.*, 2004). A limitation of this study is the potential selectivity of GR32191B for TP receptors over FP receptors. However, the data indicate that the larger inhibition of the PVAT response seen with AL8810 in PCAs from males is likely to be due to greater responsiveness and FP receptor expression in males compared to females. Similarly, the greater effect of GR32191B on PVAT responses in females compared to males appears to be due to greater release of thromboxane.

In conclusion, these data demonstrate that PVAT is able to regulate porcine coronary arterial tone through the release of thromboxane and $PGF_{2\alpha}$. To the best of the author's knowledge, this is the first study that identifies sex differences in COX metabolites in the PVAT response, where thromboxane has a role in PVAT-dependant vasoconstriction in females while PVAT-derived $PGF_{2\alpha}$ plays a role in the contraction of PCAs from males. These differences can be explained by a greater release of thromboxane from PVAT from female animals and greater expression of FP receptors on the porcine coronary artery from males. It is clear that there are sex differences in the regulation of vascular tone, including the role of EDH (Wong *et al.*, 2014b). The data presented enhance our knowledge of the mechanisms underlying these sex differences by demonstrating differences in the adipose-derived contractile factors released from coronary artery PVAT. Adipose tissue, including PVAT, changes under pathological conditions such as obesity. In the porcine coronary artery, obesity enhances the contractile responses of PVAT (Owen *et al.*, 2013). Whether this is due to altered release of prostanoids is unknown. Furthermore, whether the sex difference in the release of prostanoids is maintained in obesity is unknown. Future studies should explore whether these sex differences in PVAT are maintained under pathological conditions. The following chapter describes

reactive oxygen species as other ADCFs and shows their connection with prostanoids in PVAT-coronary arterial tone coupling.

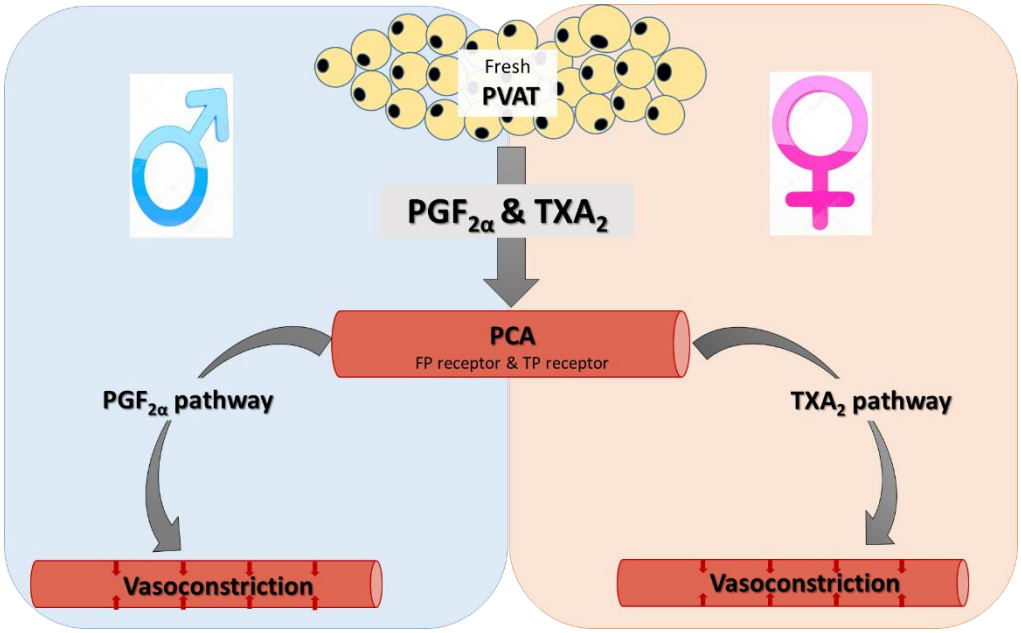


Figure 3.13 Hypothesized schematic diagram of sex differences in the contractile response of PCA to fresh PVAT. Present study demonstrated a clear sex differences in PVAT function where PVAT can mediate vasoconstriction in PCAs via thromboxane A_2 (TXA_2) and $PGF_{2\alpha}$ in females and males, respectively.

Chapter Four

Role of reactive oxygen species in perivascular adipose tissue-induced vasoconstriction: influence of sex

4.1 Introduction

Reactive oxygen species (ROS), including superoxide anion (O_2^-) and hydrogen peroxide (H_2O_2) are generated by all cell types and act as intercellular and intracellular signalling molecules (Thannickal and Fanburg, 2000). However, the highly reactive nature of ROS also possesses potential deleterious effects on cellular integrity and function resulting in oxidative stress in cardiovascular diseases such as hypertension and atherosclerosis (de Champlain *et al.*, 2004; Fortepiani and Reckelhoff, 2005). Although there are many enzymes which can generate ROS (such as cyclooxygenases, lipoxygenase, xanthine oxidase, cytochrome P450, enzymes of the mitochondrial electron transport chain), NADPH oxidases (Nox) have been identified as a major source of ROS generation within the vasculature (Wind *et al.*, 2010; Wong *et al.*, 2015a). Nox enzymes are transmembraneous proteins which consist of seven isoforms: Nox1 to Nox5 and Duox1 and Duox2 (Streeter *et al.*, 2013).

It has previously been demonstrated that there are sex differences in the expression of Nox isoforms in the porcine coronary artery, correlating with differences in the role of these isoforms in the regulation of endothelium-dependent relaxant responses, with the indication that Nox-derived ROS inhibits endothelium-dependent responses in males, but not females (Wong *et al.*, 2015a). Other studies on rat cerebral arteries and rat aortae have shown that oxidative stress levels are higher in males compared with females (Brandes and Mugge, 1997; Miller *et al.*, 2007). In contrast, White *et al.* (2005) have found that oestrogen induces vasocontraction of porcine coronary arteries (PCA) via generation of superoxide (O_2^-) in vascular smooth muscle (White *et al.*, 2005).

PVAT has recently been identified as a source of ROS (Fleenor *et al.*, 2014). A study conducted by Gao *et al.*, (2006) on the superior mesenteric artery of Wistar-Kyoto rats has showed that PVAT could augment the arterial contractile response to perivascular nerve stimulation via the production of ROS, specifically superoxide (Gao *et al.*, 2006). In addition to sex differences in the risks for CVD (Villar *et al.*, 2008; Maas and Appelman, 2010), there are also sex differences in oxidative stress levels (Brunelli *et al.*, 2014). Therefore, understanding the nature of these differential Nox-induced ROS in females and males is essential for identifying novel strategies to appropriately target

cardiovascular diseases. Although it has previously been identified that there are sex differences in the regulation of coronary arterial tone by Nox-derived ROS, it is unknown whether there are similar sex differences in the role of Nox in PVAT-induced regulation of vascular tone. Therefore, in this chapter the role of Nox isoforms in the contractile responses in coronary arteries from male and female pigs was compared.

4.2 Materials and Methods

4.2.1 Tissue preparation

Tissues were set up as previously described in Chapter 2.

4.2.2 Functional responses in the isolated porcine coronary arteries

The method is previously described in Chapter 2. Relevant test compounds were then added with 60 minutes incubation time. The following test compounds were used: N-acetyl-L-cysteine (NAC) (10 mM) as a reactive oxygen scavenger, diphenyliodonium chloride (DPI) (10 µM) as a non-selective Nox inhibitor (Fleming *et al.*, 2001); 2-acetylphenothiazine (ML171) (100 µM) (Gianni *et al.*, 2010) as a selective Nox 1 inhibitor, and Phox-I2 (100 µM) (Bosco *et al.*, 2012) as a selective Nox 2 inhibitor to determine the role of Nox1 and Nox2, respectively. In addition, GKT137831 (10 µM) (Green *et al.*, 2012), a recently described pyrazolopyridinedione derivative that inhibits Nox4 and Nox1 (Aoyama *et al.*, 2012), was used to further investigate the role of Nox4. All these inhibitors were incubated with the coronary segment prior to addition of PVAT (0.3 g). A separate series of experiments were performed to determine the role of ROS in prostanoid-induced vasoconstriction. Firstly, cumulative concentration-response curves to the TXA_2 mimetic U46619 (1 nM-300 nM) were constructed in the presence or absence of DPI and ML171 in coronary artery segments from male and female pigs. Secondly, the response of tissues to a single concentration of $PGF_{2\alpha}$ (1 µM) were determined in the presence and absence of DPI and ML171 as well. In experiments using DMSO as the solvent of the drugs (see Materials Section 4.2.6), DMSO 0.1 % (v/v) was added to the arteries as vehicle controls.

4.2.3 Protein Expression of Nox Subunits

Protein expression of NADPH-oxidase catalytic subunits, Nox1, Nox2, and Nox4 were measured in both PVAT and coronary artery from male and female pigs using immunoblotting. PVAT and PCAs were homogenized on ice in lysis buffer with protease inhibitor cocktail (Calbiochem, VWR International Ltd, Lutterworth, Leicestershire, UK) (Appendix A) using a 0.2ml glass homogenizer. Protein concentration was determined using a Lowry assay. After addition of 6x Laemmli sample buffer (Appendix A) to the samples, homogenates were heated at 100^{o}C for 5 min and centrifuged at 13000 ×g for 1

min. Equal amounts of protein were loaded onto a 4–20% Mini-PROTEAN TGX precast gel (Bio-Rad, Hemel Hempstead, Hertfordshire, UK) and transferred onto nitrocellulose membrane (GE Healthcare, Little Chalfont, Buckinghamshire, UK) using a Bio-Rad mini-Transblot.

Membranes were blocked in 5% (w/v) non-fat milk in Tris-buffered saline containing 0.1% (v/v) Tween 20 (TBS-T) (Appendix A) for 1 hour at room temperature and then incubated overnight at 4°C with the appropriate primary antibody (rabbit polyclonal anti-NOX1 antibody (ab137603 Abcam®, Cambridge, UK) (1:500), rabbit polyclonal anti-gp91-phox antibody (sc-20782 Santa Cruz Biotechnology, Insight Biotechnology Ltd, Wembley, Middlesex, UK) (1:500), rabbit monoclonal anti-NOX4 antibody (ab109225 Abcam®) (1:1000)). For validating equal loading, mouse anti-myosin light chains (MLC) antibody (Sigma-Aldrich, Poole, Dorset, UK) (1:1000) or mouse monoclonal anti-β-actin antibody (Sigma-Aldrich, Poole, Dorset, UK) (1:100,000) were used as loading controls. After washing with Tris-buffered saline containing 0.1% (v/v) Tween 20, membranes were then incubated with secondary antibody IRDye 800CW Goat anti-rabbit IgG (1:10,000) and IRDye® 680LT Goat anti-mouse IgG (1:10,000) (LI-COR Biosciences, Cambridge, UK) for 1 hour at 37°C. After washing with TBS-T buffer, immunoreactive bands were detected using a LI-COR Odyssey Infrared Imaging Scanner and densities of bands were determined using Image Studio (Version 3.1 LI-COR Biosciences). Relative densities of immunoreactive bands were normalized to intensity of corresponding bands for β–actin or MLC, as appropriate.

4.2.4 Quantification of superoxide anion production by lucigenin chemiluminescence assay

NADPH oxidase activity (superoxide anion production) of PVAT and PCAs was measured using lucigenin-enhanced chemiluminescence method (Guzik and Channon, 2005; Wind *et al.*, 2010). Briefly, fresh PVAT and PCAs from females and males were finely excised and cut into segments ~2 cm long. Segments of PVAT and PCAs were then homogenized in Krebs–HEPES buffer (pH 7.4) consisting of 99 mM NaCl, 4.7 mM KCl, 1.9 mM $CaCl_2$, 1.2 mM $MgSO_4$, 1 mM KH_2PO_4, 25 mM $NaHCO_3$, 11.1 mM glucose, 20 mM HEPES and protease inhibitor cocktail Set I (Calbiochem, VWR International Ltd, Lutterworth,

Leicestershire, UK) (Appendix A) in a Precellys® 24 Tissue Homogenizer. For removing cell debris, homogenates were then centrifuged at 1000 ×g for 10 min at 4°C. Protein concentrations of the supernatants were determined by the Bradford method (Bradford, 1976). Equal amounts of supernatant were incubated at 37 °C for 20 min in the absence or presence of 10 µM DPI, 100 µM ML-171, 100 µM Phox-I2 or 10 µM GKT137831 with a final concentration of 5 µM lucigenin. In a separate set of experiments, pre-incubation of PVAT and PCA with and without 1 nM U46619 or 1 µM $PGF_{2\alpha}$ at 37ºC for 30 min was done to investigate the connection between ROS and prostanoids in both sexes whilst pre-incubation of PVAT with the inflammatory mimetic substance LPS (5 µg/ml) at 37ºC for 4 hrs was performed to investigate the impact of inflammation on PVAT function (Tomita *et al.*, 2005). To start the reaction, 100 µM NADPH (Sigma-Aldrich, Poole, Dorset, UK) was then added into each well (total volume of 100 µl) and allowed to equilibrate in a semi-dark environment for 5 min. Photon emission was measured using Top Count NXT (PerkinElmer, Cambridge, Cambridgeshire, UK) set to single photon-counting mode for 10 s per well. Background counts (in the absence of homogenate) were subtracted and O_2^- production normalized to total protein content.

4.2.5. Quantification of hydrogen peroxide production using luciferin-enhanced chemiluminescence assay and Amplex Red

The levels of H_2O_2 production were measured in PVAT and PCA homogenates using two different sensitive and specific techniques, luciferin-enhanced chemiluminescence and Amplex Red, to confirm the result, which is not dependent upon a specific probe employed. After homogenization of the PVAT and PCA in Tris-buffered saline containing 0.1% (v/v) Tween 20, along with protease inhibitor cocktail (Calbiochem) (Appendix A), equal volumes of homogenate (30 µl) were incubated with and without 10 µM GKT137831 at 37°C for 20 min. In a separate experiment, H_2O_2 production was determined by incubating PVAT samples with and without 5 µg/ml of the inflammatory mimetic substance LPS at 37ºC for 4hrs to investigate the impact of inflammation on H_2O_2 production. H_2O_2 production was determined using both a ROS-Glo™ H_2O_2 assay (G8820, Promega, UK) and Amplex Red (10 µM) in the presence of horseradish peroxidase (0.6 UmL^{-1}). Absorbance was read at 590

nm with excitation of 530 nm using FLUOstar Galaxy (BMG Labtech Ltd, Aylesbury, Bucks, UK). In case of ROS-Glo^{TM} H_2O_2 assay, photon emission was measured using Top Count NXT. In both assays, background counts (in the absence of homogenate) were subtracted and H_2O_2 production normalized to total protein content.

4.2.6 Materials

All drugs were purchased from Sigma-Aldrich (Poole, Dorset, UK) except for DPI and ML171 from Tocris Bioscience (Bristol, UK), and GKT137831 and $PGF_{2\alpha}$ from Cayman Chemicals (Cambridge, UK). Stock solutions of DPI, ML171, Phox-I2, GKT137831 and $PGF_{2\alpha}$ were dissolved in dimethyl sulfoxide (DMSO) whereas stock solution of NAC and LPS were dissolved in distilled water. Stock solutions of U46619 were made to 10 mM in ethanol. All further dilutions of the stock solutions were made using distilled water.

4.2.7 Statistical analysis

Data are presented and were analysed as described in Chapter 2.

4.3 Results

4.3.1 Role of reactive oxygen species in PVAT-induced vasoconstriction

As shown in the chapter 3, addition of PVAT (0.3 g) to the organ baths caused a time-dependent contraction of the coronary arteries from both male and female pigs (Figure 4.1). There was no apparent difference in the profile of contraction between male and females. To determine the role of ROS in the PVAT vasomotor effect, PCAs were preincubated with ROS scavenger prior to addition of PVAT. In the presence of the ROS scavenger, N-acetyl-L-cysteine (NAC), the PVAT-induced contractions were partially, but significantly attenuated compared to control in coronary arteries from both male and female pigs (Figure 4.1).

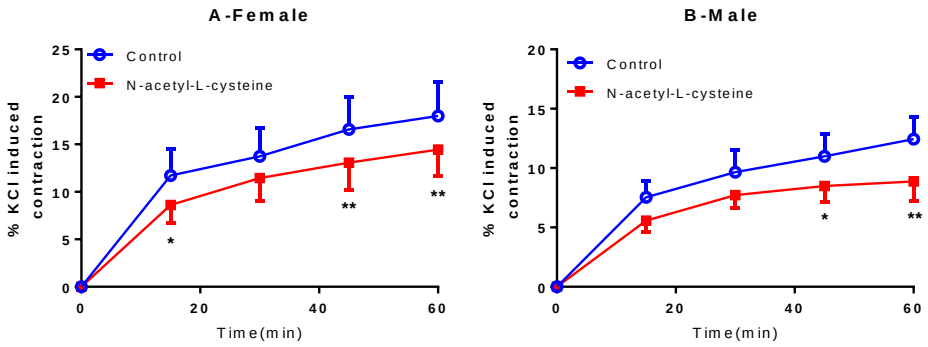


Figure 4.1: Effects of reactive oxygen species scavenger N-acetyl-L-cysteine on the PVAT-induced contraction of coronary artery segments from female **(A)** and male **(B)** pigs. Arteries were pre-incubated without (control) or with 10 mM N-acetyl-L-cysteine before addition of PVAT. Values are expressed as a percentage of the contraction to 60 mM KCl and are mean ± S.E.M. of 10 experiments. * P<0.05 and ** P<0.01, two-way ANOVA followed by a Sidak's *post hoc* test vs control values.

4.3.2 The effects of Nox inhibitors on PVAT-induced vasoconstriction in PCAs from female and male pigs

In order to determine the role of Nox isoforms in the PVAT-induced contraction, coronary artery segments were pre-incubated with different Nox inhibitors prior to addition of PVAT. Treatment with the non-selective Nox inhibitor DPI (10 µM) caused a complete inhibition of the PVAT-induced contraction in coronary arteries from both male and female pigs (Figure 4.2 A, B). Pre-incubation with

the Nox1-selective inhibitor ML171 (100 µM) caused partial inhibition of the contraction (Figure 4.3 A,B), whereas the Nox2-selective inhibitor Phox-I2 (10 µM) caused complete inhibition (Figure 4.3 C,D). The Nox1/4 inhibitor GKT137831 (10 µM) also inhibited the PVAT-induced contractions, with an apparent greater effect in coronary arteries from male compared to PCAs from female (Figure 4.3 E,F).

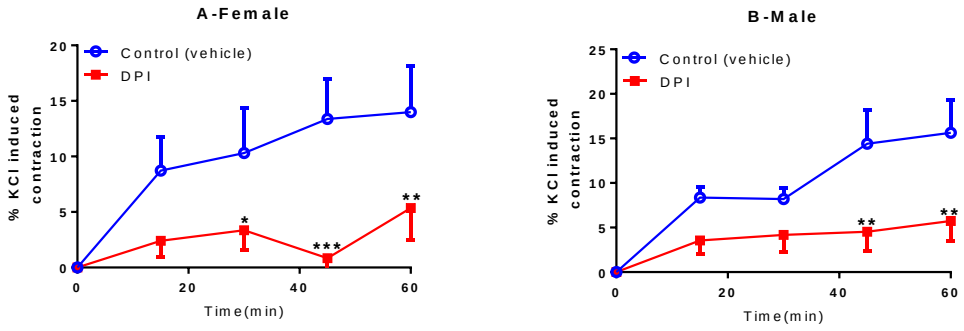


Figure 4.2: Effects of non-selective Nox inhibition on the PVAT-induced contractions of coronary arteries from female and male pigs in the absence (control vehicle) or presence of 10 µM DPI **(A & B)**. Values are expressed as a percentage of the contraction to 60 mM KCl and are mean ± S.E.M. of 6 experiments. * P<0.05, ** P<0.01 and *** P<0.001, two-way ANOVA followed by a Sidak's *post hoc* test vs control values.

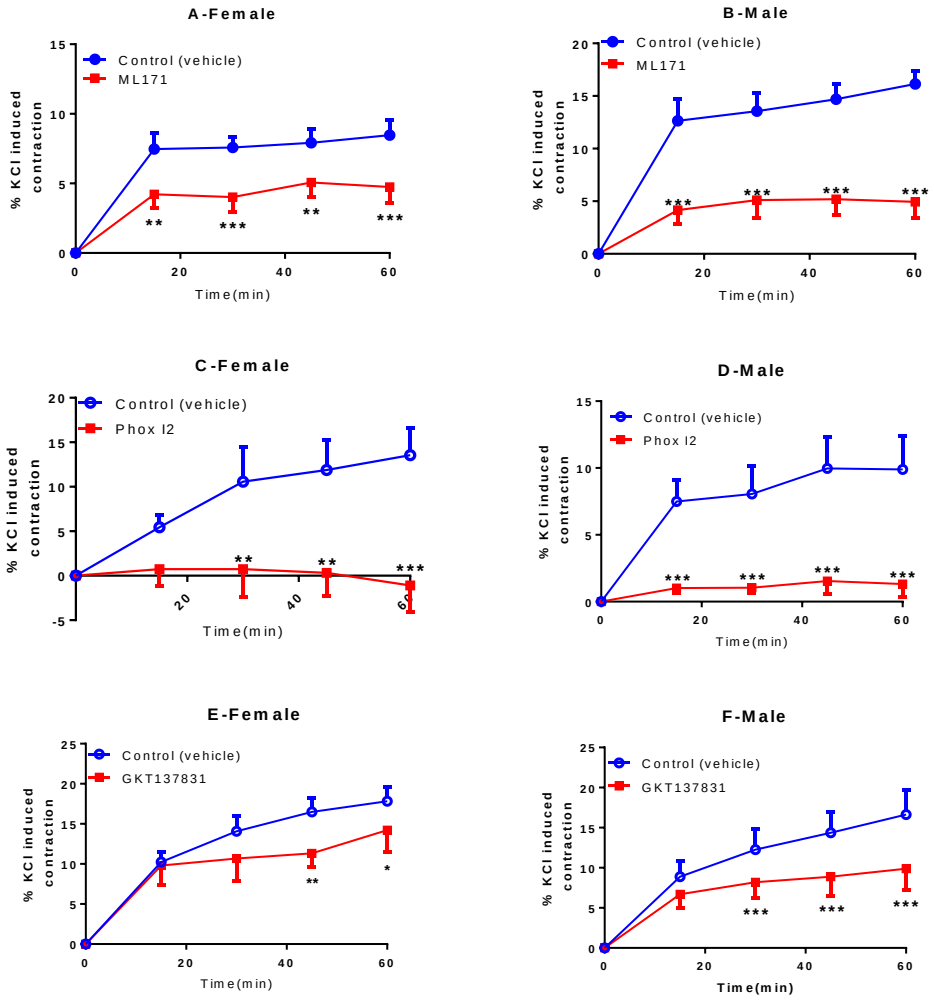


Figure 4.3: Effects of Nox inhibition on the PVAT-induced contractions of coronary arteries from female and male pigs in the absence (control vehicle) or presence of 100 μM ML-171 **(A & B);** 100 μM Phox-I2 **(C & D)**; or 10 μM GKT137831 **(E & F)**. Values are expressed as a percentage of the contraction to 60 mM KCl and are mean ± S.E.M. of 6 experiments. * P<0.05, ** P<0.01 and *** P<0.001, two-way ANOVA followed by a Sidak's *post hoc* test vs control values.

4.3.3 Measurement of superoxide anion production in coronary artery PVAT

The contractile studies indicated that Nox-derived ROS play a role in the PVAT-induced contraction in the porcine coronary artery. In order to determine whether the PVAT could be the source of the ROS, the activity and expression of Nox isoforms have been measured. In the presence of NADPH, ROS production by PVAT was significantly augmented in both sexes (Figure 4.4 A, B). Treatment

of the homogenate with the non-selective Nox inhibitor DPI significantly blocked ROS production in PVAT from both sexes, confirming that the ROS detected by chemiluminescence was Nox-dependent. In addition, the level of DPI-inhibitable chemiluminescence did not differ between sexes (Figure 4.4C). There was no difference in the level of total ROS production in PVAT from both sexes (Figure 4.4D). Incubation of PVAT homogenate with either the Nox1 inhibitor ML171 or the Nox2 inhibitor Phox-I2 significantly reduced ROS production in both females and males (Figure 4.5 A-D). In contrast, the Nox 1 and 4 inhibitor GKT137831 did not inhibit the superoxide production in PVAT from either sex (Figure 4.5 E, F) (Table 1).

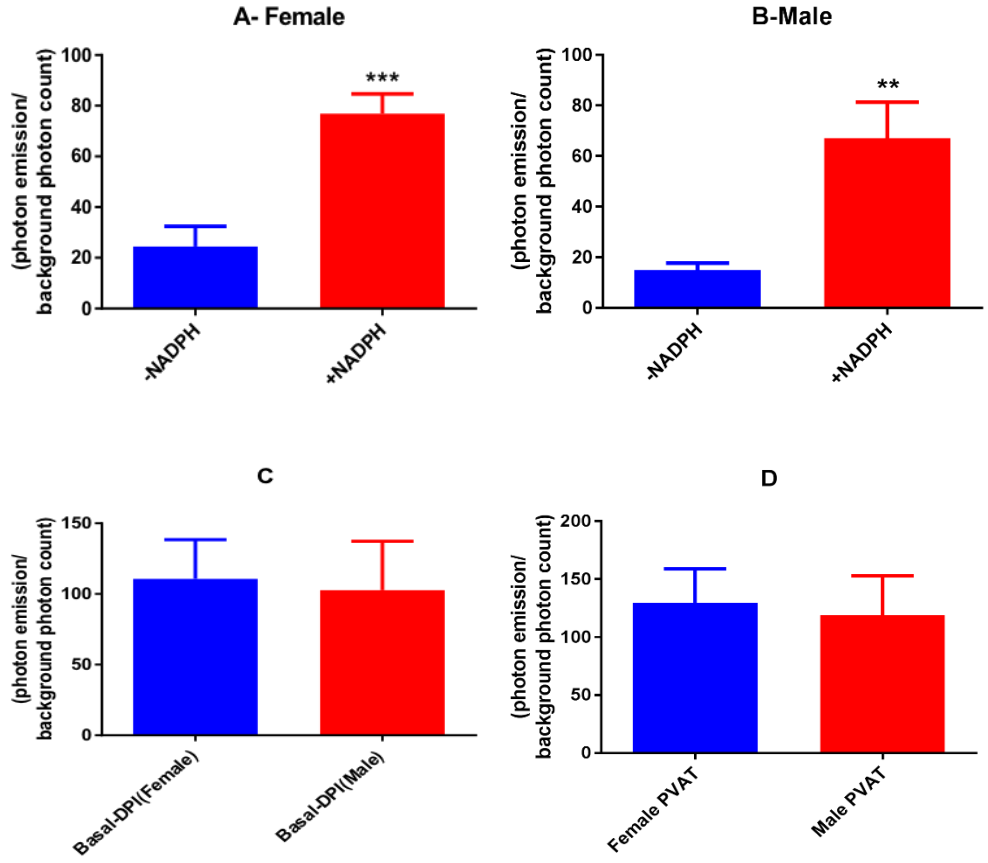


Figure 4.4: NADPH oxidase activities using lucigenin-enhanced chemiluminescence method in PVAT homogenates from female and male pigs. After 20 min incubation with 5 µM lucigenin and 10 µM DPI, 100 µM NADPH was added and measurements were taken in an interval of 10 s per well. Data are expressed as a basal fold from tissue blank and are mean± S.E.M. of 10

experiments. ** P<0.01 and *** P<0.001, paired (A,B) and unpaired (C,D) Student's 2-tailed *t*-test.

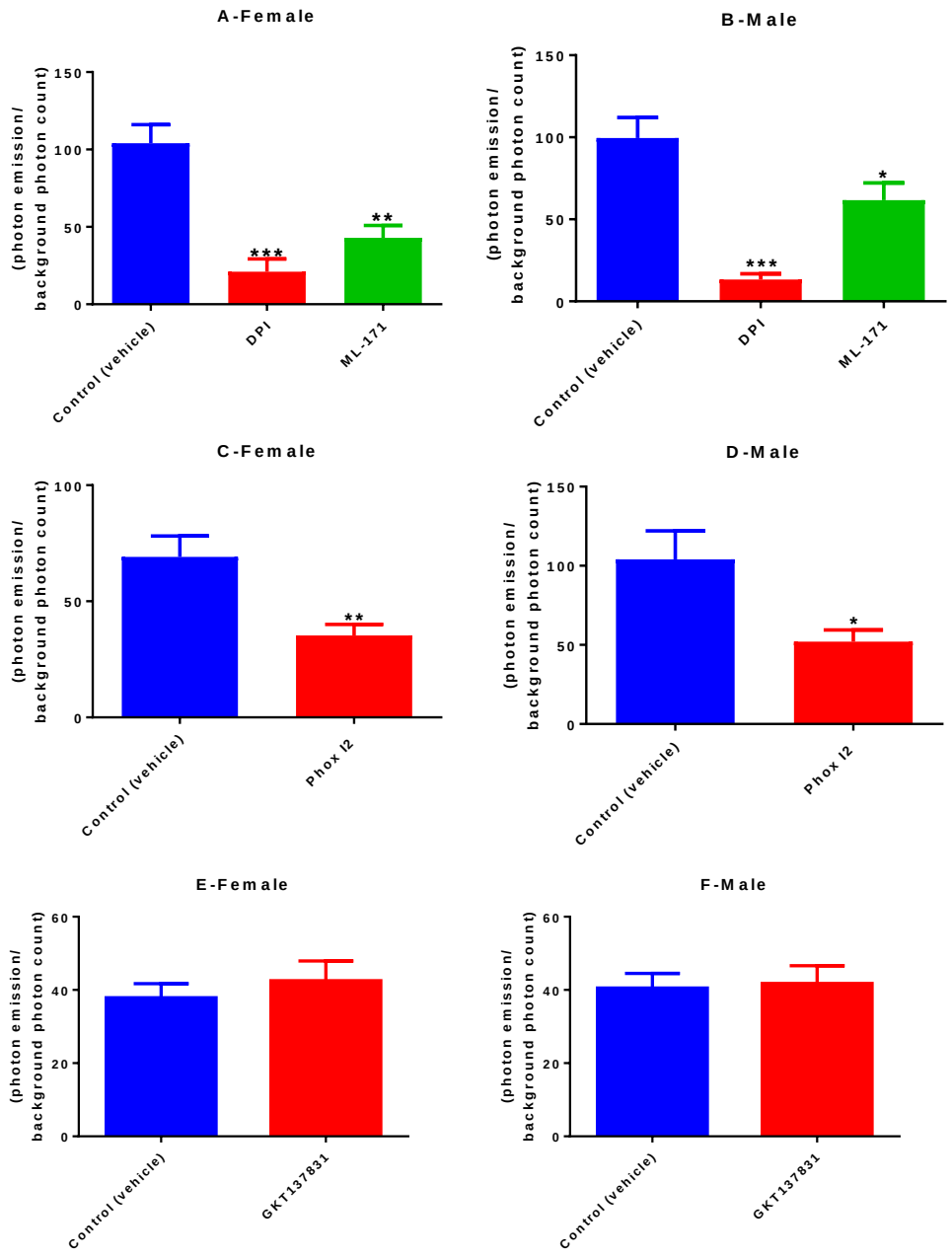


Figure 4.5: Detection of NADPH oxidase activity using the lucigenin chemiluminescence method in coronary artery PVAT homogenates from male and female pigs in the absence (control vehicle) or presence of 10 μM DPI or 100 μM ML-171 **(A & B)**; 100 μM Phox-I2 **(C & D)**; or 10 μM GKT137831 **(E & F).** After 20min incubation with inhibitors, 100 μM NADPH was added and

measurements were taken in an interval of 10 s per well. Data are expressed as fold change from tissue blank and are mean± S.E.M. of 10 experiments. * P<0.05, ** P<0.01 and *** P<0.001, one way ANOVA followed by a Sidak's *post hoc* test (A & B) and 2-tailed, Student's paired *t*-test (C-F) vs control values.

4.3.4 Measurement of hydrogen peroxide production

Amplex Red assay was used to measure the level of H_2O_2 production in PVAT from both sexes. There was no effect of the Nox1/4 inhibitor GKT137831 on the level of H_2O_2 production in PVAT from both sexes (Figure 4.6 A, B)

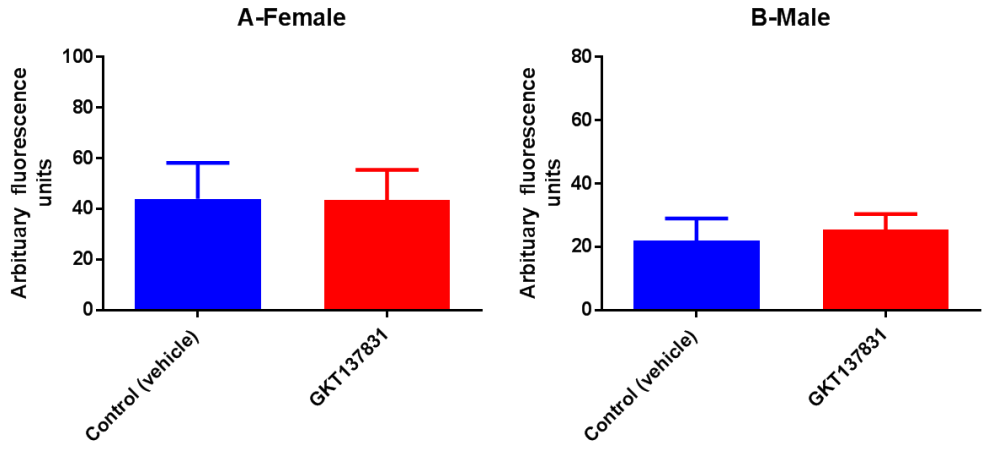


Figure 4.6: Measurement of H_2O_2 levels in the PVAT homogenate in the absence (control vehicle) or presence of 10 μM GKT137831 in **(A)** female or **(B)** male pigs. Data are expressed as arbitrary fluorescence units and are mean ± S.E.M. of 9 experiments.

4.3.5 Measurement of superoxide anion production in coronary artery

Although the contractile responses to PVAT indicate that Nox-derived ROS are involved in the contraction, the source of the ROS could be within the coronary artery itself, rather than the PVAT. Therefore, Nox isoform activity and expression was also determined in coronary artery segments. Nox activity was detected in PCA homogenates from both females and males with no sex difference in the total Nox activity (Figure 4.7 A). This ROS production was significantly inhibited by pre-incubation with DPI, ML171 and Phox-I2 in both females and males compared to their respective controls (Figure 4.7 B-E). GKT13731 reduced superoxide production in coronary artery homogenates from female pigs, but was without effect in coronary arteries from male pigs (Figure 4.7 F, G) (Table 4.1).

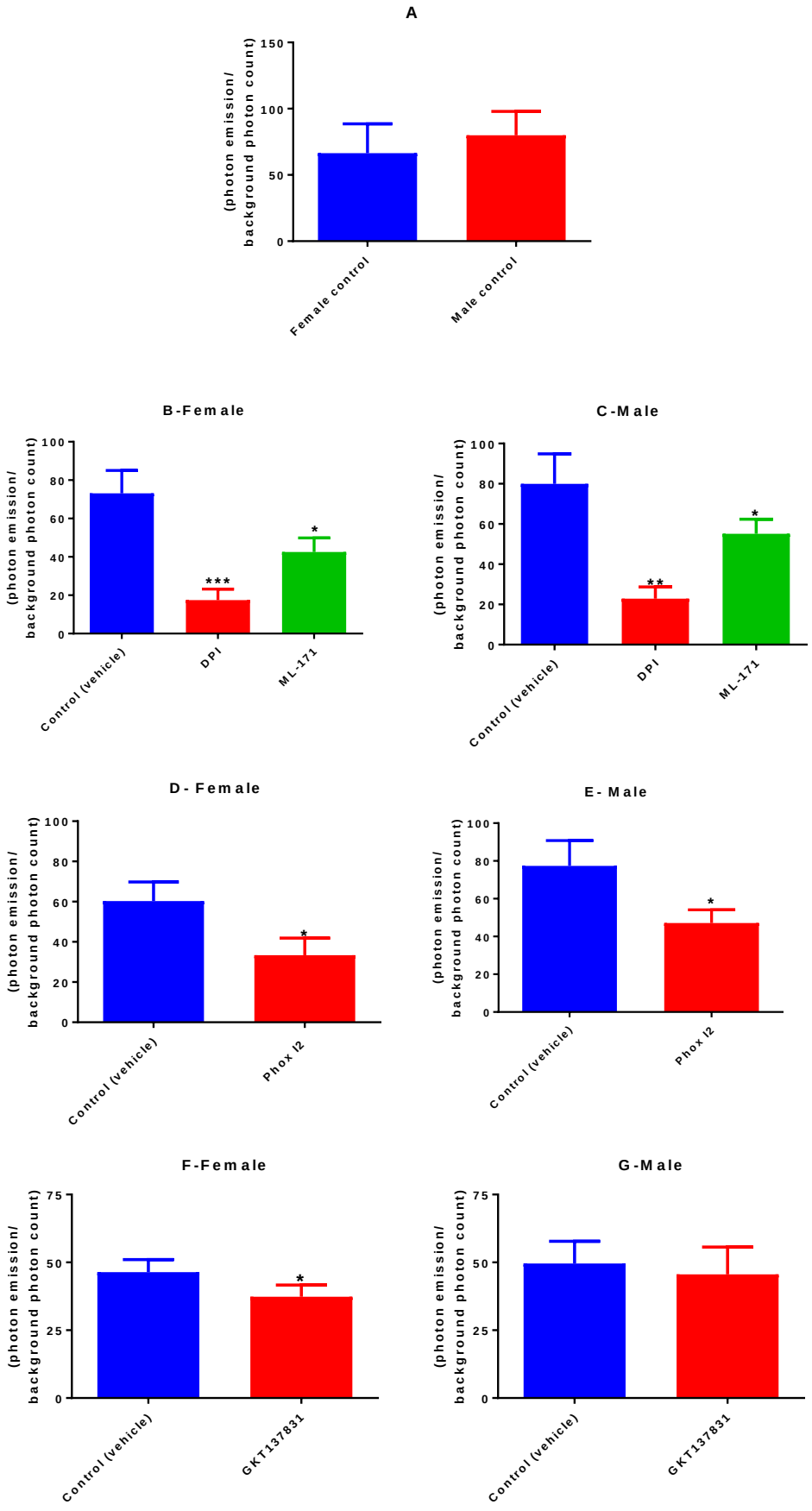

A
(photon emission/ background photon count)
150
100
50
0
Female control
Male control
B-Female
(photon emission/ background photon count)
100
80
60
40
20
0
***
*
Control (vehicle)
DPI
ML-171
C-Male
(photon emission/ background photon count)
100
80
60
40
20
0
**
*
Control (vehicle)
DPI
ML-171
D- Female
(photon emission/ background photon count)
100
80
60
40
20
0
*
Control (vehicle)
Phox I2
E- Male
(photon emission/ background photon count)
100
80
60
40
20
0
*
Control (vehicle)
Phox I2
F-Female
(photon emission/ background photon count)
75
50
25
0
*
Control (vehicle)
GKT137831
G-Male
(photon emission/ background photon count)
75
50
25
0
Control (vehicle)
GKT137831

Figure 4.7: NADPH oxidase activity detected using the lucigenin chemiluminescence method in porcine coronary arterial homogenates from male and female pigs **(A)** and, in the absence (control vehicle) or presence of 10 μM DPI or 100 μM ML-171 **(B & C)**; in the absence (control vehicle) or presence of 100 μM Phox-I2 **(D & E)**; and in the absence (control vehicle) or presence of 10 μM GKT137831 **(F & G)**. Data are expressed as fold change from tissue blank and are mean ± S.E.M. of 9 experiments. * P<0.05, ** P<0.01 and *** P<0.001, one way ANOVA followed by a Sidak's *post hoc* test (B &C), and Student's 2-tailed, paired *t*-test (D-G) vs control values.

Drugs	**PVAT (Female)**	**PVAT (Male)**	**PCA (Female)**	**PCA (Male)**
DPI	↓***	↓***	↓ ***	↓ **
ML171	↓**	↓*	↓ *	↓*
Phox-I2	↓**	↓ *	↓*	↓*
GKT137831			↓*	

Table 4.1: Summary of NADPH oxidase activities using lucigenin-enhanced chemiluminescence method in tissue homogenates of PVAT and PCA from male and female pigs and in the absence or presence of 10 μM diphenyliodonium chloride (DPI), 100 μM ML-171, 100 μM Phox-I2 or 10 μM GKT137831. Data are expressed as mean ± S.E.M of control vehicle versus drug. * P<0.05, ** P<0.01 and *** P<0.001, one way ANOVA followed by a Sidak's *post hoc* test (DPI and ML171) and Student's 2-tailed, paired *t*-test (Phox I2 and GKT137831) vs control values.

4.3.6 Measurement of hydrogen peroxide production in coronary artery

As the Nox isoforms, including Nox4, are expressed in PCA form both sexes, so the level of H_2O_2 production was measured using Amplex Red assay. Pre-incubation with GKT137831 caused a small, but significant inhibition of H_2O_2 production in PCA homogenates from both sexes (Figure 4.8 A, B). This result was confirmed using a luciferin-enhanced chemiluminescence assay (Figure 4.8 C, D).

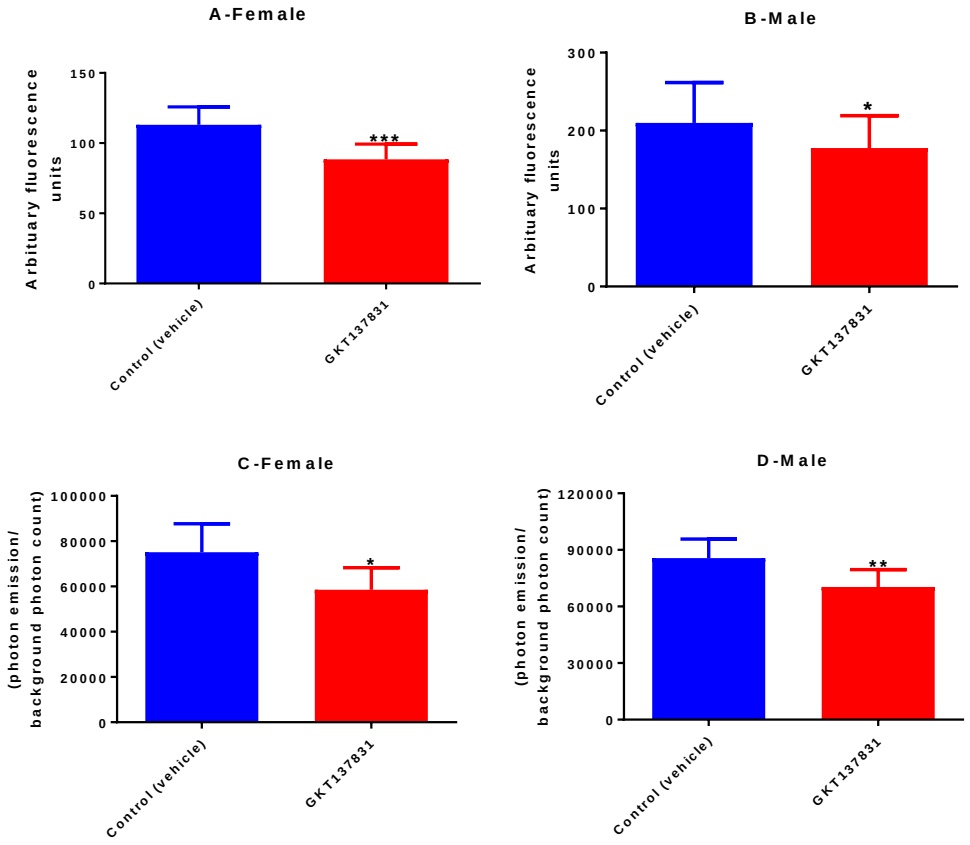


Figure 4.8: (A & B) Measurements of H_2O_2 levels in PCA homogenates using Amplex Red assay in the absence (control vehicle) or presence of 10 μM GKT137831 in PCAs from (A) female or (B) male pigs. Data are expressed as arbitrary fluorescence units and are mean ± S.E.M. of 5-6 experiments. **(C & D)** Measurement of H_2O_2 levels in PCA homogenates using luciferin-enhanced chemiluminescence assay in the absence (control vehicle) or presence of 10 μM GKT137831 in PCAs from (C) females or (D) male pigs. Data are expressed as a basal fold from tissue blank and are mean ± S.E.M. of 5-7 experiments. * P<0.05, ** P<0.01 and *** P<0.001, Student's 2-tailed, paired *t*-test vs control values.

4.3.7 Expression of Nox isoforms in PVAT

Expression of Nox1, Nox2 and Nox4 isoforms were determined in PVAT from male and female pigs using immunoblotting. A band at the predicted molecular weight of 65 kDa was detected with the anti-Nox1 antibody in PVAT from both male and female pigs, with no difference in expression (Figure 4.9). Similarly, a band at the predicted molecular weight of 60 kDa was detected with the anti-Nox2 antibody in PVAT from both male and female pigs, and again there was no difference in expression (Figure 4.10). The anti-Nox4 antibody detected a band at the predicted molecular weight of 62 kDa, with no differences in expression between male and females (Figure 4.11).

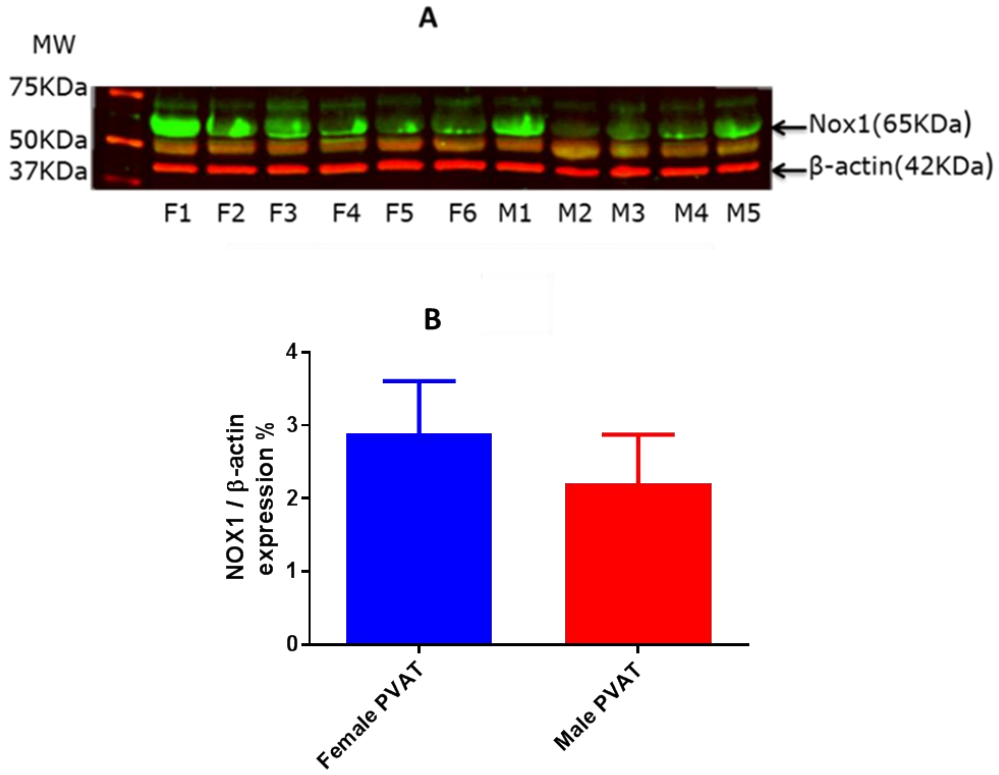


Figure 4.9: Representative immunoblot showing protein expression of the NADPH oxidase catalytic subunits: Nox1 in PVAT from female and male pigs **(A)**. Also shown is a bar chart with levels of Nox1 expressed as a percentage to the loading control β-actin **(B)**. Values are mean ± SEM of 6 females and 5 males.

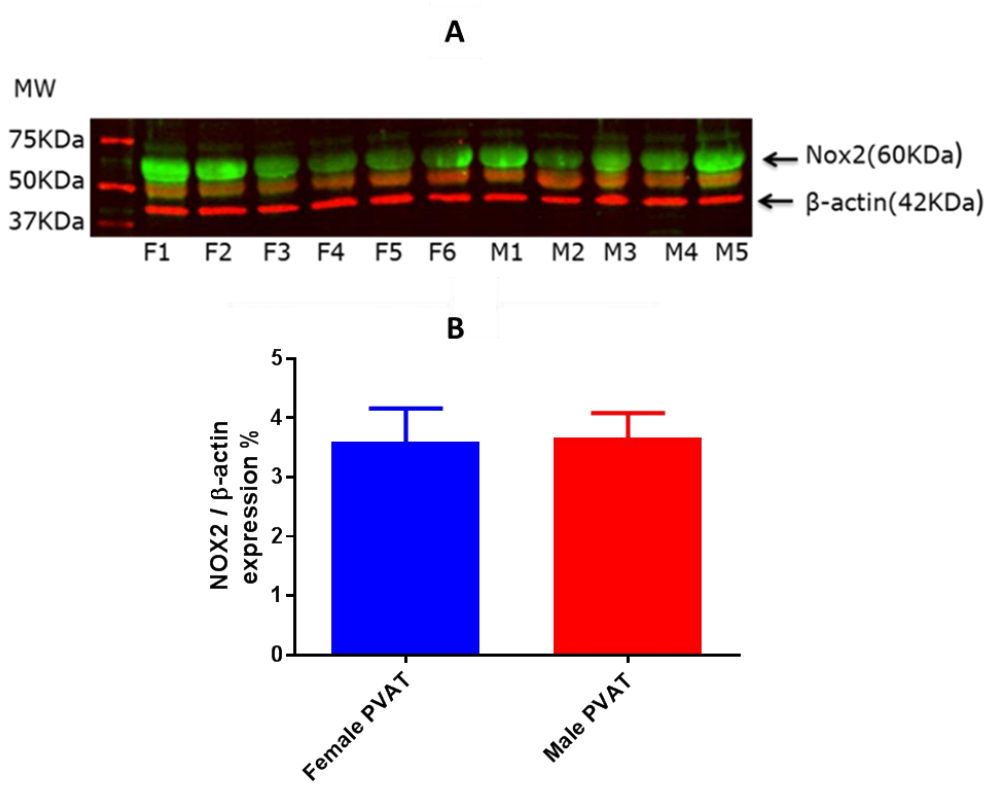


Figure 4.10: Representative immunoblot showing protein expression of the NADPH oxidase catalytic subunits: Nox2 in PVAT from female and male pigs **(A)**. Also shown is a bar chart with levels of Nox2 expressed as a percentage to the loading control β-actin **(B)**. Values are mean ± SEM of 6 females and 5 males.

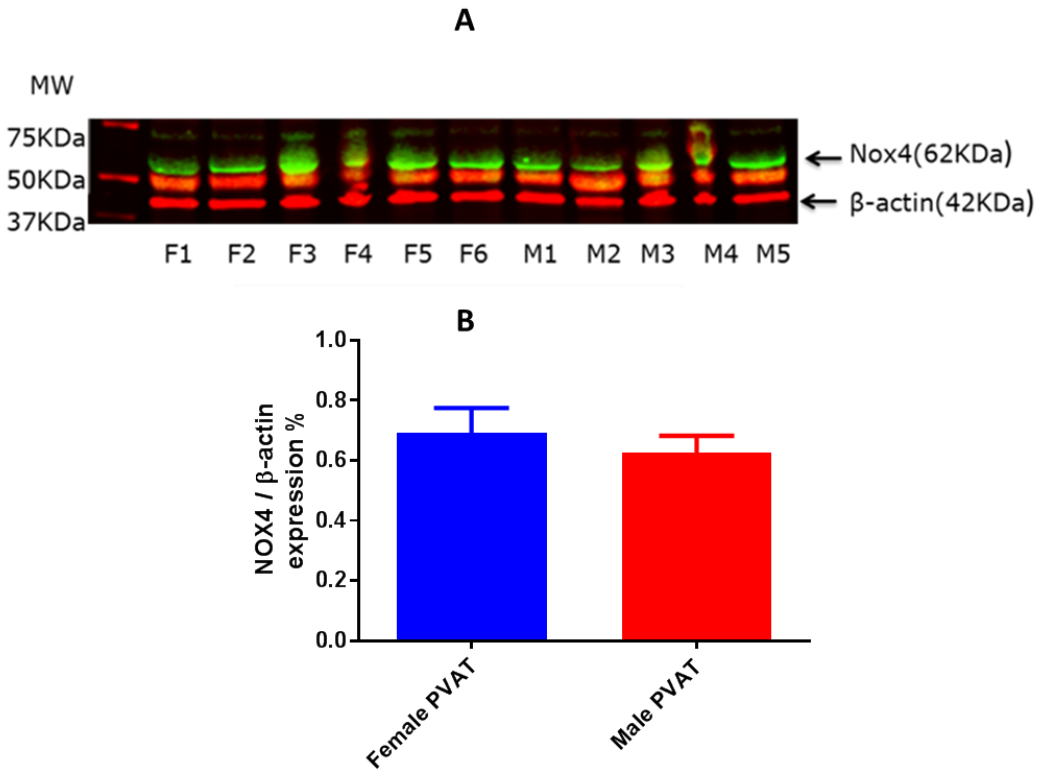


Figure 4.11: Representative immunoblot showing protein expression of the NADPH oxidase catalytic subunits: Nox4 in PVAT from female and male pigs **(A)**. Also shown is a bar chart with levels of Nox4 expressed as a percentage to the loading control β-actin **(B)**. Values are mean ± SEM of 6 females and 5 males.

4.3.8 Expression of Nox isoforms in coronary artery

As the activity of the Nox isoforms was identified in coronary arteries, the expression of Nox isoforms in PCAs was measured using Immunoblotting to confirm the effect of ROS in the coronary arteries. Bands to Nox1, 2 and 4 were also detected in porcine coronary arteries from male and female pigs. Significantly greater Nox1 expression was detected in coronary arteries from females compared to PCAs from males (Figure 4.12), whilst Nox4 expression was higher in males compared to females (Figure 4.14). There was no difference in expression of Nox2 between male and females (Figure 4.13).

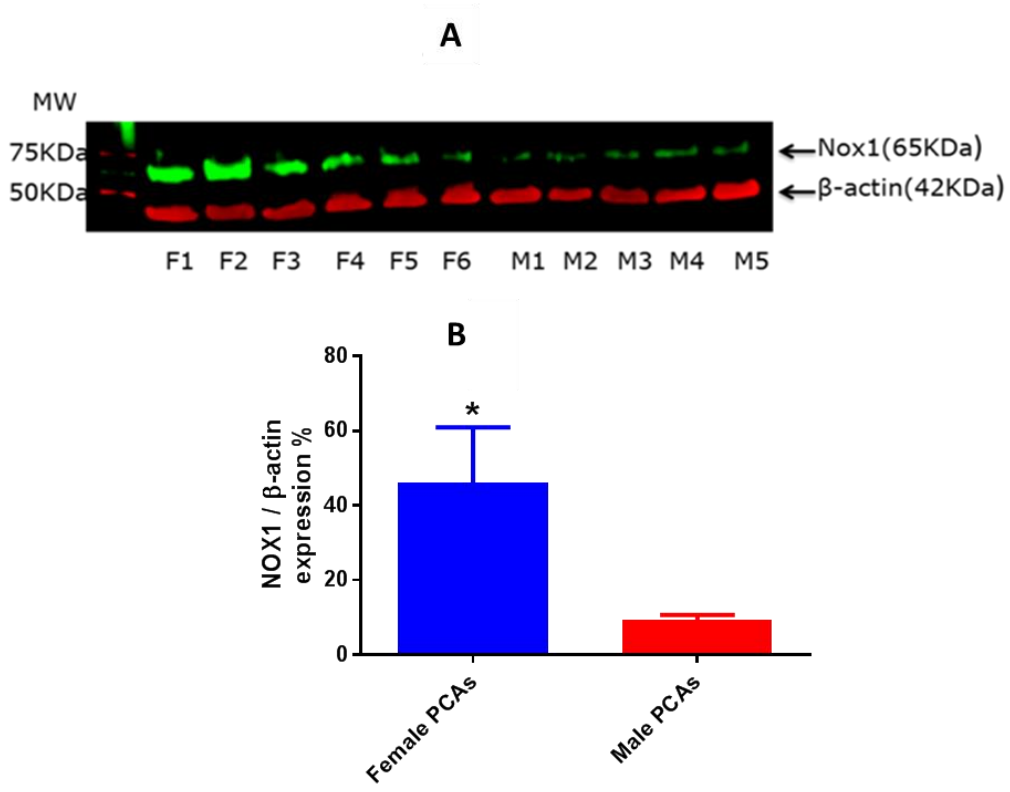


Figure 4.12: Representative immunoblot showing protein expression of Nox1 in coronary arteries from female and male pigs **(A)**. Also shown is a histogram with level of Nox1 expressed as a percentage to the loading control β-actin **(B)**. Values are mean ± SEM of 6 females and 5 males. *P<0.05, Student's 2-tailed unpaired *t*-test.

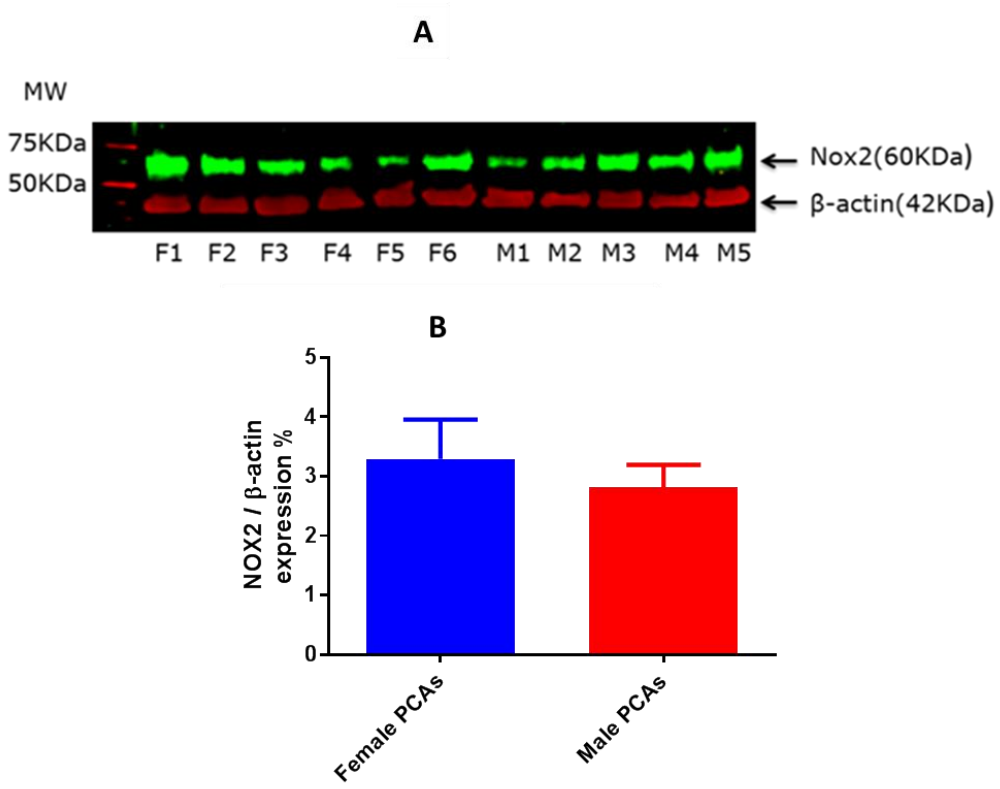


Figure 4.13: Representative immunoblot showing protein expression of Nox2 in coronary arteries from female and male pigs **(A)**. Also shown are histogram with level of Nox2 expressed as a percentage to the loading control β-actin **(B)**. Values are mean ± SEM of 6 females and 5 males.

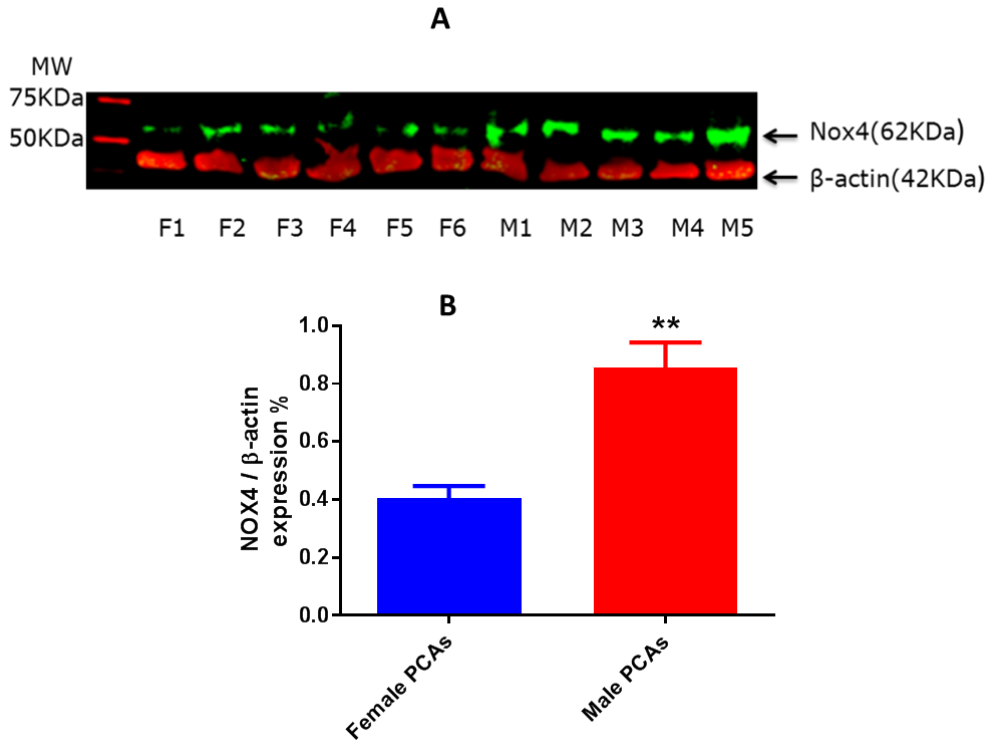


Figure 4.14: Representative immunoblot showing protein expression of Nox4 in coronary arteries from female and male pigs **(A)**. Also shown are histogram with level of Nox4 expressed as a percentage to the loading control β-actin **(B)**. Values are mean ± SEM of 6 females and 5 males. **P<0.01, Student's 2-tailed unpaired *t*-test.

4.3.9 Effects of Prostanoids on the ROS productions

4.3.9.1 Effect of U46619 on superoxide anion production

Superoxide anion production was determined in the absence and presence of U46619 in both PVAT and PCAs homogenates from both sexes to determine the effect of U46619 on ROS production. Pre-incubation with U46619 did not enhance the superoxide anion production in PVAT homogenate from both sexes (Figure 4.15 A,B) whilst pre-incubation of the PCA homogenate with U46619 caused an increase in O_2^- production in PCAs from females only (Figure 4.15 C,D). However, pre-treatment of the coronary rings with DPI inhibited the U46619-induced contraction in both sexes (Figure 4.16 A, B) whereas selective Nox1 antagonist (ML171) inhibited the contractile response to U46619 in female PCAs only (Figure 4.16 C, D).

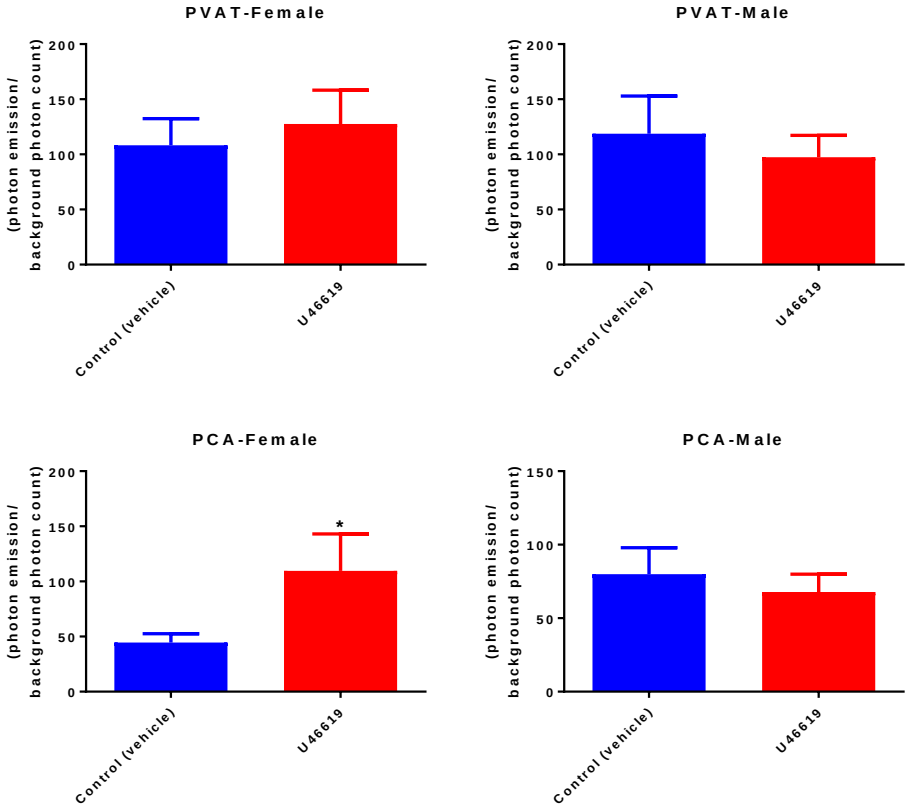


Figure 4.15: Measurement of O_2^- levels in PVAT **(A & B)** and PCA **(C & D)** homogenates using lucigenin-enhanced chemiluminescence assay in the absence (control vehicle) or presence of 100 nM U46619 in PVAT and PCAs from (A,C) females or (B,D) male pigs. Data are expressed as a basal fold from tissue blank and are mean± S.E.M. of 16-12 experiments. * P<0.05, Student's 2-tailed, paired *t*-test vs control values.

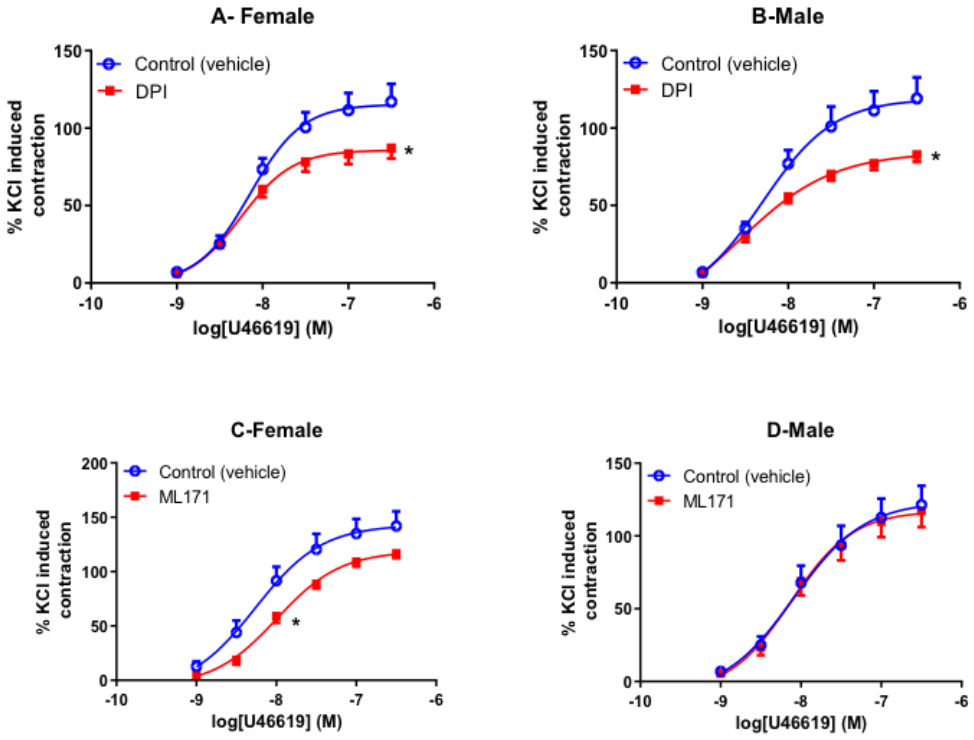


Figure 4.16: Effects of different Nox inhibitors on the U46619-induced contractions of coronary arteries from female and male pigs in the absence (control vehicle) or presence of 10 µM DPI **(A & B)** and 100 µM ML-171 **(C & D)**. Values are expressed as a percentage of the contraction to 60 mM KCl and are mean ± S.E.M. of 6 experiments. * P<0.05, 2-tailed, paired Student's *t*-test vs control values.

4.3.9.2 Effect of $PGF_{2\alpha}$ on superoxide anion production

To determine the effect of another prostanoid, $PGF_{2\alpha}$, on ROS production, superoxide anion production was determined in the absence and presence of $PGF_{2\alpha}$ in both PVAT and PCAs homogenates from both sexes. Using the lucigenin induced-chemiluminescence assay, $PGF_{2\alpha}$ had no effect on the O_2^- production in PVAT from both sexes (Figure 4.17 A,B). Like U46619, $PGF_{2\alpha}$ increased the O_2^- production in PCA homogenate from females only (Figure 4.17 C, D). Functional studies showed inhibition of the contractility of female PCAs to $PGF_{2\alpha}$ in the presence of Nox antagonists (DPI and ML171) compared to vehicle control (Figure 4.18 A, B) while there was no effect of the same antagonists on the $PGF_{2\alpha}$-induced contraction of male PCAs (Figure 4.18 C, D).

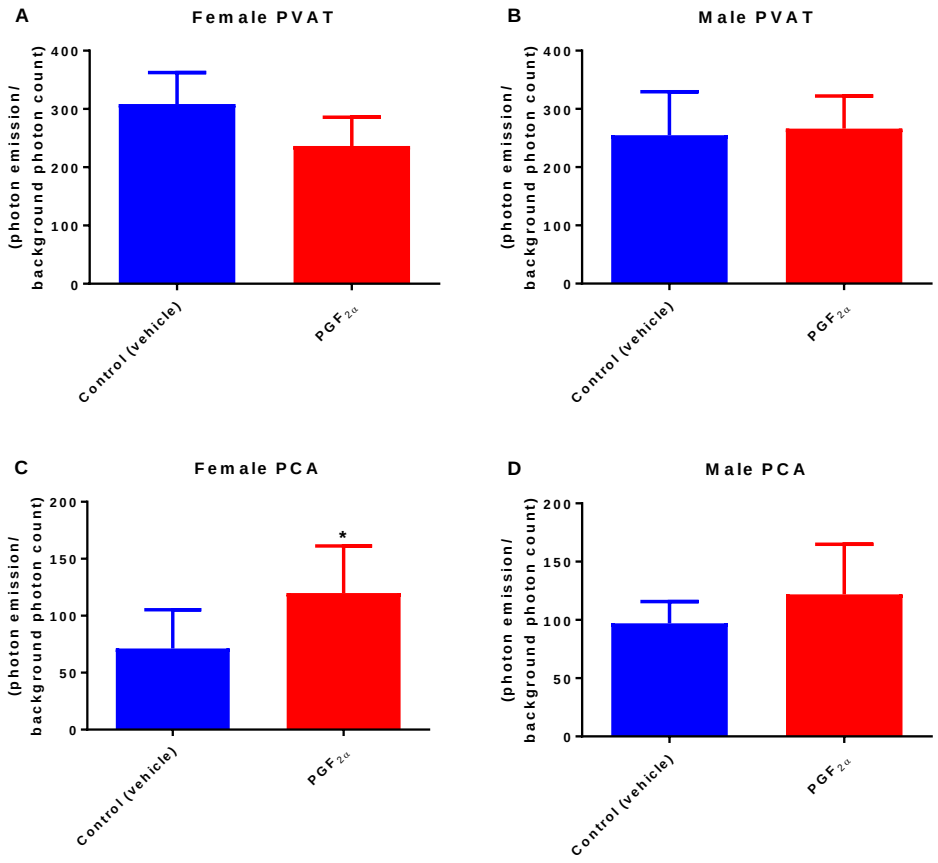


Figure 4.17: Measurement of O_2^- levels in PVAT **(A & B)** and PCA **(C & D)** homogenates using lucigenin-enhanced chemiluminescence assay in the absence (control vehicle) or presence of 1 μM $PGF_{2\alpha}$ in PVAT and PCAs from (A,C) females or (B,D) male pigs. Data are expressed as a basal fold from tissue blank and are mean ± S.E.M. of 8 experiments for all graphs. * P<0.05, Student's 2-tailed, paired *t*-test vs control values.

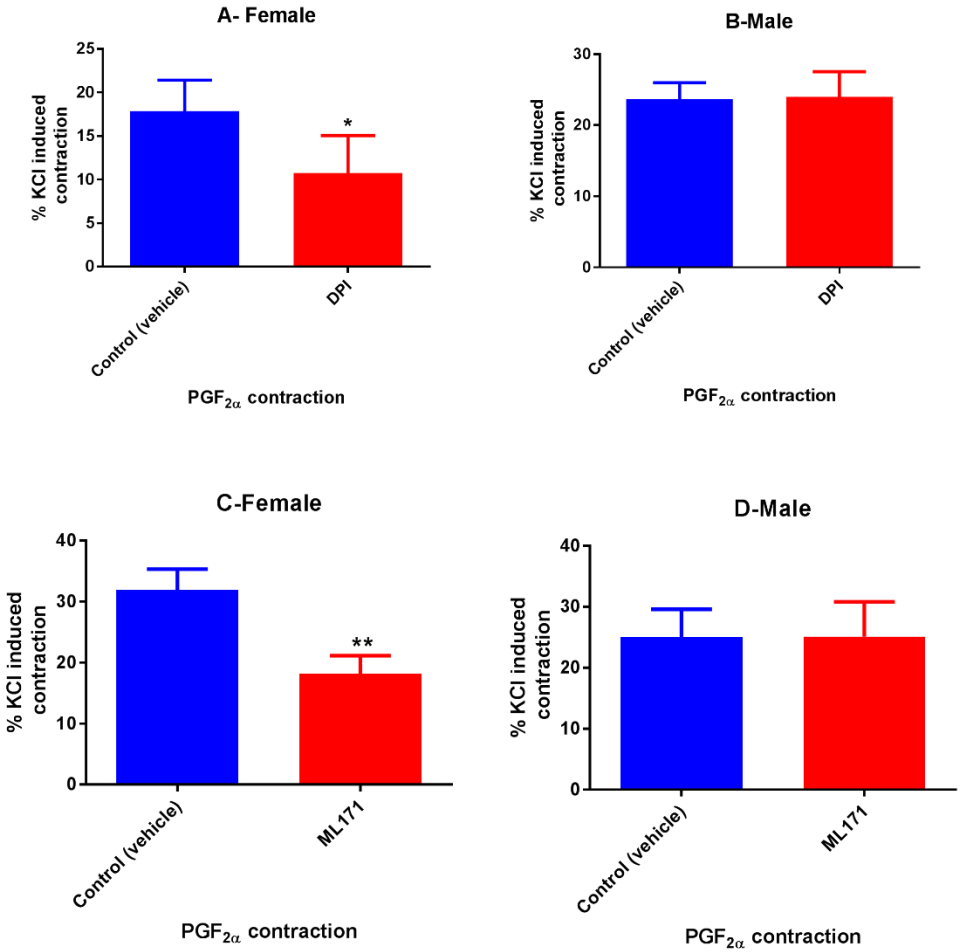


Figure 4.18: Effects of different Nox inhibitors on the 1µM $PGF_{2\alpha}$-induced contraction of coronary arteries from female and male pigs in the absence (control vehicle) or presence of 10 µM DPI **(A & B)** and 100 µM ML-171 **(C & D)**. Values are expressed as a percentage of the contraction to 60 mM KCl and are mean ± S.E.M. of 6 experiments for all graphs. * P<0.05, Student's 2-tailed, paired *t*-test vs control values.

4.3.10 Effect of LPS on PVAT function

To investigate the effects of inflammation on the function of PVAT in production of ROS, PVAT pieces were incubated with and without 5 µg/ml of LPS for 4hrs, and then H_2O_2 and O_2^- production are measured. Pre-incubation of PVAT with LPS significantly enhanced H_2O_2 production in PVAT from both sexes (Figure 4.19 A,B). However, the same pre-treatment did not affect the O_2^- production in PVAT from both sexes (Figure 4.20 A,B).

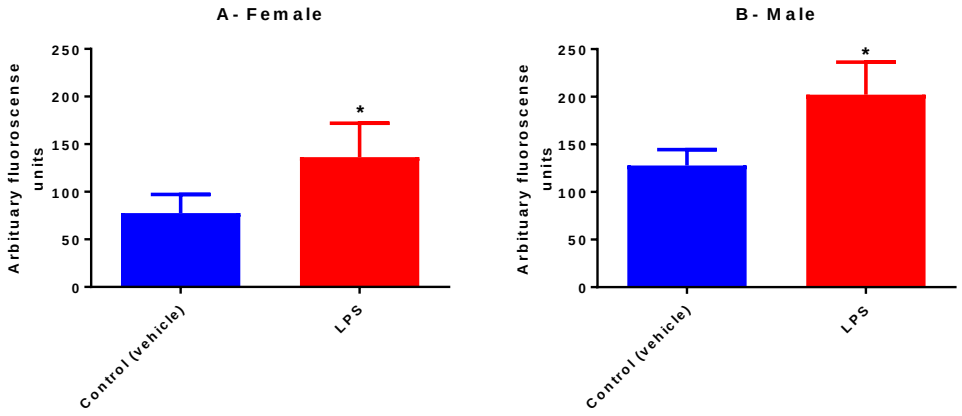


Figure 4.19: Measurement of H_2O_2 levels in the PVAT homogenate using Amplex Red assay after pre-incubation without (control vehice) or with 5 µg/ml (LPS) in **(A)** female and **(B)** male pigs. Data are expressed as arbitrary fluorescence units and are mean ± S.E.M. of 6 experiments. * P<0.05, paired Student *t*-test vs control values.

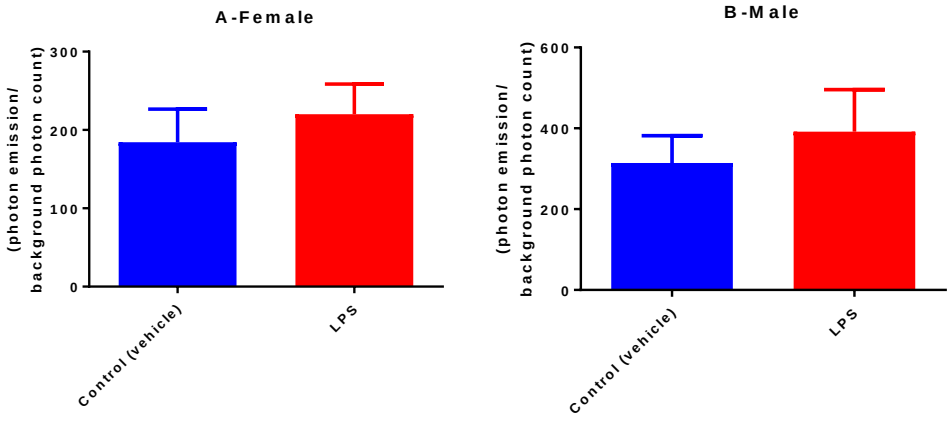


Figure 4.20: Measurement of O_2^- production using lucigenin-enhanced chemiluminescence method in PVAT homogenates after pre-incubation without (control vehicle) or with 5 µg/ml lipopolysaccharide (LPS) in **(A)** female and **(B)** male pigs. Data are expressed as a basal fold from tissue blank and are mean ± S.E.M. of 5-6 experiments vs control values.

4.4 Discussion

Reactive oxygen species (ROS) play an important role in both physiology and pathophysiology of the vasculature, including hypertension, and can cause either vasodilatation or vasoconstriction, depending on the species produced (Montezano and Touyz, 2014). The NADPH oxidase (Nox) family of enzymes is an important source of ROS within the vasculature. Sex differences have been previously demonstrated in the expression of Nox isoforms in the porcine coronary artery, which correlate with sex differences in the role of ROS in the regulation of endothelium-dependent vasodilatation (Wong *et al.*, 2015a). Adipose tissue is an important source of ROS and previous studies have demonstrated that Nox-derived ROS released from the adipose tissue surrounding blood vessels can regulate blood vessel tone (Gao *et al.*, 2006). Indeed, ROS may play a role in bi-directional signalling between coronary artery PVAT and the vascular smooth muscle (Antonopoulos *et al.*, 2015). Noteworthy, no previous study has specifically addressed whether sex influences the activity of different Nox isoforms in PVAT in the coronary circulation. In this chapter, sex differences in Nox expression and ROS production in the PVAT surrounding the coronary arteries were investigated. Furthermore, it was determined whether there were sex differences in the regulation of tone by PVAT-derived ROS. This chapter has showed that the PVAT-induced contraction of the porcine coronary artery is dependent upon Nox activity, although there are no sex differences in this response. The source of the ROS could be either the PVAT or the coronary artery itself as both express Nox isoforms.

ROS regulate vascular tone and, depending on the ROS produced (hydrogen peroxide or superoxide anion), can elicit both vasorelaxant and vasoconstrictor effects (White *et al.*, 2005; Wong *et al.*, 2014a). A previous study in rat superior mesenteric artery indicated that PVAT could produce ROS to enhance vascular tone (Gao *et al.*, 2006). However, non-selective Nox inhibitors (apocynin and DPI) were used to elucidate the role of ROS. In fact, no previous study has specifically addressed which Nox isoforms are expressed in PVAT and, therefore, which isoforms are involved in the regulation of vascular tone by PVAT.

In order to determine the role of Nox-derived ROS in the regulation of coronary artery tone by PVAT, segments of porcine coronary artery with fat removed were set up in isolated tissue baths and treated with the Nox inhibitors prior to re-addition of PVAT. Addition of PVAT produced a slow developing contraction in line with chapter 3 and other experiments in the porcine coronary artery (Owen *et al.,* 2013). The antioxidant N-acetylcysteine reduced the contraction in coronary arteries from male and female pigs (Figure 4.1). These data suggest that the PVAT-induced contraction in the coronary circulation is mediated, in part, by endogenous ROS. Pre-incubation with the non-selective Nox inhibitor DPI completely inhibited the PVAT-induced contraction (Figure 4.2), indicating a role for Nox-derived ROS in the contractile response. The Nox1 inhibitor ML171 produced a partial inhibition of the contraction (Figure 4.3 A,B), whereas the Nox2 inhibitor phox-I2 caused complete inhibition of the contraction (Figure 4.3 C,D), indicating a role for Nox1 and Nox2 in the response. It is possible that phox-I2 inhibits Nox1 as well as Nox2, which would explain why there is complete inhibition with this compound, but only partial inhibition with ML171. There was no apparent difference in the effect of ML171 and phox-I2 between tissues from male and female animals. The Nox1/4 inhibitor GKT137831 also caused partial inhibition of the PVAT-induced contraction in both male and females (Figure 4.3 E,F).

These data indicate a role for Nox-derived ROS in PVAT-induced contraction in the porcine coronary artery. The source of the ROS could be from either the PVAT or the artery itself. In an attempt to clarify the source, the expression and activity of the Nox isoforms were investigated in the PVAT and the artery. In this study, protein expression of all three Nox isoforms (Nox1, Nox2 and Nox4) was identified in the PVAT from both sexes (Figures 4.9, 4.10, 4.11). To measure ROS production, lucigenin-stimulated chemiluminescence and Amplex Red were used to detect O_2^- and H_2O_2, respectively. Lucigenin-enhanced chemiluminescence assay is used because it is one of the most sensitive and convenient methods to detect ROS released from various cells (Minkenberg and Ferber, 1984; Caldiz *et al.,* 2007). The lucigenin-enhanced chemiluminescence has been widely shown to be a useful method for detecting and quantifying the O_2^- formation in comparison with other methods of ROS

detection such as NBT reduction, O_2 consumption and cytochrome c reduction as the lucigenin probe is very sensitive to ROS (Yamazaki *et al.*, 2011). Amplex Red is a highly sensitive and stable substrate for horseradish peroxidase (HRP) with selectivity for H_2O_2 allowing measurement of H_2O_2 at concentrations as low as 50 nM. This property made the Amplex Red a commonly used technique for measurement of low levels of H_2O_2 in different biological samples. Another advantage of this assay is that HRP is active over a wide pH range (Rhee *et al.*, 2010). Using lucigenin, NADPH-stimulated chemiluminescence that was inhibited by the Nox inhibitor diphenyleneiodonium (DPI) was detected, indicating a Nox-mediated production (Figure 4.4). Chemiluminescence was also reduced using the selective Nox1 inhibitor ML171 and the selective Nox2 inhibitor Phox-I2 (Figure 4.5), indicating a role for Nox1 and Nox2, correlating with expression. There was no difference in either expression or activity between males and females. Although Nox4 expression was detected in PVAT, there was no evidence for Nox4-induced ROS production since the Nox1/4 inhibitor GKT137831 had no effect on lucigenin chemiluminescence (Figure 4.5 E,F). Nox4 produces H_2O_2 (Nisimoto *et al.*, 2014). Therefore, the effect of GKT137831 on H_2O_2 production was determined using Amplex Red. Again, GKT137831 had no effect on the Amplex Red signal (Figure 4.6), indicating that there is no detectable Nox4 activity under these conditions.

Nox1, 2 and 4 were also expressed in the porcine coronary artery. Again, NADPH-stimulated lucigenin chemiluminescence was measured, which could be inhibited by DPI, the Nox1 inhibitor ML171 and the Nox2 inhibitor phox-I2 (Figure 4.7). Although there was a greater expression of Nox1 in arteries from females compared to males (Figure 4.12), NADPH-stimulated chemiluminescence in arteries from both male and females was inhibited by ML171 (Figure 4.7). Furthermore, this difference in Nox1 expression did not correlate with the sensitivity of the PVAT-induced contraction to ML171, in that the contraction in males appeared to be inhibited more by ML171 than females. Nox4 expression was higher in coronary arteries from males compared to females (Figure 4.14). However, there was no apparent difference in sensitivity of H_2O_2 production to GKT137831. GKT137831 is a dual Nox1/4 inhibitor. Therefore, it is possible that the increase in expression of Nox4 in arteries from

males is balanced by the increase in Nox1 expression in females in this case. Noteworthy, a previous study conducted on the distal part of the coronary arteries, not the proximal portion like in the present study, showed a different profile of expression of these three enzymes (Wong *et al.*, 2015a). The authors showed that Nox1 and Nox2 expression in PCAs was higher in males compared to females whilst Nox4 was higher in females. The differences may be due to differences in the thickness and diameter of these two parts. On the other hand, PVAT is present mostly around the proximal PCA. This can raise an interesting question; could the existence of PVAT be a possible cause of the variation in Nox isoform expression between these different anatomical positions? It is for future work to identify the variation in the signalling in these different parts of the coronary artery.

The data presented here indicate that PVAT-induced contractions are mediated by release of ROS. Although Nox isoforms are expressed in both PVAT and the coronary artery, it is not possible to determine which the source of ROS leading to the contraction is. It is possible that a substance released from PVAT stimulates the production of ROS in the coronary artery in order to initiate a contraction. TP stimulation can increase the production of ROS and peroxynitrites by up-regulating PKC-dependent Nox activation in bovine aortic endothelial cells. (Zhang *et al.*, 2011). In addition, Martinez-Revelles *et al.*, (2013) showed that COX2 inhibitor celecoxib could normalize the increased O_2^- - and H_2O_2 production, (Nox1, Nox2 and Nox4) expression and activity, and the participation of ROS in vascular responses in hypertensive models (Martinez-Revelles *et al.*, 2013). The same group presented a review indicating that these two pathways act in concert to induce vascular dysfunction (Hernanz *et al.*, 2014). Furthermore, it was previously demonstrated in Chapter 3 that the prostanoids TXA_2 and $PGF_{2\alpha}$ are expressed and released from PVAT and play a role in the PVAT-induced contraction in porcine coronary arteries. Therefore, it was determined whether these compounds stimulate ROS production in PVAT or PCAs and whether the contractile response to these compounds involves Nox activity. Neither the thromboxane mimetic U46619 and $PGF_{2\alpha}$ increased ROS production in PVAT but both compounds could significantly enhance the ROS production in female PCAs only, but not male PCAs (Figure 4.15, 4.17). The

contractility response of PCAs to U46619 was reduced in both sexes in the presence of DPI, and in females only in the presence of ML171 (Figure 4.16). Although DPI inhibited the U46619 contraction in both sexes, this could be explained by the fact that DPI could cause endothelium-independent relaxation by activation of the guanylate cyclase, which is independent of Nox inhibition (Dodd-o *et al.*, 1997), and particularly because of the ability of the cGMP to phosphorylate TXA_2 receptor, resulting in feedback inhibition (Wang *et al.*, 1998). In addition, both DPI and ML171 could inhibit $PGF_{2\alpha}$–induced vasoconstriction in females PCAs only (Figure 4.18). These data suggest a significant role of ROS, at least partly, in the TXA_2 and $PGF_{2\alpha}$-induced vasoconstriction in females only. Taking all the data together, it is proposed for the first time that the ROS-dependency of the PVAT-induced contraction is as a result of release of prostanoids from the PVAT which subsequently produce a ROS-dependent contractile response in the PCA from female, rather than PVAT-derived ROS mediating the contractile response.

In addition, Chapter 6 has showed that another adipocyte-derived compound chemerin can also signal through Nox in vascular smooth muscle cells, a finding that is supported by the study of (Neves *et al.*, 2015) (see Chapter 6). Although the roles of prostanoids and chemerin are identified as contractile agents which are derived from PVAT and could induce the ROS-mediated vasoconstriction, other adipocytes-derived constrictor factors cannot be excluded. Angiotensin II, for instance, stimulates Nox-dependent production of ROS in smooth muscle cells (Nguyen Dinh Cat and Touyz, 2011), and it has also been implicated in the regulation of vascular tone by PVAT (Lu *et al.*, 2010).

PVAT has been found to be altered by expanding and accumulating inflammatory cells in pathophysiological conditions, such as obesity and diabetes, altering the production of various adipokines and inflammatory cytokines (Brown *et al.*, 2014). For instance, endovascular wire injury caused marked downregulation of adiponectin expression and upregulation of proinflammatory cytokines, such as monocyte chemoattractant protein-1 (MCP-1), TNF-α, IL-6, and plasminogen activator inhibitor type-1, in PVAT (Takaoka *et al.*, 2010). PVAT-induced contractions in coronary arteries are enhanced in obese pigs (Owen *et al.*, 2013). Furthermore, alterations in PVAT signalling in

blood vessels from overweight patients with type 2 diabetes are associated with increases in Nox activity in vascular smooth muscle (Antonopoulos *et al.*, 2015). Indeed, obesity leads to the development of an inflammatory phenotype in adipose tissue (Calabro and Yeh, 2007). In addition, inflammation is considered as one of the reasons for enhancing generation of ROS (Yang *et al.*, 2007). So increased Nox expression and activity in PVAT may also influence the contractile effects on PVAT in the coronary circulation. To study the effect of inflammation on PVAT, lipopolysaccharide from Escherichia coli (LPS) was used. Bacterial LPS has been extensively used in models studying inflammation because of its ability to stimulate production of different proinflammatory cytokines, such as TNF-α, IL-1β or IL-6 (Ngkelo *et al.*, 2012). Using LPS to stimulate inflammation in PVAT, the data in the present study demonstrate that LPS could enhance H_2O_2 production in PVAT from both sexes (Figure 4.19). However, there was no effect of LPS on the O_2^- generation in PVAT from either sex (Figure 4.20). In addition, a pilot study attempted to address the effect of LPS on the contractility response of PCAs. However, LPS inhibited PVAT-induced contraction rather than enhance PVAT-induced vasoconstriction, as expected (Appendix C). The latter result could be explained by the enhancement of nitric oxide synthase (NOS) activity (McKenna, 1992; Nakayama *et al.*, 1992) or/and the inhibition of Ca^{2+} influx via L-type calcium channel (Hobai *et al.*, 2015).

In summary, this study demonstrates that PVAT from coronary artery initiates vasoconstriction through Nox-dependent ROS production. Both PVAT and the artery itself express Nox isoforms and Nox-dependent ROS production can be measured in both tissues. TXA_2 and $PGF_{2\alpha}$ could enhance vasoconstriction via increasing ROS production in females only. As PVAT can release these prostanoids and increase the vascular tone of PCAs (Chapter 3), it also can be concluded that PVAT can induce vasoconstriction by releasing prostanoids that enhance the ROS activity in PCAs from females only. Despite sex differences in the expression of Nox isoforms in the porcine coronary artery, there was no difference in the role of Nox isoforms in the PVAT-induced contraction between male and female animals.

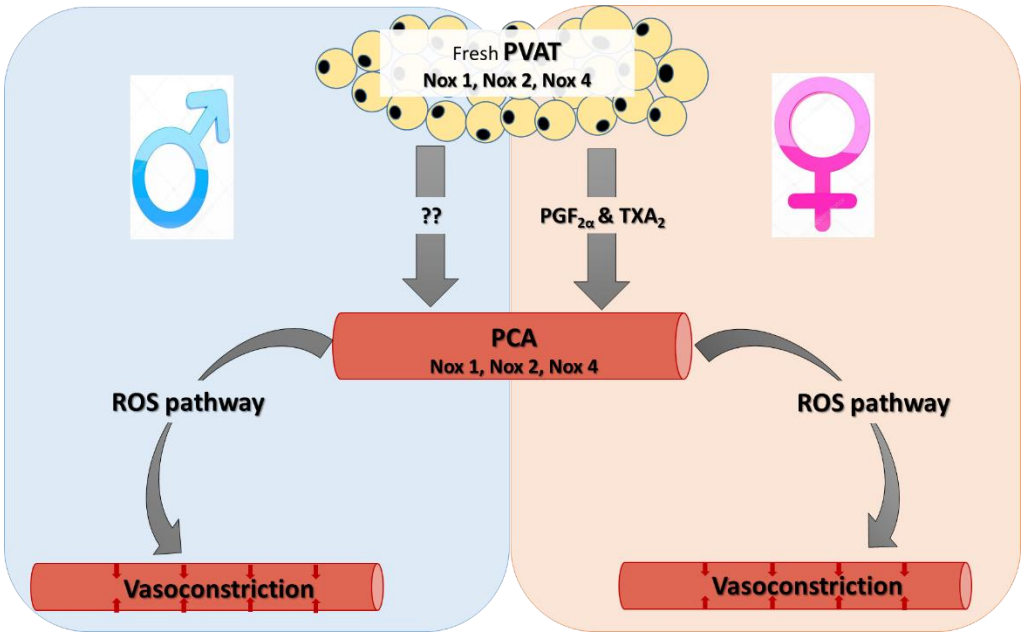


Figure 4.16 Hypothesized schematic diagram of sex differences in the contractile response of PCA to fresh PVAT. Present study demonstrated that PVAT can mediate vasoconstriction in PCAs via reactive oxygen species pathway in both sexes with thromboxane A_2 (TXA_2) and $PGF_{2\alpha}$ as ADCFs that could induce this pathway in females only.

Chapter Five

Effects of sexual dimorphism on the role of perivascular adipose tissue-derived chemerin in the regulation of vascular tone of porcine coronary artery

5.1 Introduction

Chemerin is a 16 kDa protein that was discovered in 1997 (Nagpal *et al.*, 1997) and is known to has a role in the maintenance of the normal physiology of the skin. Chemerin (also known as retinoic acid receptor responder gene 2, RARRES2) acts as a chemoattractant for monocytes and macrophages (Nagpal *et al.*, 1997; Samson *et al.*, 1998), with well-established roles in inflammation and obesity (Sell *et al.*, 2010; Chakaroun *et al.*, 2012; Landgraf *et al.*, 2012). Chemerin is present in many isoforms such as chemerin F^{156} (Meder *et al.*, 2003), chemerin K^{158} (Zhao *et al.*, 2011), chemerin A^{155} (Zabel *et al.*, 2005) and the most active form chemerin S^{157} (Yamaguchi *et al.*, 2011).

Elevated levels of chemerin have been positively correlated with coronary artery disease (Lin *et al.*, 2012), pre-eclampsia (Stepan *et al.*, 2011), metabolic syndrome (Dong *et al.*, 2011), renal dysfunction, and may be predictive for other cardiovascular events (Leiherer *et al.*, 2016). In addition, a recent study in humans has showed a positive correlation between chemerin and LDL cholesterol and a negative correlation between chemerin and HDL cholesterol levels in obese patients (Lorincz *et al.*, 2014). In addition to the discovery of multiple receptors for chemerin and a vast collection of associations with various pathologies, chemerin has a global role in human physiology and pathology by regulating chemotactic, adipogenic and angiogenic functions (Ferland and Watts, 2015). Goralski *et al.*, (2007) have found that chemerin/CMKLR1 axis has a critical role in signalling in adipocytes by regulating adipogenesis and metabolic homeostasis. CMKLR1 expression and chemerin expression and secretion increased with adipogenesis (Goralski *et al.*, 2007). In addition, chemerin could induce endothelial angiogenesis in human endothelial cells by activating MAPK and Akt kinases pathways (Kaur *et al.*, 2010). Although the epidemiology and associations between chemerin and different pathological conditions is being investigated, knowledge of its general mechanisms of action has yet to be fully established.

As discussed in the General Introduction, PVAT dysfunction is a major factor in the pathogenesis of many cardiovascular diseases (CVD) including hypertension and atherosclerosis. For instance, there is evidence that increased PVAT mass around coronary artery has been linked with increased prevalence

of CVD (Mahabadi *et al.*, 2010; Nakamura *et al.*, 2014). Watts and co-workers have characterized the role of chemerin in PVAT and highlighted the correlation between PVAT-derived chemerin and augmentation of the vascular tone of thoracic aorta of mice and rats, and superior mesenteric arteries of rats (Watts *et al.*, 2013). They found that chemerin can amplify electrical field-stimulated contraction through activation of the chemerin receptor, ChemR23, in the isolated rat superior mesenteric artery (Darios *et al.*, 2016).

Sex-related differences have been suggested to contribute to the risk for cardiovascular diseases in association with obesity and metabolic syndrome (Coatmellec-Taglioni *et al.*, 2002; Lima *et al.*, 2012). A recent report demonstrated sex differences in chemerin mRNA expression levels of subcutaneous adipose tissue, with expression significantly higher in women than men (Alfadda *et al.*, 2012). However, sex differences in the role of PVAT-derived chemerin in vascular regulation has not been determined. Therefore the aim of the present study was to investigate the influence of the sex on the PVAT-derived chemerin in regulating the isolated porcine coronary arterial tone.

5.2 Materials and Methods

5.2.1 Tissue preparation

Tissues were set up as previously described in Chapter 2.

5.2.2 Functional responses in the isolated porcine coronary arteries

The method is described in Chapter 2. Cumulative concentration-response curves to chemerin-9 (100 nM-30 μM) were constructed in coronary arterial segments from male and female pigs. To investigate the role of ROS in chemerin-induced vasoconstriction, coronary segments were incubated with ML171 (100 μM) as a Nox1 inhibitor (Gianni *et al.*, 2010) for an hour before adding a single concentration (10 μM) of chemerin-9 to U46619-precontracted vessels. Pre-incubation with a chemerin antibody (1:500; ABIN1857924, Antibodies-online Inc., Atlanta, USA) was performed to determine the role of chemerin in PVAT-induced vasoconstriction. Additionally, other experiments were performed to determine the role of chemerin in U46619-induced vasoconstriction. Cumulative concentration-response curves to the U46619 (1

nM-300 nM) were constructed in the presence or absence of chemerin antibody in coronary artery segments from pigs. DMSO (0.1% v/v) was used as vehicle controls, as appropriate.

5.2.3 Determination of levels of mRNA expression of chemerin and ChemR23 by RT-PCR.

RNA was extracted from PVAT and PCA using Tri-Reagent (Sigma-Aldrich, USA) and purified with RNeasy (Qiagen, Valencia, CA) columns. RNA was quantitated using the NanoDrop 2000 (Thermo Scientific, USA) spectrophotometer. cDNA was prepared by reverse transcription (RT) reaction from 500 ng total RNA using the Affinity Script Multiple Temperature Reverse Transcriptase (Agilent Technologies, USA) according to the manufacturer's instructions. Chemerin and ChemR23 expression levels were quantified by RT-PCR using the SYBR Green master mix kit (Applied Biosystem, USA). Primers for PCR amplifications were ordered from Eurofins Genomics (Ebersberg, Germany). Primer sequences are listed in Appendix E. qRT-PCR was carried out using an Applied Biosystem Step OnePlus™ Thermocycler for 40 cycles. In this study, relative expression levels were determined using the relative standard curve method. Relative gene expression was normalized to the housekeeping gene, glyceraldehyde-3-phosphate dehydrogenase (GAPDH). Results are expressed as the mean ± SEM of the C_T value obtained.

5.2.4 Quantification of NADPH oxidase activity by lucigenin chemiluminescence assay

The method is previously described in Chapter 4. However, in this chapter, equal amount of supernatant (30 µl) was incubated at 37°C for 20 min in the absence or presence of 30 µM chemerin with a final concentration of 5 µM lucigenin.

5.2.5 Statistical analysis

Data are presented and analysed as described in Chapter 2.

5.2.6 Materials

Chemerin-9 was purchased from GenScript (cat # RP20248; Piscataway, NJ, USA) while ML171 from Tocris Bioscience (Bristol, UK). Stock solutions of chemerin-9 was dissolved in distilled water whereas DPI was dissolved in dimethyl sulfoxide (DMSO).

5.3 Results

5.3.1 Responsiveness of PCAs to chemerin-9

To investigate the sensitivity of coronary arteries to chemerin, cumulative concentration-response curves to chemerin-9 were conducted on PCAs segments from females and males. The responsiveness of female PCAs to chemerin-9 was greater compared to male PCAs (females: 18.4 ± 7.1% of KCl; males: 8.6 ± 1.1% of KCl) (Figure 5.1).

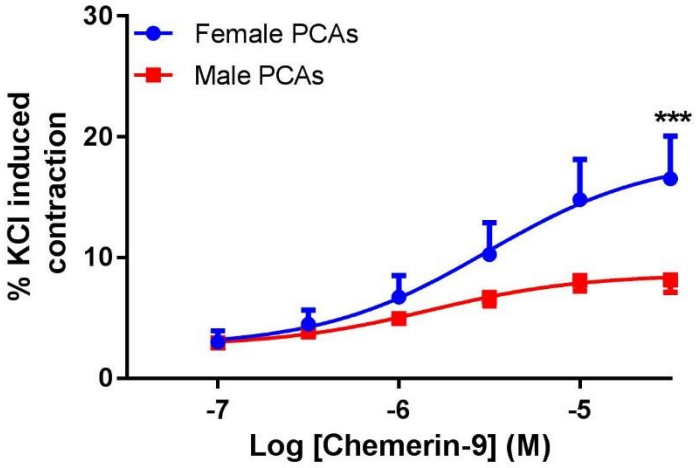


Figure 5.1: Log concentration-response curves for the vasoconstrictor effects of chemerin-9 in coronary arteries from female (n=6) and male (n=9) pigs. Data are expressed as a percentage of the contraction to 60 mM KCl and are mean ± S.E.M. of experiments. *** indicates P<0.001, 2-tailed, unpaired Student's *t*-test.

5.3.2 ROS production by chemerin-9

In order to determine whether chemerin can act through activation of Nox enzyme, ROS production have been measured in the presence and absence of chemerin-9 in coronary arteries from both sexes. Chemerin-9 evoked a significant ROS production in homogenates of female PCAs compared to their respective controls whilst no enhancement was noticed in homogenate of male arteries (Figure 5.2).

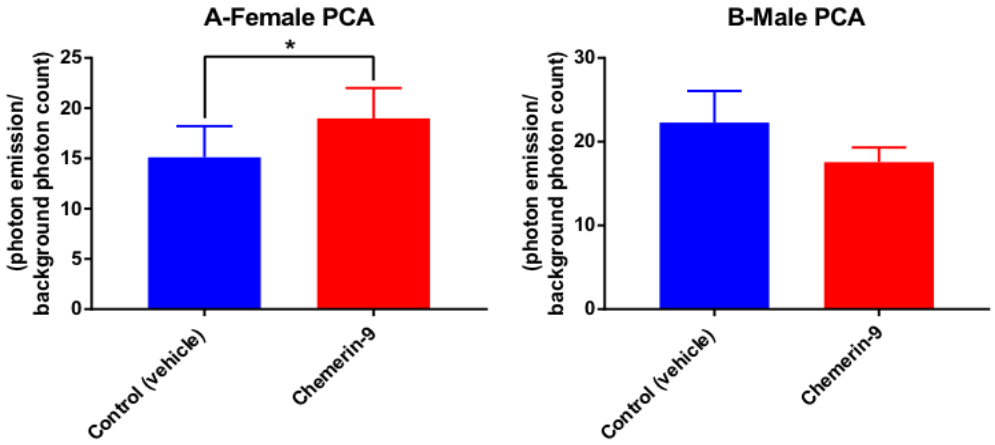


Figure 5.2: NADPH oxidase activity determined using lucigenin-enhanced chemiluminescence method in PCA homogenates from female **(A)** and male **(B)** pigs. After 20 min incubation without (control vehicle) or with 30 µM chemerin-9 and 5 µM lucigenin, 100 µM NADPH was added and measurements were taken in an interval of 10 s per well. Data are expressed as a basal fold from tissue blank and are mean± S.E.M. of 6(A)-5(B) experiments. * P<0.05, 2-tailed, paired Student's *t*-test vs control values.

5.3.3 The effects of Nox antagonist on chemerin9-induced vasoconstriction in PCAs

As chemerin only produced ROS in PCAs from females, then the role of Nox in the chemerin-9 -induced contraction was determined. Therefore, coronary arterial segments were pre-incubated with ML171 (100 µM) prior to addition of chemerin-9. Pre-incubation with the Nox inhibitor inhibited the PVAT-induced contractions in PCA from females, but not males (Figure 5.3).

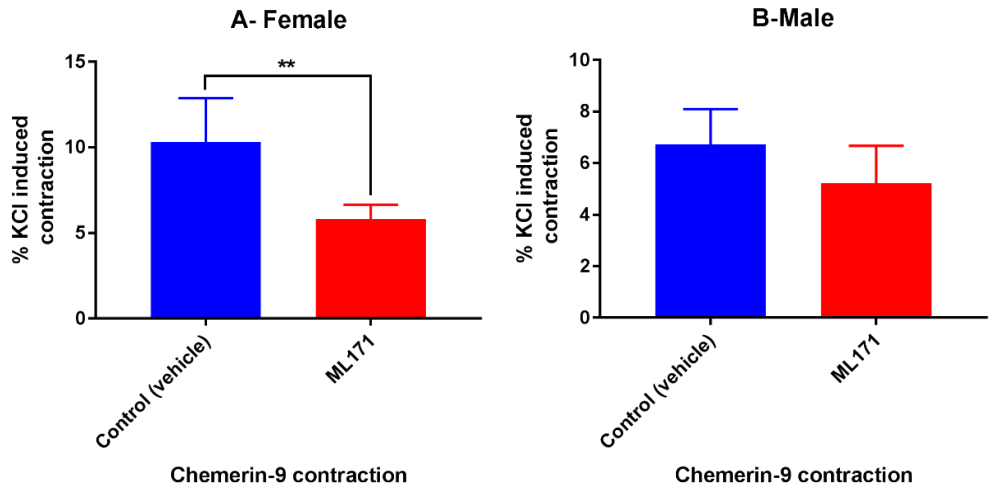


Figure 5.3: Effects of Nox inhibitor on the chemerin-9 (30 µM)-induced contraction of coronary arteries from female **(A)** and male **(B)** pigs in the absence (control vehicle) or presence of 100 µM ML171. Values are expressed as a percentage of the contraction to 60 mM KCl and are mean ± S.E.M. of 8 (A) and 6 (B) experiments. ** P<0.01, 2-tailed, paired Student's *t*-test vs control values.

5.3.4 mRNA expression of chemerin and ChemR23

mRNA expression of ChemR23 in PCAs from both sexes was determined using RT-PCR in order to investigate whether differences in the contractile response to chemerin could be due to the sex difference in expression of the chemerin receptor, and, as a comparison, mRNA of chemerin in PVAT was also examined. RT-PCR confirmed the expression of chemerin (RARRES2) mRNA in the PVAT and ChemR23 receptor (CMKLR1) mRNA in porcine coronary arteries. However, there were no significant sex differences in the expression of either chemerin or its receptor ChemR23 (Figure 5.4 A, B).

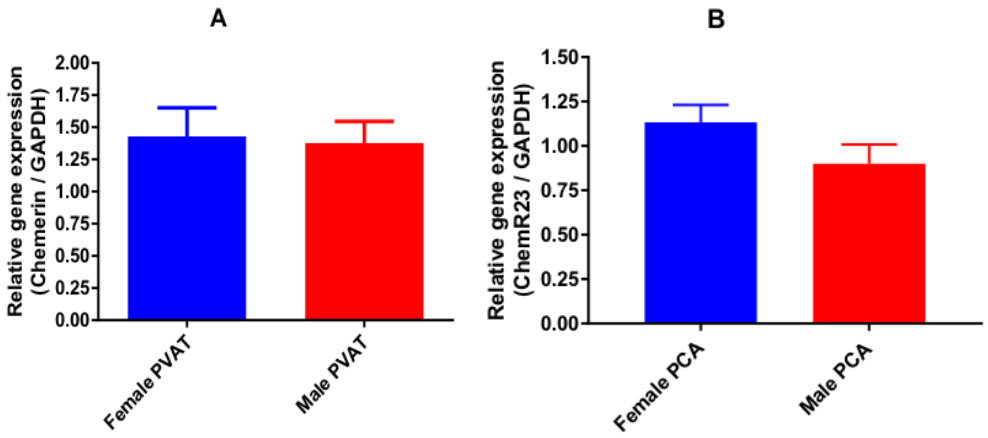


Figure 5.4: Expression of chemerin mRNA in PVAT **(A)** and ChemR23 mRNA in PCAs **(B)** in both genders. (A) The relative expression of chemerin mRNA in PVAT normalised to GAPDH in females (n = 10) and males (n = 10). (B) The relative expression of ChemR23 mRNA in PCAs normalised to GAPDH in females (n = 10) and males (n = 8). Data are expressed as mean ± SEM.

5.3.5 Role of chemerin in PVAT-mediated vasoconstriction

A previous study has indicated that chemerin acts as an adipocyte-derived constricting factor. Therefore, the functional role of chemerin in the PVAT-induced vasoconstriction was examined. Segments of coronary arteries from both sexes were pre-treated with a chemerin antibody, in order to bind any released chemerin. In the presence of the chemerin antibody, the PVAT-induced contraction was abolished in both sexes (Figure 5.5 A,B).

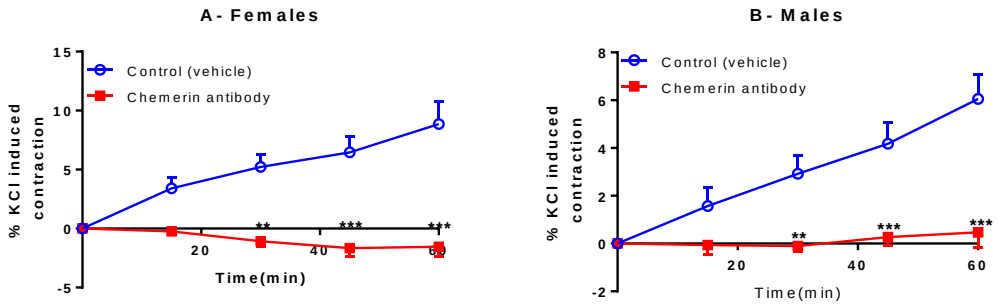


Figure 5.5: Effects of pre-incubation with chemerin antibody on PVAT vasomotor function. PVAT (0.3 g)–induced vasoconstriction in the absence (control vehicle) or the presence of chemerin antibody in PCAs from females **(A)** and males **(B)**. Data are expressed as a percentage of the contraction to 60

mM KCl and are mean ± S.E.M. of 5(A) - 6(B) experiments. ** indicates P<0.01, *** indicates P<0.001, two-way ANOVA followed by a Sidak's *post hoc* test vs control values.

5.3.6 Role of chemerin in U46619-induced vasoconstriction

In order to investigate whether chemerin can affect another signalling pathway and cause vasoconstriction, the effect of chemerin on U46619 contraction was determined. PCAs are preincubated with and without chemerin antibody before addition of cumulative concentrations of U46619. Pre-treatment of the coronary arterial rings with chemerin antibody inhibited the U46619-induced contraction in PCAs in that the log EC_{50} was significantly reduced in the rings pre-incubated with chemerin antibody (pEC_{50} = 7.65 ± 0.13) compared to control (pEC_{50} = 8 ± 0.07) (Figure 5.6).

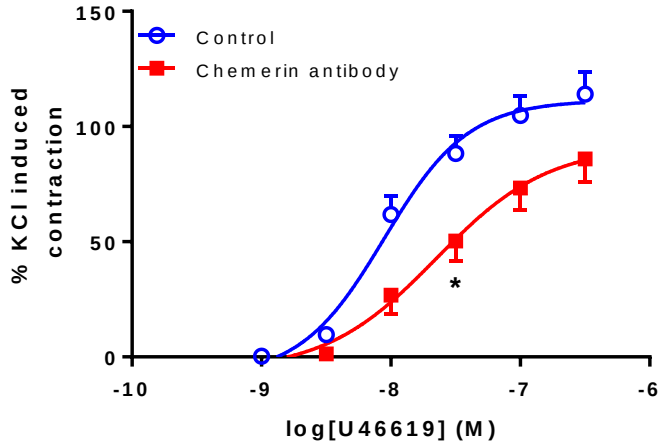


Figure 5.6: Log concentration-response curves for the vasoconstrictor effects of U46619 in the absence (control vehicle) or presence of chemerin antibody in coronary arteries from pigs. Values are expressed as a percentage of the contraction to 60 mM KCl and are mean ± S.E.M. of 4 experiments. * P<0.05, 2-tailed, paired Student's *t*-test vs control values.

5.4 Discussion

Chemerin is an important mediator in both physiology and pathophysiology. Chemerin, which could be derived from PVAT, is able to enhance vasoconstriction but its signalling pathway, or pathways, have not been fully addressed. This study is noteworthy, in that it demonstrates a novel impact of sex differences on the chemerin function in regulating the vascular tone of PCA. In addition, it expands the list of factors which affect PVAT function and highlights the role of sexual dimorphism in regulation of cardiovascular pathophysiology.

The effects of chemerin-9 peptide were investigated on the contractility of PCAs. Chemerin induced vasoconstriction in PCA from both sexes but with significantly higher response in PCA from females compared to male PCAs (Figure 5.1). In this study, the peptide chemerin-9 was used because it is the only peptide that has similar potency as recombinant chemerin in the activation of the chemerin receptor ChemR23 (Wittamer *et al.*, 2004). A study conducted by Darios *et al.*, (2016) found that chemerin augmented electrical field-stimulation-induced vasoconstriction in rat superior mesenteric arteries (Darios *et al.*, 2016), which supports the idea of the ability of chemerin to increase the vascular tone. A study in rat aorta and mesenteric blood vessels showed that PVAT-derived chemerin could be a potential factor which is responsible for arterial contraction. (Watts *et al.*, 2013). This supports the data presented here, confirming that chemerin can induce vasoconstriction.

In order to determine whether chemerin is involved in PVAT-induced contraction, and due to unavailability of chemerin antagonist, an anti-chemerin antibody was used to bind any chemerin released from the PVAT and prevent it from activating the receptor on the artery. Under these conditions, the presence of the chemerin antibody completely prevented the PVAT-induced vasoconstriction, indicating that chemerin is likely to be the mediator released from the fat (Figure 5.5). Further experiments have showed that chemerin antibody can also inhibit the contractile response of PCA to U46619 which suggests a crucial role of chemerin in TXA_2-induced contraction as well (Figure 5.6). Noteworthy, Watts *et al.*, (2013) have reported a similar inhibitory effect of ChemR23 antagonist CCX832 but on the contractile response to $PGF_{2\alpha}$ and

phenylephrine (Watts *et al.*, 2013). Thus, the effect of chemerin antibody could be due to the inhibition of the chemerin itself and/or other bioactive signalling substances, like TXA_2, that are released from PVAT and enhance the contractility of the coronary arterial segments. Additionally, this raised another question about whether PVAT-derived chemerin can cause vasoconstriction directly and/or by stimulating other ADCF to provoke vasoconstriction?

In order to determine whether differences in expression of the chemerin receptor could explain the sex difference in the contractile response to chemerin, mRNA expression of ChemR23 in PCAs from both sexes was determined and, as a comparison, mRNA of chemerin in PVAT was also examined. The RT-PCR results confirmed the existence of chemerin and its receptor in PVAT and PCA, respectively. However, no sexual dimorphism was identified in their expression (Figure 5.4). Although the expression of ChemR23 was investigated here, chemerin has been identified to act through G protein-coupled receptor 1 (GPR1) (Barnea *et al.*, 2008) and C-C chemokine receptor-like 2 (CCRL2) (Zabel *et al.*, 2008) as well. However, this study focused on ChemR23 rather than GPR1 or CCRL2 receptors because a recent report showed that CCX832, a newly described ChemR23 antagonist, inhibits chemerin-stimulated contraction. CCX823 does not possess affinity to the other chemerin receptors (GPR1 and CCLR2), indicating a major role for ChemR23 in chemerin-induced vascular smooth muscle contraction (Watts *et al.*, 2013). Interestingly, the results in the present study are in line with the study by Kostopoulos *et al.*, (2014) conducted on human aorta and coronary vessels which showed chemerin and ChemR23 expression in human arteries and PVAT (Kostopoulos *et al.*, 2014). Moreover, this is supported by another study which has identified the presence of highest mRNA levels of chemerin and its receptor in mature adipocytes which become even higher after feeding the mice with high-fat diet (Roh *et al.*, 2007). Therefore, the data presented here demonstrate that chemerin is present in coronary artery PVAT and the presence of the receptor on the coronary artery itself indicates that PVAT-derived chemerin has the potential to modify vascular function.

Because of these previous results and as the sex difference in the contractile response to chemerin could not be explained by a difference in

ChemR23 expression, chemerin signalling in PCA was investigated. It has been already demonstrated that ROS, and particularly O_2^-, can induce vasoconstriction in different anatomical regions and different species (Peters *et al.*, 2000; Gao *et al.*, 2006). In the previous chapter (Chapter 4), it was demonstrated that ROS can be produced in the PVAT and is involved in PVAT-induced contractions of the PCA. Chemerin has been shown to activate ROS generation in human microvascular endothelial cells and VSMC (Neves *et al.*, 2015). Therefore, the effects of chemerin on the NADPH oxidase (Nox)-derived ROS production, particularly O_2^-, were determined in PCAs from both sexes. Using lucigenin-induced chemiluminescence assay, the data of this study showed for the first time that chemerin can increase O_2^- production in PCA homogenate from females but not males (Figure 5.2). As demonstrated in Chapter 4, many isoforms of Nox are present in PCA but the main 2 isoforms that are responsible for production of vasocontractile O_2^- are Nox1 and Nox2. Interestingly, it was found that Nox1 expression was higher in female PCAs compared to males PCAs while Nox2 levels were the same in both sexes (Chapter 4). Therefore, differences in chemerin-induced ROS production through Nox1 could explain the larger contractions to chemerin in PCAs from female animals. Interestingly, this was confirmed by a functional study demonstrating that the Nox1-selective inhibitor ML171 inhibited the contractile responses of the coronary arteries to chemerin only in females (Figure 5.3). This study is supported by a previous report which, although it did not study the effect of sex variance, found that incubation of rat aorta with chemerin enhanced ROS generation along with reduced NO production and guanylyl cyclase activity (Neves *et al.*, 2014). In this latter study, the relaxant responses to different vasodilators are reduced in chemerin-treated vessels, then retrieved by using an O_2^- scavenger (tiron) and SOD mimetic (tempol). Taken together, these data indicate that chemerin regulates vascular tone through production of ROS.

ChemR23 receptor has been found to be expressed on smooth muscle and foam cells in human atherosclerotic lesions (Kostopoulos *et al.*, 2014). These reports, in addition to reports of an inhibitory effect of chemerin on NO-induced relaxation and cGMP signalling in the vasculature (Neves *et al.*, 2014), proposed a potential role of chemerin in atherosclerosis, preeclampsia,

hypertension, and overall metabolic syndrome. In addition, Bozaoglu *et al.*, (2007) reported, for the first time, that serum chemerin levels are associated with body mass index, circulating triglycerides, and blood pressure. They found that the higher levels of gene expression of chemerin and its receptor, CMKLR1, in adipose tissue were significantly associated with obese and type 2 diabetic Mexican–American subjects (Bozaoglu *et al.*, 2007). A similar study in a Mauritian and Caucasian population confirmed the correlation between serum chemerin with adiposity and several key aspects of the metabolic syndrome (Stejskal *et al.*, 2008). A recent meta-analysis was performed to investigate the association between chemerin and obesity. It has been reported that chemerin could play a significant role in the pathophysiology of obesity (Li *et al.*, 2014). The demonstration in the present study that chemerin induces vasoconstriction of the porcine coronary artery, may indicate a role for PVAT-derived chemerin in obesity-related coronary artery disease. Interestingly, other studies have reported increased serum levels of chemerin in different cardiovascular diseases such as hypertension (Stejskal *et al.*, 2008; Dong *et al.*, 2011), preeclampsia (Stepan *et al.*, 2011) and coronary artery diseases (Dong *et al.*, 2011). As sex differences were demonstrated in the response of the porcine coronary artery to chemerin, it would be of interest to determine whether the increases in serum levels of chemerin seen in these conditions are also associated with sex differences in contractile responses to chemerin, as seen in this present study.

In conclusion, this study demonstrates, for the first time, the presence of a sexual dimorphism in the contractile response to chemerin. Furthermore, this study demonstrates the presence of chemerin in coronary artery PVAT and ChemR23 in coronary arteries themselves. This study also demonstrates a sexual dimorphism in the ability of chemerin to induce ROS production in PCAs, which underlies the difference in the contractile response to chemerin. Overall, these data demonstrate that PVAT is an important source of this adipokine in the coronary circulation. As chemerin levels change in obesity, these changes in chemerin levels and/or signalling may have an impact on coronary artery tone. Establishing chemerin as a key mediator in the PVAT and its impact on coronary circulation in obesity will allow a better understanding of the cardiovascular pathophysiology.

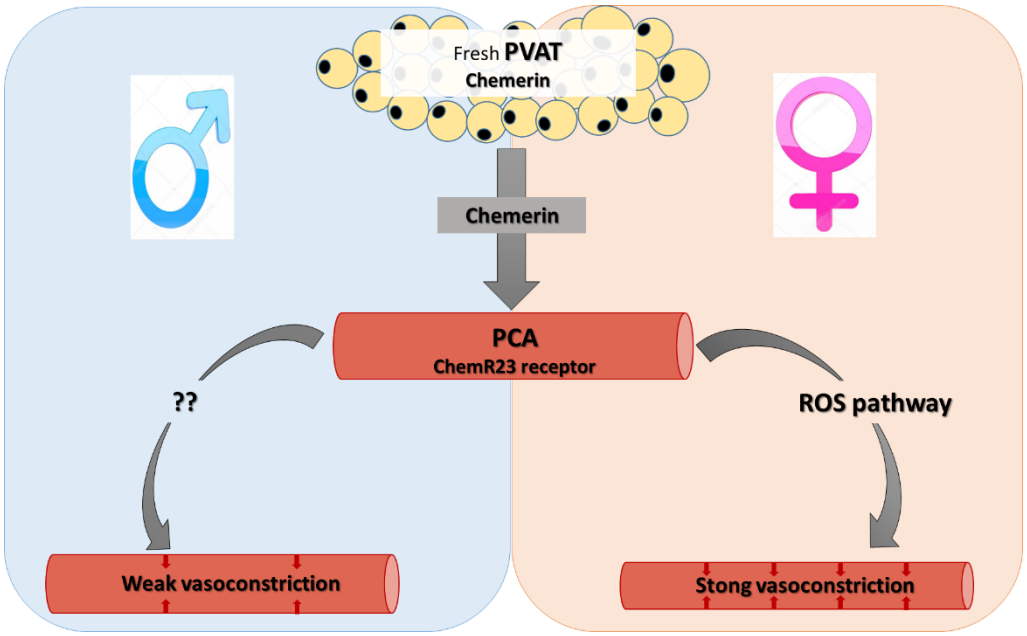


Figure 5.7: Hypothesized schematic diagram of sex differences in the contractile response of PCA to fresh PVAT. Present study demonstrated that PVAT-derived chemerin can mediate stronger vasoconstriction in PCAs from females than males PCAs, with an important role of reactive oxygen species (ROS) as a signalling pathway in females PCAs only.

Chapter six

General Discussion

6.1 Dual effect of PVAT on the vascular tone of PCA

The recognition that perivascular adipose tissue is not simply a reservoir for lipid storage but is also a complex endocrine organ, has led to substantial research efforts to establish the mechanistic links between the PVAT and vascular tone regulation. In addition, female and male animals are often used interchangeably in experimental studies with little consideration given to differences in PCA responses to PVAT between the sexes. Therefore, despite numerous reports outlining the importance of consideration of sex differences in biomedical research (Miller *et al.*, 2007; Bhatia *et al.*, 2012), little specific information is available on the mechanisms of the vasomotor effect of PVAT in each sex. The present study aimed to determine the effects of PVAT on vascular control and identified clear gender differences and ability of PVAT to reduce and promote constriction in PCAs, depending on the condition of storing the tissue.

(Chapter 2) The present study suggests a significant relaxant or at least anticontractile effects of PVAT, which had been stored overnight, on the coronary arterial tone. The PVAT-mediated relaxation observed in female, but not male, porcine coronary arteries was identified by using both attached and separated PVAT, and does not appear to be dependent upon the contractile agents employed, as similar effects were obtained after cumulative contraction with both U46619 and ET-1. Studies by Gao *et al.*, (2007) and Malinowski et *al.*, (2008) have shown that PVAT reduces vascular tone in rat aorta and human internal thoracic arteries, respectively (Gao *et al.*, 2007; Malinowski *et al.*, 2008). The present results are consistent with these studies. The functional responses were studied on isolated tissues in an isometric tension recording system (organ bath). Although this technique is considered as a corner stone in the pharmacology and physiology experiments because of a lot of the advantageous characteristics, some disadvantages could be encounter such as tissues may experience different degrees of damage during surgical removal or placement of rings on hooks. Additionally, tissues may change in their responsiveness throughout the day such that time controls become a necessary control for every experiment. The involvement of NO and COX metabolites has been identified in the PVAT response with the most common adipokine, adiponectin, causing this vasorelaxation. The present study was then extended

to investigate whether there are any sex differences in the role of PVAT-derived adiponectin in controlling the vascular tone of the PCAs. Chapter 2 demonstrated that the increased effect of adiponectin in females was due to the higher responsiveness of PCA from females to adiponectin compared to males PCA, rather than a variation in the level of expression or release of adiponectin from PVAT.

Noteworthy, several clinical studies have demonstrated vascular protective effects of adiponectin as low plasma levels of adiponectin are associated with hypertension and other cardiovascular diseases (Imatoh *et al.*, 2008; Aprahamian and Sam, 2011; Kim *et al.*, 2013) and high levels of adiponectin are associated with a reduced incidence of acute coronary syndrome and acute myocardial infarction (Pischon *et al.*, 2004; Mittal *et al.*, 2013). The present study demonstrates that only PVAT from females has an anti-contractile effect on the coronary artery tone and thus may contribute to the reduced incidence of cardiovascular disease in pre-menopausal women. However, further studies are required to determine whether similar sex differences in the regulation of tone by PVAT are observed in other blood vessels, and, importantly, whether similar effects are seen in humans. In addition, it is worth to study this sexual dimorphism in PVAT function in other pathological conditions such as obesity.

In addition, the results in Chapter 2 have shown the expression and activity of both CBS and 3-MPST, but not CSE, in PVAT with no sex differences. However, the present study showed that the activity of these enzymes in porcine PVAT was low and there was no evidence that H_2S is involved in the anti-contractile effect of PVAT in the porcine coronary artery. As there is no functional effect of PVAT-derived H_2S on the vascular tone of PCA under the physiological condition used, and as it is demonstrated that H_2S activity is enhanced in hypoxia and inflammation (Osmond and Kanagy, 2014; Guo *et al.*, 2016), future studies under different pathological conditions, such as hypoxia and inflammation, may be required for further verification and understanding of the H_2S role. Furthermore, H_2S production in PVAT can be increased along with the enhancement of its anticontractile effect as a response to different pharmacological treatments such as rosiglitazone and atorvastatin

(Wojcicka *et al.*, 2011; Beltowski, 2013). Noteworthy, as there is no inhibitor of 3-MPST, so it cannot be excluded that H_2S from 3-MPST is involved in the PVAT effect.

Next, PVAT was used directly upon arrival from abattoir to check if it would result in a different response. Surprisingly, response to PVAT was totally different in that PVAT caused vasoconstriction rather than vasorelaxation. So the next work was focused on fresh PVAT function. **(Chapter 3)** It became increasingly clear that PVAT plays a role in cardiovascular pathophysiology. For instance, an apparent link has been found between an increase in PVAT and coronary artery disease (Verhagen and Visseren, 2011). As prostanoids have previously been proposed to be a novel regulator of arterial vasoconstriction through the release of COX-derived ADCF factors released from PVAT causing vasoconstriction in isolated aortae from mice (Meyer *et al.*, 2013), Chapter 3 explored the role of sex differences in PVAT-derived prostanoids in vasoconstriction in PCAs. The present study has identified that the cyclooxygenase products (TXA_2 and $PGF_{2\alpha}$) are released from coronary artery PVAT as COX antagonists inhibited the contractile effect of PVAT, while a PLA_2 stimulator augmented this vasoconstriction in both sexes. These observations are in line with a previous work on carotid, thoracic and mesenteric arteries from mice, which found that PVAT exerted its contractile effects by secreting prostanoids which could be inhibited by indomethacin in a dose-dependent manner (Chang *et al.*, 2012b). In addition, the present study demonstrated that whilst PVAT-derived TXA_2 plays a role in PCAs from female pigs, $PGF_{2\alpha}$ appears to be more important in the PVAT-induced vasoconstriction in PCAs from male pigs. These sex variations are due to a greater release of TXA_2 from female PVAT and higher responsiveness of $PGF_{2\alpha}$ in males PCAs. However, further work involving in vivo studies may provide information about the overall effect on different vascular bed and in different sexes, which may be important for any clinical use in future. For instances, the effect of the pharmacological inhibition of these prostanoids can be determined on the blood pressure in animals of different sexes. In addition, knock out mice in which the prostanoids machinery of PVAT is targeted can be utilized to identify the particular role of PVAT in maintenance of blood pressure in either sex.

(Chapter 4) Chapter 4 demonstrated that PVAT could act via reactive oxygen species in both sexes. Although immunoblot analysis identified the expression of different Nox isoforms in both PVAT and PCA, the present study did not detect any differences in protein expression for Nox enzymes in PVAT from male and female pigs whilst significant changes were found in PCAs from different genders in that Nox1 expression was higher in females whereas Nox4 expression was higher in males. In addition, PVAT-induced vasoconstriction was inhibited by differential inhibition of Nox isoenzymes (Nox1, Nox2 and Nox4) without sex differences. Although the present study used selective Nox antagonists such as ML171, PhoxI2 and GKT137831, future studies involving more selective antagonists may be required. This study was then extended to examine if there are specific bioactive signalling molecules in PVAT that could affect the ROS production. As the COX-derived metabolites have been identified in Chapter 3 as ADCFs, so the prostanoid effects on ROS production have been investigated in PVAT and PCAs, and in both female and male pigs as well. Chapter 4 demonstrated that both U46619 and $PGF_{2\alpha}$ could augment the ROS production and, consequently the vasoconstriction in PCAs from females only. The signalling molecules in PVAT which evoke the ROS–mediated response in PCA from males were not examined in the present study. Therefore, further work is required to investigate the mechanism by which PVAT-derived ROS can enhance the vasoconstriction in males. Indeed, a previous study on thoracic aorta and superior mesenteric artery of Sprague-Dawley male rat identified the presence of an active, functional catecholamine pool in arterial PVAT (Ayala-Lopez *et al.*, 2014). Given that different studies reported that adrenoceptor activation can induce ROS production (Gayen *et al.*, 2010; Andersson *et al.*, 2011) so it can be speculated that the adrenergic components (e.g. noradrenaline) could enhance ROS activity, and subsequently the PVAT-induced vasoconstriction, in males pigs. However, further studies are required to prove this speculation.

(Chapter 5) Having demonstrated sex differences in the role of vasorelaxant adipokine, adiponectin, in PVAT function in Chapter 2, Chapter 5 explored the functional effect of chemerin as another important adipokine that could be released from PVAT and affect the vascular tone of PCA, and identified

whether there is any sex difference in its action. The present study showed the presence of a chemerin signalling pathway in coronary circulation as mRNA expression of both chemerin and chemerin receptors (ChemR23) have been identified in PVAT and PCAs, respectively. The responsiveness to chemerin-9 was higher in PCAs from females compared to PCAs from males. Although there were no sex differences in the expression of both chemerin and its receptor, the present study found sex variations in chemerin signalling in coronary arteries in that ROS production is more active in females than males. This sexual dimorphism in the vascular responsiveness to chemerin is explained by the difference in downstream regulation as chemerin can stimulate ROS production in PCAs from females only. Additionally, the present study showed that Nox1 antagonist could inhibit chemerin-induced contraction in females only. The limitation of the present study was the lack of a direct evidence of the effect of PVAT-derived chemerin on the vascular tone of PCAs because of the unavailability of chemerin antagonist. However, using chemerin antibody, as alternative to ChemR23 antagonist, caused inhibition of PVAT-induced vasoconstriction in both sexes suggesting the probability of chemerin to be the mediator released from the fat. Additionally, the present study showed that the chemerin antibody can reduce the responsiveness of PCAs to U46619. A study by Watts *et al.,* (2013) has showed that a ChemR23 antagonist could inhibit the prostaglandin $F_{2\alpha}$-induced contraction in male Sprague-Dawley rats (Watts *et al.*, 2013). The findings of the latter study could explain and link the results of Chapters 3 and 5 in that chemerin could induce vasoconstriction via augmentation of $PGF_{2\alpha}$ signalling in male PCAs.

Putting together the results from Chapters 2, 3, 4 and 5, the present study demonstrates a dual effect of the vasomotor function of PVAT on the coronary arterial tone in that PVAT can produce and release both vasorelaxant and vasocontractile signalling factors (Figure 6.1). In addition, significant sex differences have been identified in the PVAT-vascular coupling in all the chapters which highlights the importance of taking into account potential sex differences in the responses during performing the cardiovascular research. Although PVAT from both sexes have the same histological appearance and expression profile of the studied signalling molecules such as adiponectin,

TXA_2, $PGF_{2\alpha}$, Nox1, Nox2, Nox4 and chemerin, a substantial functional difference has been revealed in all of these pathways in their vasomotor regulation. The reason behind these sex differences in fat-vascular coupling were mostly due to the variations in the coronary artery itself rather than PVAT, apart from the varied TXA_2 release from PVAT. Moreover, taken together the results from Chapters 3 and 4, TXA_2 released from PVAT can cause vasoconstriction only in females via, at least partly, evoking ROS production. On the other hand, PVAT-derived $PGF_{2\alpha}$ can enhance vasoconstriction in males only, and via a pathway/pathways that does not include ROS metabolites. This could be due to a greater expression of the O_2^- producing enzyme (Nox1) in PCAs from females compared to males. Noteworthy, Chapter 6 also showed an active ROS mechanism responsible for chemerin-induced vasoconstriction in PCAs from females only. It can be speculated that in situations of high oxidative stress, such as obesity, this variation in PVAT function can be translated into higher PVAT-induced vasoconstriction in females rather than males. As the available studies are performed on one sex, a future study is required to investigate the effect of obesity on these PVAT-derived signalling pathways in different sexes. In addition, the present study showed that non-physiological conditions could affect the vasomotor function of PVAT but without sex differences. PLA_2 stimulator (melittin) enhanced PVAT-induced vasoconstriction by enhancing prostanoids action and release from PVAT (Chapter 3). Furthermore, inflammatory condition caused augmentation of H_2O_2 production, but not O_2^-, in PVAT from both sexes (Chapter 4). A study by (Fleenor *et al.*, 2014) found that superoxide signalling in aortic PVAT can act as a novel mechanism and potential therapeutic target in large elastic artery stiffening and increased CVD risk with aging. Noteworthy, as PVAT from different vessels and different species are phenotypically and functionally different, further work is needed to explore the vascular-bed and species differences in PVAT function, and eventually, to uncover ways to ameliorate cardiovascular disease by targeting therapeutic approaches to PVAT.

6.2 Vasomotor effects of PVAT in different conditions

In this study, two different conditions of the PVAT were used which showed totally different effects. Firstly, PVAT stored overnight at 4^{o}C mediated vasorelaxation/or at least anticontractile effect in PCA from females only (Chapter 2) in which adiponectin was identified as ADRF which acts through NO and COX pathways. Secondly, fresh PVAT, which was added directly upon arrival from abattoir, induced vasoconstriction in PCAs from both sexes in which prostanoids, reactive oxygen species and chemerin were the ADCFs that are responsible for this contraction (Chapter 3, 4, 5). To clarify this variation in the PVAT vasomotor function, the fat was dissected upon arrival from the abattoir, maintained in Krebs'-Henseleit solution at room temperature and stored overnight with continued oxygenation with carbogen (95% O_2, % CO_2) to investigate the possible effect of hypoxia on PVAT. Interestingly, PVAT-induced vasoconstriction was restored in both sexes (see in Appendix D). These data suggest that the contractile response is lost when the tissues become hypoxic. Noteworthy, the effects of hypoxia on PVAT have been studied in different anatomical sites and different species, and showed controversial effects (Maenhaut *et al.*, 2010; Withers *et al.*, 2011). In line with the present study, Maenhaut *et al.* (2010) demonstrated that hypoxia can induce the vasorelaxant effect of PVAT in mouse aorta which was independent of the endothelium and soluble guanylyl cyclase. Although the authors found no role of lactate, adenosine, CO and H_2S in the hypoxic response they admitted that an unidentified "adipocyte-derived relaxing factor" could not be excluded (Maenhaut *et al.*, 2010). On the other hand, hypoxia inhibited the anticontractile effect of PVAT in mesenteric arteries from rat. Macrophage activation was considered as a key modulator of the enhancement of the contractility in the arteries after induction of inflammation by hypoxia and aldosterone (Withers *et al.*, 2011). Furthermore, it cannot be excluded whether the hypoxia could affect the stability of the bioactive molecules and/or their receptors in PVAT or PCAs, respectively. It is for future studies to investigate how hypoxia can affect these different scenarios in PVAT-vascular coupling.

The present study showed the complexity of PVAT physiology as the same coronary PVAT has both vasorelaxant and vasoconstrictor signalling

molecules which are functionally active. Additionally, this study identifies a significant impact of sex on the PVAT function (Figure 6.1). Understanding the nature of these differential signalling pathways in females and males is essential for identifying novel strategies to appropriately target cardiovascular diseases. Indeed, it is unclear whether it would be better to potentiate the actions of anti-atherogenic adipocytokines, or inhibit the actions of pro-atherogenic adipocytokines, or both (Andrade-Oliveira *et al.*, 2015). It is also unclear which cell type within the PVAT needs to be targeted or which key transcriptional pathways need to be modified to improve its overall secretory profile. Indeed, producing a drug that can target adiponectin, TXA_2, $PGF_{2\alpha}$ or chemerin in PVAT to reduce the risk of ischaemic heart disease in a specific gender could be a promising strategy to treat the cardiovascular diseases (e.g as a meta-analysis showed a significant increase in plasma adiponectin levels following statin therapy (Chrusciel *et al.*, 2016), could statins have more advantageous pleiotropic effects in women rather than men due to the increased adiponectin activity in females coronary arteries compared to the males arteries?).

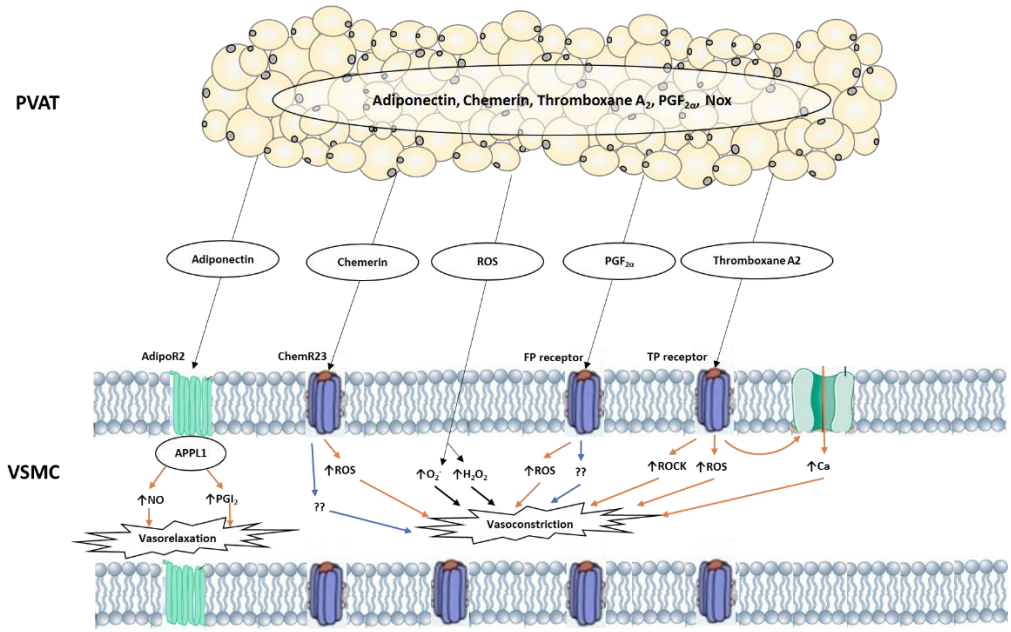


Figure 6.1: Hypothesized schematic diagram of sex differences in the contractile response of PCA to PVAT. Present study demonstrated that PVAT-derived adiponectin, chemerin, ROS, $PGF_{2\alpha}$ and thromboxane A_2 can regulate the vascular tone of PCAs from females (red arrows), males (blue arrows) or both sexes (black arrows). Adiponectin binds to AdipoR2 and causes vasorelaxation in females PCAs via signalling through APPL1 and increasing nitric oxide and prostacyclin. Chemerin binds to ChemR23 and causes vasoconstriction via increasing ROS in females PCAs and unknown mechanism in males PCAs. Superoxide anion O_2^- and hydrogen peroxide H_2O_2 cause vasoconstriction in both sexes. $PGF_{2\alpha}$ binds to FP receptor and causes vasoconstriction via increasing ROS in females PCAs and unknown mechanism in males PCAs. Thromboxane A_2 binds to TP receptor and causes vasoconstriction in PCAs from females via increasing ROS, activating Rho kinase pathway (ROCK) and enhancing influx of calcium through opening L-type Ca^{2+} channels.

6.3 Conclusions

The present study revealed clear sex differences in the PVAT function in PCAs and addressed diverse effect of PVAT on vascular tone in different conditions (fresh and stored overnight at 4^{o}C PVAT). This study also investigated different signalling pathways that are involved in regulation of coronary arterial tone by PVAT. Chapter 2 showed an anti-contractile response in PCAs to (stored overnight) PVAT from female, but not male pigs, which appears to be due to increased adiponectin activity. In contrast, no obvious functional role has been identified for H_2S in this PVAT-induced vasorelaxation despite the identified expression of its synthesizing enzymes (CBS and 3-MPST).

Chapter 3 further demonstrated sex differences in the PVAT function where fresh PVAT added to segments of porcine coronary artery produced a contractile response due to prostanoids release. In addition, this study identified sex differences in COX metabolites in the PVAT response, where thromboxane has a role in PVAT-dependant vasoconstriction in females while PVAT-derived $PGF_{2\alpha}$ plays a role in the contraction of PCAs from males. Chapter 4 showed that the fresh PVAT-induced contraction of the porcine coronary artery is dependent upon Nox activity, although there are no sex differences in this response. In addition, Chapter 4 demonstrated that TXA_2 and $PGF_{2\alpha}$ could enhance vasoconstriction via increasing ROS production in females only which suggest also that PVAT can induce vasoconstriction by releasing prostanoids that enhance the ROS activity only in PCAs from females. Chapter 5 suggested that PVAT is an important source of chemerin in the coronary circulation. Furthermore, this study demonstrated a novel impact of sex on the chemerin function in regulating the vascular tone of PCA as chemerin can induce vasoconstriction via ROS production in females only. Therefore, this study has revealed for the first time a significant sexual dimorphism in the signalling pathways involved in the vascular-PVAT coupling which highlighted the importance of taking into account potential sex differences in the responses to PVAT and that sex-specific drug treatment may represent a potential strategy in the treatment of cardiovascular diseases.

Appendices

A. List of buffers and chemicals used for immunoblotting

Table 1. Lysis buffer

	Concentration
Tris	20 mM
EGTA	1 mM
Sucrose	320 mM
Triton X100	0.1%
Sodium fluoride	1 mM
β-glycerophosphate	10 mM
pH to 7.6	

Table 1 List of materials in lysis buffer.

Table 3. Tris-buffered saline containing 0.1% Tween 20 (TBS-T)

	Concentration
Tris	25 mM
NaCl	125 mM
Tween 20	0.1%
pH to 7.6	

Table 3 List of materials in TBS-T.

Table 4. 6x solubilisation buffer

	Concentration	
24% SDS	4%	2.4 g
30% Glycerol	5%	3 mL
β-mercaptoethanol	5%	3 mL
2.5% BPB	0.01%	240 µL
1.5 M Tris-HCl	0.0625 M	2.5 mL
Make up to 10 mL (Store at -20°C)		

Table 4 List of materials in 6x solubilisation buffer.

Table 5. Protease Inhibitor Cocktail Set I (Calbiochem)

Product	Concentration	Target protease
AEBSF hydrochloride	500 µM	Serine proteases
Aprotinin, bovine lung, Crystalline	150 nM	Serine proteases and esterases
E-64 Protease inhibitor	1 µM	Cysteine proteases
EDTA, disodium	0.5 mM	Metalloproteases
Leupeptin, hemisulfate	1 µM	Cysteine and trypsin-like proteases

Table 5 List of materials in protease inhibitor cocktail Set I

Table 6. 10X electrophoresis buffer

Tris	30.3 g
Glycine	144 g
Dissolve in dH_2O	8 L
Add methanol	2 L
Store at 4°C	

Table 6 List of materials in 10X electrophoresis buffer

Table 7. Transfer buffer

Tris	30.3 g
Glycine	144 g
SDS	10 g
Make up to 1 L in dH_2O	

Table 7 List of materials in transfer buffer

B. Immunoblots

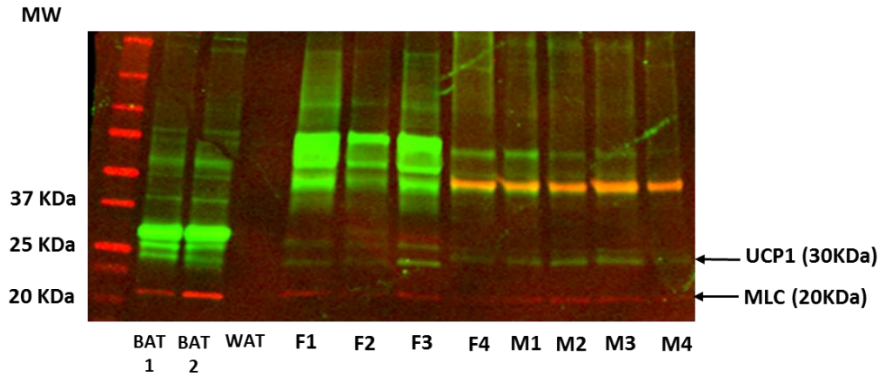


Figure 1: Full immunoblot showing expression of the uncoupling protein1 (UCP1) in PVAT from female and male pigs compared to interscapular brown adipose tissue (BAT1), aortic brown adipose tissue (BAT2) and epididymal white adipose tissue (WAT) (see Figure 2.4).

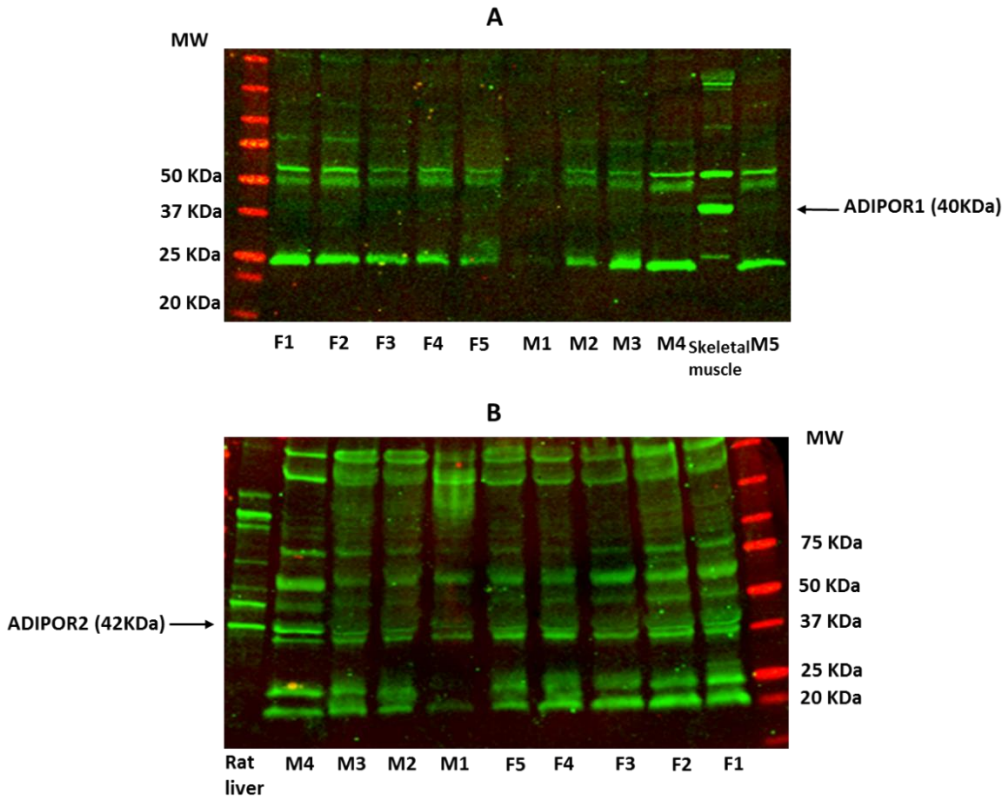


Figure 2: Full immunoblots of expression of adiponectin receptors. **(A)** Expression of AdipoR1 (40 kDa) levels in 20 µg of PCA from female (F1-F6) and male (M1-M5) pigs. Porcine skeletal muscle is used as a positive control. **(B)** Expression of AdipoR2 (42 kDa) (20 kDa) levels in 20 µg of PCA from

female (F1-F5) and male (M1-M4) pigs. Rat liver was used as a positive control (see Figure 2.9).

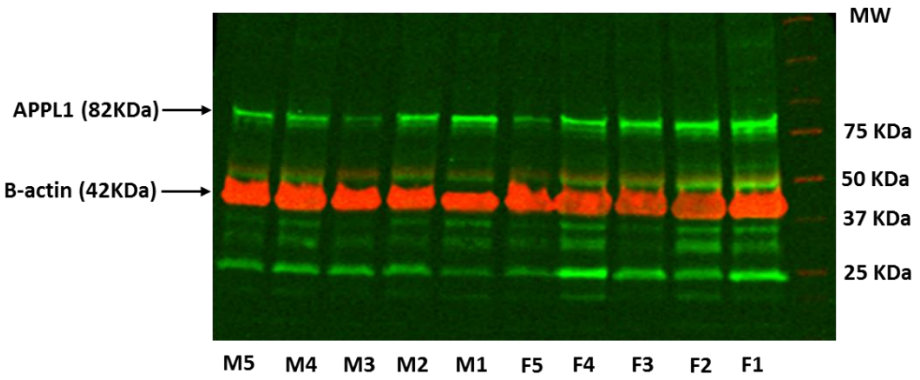


Figure 3: Full immunoblot of expression of adiponectin binding protein APPL1 (82 kDa) and β-actin (42 kDa) levels in 20 µg of PCA from female (F1-F5) and male (M1-M5) pigs (see Figure 2.10).

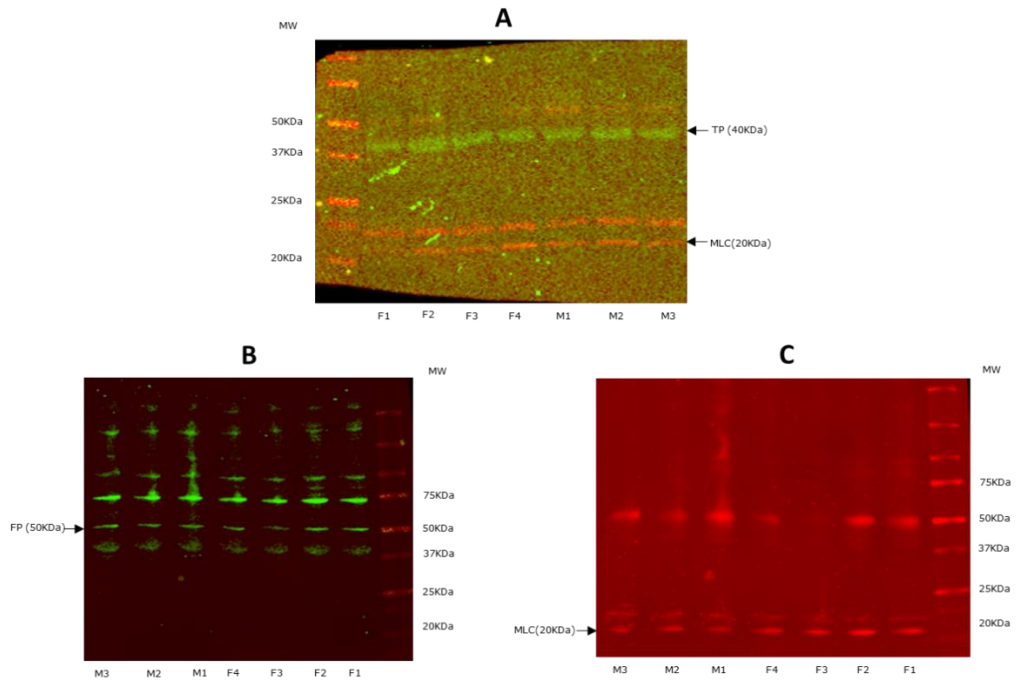


Figure 4: Full immunoblots showing **(A)** Expression of TP receptor (40 kDa) and MLC (20 kDa) levels in 20 µg of 6 female and 8 male PCAs. **(B)** Expression of FP receptor (50 kDa) and **(C)** MLC (20 kDa) levels in 20 µg of 7 female and 8 male PCAs (see Figure 3.5 and 3.6).

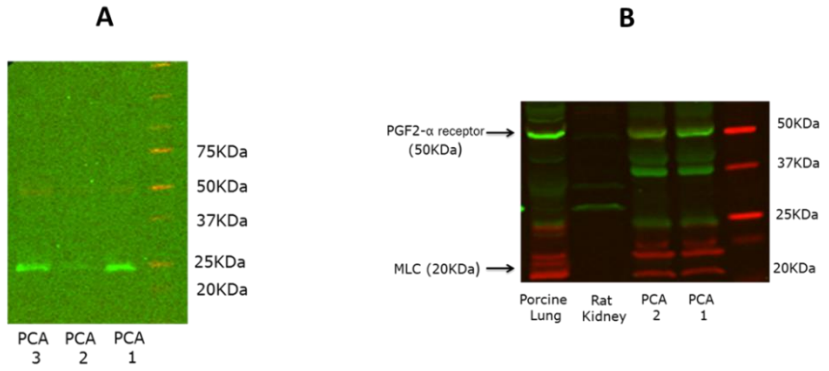


Figure 5: (A) Negative control blot: Immunoblot incubated with secondary antibodies only (without primary antibody). **(B)** Positive control blot: Immunoblot showing expression of FP receptor (50 kDa) and MLC (20 kDa) levels in 20 µg of coronary arteries and porcine lung tissue as a positive control (see Figure 3.6).

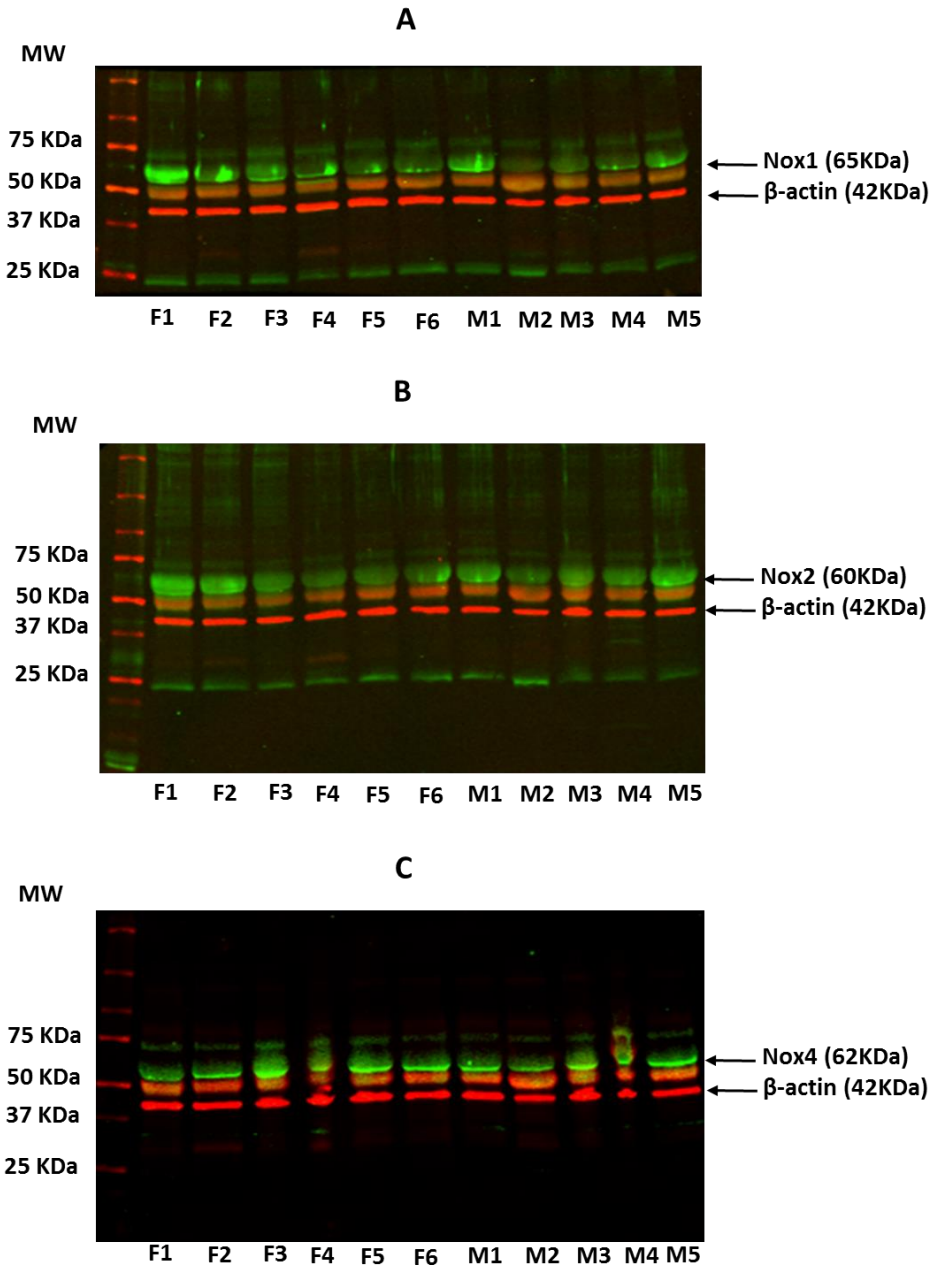


Figure 6: Full immunoblots showing protein expression of the NADPH oxidase catalytic subunits: Nox1**(A),** Nox2**(B)** and Nox4**(C)** in PVAT from female and male pigs (see Figure 4.9, 4.10, 4.11).

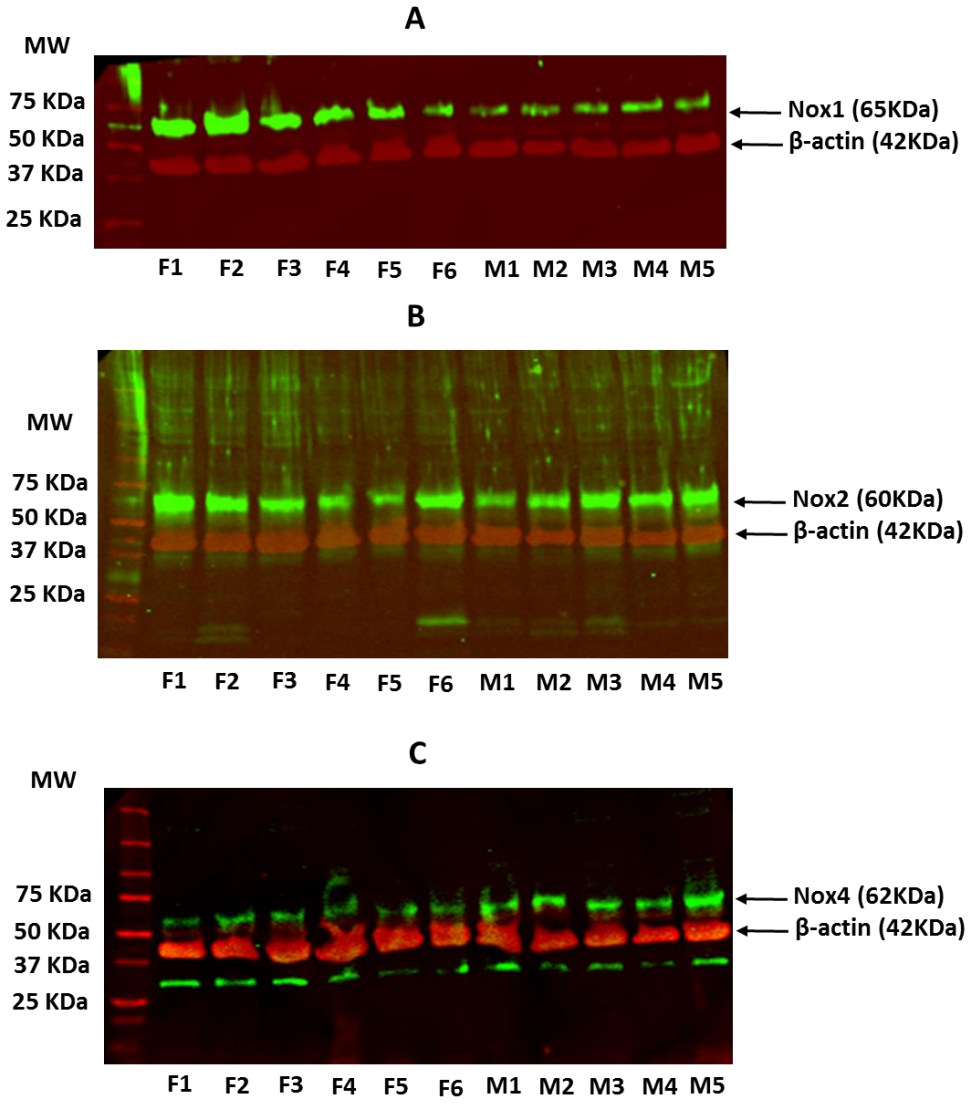


Figure 7: Full immunoblots showing protein expression of the NADPH oxidase catalytic subunits: Nox1**(A),** Nox2**(B)** and Nox4**(C)** in PCA from female and male pigs (see Figure 4.12, 4.13, 4.14).

C. LPS effect on PVAT-induced contractions of PCAs (Pilot study)

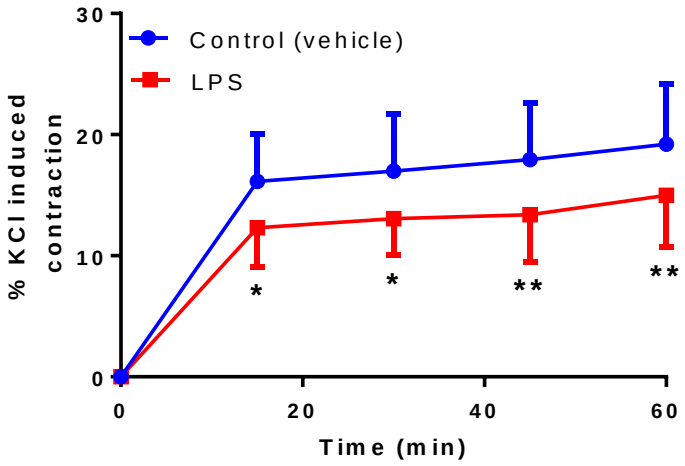


Figure 8: Effects of LPS on the PVAT-induced contractions of coronary arteries from pigs in the absence (control vehicle) or presence of 5 µg/ml LPS. Values are expressed as a percentage of the contraction to 60 mM KCl and are mean ± S.E.M. of 4 experiments. * P<0.05, ** P<0.01, two-way ANOVA followed by a Sidak's *post hoc* test versus control values.

D. Effect of overnight continuous oxygenation on the vasomotor effect of PVAT in PCAs

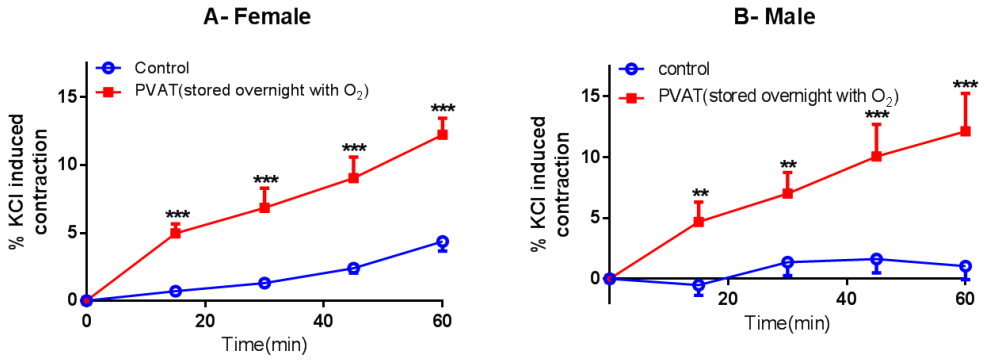


Figure 9: Contractile responses of the PCAs to (0.3 g) PVAT stored overnight with continuous oxygenation in female **(A)** and male **(B)** PCAs. Data are expressed as a percentage change from 60 mM KCl and are mean ± SEM of arteries from 6 (A) and 6 (B) different animals. ** indicates P< 0.01, ****P* < 0.001 (2-way ANOVA followed by a Sidak's *post-hoc* test) versus control values.

E. Sequence of primers

1- SYB pig, Sus scrofa retinoic acid receptor responder 2 (RARRES2), mRNA

Forward CAACGGGAGAAAGCGGAAGT

Reverse GTCTCTATGGGGCAGTGAACC.

2- SYB pig, Sus scrofa chemerin chemokine-like receptor 1 (CMKLR1), mRNA

Forward TTCTCCCGTCTGGTCAATGC

Reverse CTCAGAGCATGCTGGTCTCC.

3- SYB pig, Sus scrofa glyceraldehyde-3-phosphate dehydrogenase (GAPDH), mRNA -

Forward GACCAGGTTGTGTCCTGTGAC

Reverse GAGCTTGACGAAGTGGTCGTT.

References

ABBOTT, N. J. 2000. Inflammatory mediators and modulation of blood-brain barrier permeability. *Cell Mol Neurobiol,* 20**,** 131-47.

AHERNE, W. & HULL, D. 1966. Brown adipose tissue and heat production in the newborn infant. *J Pathol Bacteriol,* 91**,** 223-34.

ALFADDA, A. A., SALLAM, R. M., CHISHTI, M. A., MOUSTAFA, A. S., FATMA, S., ALOMAIM, W. S., AL-NAAMI, M. Y., BASSAS, A. F., CHROUSOS, G. P. & JO, H. 2012. Differential patterns of serum concentration and adipose tissue expression of chemerin in obesity: adipose depot specificity and gender dimorphism. *Mol Cells,* 33**,** 591-6.

ANDERSSON, D. C., FAUCONNIER, J., YAMADA, T., LACAMPAGNE, A., ZHANG, S. J., KATZ, A. & WESTERBLAD, H. 2011. Mitochondrial production of reactive oxygen species contributes to the beta-adrenergic stimulation of mouse cardiomycytes. *J Physiol,* 589**,** 1791-801.

ANDRADE-OLIVEIRA, V., CAMARA, N. O. & MORAES-VIEIRA, P. M. 2015. Adipokines as drug targets in diabetes and underlying disturbances. *J Diabetes Res,* 2015**,** 681612.

ANTONOPOULOS, A. S., MARGARITIS, M., COUTINHO, P., SHIRODARIA, C., PSARROS, C., HERDMAN, L., SANNA, F., DE SILVA, R., PETROU, M., SAYEED, R., KRASOPOULOS, G., LEE, R., DIGBY, J., REILLY, S., BAKOGIANNIS, C., TOUSOULIS, D., KESSLER, B., CASADEI, B., CHANNON, K. M. & ANTONIADES, C. 2015. Adiponectin as a link between type 2 diabetes and vascular NADPH oxidase activity in the human arterial wall: the regulatory role of perivascular adipose tissue. *Diabetes,* 64**,** 2207-19.

AOYAMA, T., PAIK, Y. H., WATANABE, S., LALEU, B., GAGGINI, F., FIORASO-CARTIER, L., MOLANGO, S., HEITZ, F., MERLOT, C., SZYNDRALEWIEZ, C., PAGE, P. & BRENNER, D. A. 2012. Nicotinamide adenine dinucleotide phosphate oxidase in experimental liver fibrosis: GKT137831 as a novel potential therapeutic agent. *Hepatology,* 56**,** 2316-27.

APRAHAMIAN, T. R. & SAM, F. 2011. Adiponectin in cardiovascular inflammation and obesity. *Int J Inflam,* 2011**,** 376909.

ARITA, Y., KIHARA, S., OUCHI, N., TAKAHASHI, M., MAEDA, K., MIYAGAWA, J., HOTTA, K., SHIMOMURA, I., NAKAMURA, T., MIYAOKA, K., KURIYAMA, H., NISHIDA, M., YAMASHITA, S., OKUBO, K., MATSUBARA, K., MURAGUCHI, M., OHMOTO, Y., FUNAHASHI, T. & MATSUZAWA, Y. 2012. Paradoxical decrease of an adipose-specific protein, adiponectin, in obesity. 1999. *Biochem Biophys Res Commun,* 425**,** 560-4.

AVRAM, A. S., AVRAM, M. M. & JAMES, W. D. 2005. Subcutaneous fat in normal and diseased states: 2. Anatomy and physiology of white and brown adipose tissue. *J Am Acad Dermatol,* 53**,** 671-83.

AYALA-LOPEZ, N., MARTINI, M., JACKSON, W. F., DARIOS, E., BURNETT, R., SEITZ, B., FINK, G. D. & WATTS, S. W. 2014. Perivascular adipose tissue contains functional catecholamines. *Pharmacol Res Perspect,* 2**,** e00041.

AYALA-LOPEZ, N. & WATTS, S. W. 2016. New actions of an old friend: perivascular adipose tissue's adrenergic mechanisms. *Br J Pharmacol*.

BABIOR, B. M., LAMBETH, J. D. & NAUSEEF, W. 2002. The neutrophil NADPH oxidase. *Arch Biochem Biophys,* 397**,** 342-4.

BAILEY, J. M., MAKHEJA, A. N., BUTLER, J. & SALATA, K. 1979. Anti-inflammatory drugs in experimental atherosclerosis. Part 4. Inhibition of atherosclerosis in vivo and

thromboxane synthesis and platelet aggregation in vitro. *Atherosclerosis,* 32**,** 195-203.

BARANDIER, C., MONTANI, J. P. & YANG, Z. 2005. Mature adipocytes and perivascular adipose tissue stimulate vascular smooth muscle cell proliferation: effects of aging and obesity. *Am J Physiol Heart Circ Physiol,* 289**,** H1807-13.

BARNEA, G., STRAPPS, W., HERRADA, G., BERMAN, Y., ONG, J., KLOSS, B., AXEL, R. & LEE, K. J. 2008. The genetic design of signaling cascades to record receptor activation. *Proc Natl Acad Sci U S A,* 105**,** 64-9.

BARRETT-CONNOR, E. 1997. Sex differences in coronary heart disease. Why are women so superior? The 1995 Ancel Keys Lecture. *Circulation,* 95**,** 252-64.

BARRY-LANE, P. A., PATTERSON, C., VAN DER MERWE, M., HU, Z., HOLLAND, S. M., YEH, E. T. & RUNGE, M. S. 2001. p47phox is required for atherosclerotic lesion progression in ApoE(-/-) mice. *J Clin Invest,* 108**,** 1513-22.

BARTELINK, M. L., VAN DE LISDONK, E., VAN DEN HOOGEN, H., WOLLERSHEIM, H. & VAN WEEL, C. 1993. Migraine in family practice: prevalence and influence of sex hormonal status. *Fam Med,* 25**,** 331-6.

BELL, A., GAGNON, A., DODS, P., PAPINEAU, D., TIBERI, M. & SORISKY, A. 2002. TSH signaling and cell survival in 3T3-L1 preadipocytes. *Am J Physiol Cell Physiol,* 283**,** C1056-64.

BELTOWSKI, J. 2013. Endogenous hydrogen sulfide in perivascular adipose tissue: role in the regulation of vascular tone in physiology and pathology. *Can J Physiol Pharmacol,* 91**,** 889-98.

BHATIA, K., ELMARAKBY, A. A., EL-REMESSY, A. B. & SULLIVAN, J. C. 2012. Oxidative stress contributes to sex differences in angiotensin II-mediated hypertension in spontaneously hypertensive rats. *Am J Physiol Regul Integr Comp Physiol,* 302**,** R274-82.

BIRUKOV, K. G. 2009. Cyclic stretch, reactive oxygen species, and vascular remodeling. *Antioxid Redox Signal,* 11**,** 1651-67.

BOS, C. L., RICHEL, D. J., RITSEMA, T., PEPPELENBOSCH, M. P. & VERSTEEG, H. H. 2004. Prostanoids and prostanoid receptors in signal transduction. *Int J Biochem Cell Biol,* 36**,** 1187-205.

BOSCO, E. E., KUMAR, S., MARCHIONI, F., BIESIADA, J., KORDOS, M., SZCZUR, K., MELLER, J., SEIBEL, W., MIZRAHI, A., PICK, E., FILIPPI, M. D. & ZHENG, Y. 2012. Rational design of small molecule inhibitors targeting the Rac GTPase-p67(phox) signaling axis in inflammation. *Chem Biol,* 19**,** 228-42.

BOZAOGLU, K., BOLTON, K., MCMILLAN, J., ZIMMET, P., JOWETT, J., COLLIER, G., WALDER, K. & SEGAL, D. 2007. Chemerin is a novel adipokine associated with obesity and metabolic syndrome. *Endocrinology,* 148**,** 4687-94.

BRADFORD, M. M. 1976. A rapid and sensitive method for the quantitation of microgram quantities of protein utilizing the principle of protein-dye binding. *Anal Biochem,* 72**,** 248-54.

BRANDES, R. P. & MUGGE, A. 1997. Gender differences in the generation of superoxide anions in the rat aorta. *Life Sci,* 60**,** 391-6.

BRIAN, J. E., JR. & FARACI, F. M. 1998. Tumor necrosis factor-alpha-induced dilatation of cerebral arterioles. *Stroke,* 29**,** 509-15.

BROWN, N. K., ZHOU, Z., ZHANG, J., ZENG, R., WU, J., EITZMAN, D. T., CHEN, Y. E. & CHANG, L. 2014. Perivascular adipose tissue in vascular function and disease: a review of current research and animal models. *Arterioscler Thromb Vasc Biol,* 34**,** 1621-30.

BRUCE, C. R., MERTZ, V. A., HEIGENHAUSER, G. J. & DYCK, D. J. 2005. The stimulatory effect of globular adiponectin on insulin-stimulated glucose uptake and fatty

acid oxidation is impaired in skeletal muscle from obese subjects. *Diabetes,* 54**,** 3154-60.

BRUNELLI, E., DOMANICO, F., LA RUSSA, D. & PELLEGRINO, D. 2014. Sex differences in oxidative stress biomarkers. *Curr Drug Targets,* 15**,** 811-5.

BRUNETTI, L., ORLANDO, G., RECINELLA, L., MICHELOTTO, B., FERRANTE, C. & VACCA, M. 2004. Resistin, but not adiponectin, inhibits dopamine and norepinephrine release in the hypothalamus. *Eur J Pharmacol,* 493**,** 41-4.

BUECHLER, C., WANNINGER, J. & NEUMEIER, M. 2010. Adiponectin receptor binding proteins--recent advances in elucidating adiponectin signalling pathways. *FEBS Lett,* 584**,** 4280-6.

BULLOCH, J. M. & DALY, C. J. 2014. Autonomic nerves and perivascular fat: interactive mechanisms. *Pharmacol Ther,* 143**,** 61-73.

BURKE, T. M. & WOLIN, M. S. 1987. Hydrogen peroxide elicits pulmonary arterial relaxation and guanylate cyclase activation. *Am J Physiol,* 252**,** H721-32.

BUSSEY, C. E., WITHERS, S. B., ALDOUS, R. G., EDWARDS, G. & HEAGERTY, A. M. 2016. Obesity-Related Perivascular Adipose Tissue Damage Is Reversed by Sustained Weight Loss in the Rat. *Arterioscler Thromb Vasc Biol,* 36**,** 1377-85.

CALABRO, P. & YEH, E. T. 2007. Obesity, inflammation, and vascular disease: the role of the adipose tissue as an endocrine organ. *Subcell Biochem,* 42**,** 63-91.

CALDIZ, C. I., GARCIARENA, C. D., DULCE, R. A., NOVARETTO, L. P., YEVES, A. M., ENNIS, I. L., CINGOLANI, H. E., CHIAPPE DE CINGOLANI, G. & PEREZ, N. G. 2007. Mitochondrial reactive oxygen species activate the slow force response to stretch in feline myocardium. *J Physiol,* 584**,** 895-905.

CAMHI, S. M., BRAY, G. A., BOUCHARD, C., GREENWAY, F. L., JOHNSON, W. D., NEWTON, R. L., RAVUSSIN, E., RYAN, D. H., SMITH, S. R. & KATZMARZYK, P. T. 2011. The relationship of waist circumference and BMI to visceral, subcutaneous, and total body fat: sex and race differences. *Obesity (Silver Spring),* 19**,** 402-8.

CANNON, B. & NEDERGAARD, J. 2004. Brown adipose tissue: function and physiological significance. *Physiol Rev,* 84**,** 277-359.

CAVE, A. C., BREWER, A. C., NARAYANAPANICKER, A., RAY, R., GRIEVE, D. J., WALKER, S. & SHAH, A. M. 2006. NADPH oxidases in cardiovascular health and disease. *Antioxid Redox Signal,* 8**,** 691-728.

CHAKAROUN, R., RASCHPICHLER, M., KLOTING, N., OBERBACH, A., FLEHMIG, G., KERN, M., SCHON, M. R., SHANG, E., LOHMANN, T., DRESSLER, M., FASSHAUER, M., STUMVOLL, M. & BLUHER, M. 2012. Effects of weight loss and exercise on chemerin serum concentrations and adipose tissue expression in human obesity. *Metabolism,* 61**,** 706-14.

CHALDAKOV, G. N., BELTOWSKY, J., GHENEV, P. I., FIORE, M., PANAYOTOV, P., RANCIC, G. & ALOE, L. 2012. Adipoparacrinology--vascular periadventitial adipose tissue (tunica adiposa) as an example. *Cell Biol Int,* 36**,** 327-30.

CHALDAKOV, G. N., FIORE, M., GHENEV, P. I., BELTOWSKI, J., RANCIC, G., TUNCEL, N. & ALOE, L. 2014. Triactome: neuro-immune-adipose interactions. Implication in vascular biology. *Front Immunol,* 5**,** 130.

CHALDAKOV, G. N., TONCHEV, A. B., STANKULOV, I. S., GHENEV, P. I., FIORE, M., ALOE, L., RANCIC, G., PANAYOTOV, P. & KOSTOV, D. D. 2007. Periadventitial adipose tissue (tunica adiposa): enemy or friend around? *Arch Pathol Lab Med,* 131**,** 1766; author reply 1766-7.

CHANG, L., MILTON, H., EITZMAN, D. T. & CHEN, Y. E. 2013. Paradoxical roles of perivascular adipose tissue in atherosclerosis and hypertension. *Circ J,* 77**,** 11-8.

CHANG, L., VILLACORTA, L., LI, R., HAMBLIN, M., XU, W., DOU, C., ZHANG, J., WU, J., ZENG, R. & CHEN, Y. E. 2012a. Loss of perivascular adipose tissue on peroxisome proliferator-activated receptor-gamma deletion in smooth muscle cells impairs intravascular thermoregulation and enhances atherosclerosis. *Circulation,* 126**,** 1067-78.

CHANG, L., VILLACOTA, L., DOU, C., CHEN, E. & ZHANG, J. 2012b. Perivascular adipose tissue-derived prostaglandins constrict vessel [abstract] *Hypertension,* 60.

CHANG, M. Y., HO, F. M., WANG, J. S., KANG, H. C., CHANG, Y., YE, Z. X. & LIN, W. W. 2010. AICAR induces cyclooxygenase-2 expression through AMP-activated protein kinase-transforming growth factor-beta-activated kinase 1-p38 mitogen-activated protein kinase signaling pathway. *Biochem Pharmacol,* 80**,** 1210-20.

CHATTERJEE, T. K., STOLL, L. L., DENNING, G. M., HARRELSON, A., BLOMKALNS, A. L., IDELMAN, G., ROTHENBERG, F. G., NELTNER, B., ROMIG-MARTIN, S. A., DICKSON, E. W., RUDICH, S. & WEINTRAUB, N. L. 2009. Proinflammatory phenotype of perivascular adipocytes: influence of high-fat feeding. *Circ Res,* 104**,** 541-9.

CHEN, J. Q., CAMMARATA, P. R., BAINES, C. P. & YAGER, J. D. 2009. Regulation of mitochondrial respiratory chain biogenesis by estrogens/estrogen receptors and physiological, pathological and pharmacological implications. *Biochim Biophys Acta,* 1793**,** 1540-70.

CHEN, M. B., MCAINCH, A. J., MACAULAY, S. L., CASTELLI, L. A., O'BRIEN P, E., DIXON, J. B., CAMERON-SMITH, D., KEMP, B. E. & STEINBERG, G. R. 2005. Impaired activation of AMP-kinase and fatty acid oxidation by globular adiponectin in cultured human skeletal muscle of obese type 2 diabetics. *J Clin Endocrinol Metab,* 90**,** 3665-72.

CHENG, K. K., LAM, K. S., WANG, Y., HUANG, Y., CARLING, D., WU, D., WONG, C. & XU, A. 2007. Adiponectin-induced endothelial nitric oxide synthase activation and nitric oxide production are mediated by APPL1 in endothelial cells. *Diabetes,* 56**,** 1387-94.

CHENG, Y., NDISANG, J. F., TANG, G., CAO, K. & WANG, R. 2004. Hydrogen sulfide-induced relaxation of resistance mesenteric artery beds of rats. *Am J Physiol Heart Circ Physiol,* 287**,** H2316-23.

CHO, Y., LEE, S. E., LEE, H. C., HUR, J., LEE, S., YOUN, S. W., LEE, J., LEE, H. J., LEE, T. K., PARK, J., HWANG, S. J., KWON, Y. W., CHO, H. J., OH, B. H., PARK, Y. B. & KIM, H. S. 2011. Adipokine resistin is a key player to modulate monocytes, endothelial cells, and smooth muscle cells, leading to progression of atherosclerosis in rabbit carotid artery. *J Am Coll Cardiol,* 57**,** 99-109.

CHOWEN, J. A., GARCIA-SEGURA, L. M., GONZALEZ-PARRA, S. & ARGENTE, J. 1996. Sex steroid effects on the development and functioning of the growth hormone axis. *Cell Mol Neurobiol,* 16**,** 297-310.

CHRUSCIEL, P., SAHEBKAR, A., REMBEK-WIELICZKO, M., SERBAN, M. C., URSONIU, S., MIKHAILIDIS, D. P., JONES, S. R., MOSTEORU, S., BLAHA, M. J., MARTIN, S. S., RYSZ, J., TOTH, P. P., LIP, G. Y., PENCINA, M. J., RAY, K. K., BANACH, M., LIPID & BLOOD PRESSURE META-ANALYSIS COLLABORATION, G. 2016. Impact of statin therapy on plasma adiponectin concentrations: A systematic review and meta-analysis of 43 randomized controlled trial arms. *Atherosclerosis,* 253**,** 194-208.

CINTI, S. 2005. The adipose organ. *Prostaglandins Leukot Essent Fatty Acids,* 73**,** 9-15.

CINTI, S. 2011. Between brown and white: novel aspects of adipocyte differentiation. *Ann Med,* 43**,** 104-15.

CNOP, M., HAVEL, P. J., UTZSCHNEIDER, K. M., CARR, D. B., SINHA, M. K., BOYKO, E. J., RETZLAFF, B. M., KNOPP, R. H., BRUNZELL, J. D. & KAHN, S. E. 2003.

Relationship of adiponectin to body fat distribution, insulin sensitivity and plasma lipoproteins: evidence for independent roles of age and sex. *Diabetologia,* 46**,** 459-69.

COATMELLEC-TAGLIONI, G., DAUSSE, J. P., GIUDICELLI, Y. & RIBIERE, C. 2002. Gender difference in diet-induced obesity hypertension: implication of renal alpha2-adrenergic receptors. *Am J Hypertens,* 15**,** 143-9.

COLEMAN, R. A., SMITH, W. L. & NARUMIYA, S. 1994. International Union of Pharmacology classification of prostanoid receptors: properties, distribution, and structure of the receptors and their subtypes. *Pharmacol Rev,* 46**,** 205-29.

CONSIDINE, R. V., SINHA, M. K., HEIMAN, M. L., KRIAUCIUNAS, A., STEPHENS, T. W., NYCE, M. R., OHANNESIAN, J. P., MARCO, C. C., MCKEE, L. J., BAUER, T. L. & ET AL. 1996. Serum immunoreactive-leptin concentrations in normal-weight and obese humans. *N Engl J Med,* 334**,** 292-5.

CORBOULD, A. 2007. Chronic testosterone treatment induces selective insulin resistance in subcutaneous adipocytes of women. *J Endocrinol,* 192**,** 585-94.

COSTA, R. M., FILGUEIRA, F. P., TOSTES, R. C., CARVALHO, M. H., AKAMINE, E. H. & LOBATO, N. S. 2016. H2O2 generated from mitochondrial electron transport chain in thoracic perivascular adipose tissue is crucial for modulation of vascular smooth muscle contraction. *Vascul Pharmacol,* 84**,** 28-37.

COUSIN, B., MUNOZ, O., ANDRE, M., FONTANILLES, A. M., DANI, C., COUSIN, J. L., LAHARRAGUE, P., CASTEILLA, L. & PENICAUD, L. 1999. A role for preadipocytes as macrophage-like cells. *FASEB J,* 13**,** 305-12.

CYPESS, A. M., LEHMAN, S., WILLIAMS, G., TAL, I., RODMAN, D., GOLDFINE, A. B., KUO, F. C., PALMER, E. L., TSENG, Y. H., DORIA, A., KOLODNY, G. M. & KAHN, C. R. 2009. Identification and importance of brown adipose tissue in adult humans. *N Engl J Med,* 360**,** 1509-17.

DA COSTA, R. M., FAIS, R. S., DECHANDT, C. R., LOUZADA-JUNIOR, P., ALBERICI, L. C., LOBATO, N. S. & TOSTES, R. C. 2016. Increased mitochondrial ROS generation mediates the loss of the anti-contractile effects of perivascular adipose tissue in high-fat diet obese mice. *Br J Pharmacol*.

DABROWSKA, R., AROMATORIO, D., SHERRY, J. M. & HARTSHORNE, D. J. 1977. Composition of the myosin light chain kinase from chicken gizzard. *Biochem Biophys Res Commun,* 78**,** 1263-72.

DARIOS, E. S., WINNER, B. M., CHARVAT, T., KRASINKSI, A., PUNNA, S. & WATTS, S. W. 2016. The adipokine chemerin amplifies electrical field-stimulated contraction in the isolated rat superior mesenteric artery. *Am J Physiol Heart Circ Physiol,* 311**,** H498-507.

DASHWOOD, M. R., DOOLEY, A., SHI-WEN, X., ABRAHAM, D. J. & SOUZA, D. S. 2007. Does periadventitial fat-derived nitric oxide play a role in improved saphenous vein graft patency in patients undergoing coronary artery bypass surgery? *J Vasc Res,* 44**,** 175-81.

DAVIS, K. E., M, D. N., SUN, K., W, M. S., J, D. B., J, A. Z., ZEVE, D., L, D. H., D, W. C., L, M. G., XU, Y., Z, V. W., S, A. K. & CLEGG, D. J. 2013. The sexually dimorphic role of adipose and adipocyte estrogen receptors in modulating adipose tissue expansion, inflammation, and fibrosis. *Mol Metab,* 2**,** 227-42.

DE CHAMPLAIN, J., WU, R., GIROUARD, H., KARAS, M., A, E. L. M., LAPLANTE, M. A. & WU, L. 2004. Oxidative stress in hypertension. *Clin Exp Hypertens,* 26**,** 593-601.

DEMERATH, E. W., SUN, S. S., ROGERS, N., LEE, M., REED, D., CHOH, A. C., COUCH, W., CZERWINSKI, S. A., CHUMLEA, W. C., SIERVOGEL, R. M. & TOWNE, B. 2007. Anatomical patterning of visceral adipose tissue: race, sex, and age variation. *Obesity (Silver Spring),* 15**,** 2984-93.

DIDION, S. P. & FARACI, F. M. 2002. Effects of NADH and NADPH on superoxide levels and cerebral vascular tone. *Am J Physiol Heart Circ Physiol,* 282**,** H688-95.

DING, Q., WANG, Z. & CHEN, Y. 2009. Endocytosis of adiponectin receptor 1 through a clathrin- and Rab5-dependent pathway. *Cell Res,* 19**,** 317-27.

DODD-O, J. M., ZHENG, G., SILVERMAN, H. S., LAKATTA, E. G. & ZIEGELSTEIN, R. C. 1997. Endothelium-independent relaxation of aortic rings by the nitric oxide synthase inhibitor diphenyleneiodonium. *Br J Pharmacol,* 120**,** 857-64.

DONG, B., JI, W. & ZHANG, Y. 2011. Elevated serum chemerin levels are associated with the presence of coronary artery disease in patients with metabolic syndrome. *Intern Med,* 50**,** 1093-7.

DONOVAN, J., WONG, P. S., ROBERTS, R. E., GARLE, M. J., ALEXANDER, S. P. H., DUNN, W. R. & RALEVIC, V. 2017. A critical role for cystathionine-beta-synthase in hydrogen sulfide-mediated hypoxic relaxation of the coronary artery. *Vascul Pharmacol,* 93-95**,** 20-32.

DROGE, W. 2002. Free radicals in the physiological control of cell function. *Physiol Rev,* 82**,** 47-95.

EGAN, K. M., LAWSON, J. A., FRIES, S., KOLLER, B., RADER, D. J., SMYTH, E. M. & FITZGERALD, G. A. 2004. COX-2-derived prostacyclin confers atheroprotection on female mice. *Science,* 306**,** 1954-7.

ENGELI, S. 2005. Is there a pathophysiological role for perivascular adipocytes? *Am J Physiol Heart Circ Physiol,* 289**,** H1794-5.

ENGELI, S., SCHLING, P., GORZELNIAK, K., BOSCHMANN, M., JANKE, J., AILHAUD, G., TEBOUL, M., MASSIERA, F. & SHARMA, A. M. 2003. The adipose-tissue renin-angiotensin-aldosterone system: role in the metabolic syndrome? *Int J Biochem Cell Biol,* 35**,** 807-25.

ERNST, M. C., HAIDL, I. D., ZUNIGA, L. A., DRANSE, H. J., ROURKE, J. L., ZABEL, B. A., BUTCHER, E. C. & SINAL, C. J. 2012. Disruption of the chemokine-like receptor-1 (CMKLR1) gene is associated with reduced adiposity and glucose intolerance. *Endocrinology,* 153**,** 672-82.

ERNST, M. C. & SINAL, C. J. 2010. Chemerin: at the crossroads of inflammation and obesity. *Trends Endocrinol Metab,* 21**,** 660-7.

FANG, L., ZHAO, J., CHEN, Y., MA, T., XU, G., TANG, C., LIU, X. & GENG, B. 2009. Hydrogen sulfide derived from periadventitial adipose tissue is a vasodilator. *J Hypertens,* 27**,** 2174-85.

FARACI, F. M. 2005. Oxidative stress: the curse that underlies cerebral vascular dysfunction? *Stroke,* 36**,** 186-8.

FARACI, F. M. & DIDION, S. P. 2004. Vascular protection: superoxide dismutase isoforms in the vessel wall. *Arterioscler Thromb Vasc Biol,* 24**,** 1367-73.

FARB, M. G., TIWARI, S., KARKI, S., NGO, D. T., CARMINE, B., HESS, D. T., ZURIAGA, M. A., WALSH, K., FETTERMAN, J. L., HAMBURG, N. M., VITA, J. A., APOVIAN, C. M. & GOKCE, N. 2014. Cyclooxygenase inhibition improves endothelial vasomotor dysfunction of visceral adipose arterioles in human obesity. *Obesity (Silver Spring),* 22**,** 349-55.

FELETOU, M., VERBEUREN, T. J. & VANHOUTTE, P. M. 2009. Endothelium-dependent contractions in SHR: a tale of prostanoid TP and IP receptors. *Br J Pharmacol,* 156**,** 563-74.

FENG, X., CHEN, Y., ZHAO, J., TANG, C., JIANG, Z. & GENG, B. 2009. Hydrogen sulfide from adipose tissue is a novel insulin resistance regulator. *Biochem Biophys Res Commun,* 380**,** 153-9.

FERLAND, D. J. & WATTS, S. W. 2015. Chemerin: A comprehensive review elucidating the need for cardiovascular research. *Pharmacol Res,* 99**,** 351-61.

FESUS, G., DUBROVSKA, G., GORZELNIAK, K., KLUGE, R., HUANG, Y., LUFT, F. C. & GOLLASCH, M. 2007. Adiponectin is a novel humoral vasodilator. *Cardiovasc Res,* 75**,** 719-27.

FILOMENI, G., DE ZIO, D. & CECCONI, F. 2015. Oxidative stress and autophagy: the clash between damage and metabolic needs. *Cell Death Differ,* 22**,** 377-88.

FITZGIBBONS, T. P., KOGAN, S., AOUADI, M., HENDRICKS, G. M., STRAUBHAAR, J. & CZECH, M. P. 2011. Similarity of mouse perivascular and brown adipose tissues and their resistance to diet-induced inflammation. *Am J Physiol Heart Circ Physiol,* 301**,** H1425-37.

FLEENOR, B. S., ENG, J. S., SINDLER, A. L., PHAM, B. T., KLOOR, J. D. & SEALS, D. R. 2014. Superoxide signaling in perivascular adipose tissue promotes age-related artery stiffness. *Aging Cell,* 13**,** 576-8.

FLEMING, I., MICHAELIS, U. R., BREDENKOTTER, D., FISSLTHALER, B., DEHGHANI, F., BRANDES, R. P. & BUSSE, R. 2001. Endothelium-derived hyperpolarizing factor synthase (Cytochrome P450 2C9) is a functionally significant source of reactive oxygen species in coronary arteries. *Circ Res,* 88**,** 44-51.

FLINT, D. J., BINART, N., BOUMARD, S., KOPCHICK, J. J. & KELLY, P. 2006. Developmental aspects of adipose tissue in GH receptor and prolactin receptor gene disrupted mice: site-specific effects upon proliferation, differentiation and hormone sensitivity. *J Endocrinol,* 191**,** 101-11.

FORTEPIANI, L. A. & RECKELHOFF, J. F. 2005. Role of oxidative stress in the sex differences in blood pressure in spontaneously hypertensive rats. *J Hypertens,* 23**,** 801-5.

FORTUNO, A., RODRIGUEZ, A., GOMEZ-AMBROSI, J., FRUHBECK, G. & DIEZ, J. 2003. Adipose tissue as an endocrine organ: role of leptin and adiponectin in the pathogenesis of cardiovascular diseases. *J Physiol Biochem,* 59**,** 51-60.

FRONTINI, A. & CINTI, S. 2010. Distribution and development of brown adipocytes in the murine and human adipose organ. *Cell Metab,* 11**,** 253-6.

FRUHBECK, G. 1999. Pivotal role of nitric oxide in the control of blood pressure after leptin administration. *Diabetes,* 48**,** 903-8.

FUENTE-MARTIN, E., ARGENTE-ARIZON, P., ROS, P., ARGENTE, J. & CHOWEN, J. A. 2013. Sex differences in adipose tissue: It is not only a question of quantity and distribution. *Adipocyte,* 2**,** 128-34.

FUJIMOTO, S., ASANO, T., SAKAI, M., SAKURAI, K., TAKAGI, D., YOSHIMOTO, N. & ITOH, T. 2001. Mechanisms of hydrogen peroxide-induced relaxation in rabbit mesenteric small artery. *Eur J Pharmacol,* 412**,** 291-300.

GABELLA, G. 1984. Structural apparatus for force transmission in smooth muscles. *Physiol Rev,* 64**,** 455-77.

GALVEZ-PRIETO, B., BOLBRINKER, J., STUCCHI, P., DE LAS HERAS, A. I., MERINO, B., ARRIBAS, S., RUIZ-GAYO, M., HUBER, M., WEHLAND, M., KREUTZ, R. & FERNANDEZ-ALFONSO, M. S. 2008. Comparative expression analysis of the renin-angiotensin system components between white and brown perivascular adipose tissue. *J Endocrinol,* 197**,** 55-64.

GAO, Y. J. 2007. Dual modulation of vascular function by perivascular adipose tissue and its potential correlation with adiposity/lipoatrophy-related vascular dysfunction. *Curr Pharm Des,* 13**,** 2185-92.

GAO, Y. J., HOLLOWAY, A. C., ZENG, Z. H., LIM, G. E., PETRIK, J. J., FOSTER, W. G. & LEE, R. M. 2005a. Prenatal exposure to nicotine causes postnatal obesity and altered perivascular adipose tissue function. *Obes Res,* 13**,** 687-92.

GAO, Y. J., LU, C., SU, L. Y., SHARMA, A. M. & LEE, R. M. 2007. Modulation of vascular function by perivascular adipose tissue: the role of endothelium and hydrogen peroxide. *Br J Pharmacol,* 151**,** 323-31.

GAO, Y. J., TAKEMORI, K., SU, L. Y., AN, W. S., LU, C., SHARMA, A. M. & LEE, R. M. 2006. Perivascular adipose tissue promotes vasoconstriction: the role of superoxide anion. *Cardiovasc Res,* 71**,** 363-73.

GAO, Y. J., ZENG, Z. H., TEOH, K., SHARMA, A. M., ABOUZAHR, L., CYBULSKY, I., LAMY, A., SEMELHAGO, L. & LEE, R. M. 2005b. Perivascular adipose tissue modulates vascular function in the human internal thoracic artery. *J Thorac Cardiovasc Surg,* 130**,** 1130-6.

GAYEN, J. R., ZHANG, K., RAMACHANDRARAO, S. P., MAHATA, M., CHEN, Y., KIM, H. S., NAVIAUX, R. K., SHARMA, K., MAHATA, S. K. & O'CONNOR, D. T. 2010. Role of reactive oxygen species in hyperadrenergic hypertension: biochemical, physiological, and pharmacological evidence from targeted ablation of the chromogranin a (Chga) gene. *Circ Cardiovasc Genet,* 3**,** 414-25.

GIANNI, D., TAULET, N., ZHANG, H., DERMARDIROSSIAN, C., KISTER, J., MARTINEZ, L., ROUSH, W. R., BROWN, S. J., BOKOCH, G. M. & ROSEN, H. 2010. A novel and specific NADPH oxidase-1 (Nox1) small-molecule inhibitor blocks the formation of functional invadopodia in human colon cancer cells. *ACS Chem Biol,* 5**,** 981-93.

GIL-ORTEGA, M., STUCCHI, P., GUZMAN-RUIZ, R., CANO, V., ARRIBAS, S., GONZALEZ, M. C., RUIZ-GAYO, M., FERNANDEZ-ALFONSO, M. S. & SOMOZA, B. 2010. Adaptative nitric oxide overproduction in perivascular adipose tissue during early diet-induced obesity. *Endocrinology,* 151**,** 3299-306.

GILLIGAN, D. M., QUYYUMI, A. A. & CANNON, R. O., 3RD 1994. Effects of physiological levels of estrogen on coronary vasomotor function in postmenopausal women. *Circulation,* 89**,** 2545-51.

GOLLASCH, M. 2012. Vasodilator signals from perivascular adipose tissue. *Br J Pharmacol,* 165**,** 633-42.

GOLLASCH, M. 2017. Adipose-Vascular Coupling and Potential Therapeutics. *Annu Rev Pharmacol Toxicol,* 57**,** 417-436.

GOODMAN-GRUEN, D. & BARRETT-CONNOR, E. 1996. Sex differences in measures of body fat and body fat distribution in the elderly. *Am J Epidemiol,* 143**,** 898-906.

GORALSKI, K. B., MCCARTHY, T. C., HANNIMAN, E. A., ZABEL, B. A., BUTCHER, E. C., PARLEE, S. D., MURUGANANDAN, S. & SINAL, C. J. 2007. Chemerin, a novel adipokine that regulates adipogenesis and adipocyte metabolism. *J Biol Chem,* 282**,** 28175-88.

GORRES, B. K., BOMHOFF, G. L., GUPTE, A. A. & GEIGER, P. C. 2011. Altered estrogen receptor expression in skeletal muscle and adipose tissue of female rats fed a high-fat diet. *J Appl Physiol (1985),* 110**,** 1046-53.

GOSSL, M., HERRMANN, J., TANG, H., VERSARI, D., GALILI, O., MANNHEIM, D., RAJKUMAR, S. V., LERMAN, L. O. & LERMAN, A. 2009. Prevention of vasa vasorum neovascularization attenuates early neointima formation in experimental hypercholesterolemia. *Basic Res Cardiol,* 104**,** 695-706.

GREEN, D. E., MURPHY, T. C., KANG, B. Y., KLEINHENZ, J. M., SZYNDRALEWIEZ, C., PAGE, P., SUTLIFF, R. L. & HART, C. M. 2012. The Nox4 inhibitor GKT137831 attenuates hypoxia-induced pulmonary vascular cell proliferation. *Am J Respir Cell Mol Biol,* 47**,** 718-26.

GREENHILL, C. 2016. Adipose tissue: Sex differences in adipogenesis. *Nat Rev Endocrinol,* 12**,** 497.

GREENSTEIN, A. S., KHAVANDI, K., WITHERS, S. B., SONOYAMA, K., CLANCY, O., JEZIORSKA, M., LAING, I., YATES, A. P., PEMBERTON, P. W., MALIK, R. A. & HEAGERTY, A. M. 2009. Local inflammation and hypoxia abolish the protective anticontractile properties of perivascular fat in obese patients. *Circulation,* 119**,** 1661-70.

GUILLABERT, A., WITTAMER, V., BONDUE, B., GODOT, V., IMBAULT, V., PARMENTIER, M. & COMMUNI, D. 2008. Role of neutrophil proteinase 3 and mast cell chymase in chemerin proteolytic regulation. *J Leukoc Biol,* 84**,** 1530-8.

GUO, F. F., YU, T. C., HONG, J. & FANG, J. Y. 2016. Emerging Roles of Hydrogen Sulfide in Inflammatory and Neoplastic Colonic Diseases. *Front Physiol,* 7**,** 156.

GUYTON, A. C. & HALL, J. E. 1996. *Textbook of Medical Physiology*, W.B. Saunders.

GUZIK, T. J. & CHANNON, K. M. 2005. Measurement of vascular reactive oxygen species production by chemiluminescence. *Methods Mol Med,* 108**,** 73-89.

GUZIK, T. J., MARVAR, P. J., CZESNIKIEWICZ-GUZIK, M. & KORBUT, R. 2007. Perivascular adipose tissue as a messenger of the brain-vessel axis: role in vascular inflammation and dysfunction. *J Physiol Pharmacol,* 58**,** 591-610.

HAMLAT-KHENNAF, N., NEGGAZI, S., AYARI, H., FEUGIER, P., BRICCA, G., AOUICHAT-BOUGUERRA, S. & BEYLOT, M. 2017. [Inflammation in the perivascular adipose tissue and atherosclerosis]. *C R Biol,* 340**,** 156-163.

HARMS, M. & SEALE, P. 2013. Brown and beige fat: development, function and therapeutic potential. *Nat Med,* 19**,** 1252-63.

HART, R. & GREAVES, D. R. 2010. Chemerin contributes to inflammation by promoting macrophage adhesion to VCAM-1 and fibronectin through clustering of VLA-4 and VLA-5. *J Immunol,* 185**,** 3728-39.

HAVEL, P. J. 2004. Update on adipocyte hormones: regulation of energy balance and carbohydrate/lipid metabolism. *Diabetes,* 53 Suppl 1**,** S143-51.

HE, G. W. & YANG, C. Q. 1999. Inhibition of vasoconstriction by the thromboxane A2 antagonist GR32191B in the human radial artery. *Br J Clin Pharmacol,* 48**,** 207-15.

HE, Q., HORLICK, M., THORNTON, J., WANG, J., PIERSON, R. N., JR., HESHKA, S. & GALLAGHER, D. 2002. Sex and race differences in fat distribution among Asian, African-American, and Caucasian prepubertal children. *J Clin Endocrinol Metab,* 87**,** 2164-70.

HEATON, J. M. 1972. The distribution of brown adipose tissue in the human. *J Anat,* 112**,** 35-9.

HELLSTROM, L., WAHRENBERG, H., HRUSKA, K., REYNISDOTTIR, S. & ARNER, P. 2000. Mechanisms behind gender differences in circulating leptin levels. *J Intern Med,* 247**,** 457-62.

HENRICHOT, E., JUGE-AUBRY, C. E., PERNIN, A., PACHE, J. C., VELEBIT, V., DAYER, J. M., MEDA, P., CHIZZOLINI, C. & MEIER, C. A. 2005. Production of chemokines by perivascular adipose tissue: a role in the pathogenesis of atherosclerosis? *Arterioscler Thromb Vasc Biol,* 25**,** 2594-9.

HERNANZ, R., BRIONES, A. M., SALAICES, M. & ALONSO, M. J. 2014. New roles for old pathways? A circuitous relationship between reactive oxygen species and cyclo-oxygenase in hypertension. *Clin Sci (Lond),* 126**,** 111-21.

HOBAI, I. A., MORSE, J. C., SIWIK, D. A. & COLUCCI, W. S. 2015. Lipopolysaccharide and cytokines inhibit rat cardiomyocyte contractility in vitro. *J Surg Res,* 193**,** 888-901.

HOLMSTROM, K. M. & FINKEL, T. 2014. Cellular mechanisms and physiological consequences of redox-dependent signalling. *Nat Rev Mol Cell Biol,* 15**,** 411-21.

HOTAMISLIGIL, G. S., SHARGILL, N. S. & SPIEGELMAN, B. M. 1993. Adipose expression of tumor necrosis factor-alpha: direct role in obesity-linked insulin resistance. *Science,* 259**,** 87-91.

HUANG, C. C., CHEN, K. L., CHEUNG, C. H. & CHANG, J. Y. 2013. Autophagy induced by cathepsin S inhibition induces early ROS production, oxidative DNA damage, and cell death via xanthine oxidase. *Free Radic Biol Med,* 65**,** 1473-86.

HUANG, F., LEZAMA, M. A., ONTIVEROS, J. A., BRAVO, G., VILLAFANA, S., DEL-RIO-NAVARRO, B. E. & HONG, E. 2010. Effect of losartan on vascular function in fructose-fed rats: the role of perivascular adipose tissue. *Clin Exp Hypertens,* 32**,** 98-104.

IANNONE, F. & LAPADULA, G. 2011. Chemerin/ChemR23 pathway: a system beyond chemokines. *Arthritis Res Ther,* 13**,** 104.

IBRAHIM, M. M. 2010. Subcutaneous and visceral adipose tissue: structural and functional differences. *Obes Rev,* 11**,** 11-8.

IMATOH, T., MIYAZAKI, M., MOMOSE, Y., TANIHARA, S. & UNE, H. 2008. Adiponectin levels associated with the development of hypertension: a prospective study. *Hypertens Res,* 31**,** 229-33.

JAPP, A. G. & NEWBY, D. E. 2008. The apelin-APJ system in heart failure: pathophysiologic relevance and therapeutic potential. *Biochem Pharmacol,* 75**,** 1882-92.

JIALAL, I., DEVARAJ, S., KAUR, H., ADAMS-HUET, B. & BREMER, A. A. 2013. Increased chemerin and decreased omentin-1 in both adipose tissue and plasma in nascent metabolic syndrome. *J Clin Endocrinol Metab,* 98**,** E514-7.

JOHN, H., HIERER, J., HAAS, O. & FORSSMANN, W. G. 2007. Quantification of angiotensin-converting-enzyme-mediated degradation of human chemerin 145-154 in plasma by matrix-assisted laser desorption/ionization-time-of-flight mass spectrometry. *Anal Biochem,* 362**,** 117-25.

JOHNS, D. G. & WEBB, R. C. 1998. TNF-alpha-induced endothelium-independent vasodilation: a role for phospholipase A2-dependent ceramide signaling. *Am J Physiol,* 275**,** H1592-8.

JONES, D. A., CARLTON, D. P., MCINTYRE, T. M., ZIMMERMAN, G. A. & PRESCOTT, S. M. 1993. Molecular cloning of human prostaglandin endoperoxide synthase type II and demonstration of expression in response to cytokines. *J Biol Chem,* 268**,** 9049-54.

JUDKINS, C. P., DIEP, H., BROUGHTON, B. R., MAST, A. E., HOOKER, E. U., MILLER, A. A., SELEMIDIS, S., DUSTING, G. J., SOBEY, C. G. & DRUMMOND, G. R. 2010. Direct evidence of a role for Nox2 in superoxide production, reduced nitric oxide bioavailability, and early atherosclerotic plaque formation in ApoE-/- mice. *Am J Physiol Heart Circ Physiol,* 298**,** H24-32.

KADOWAKI, T. & YAMAUCHI, T. 2005. Adiponectin and adiponectin receptors. *Endocr Rev,* 26**,** 439-51.

KAJIMURA, S. & SAITO, M. 2014. A new era in brown adipose tissue biology: molecular control of brown fat development and energy homeostasis. *Annu Rev Physiol,* 76**,** 225-49.

KARASTERGIOU, K., SMITH, S. R., GREENBERG, A. S. & FRIED, S. K. 2012. Sex differences in human adipose tissues - the biology of pear shape. *Biol Sex Differ,* 3**,** 13.

KATSUYAMA, M. 2010. NOX/NADPH oxidase, the superoxide-generating enzyme: its transcriptional regulation and physiological roles. *J Pharmacol Sci,* 114**,** 134-46.

KAUR, J., ADYA, R., TAN, B. K., CHEN, J. & RANDEVA, H. S. 2010. Identification of chemerin receptor (ChemR23) in human endothelial cells: chemerin-induced endothelial angiogenesis. *Biochem Biophys Res Commun,* 391**,** 1762-8.

KAWAHITO, H., YAMADA, H., IRIE, D., KATO, T., AKAKABE, Y., KISHIDA, S., TAKATA, H., WAKANA, N., OGATA, T., IKEDA, K., UEYAMA, T., MATOBA, S., MORI, Y. & MATSUBARA, H. 2013. Periaortic adipose tissue-specific activation of the renin-angiotensin system contributes to atherosclerosis development in uninephrectomized apoE-/- mice. *Am J Physiol Heart Circ Physiol,* 305**,** H667-75.

KETONEN, J., SHI, J., MARTONEN, E. & MERVAALA, E. 2010. Periadventitial adipose tissue promotes endothelial dysfunction via oxidative stress in diet-induced obese C57Bl/6 mice. *Circ J,* 74**,** 1479-87.

KIM, D. H., KIM, C., DING, E. L., TOWNSEND, M. K. & LIPSITZ, L. A. 2013. Adiponectin levels and the risk of hypertension: a systematic review and meta-analysis. *Hypertension,* 62**,** 27-32.

KIMURA, K., TSUDA, K., BABA, A., KAWABE, T., BOH-OKA, S., IBATA, M., MORIWAKI, C., HANO, T. & NISHIO, I. 2000. Involvement of nitric oxide in endothelium-dependent arterial relaxation by leptin. *Biochem Biophys Res Commun,* 273**,** 745-9.

KOHN, C., SCHLEIFENBAUM, J., SZIJARTO, I. A., MARKO, L., DUBROVSKA, G., HUANG, Y. & GOLLASCH, M. 2012. Differential effects of cystathionine-gamma-lyase-dependent vasodilatory H2S in periadventitial vasoregulation of rat and mouse aortas. *PLoS One,* 7**,** e41951.

KOSTOPOULOS, C. G., SPIROGLOU, S. G., VARAKIS, J. N., APOSTOLAKIS, E. & PAPADAKI, H. H. 2014. Chemerin and CMKLR1 expression in human arteries and periadventitial fat: a possible role for local chemerin in atherosclerosis? *BMC Cardiovasc Disord,* 14**,** 56.

KOTANI, K., TOKUNAGA, K., FUJIOKA, S., KOBATAKE, T., KENO, Y., YOSHIDA, S., SHIMOMURA, I., TARUI, S. & MATSUZAWA, Y. 1994. Sexual dimorphism of age-related changes in whole-body fat distribution in the obese. *Int J Obes Relat Metab Disord,* 18**,** 207-2.

KOUMANOV, K., MOMCHILOVA, A. & WOLF, C. 2003. Bimodal regulatory effect of melittin and phospholipase A2-activating protein on human type II secretory phospholipase A2. *Cell Biol Int,* 27**,** 871-7.

KUO, M. M., KIM, D. H., JANDU, S., BERGMAN, Y., TAN, S., WANG, H., PANDEY, D. R., ABRAHAM, T. P., SHOUKAS, A. A., BERKOWITZ, D. E. & SANTHANAM, L. 2016. MPST but not CSE is the primary regulator of hydrogen sulfide production and function in the coronary artery. *Am J Physiol Heart Circ Physiol,* 310**,** H71-9.

LAFONTAN, M. & BERLAN, M. 1993. Fat cell adrenergic receptors and the control of white and brown fat cell function. *J Lipid Res,* 34**,** 1057-91.

LAMBETH, J. D. 2004. NOX enzymes and the biology of reactive oxygen. *Nat Rev Immunol,* 4**,** 181-9.

LAMERS, D., SCHLICH, R., GREULICH, S., SASSON, S., SELL, H. & ECKEL, J. 2011. Oleic acid and adipokines synergize in inducing proliferation and inflammatory signalling in human vascular smooth muscle cells. *J Cell Mol Med,* 15**,** 1177-88.

LANDGRAF, K., FRIEBE, D., ULLRICH, T., KRATZSCH, J., DITTRICH, K., HERBERTH, G., ADAMS, V., KIESS, W., ERBS, S. & KORNER, A. 2012. Chemerin as a mediator between obesity and vascular inflammation in children. *J Clin Endocrinol Metab,* 97**,** E556-64.

LANGENBERG, C., BERGSTROM, J., SCHEIDT-NAVE, C., PFEILSCHIFTER, J. & BARRETT-CONNOR, E. 2006. Cardiovascular death and the metabolic syndrome: role of adiposity-signaling hormones and inflammatory markers. *Diabetes Care,* 29**,** 1363-9.

LAU, W. B., TAO, L., WANG, Y., LI, R. & MA, X. L. 2011. Systemic adiponectin malfunction as a risk factor for cardiovascular disease. *Antioxid Redox Signal,* 15**,** 1863-73.

LEE, D. L., STURGIS, L. C., LABAZI, H., OSBORNE, J. B., JR., FLEMING, C., POLLOCK, J. S., MANHIANI, M., IMIG, J. D. & BRANDS, M. W. 2006. Angiotensin II hypertension is attenuated in interleukin-6 knockout mice. *Am J Physiol Heart Circ Physiol,* 290**,** H935-40.

LEE, F. P., JEN, C. Y., CHANG, C. C., CHOU, Y., LIN, H., CHOU, C. M. & JUAN, S. H. 2010. Mechanisms of adiponectin-mediated COX-2 induction and protection against iron injury in mouse hepatocytes. *J Cell Physiol,* 224**,** 837-47.

LEE, R. M., BADER, M., ALENINA, N., SANTOS, R. A., GAO, Y. J. & LU, C. 2011. Mas receptors in modulating relaxation induced by perivascular adipose tissue. *Life Sci,* 89**,** 467-72.

LEE, R. M., LU, C., SU, L. Y. & GAO, Y. J. 2009. Endothelium-dependent relaxation factor released by perivascular adipose tissue. *J Hypertens,* 27**,** 782-90.

LEIHERER, A., MUENDLEIN, A., KINZ, E., VONBANK, A., REIN, P., FRAUNBERGER, P., MALIN, C., SAELY, C. H. & DREXEL, H. 2016. High plasma chemerin is associated with renal dysfunction and predictive for cardiovascular events - Insights from phenotype and genotype characterization. *Vascul Pharmacol,* 77**,** 60-8.

LEMBO, G., VECCHIONE, C., FRATTA, L., MARINO, G., TRIMARCO, V., D'AMATI, G. & TRIMARCO, B. 2000. Leptin induces direct vasodilation through distinct endothelial mechanisms. *Diabetes,* 49**,** 293-7.

LEMIEUX, I., PASCOT, A., COUILLARD, C., LAMARCHE, B., TCHERNOF, A., ALMERAS, N., BERGERON, J., GAUDET, D., TREMBLAY, G., PRUD'HOMME, D., NADEAU, A. & DESPRES, J. P. 2000. Hypertriglyceridemic waist: A marker of the atherogenic metabolic triad (hyperinsulinemia; hyperapolipoprotein B; small, dense LDL) in men? *Circulation,* 102**,** 179-84.

LERNER, D. J. & KANNEL, W. B. 1986. Patterns of coronary heart disease morbidity and mortality in the sexes: a 26-year follow-up of the Framingham population. *Am Heart J,* 111**,** 383-90.

LI, M., KUO, L. & STALLONE, J. N. 2008. Estrogen potentiates constrictor prostanoid function in female rat aorta by upregulation of cyclooxygenase-2 and thromboxane pathway expression. *Am J Physiol Heart Circ Physiol,* 294**,** H2444-55.

LI, Y., SHI, B. & LI, S. 2014. Association between serum chemerin concentrations and clinical indices in obesity or metabolic syndrome: a meta-analysis. *PLoS One,* 9**,** e113915.

LIMA, R., WOFFORD, M. & RECKELHOFF, J. F. 2012. Hypertension in postmenopausal women. *Curr Hypertens Rep,* 14**,** 254-60.

LIN, X., TANG, X., JIANG, Q., LIU, Q., LIN, Z., LIN, J., CHEN, L. & HONG, H. 2012. Elevated serum chemerin levels are associated with the presence of coronary artery disease in patients with type 2 diabetes. *Clin Lab,* 58**,** 539-44.

LOBATO, N. S., FILGUEIRA, F. P., AKAMINE, E. H., DAVEL, A. P., ROSSONI, L. V., TOSTES, R. C., CARVALHO, M. H. & FORTES, Z. B. 2011. Obesity induced by neonatal treatment with monosodium glutamate impairs microvascular reactivity in adult rats: role of NO and prostanoids. *Nutr Metab Cardiovasc Dis,* 21**,** 808-16.

LOHN, M., DUBROVSKA, G., LAUTERBACH, B., LUFT, F. C., GOLLASCH, M. & SHARMA, A. M. 2002. Periadventitial fat releases a vascular relaxing factor. *FASEB J,* 16**,** 1057-63.

LORINCZ, H., KATKO, M., HARANGI, M., SOMODI, S., GAAL, K., FULOP, P., PARAGH, G. & SERES, I. 2014. Strong correlations between circulating chemerin levels and lipoprotein subfractions in nondiabetic obese and nonobese subjects. *Clin Endocrinol (Oxf),* 81**,** 370-7.

LOWELL, B. B. 1998. Adaptive thermogenesis: turning on the heat. *Curr Biol,* 8**,** R517-20.

LOWRY, O. H., ROSEBROUGH, N. J., FARR, A. L. & RANDALL, R. J. 1951. Protein measurement with the Folin phenol reagent. *J Biol Chem,* 193**,** 265-75.

LU, C., SU, L. Y., LEE, R. M. & GAO, Y. J. 2010. Mechanisms for perivascular adipose tissue-mediated potentiation of vascular contraction to perivascular neuronal

stimulation: the role of adipocyte-derived angiotensin II. *Eur J Pharmacol,* 634**,** 107-12.

LU, C., ZHAO, A. X., GAO, Y. J. & LEE, R. M. 2011. Modulation of vein function by perivascular adipose tissue. *Eur J Pharmacol,* 657**,** 111-6.

LYNCH, F. M., WITHERS, S. B., YAO, Z., WERNER, M. E., EDWARDS, G., WESTON, A. H. & HEAGERTY, A. M. 2013. Perivascular adipose tissue-derived adiponectin activates BK(Ca) channels to induce anticontractile responses. *Am J Physiol Heart Circ Physiol,* 304**,** H786-95.

MAAS, A. H. & APPELMAN, Y. E. 2010. Gender differences in coronary heart disease. *Neth Heart J,* 18**,** 598-602.

MAENHAUT, N., BOYDENS, C. & VAN DE VOORDE, J. 2010. Hypoxia enhances the relaxing influence of perivascular adipose tissue in isolated mice aorta. *Eur J Pharmacol,* 641**,** 207-12.

MAENHAUT, N. & VAN DE VOORDE, J. 2011. Regulation of vascular tone by adipocytes. *BMC Med,* 9**,** 25.

MAHABADI, A. A., REINSCH, N., LEHMANN, N., ALTENBERND, J., KALSCH, H., SEIBEL, R. M., ERBEL, R. & MOHLENKAMP, S. 2010. Association of pericoronary fat volume with atherosclerotic plaque burden in the underlying coronary artery: a segment analysis. *Atherosclerosis,* 211**,** 195-9.

MALINOWSKI, M., DEJA, M. A., GOLBA, K. S., ROLEDER, T., BIERNAT, J. & WOS, S. 2008. Perivascular tissue of internal thoracic artery releases potent nitric oxide and prostacyclin-independent anticontractile factor. *Eur J Cardiothorac Surg,* 33**,** 225-31.

MAO, X., KIKANI, C. K., RIOJAS, R. A., LANGLAIS, P., WANG, L., RAMOS, F. J., FANG, Q., CHRIST-ROBERTS, C. Y., HONG, J. Y., KIM, R. Y., LIU, F. & DONG, L. Q. 2006. APPL1 binds to adiponectin receptors and mediates adiponectin signalling and function. *Nat Cell Biol,* 8**,** 516-23.

MARIMAN, E. C. & WANG, P. 2010. Adipocyte extracellular matrix composition, dynamics and role in obesity. *Cell Mol Life Sci,* 67**,** 1277-92.

MARTIN, S. S., QASIM, A. N., RADER, D. J. & REILLY, M. P. 2012. C-reactive protein modifies the association of plasma leptin with coronary calcium in asymptomatic overweight individuals. *Obesity (Silver Spring),* 20**,** 856-61.

MARTINEZ-REVELLES, S., AVENDANO, M. S., GARCIA-REDONDO, A. B., ALVAREZ, Y., AGUADO, A., PEREZ-GIRON, J. V., GARCIA-REDONDO, L., ESTEBAN, V., REDONDO, J. M., ALONSO, M. J., BRIONES, A. M. & SALAICES, M. 2013. Reciprocal relationship between reactive oxygen species and cyclooxygenase-2 and vascular dysfunction in hypertension. *Antioxid Redox Signal,* 18**,** 51-65.

MATSUMOTO, S., KISHIDA, K., SHIMOMURA, I., MAEDA, N., NAGARETANI, H., MATSUDA, M., NISHIZAWA, H., KIHARA, S., FUNAHASHI, T., MATSUZAWA, Y., YAMADA, A., YAMASHITA, S., TAMURA, S. & KAWATA, S. 2002. Increased plasma HB-EGF associated with obesity and coronary artery disease. *Biochem Biophys Res Commun,* 292**,** 781-6.

MATSUZAWA, Y. 2010. Adiponectin: a key player in obesity related disorders. *Curr Pharm Des,* 16**,** 1896-901.

MATTERN, A., ZELLMANN, T. & BECK-SICKINGER, A. G. 2014. Processing, signaling, and physiological function of chemerin. *IUBMB Life,* 66**,** 19-26.

MATTU, H. S. & RANDEVA, H. S. 2013. Role of adipokines in cardiovascular disease. *J Endocrinol,* 216**,** T17-36.

MAZUREK, T., ZHANG, L., ZALEWSKI, A., MANNION, J. D., DIEHL, J. T., ARAFAT, H., SAROV-BLAT, L., O'BRIEN, S., KEIPER, E. A., JOHNSON, A. G., MARTIN, J., GOLDSTEIN, B. J. & SHI, Y. 2003. Human epicardial adipose tissue is a source of inflammatory mediators. *Circulation,* 108**,** 2460-6.

MCFARLANE, S. I., BANERJI, M. & SOWERS, J. R. 2001. Insulin resistance and cardiovascular disease. *J Clin Endocrinol Metab,* 86**,** 713-8.

MCKENNA, T. M. 1992. Recovery of vascular tissue contractile function during sustained endotoxin exposure. *Am J Physiol,* 263**,** H1628-31.

MEDER, W., WENDLAND, M., BUSMANN, A., KUTZLEB, C., SPODSBERG, N., JOHN, H., RICHTER, R., SCHLEUDER, D., MEYER, M. & FORSSMANN, W. G. 2003. Characterization of human circulating TIG2 as a ligand for the orphan receptor ChemR23. *FEBS Lett,* 555**,** 495-9.

MENDELSOHN, M. E. & KARAS, R. H. 1999. The protective effects of estrogen on the cardiovascular system. *N Engl J Med,* 340**,** 1801-11.

MENDIZABAL, Y., LLORENS, S. & NAVA, E. 2013. Vasoactive effects of prostaglandins from the perivascular fat of mesenteric resistance arteries in WKY and SHROB rats. *Life Sci,* 93**,** 1023-32.

MENENDEZ, C., BALDELLI, R., CAMINA, J. P., ESCUDERO, B., PEINO, R., DIEGUEZ, C. & CASANUEVA, F. F. 2003. TSH stimulates leptin secretion by a direct effect on adipocytes. *J Endocrinol,* 176**,** 7-12.

MEYER, M. R., AMANN, K., FIELD, A. S., HU, C., HATHAWAY, H. J., KANAGY, N. L., WALKER, M. K., BARTON, M. & PROSSNITZ, E. R. 2012. Deletion of G protein-coupled estrogen receptor increases endothelial vasoconstriction. *Hypertension,* 59**,** 507-12.

MEYER, M. R., FREDETTE, N. C., BARTON, M. & PROSSNITZ, E. R. 2013. Regulation of vascular smooth muscle tone by adipose-derived contracting factor. *PLoS One,* 8**,** e79245.

MILLER, A. A., DRUMMOND, G. R., MAST, A. E., SCHMIDT, H. H. & SOBEY, C. G. 2007. Effect of gender on NADPH-oxidase activity, expression, and function in the cerebral circulation: role of estrogen. *Stroke,* 38**,** 2142-9.

MINKENBERG, I. & FERBER, E. 1984. Lucigenin-dependent chemiluminescence as a new assay for NAD(P)H-oxidase activity in particulate fractions of human polymorphonuclear leukocytes. *J Immunol Methods,* 71**,** 61-7.

MITTAL, A., GUPTA, M. D., MEENNAHALLI PALLEDA, G., VYAS, A. & TYAGI, S. 2013. Relationship of plasma adiponectin levels with acute coronary syndromes and coronary lesion severity in north Indian population. *ISRN Cardiol,* 2013**,** 854815.

MONTEZANO, A. C. & TOUYZ, R. M. 2014. Reactive oxygen species, vascular Noxs, and hypertension: focus on translational and clinical research. *Antioxid Redox Signal,* 20**,** 164-82.

MORAN, A., JACOBS, D. R., JR., STEINBERGER, J., STEFFEN, L. M., PANKOW, J. S., HONG, C. P. & SINAIKO, A. R. 2008. Changes in insulin resistance and cardiovascular risk during adolescence: establishment of differential risk in males and females. *Circulation,* 117**,** 2361-8.

MORITA, I., SCHINDLER, M., REGIER, M. K., OTTO, J. C., HORI, T., DEWITT, D. L. & SMITH, W. L. 1995. Different intracellular locations for prostaglandin endoperoxide H synthase-1 and -2. *J Biol Chem,* 270**,** 10902-8.

MULLEN, K. L., PRITCHARD, J., RITCHIE, I., SNOOK, L. A., CHABOWSKI, A., BONEN, A., WRIGHT, D. & DYCK, D. J. 2009. Adiponectin resistance precedes the accumulation of skeletal muscle lipids and insulin resistance in high-fat-fed rats. *Am J Physiol Regul Integr Comp Physiol,* 296**,** R243-51.

MURUGANANDAN, S., PARLEE, S. D., ROURKE, J. L., ERNST, M. C., GORALSKI, K. B. & SINAL, C. J. 2011. Chemerin, a novel peroxisome proliferator-activated receptor gamma (PPARgamma) target gene that promotes mesenchymal stem cell adipogenesis. *J Biol Chem,* 286**,** 23982-95.

NAGPAL, S., PATEL, S., JACOBE, H., DISEPIO, D., GHOSN, C., MALHOTRA, M., TENG, M., DUVIC, M. & CHANDRARATNA, R. A. 1997. Tazarotene-induced gene 2 (TIG2), a novel retinoid-responsive gene in skin. *J Invest Dermatol,* 109**,** 91-5.

NAKAMURA, K., FUSTER, J. J. & WALSH, K. 2014. Adipokines: a link between obesity and cardiovascular disease. *J Cardiol,* 63**,** 250-9.

NAKAYAMA, D. K., GELLER, D. A., LOWENSTEIN, C. J., CHERN, H. D., DAVIES, P., PITT, B. R., SIMMONS, R. L. & BILLIAR, T. R. 1992. Cytokines and lipopolysaccharide induce nitric oxide synthase in cultured rat pulmonary artery smooth muscle. *Am J Respir Cell Mol Biol,* 7**,** 471-6.

NARUMIYA, S., SUGIMOTO, Y. & USHIKUBI, F. 1999. Prostanoid receptors: structures, properties, and functions. *Physiol Rev,* 79**,** 1193-226.

NAVA, E. & LLORENS, S. 2016. The paracrine control of vascular motion. A historical perspective. *Pharmacol Res,* 113**,** 125-145.

NEDERGAARD, J., BENGTSSON, T. & CANNON, B. 2007. Unexpected evidence for active brown adipose tissue in adult humans. *Am J Physiol Endocrinol Metab,* 293**,** E444-52.

NETTLESHIP, J. E., JONES, R. D., CHANNER, K. S. & JONES, T. H. 2009. Testosterone and coronary artery disease. *Front Horm Res,* 37**,** 91-107.

NEVES, K. B., LOBATO, N. S., LOPES, R. A., FILGUEIRA, F. P., ZANOTTO, C. Z., OLIVEIRA, A. M. & TOSTES, R. C. 2014. Chemerin reduces vascular nitric oxide/cGMP signalling in rat aorta: a link to vascular dysfunction in obesity? *Clin Sci (Lond),* 127**,** 111-22.

NEVES, K. B., NGUYEN DINH CAT, A., LOPES, R. A., RIOS, F. J., ANAGNOSTOPOULOU, A., LOBATO, N. S., DE OLIVEIRA, A. M., TOSTES, R. C., MONTEZANO, A. C. & TOUYZ, R. M. 2015. Chemerin Regulates Crosstalk Between Adipocytes and Vascular Cells Through Nox. *Hypertension,* 66**,** 657-66.

NGKELO, A., MEJA, K., YEADON, M., ADCOCK, I. & KIRKHAM, P. A. 2012. LPS induced inflammatory responses in human peripheral blood mononuclear cells is mediated through NOX4 and Gialpha dependent PI-3kinase signalling. *J Inflamm (Lond),* 9**,** 1.

NGUYEN DINH CAT, A. & TOUYZ, R. M. 2011. Cell signaling of angiotensin II on vascular tone: novel mechanisms. *Curr Hypertens Rep,* 13**,** 122-8.

NICHOLSON, W. T., VAA, B., HESSE, C., EISENACH, J. H. & JOYNER, M. J. 2009. Aging is associated with reduced prostacyclin-mediated dilation in the human forearm. *Hypertension,* 53**,** 973-8.

NIELSEN, S., GUO, Z., ALBU, J. B., KLEIN, S., O'BRIEN, P. C. & JENSEN, M. D. 2003. Energy expenditure, sex, and endogenous fuel availability in humans. *J Clin Invest,* 111**,** 981-8.

NISHIZAWA, H., SHIMOMURA, I., KISHIDA, K., MAEDA, N., KURIYAMA, H., NAGARETANI, H., MATSUDA, M., KONDO, H., FURUYAMA, N., KIHARA, S., NAKAMURA, T., TOCHINO, Y., FUNAHASHI, T. & MATSUZAWA, Y. 2002. Androgens decrease plasma adiponectin, an insulin-sensitizing adipocyte-derived protein. *Diabetes,* 51**,** 2734-41.

NISIMOTO, Y., DIEBOLD, B. A., COSENTINO-GOMES, D. & LAMBETH, J. D. 2014. Nox4: a hydrogen peroxide-generating oxygen sensor. *Biochemistry,* 53**,** 5111-20.

NOOKAEW, I., SVENSSON, P. A., JACOBSON, P., JERNAS, M., TAUBE, M., LARSSON, I., ANDERSSON-ASSARSSON, J. C., SJOSTROM, L., FROGUEL, P., WALLEY, A., NIELSEN, J. & CARLSSON, L. M. 2013. Adipose tissue resting energy expenditure and expression of genes involved in mitochondrial function are higher in women than in men. *J Clin Endocrinol Metab,* 98**,** E370-8.

OHKAWA, F., IKEDA, U., KAWASAKI, K., KUSANO, E., IGARASHI, M. & SHIMADA, K. 1994. Inhibitory effect of interleukin-6 on vascular smooth muscle contraction. *Am J Physiol,* 266**,** H898-902.

OHMAN, M. K., LUO, W., WANG, H., GUO, C., ABDALLAH, W., RUSSO, H. M. & EITZMAN, D. T. 2011. Perivascular visceral adipose tissue induces atherosclerosis in apolipoprotein E deficient mice. *Atherosclerosis,* 219**,** 33-9.

OKADA-IWABU, M., YAMAUCHI, T., IWABU, M., HONMA, T., HAMAGAMI, K., MATSUDA, K., YAMAGUCHI, M., TANABE, H., KIMURA-SOMEYA, T., SHIROUZU, M., OGATA, H., TOKUYAMA, K., UEKI, K., NAGANO, T., TANAKA, A., YOKOYAMA, S. & KADOWAKI, T. 2013. A small-molecule AdipoR agonist for type 2 diabetes and short life in obesity. *Nature,* 503**,** 493-9.

OKAMOTO, E., COUSE, T., DE LEON, H., VINTEN-JOHANSEN, J., GOODMAN, R. B., SCOTT, N. A. & WILCOX, J. N. 2001. Perivascular inflammation after balloon angioplasty of porcine coronary arteries. *Circulation,* 104**,** 2228-35.

OKAMOTO, Y., FOLCO, E. J., MINAMI, M., WARA, A. K., FEINBERG, M. W., SUKHOVA, G. K., COLVIN, R. A., KIHARA, S., FUNAHASHI, T., LUSTER, A. D. & LIBBY, P. 2008. Adiponectin inhibits the production of CXC receptor 3 chemokine ligands in macrophages and reduces T-lymphocyte recruitment in atherogenesis. *Circ Res,* 102**,** 218-25.

ORSHAL, J. M. & KHALIL, R. A. 2004. Gender, sex hormones, and vascular tone. *Am J Physiol Regul Integr Comp Physiol,* 286**,** R233-49.

OSMOND, J. M. & KANAGY, N. L. 2014. Modulation of hydrogen sulfide by vascular hypoxia. *Hypoxia (Auckl),* 2**,** 117-126.

OWEN, M. K., WITZMANN, F. A., MCKENNEY, M. L., LAI, X., BERWICK, Z. C., MOBERLY, S. P., ALLOOSH, M., STUREK, M. & TUNE, J. D. 2013. Perivascular adipose tissue potentiates contraction of coronary vascular smooth muscle: influence of obesity. *Circulation,* 128**,** 9-18.

OZEN, G., TOPAL, G., GOMEZ, I., GHORRESHI, A., BOUKAIS, K., BENYAHIA, C., KANYINDA, L., LONGROIS, D., TESKIN, O., UYDES-DOGAN, B. S. & NOREL, X. 2013. Control of human vascular tone by prostanoids derived from perivascular adipose tissue. *Prostaglandins Other Lipid Mediat,* 107**,** 13-7.

PANIERI, E. & SANTORO, M. M. 2015. ROS signaling and redox biology in endothelial cells. *Cell Mol Life Sci,* 72**,** 3281-303.

PARK, Y., YANG, J., ZHANG, H., CHEN, X. & ZHANG, C. 2011. Effect of PAR2 in regulating TNF-alpha and NAD(P)H oxidase in coronary arterioles in type 2 diabetic mice. *Basic Res Cardiol,* 106**,** 111-23.

PARLEE, S. D., MCNEIL, J. O., MURUGANANDAN, S., SINAL, C. J. & GORALSKI, K. B. 2012. Elastase and tryptase govern TNFalpha-mediated production of active chemerin by adipocytes. *PLoS One,* 7**,** e51072.

PAYNE, G. A., BOHLEN, H. G., DINCER, U. D., BORBOUSE, L. & TUNE, J. D. 2009. Periadventitial adipose tissue impairs coronary endothelial function via PKC-beta-dependent phosphorylation of nitric oxide synthase. *Am J Physiol Heart Circ Physiol,* 297**,** H460-5.

PAYNE, G. A., BORBOUSE, L., KUMAR, S., NEEB, Z., ALLOOSH, M., STUREK, M. & TUNE, J. D. 2010. Epicardial perivascular adipose-derived leptin exacerbates coronary endothelial dysfunction in metabolic syndrome via a protein kinase C-beta pathway. *Arterioscler Thromb Vasc Biol,* 30**,** 1711-7.

PETERS, S. L., MATHY, M. J., PFAFFENDORF, M. & VAN ZWIETEN, P. A. 2000. Reactive oxygen species-induced aortic vasoconstriction and deterioration of functional integrity. *Naunyn Schmiedebergs Arch Pharmacol,* 361**,** 127-33.

PETRINI, S., NERI, T., LOMBARDI, S., CORDAZZO, C., BALIA, C., SCALISE, V., PAGGIARO, P., PEDRINELLI, R. & CELI, A. 2016. Leptin induces the generation of

procoagulant, tissue factor bearing microparticles by human peripheral blood mononuclear cells. *Biochim Biophys Acta,* 1860**,** 1354-61.

PISCHON, T., GIRMAN, C. J., HOTAMISLIGIL, G. S., RIFAI, N., HU, F. B. & RIMM, E. B. 2004. Plasma adiponectin levels and risk of myocardial infarction in men. *JAMA,* 291**,** 1730-7.

PLANAS, A., CLARA, A., POU, J. M., VIDAL-BARRAQUER, F., GASOL, A., DE MONER, A., CONTRERAS, C. & MARRUGAT, J. 2001. Relationship of obesity distribution and peripheral arterial occlusive disease in elderly men. *Int J Obes Relat Metab Disord,* 25**,** 1068-70.

PRATICO, D., TILLMANN, C., ZHANG, Z. B., LI, H. & FITZGERALD, G. A. 2001. Acceleration of atherogenesis by COX-1-dependent prostanoid formation in low density lipoprotein receptor knockout mice. *Proc Natl Acad Sci U S A,* 98**,** 3358-63.

RAJSHEKER, S., MANKA, D., BLOMKALNS, A. L., CHATTERJEE, T. K., STOLL, L. L. & WEINTRAUB, N. L. 2010. Crosstalk between perivascular adipose tissue and blood vessels. *Curr Opin Pharmacol,* 10**,** 191-6.

RAMOS-ALVES, F. E., DE QUEIROZ, D. B., SANTOS-ROCHA, J., DUARTE, G. P. & XAVIER, F. E. 2012. Increased cyclooxygenase-2-derived prostanoids contributes to the hyperreactivity to noradrenaline in mesenteric resistance arteries from offspring of diabetic rats. *PLoS One,* 7**,** e50593.

RAMSAY, T. G. 1996. Fat cells. *Endocrinol Metab Clin North Am,* 25**,** 847-70.

RANG, H. P. & DALE, M. M. 2012. *Rang and Dale's Pharmacology*, Elsevier/Churchill Livingstone.

RAYMENT, S. J., RALEVIC, V., BARRETT, D. A., CORDELL, R. & ALEXANDER, S. P. 2007. A novel mechanism of vasoregulation: ADP-induced relaxation of the porcine isolated coronary artery is mediated via adenosine release. *FASEB J,* 21**,** 577-85.

RAYNER, D. V. & TRAYHURN, P. 2001. Regulation of leptin production: sympathetic nervous system interactions. *J Mol Med (Berl),* 79**,** 8-20.

RECKELHOFF, J. F. 2005. Sex steroids, cardiovascular disease, and hypertension: unanswered questions and some speculations. *Hypertension,* 45**,** 170-4.

REID, G., WIELINGA, P., ZELCER, N., VAN DER HEIJDEN, I., KUIL, A., DE HAAS, M., WIJNHOLDS, J. & BORST, P. 2003. The human multidrug resistance protein MRP4 functions as a prostaglandin efflux transporter and is inhibited by nonsteroidal antiinflammatory drugs. *Proc Natl Acad Sci U S A,* 100**,** 9244-9.

RHEE, S. G., CHANG, T. S., JEONG, W. & KANG, D. 2010. Methods for detection and measurement of hydrogen peroxide inside and outside of cells. *Mol Cells,* 29**,** 539-49.

RIBAS, V., NGUYEN, M. T., HENSTRIDGE, D. C., NGUYEN, A. K., BEAVEN, S. W., WATT, M. J. & HEVENER, A. L. 2010. Impaired oxidative metabolism and inflammation are associated with insulin resistance in ERalpha-deficient mice. *Am J Physiol Endocrinol Metab,* 298**,** E304-19.

RIDKER, P. M., RIFAI, N., STAMPFER, M. J. & HENNEKENS, C. H. 2000. Plasma concentration of interleukin-6 and the risk of future myocardial infarction among apparently healthy men. *Circulation,* 101**,** 1767-72.

RITTIG, K., STAIB, K., MACHANN, J., BOTTCHER, M., PETER, A., SCHICK, F., CLAUSSEN, C., STEFAN, N., FRITSCHE, A., HARING, H. U. & BALLETSHOFER, B. 2008. Perivascular fatty tissue at the brachial artery is linked to insulin resistance but not to local endothelial dysfunction. *Diabetologia,* 51**,** 2093-9.

RIUS, M., THON, W. F., KEPPLER, D. & NIES, A. T. 2005. Prostanoid transport by multidrug resistance protein 4 (MRP4/ABCC4) localized in tissues of the human urogenital tract. *J Urol,* 174**,** 2409-14.

ROBINSON, S. 1952. Physiological effects of heat and cold. *Annu Rev Physiol,* 14**,** 73-96.

ROH, S. G., SONG, S. H., CHOI, K. C., KATOH, K., WITTAMER, V., PARMENTIER, M. & SASAKI, S. 2007. Chemerin--a new adipokine that modulates adipogenesis via its own receptor. *Biochem Biophys Res Commun,* 362**,** 1013-8.

ROURKE, J. L., DRANSE, H. J. & SINAL, C. J. 2013. Towards an integrative approach to understanding the role of chemerin in human health and disease. *Obes Rev,* 14**,** 245-62.

SACKS, H. S., FAIN, J. N., HOLMAN, B., CHEEMA, P., CHARY, A., PARKS, F., KARAS, J., OPTICAN, R., BAHOUTH, S. W., GARRETT, E., WOLF, R. Y., CARTER, R. A., ROBBINS, T., WOLFORD, D. & SAMAHA, J. 2009. Uncoupling protein-1 and related messenger ribonucleic acids in human epicardial and other adipose tissues: epicardial fat functioning as brown fat. *J Clin Endocrinol Metab,* 94**,** 3611-5.

SAHIN, A. S. & BARISKANER, H. 2007. The mechanisms of vasorelaxant effect of leptin on isolated rabbit aorta. *Fundam Clin Pharmacol,* 21**,** 595-600.

SAMSON, M., EDINGER, A. L., STORDEUR, P., RUCKER, J., VERHASSELT, V., SHARRON, M., GOVAERTS, C., MOLLEREAU, C., VASSART, G., DOMS, R. W. & PARMENTIER, M. 1998. ChemR23, a putative chemoattractant receptor, is expressed in monocyte-derived dendritic cells and macrophages and is a coreceptor for SIV and some primary HIV-1 strains. *Eur J Immunol,* 28**,** 1689-700.

SATO, A., SAKUMA, I. & GUTTERMAN, D. D. 2003. Mechanism of dilation to reactive oxygen species in human coronary arterioles. *Am J Physiol Heart Circ Physiol,* 285**,** H2345-54.

SCHERER, P. E., WILLIAMS, S., FOGLIANO, M., BALDINI, G. & LODISH, H. F. 1995. A novel serum protein similar to C1q, produced exclusively in adipocytes. *J Biol Chem,* 270**,** 26746-9.

SCHLEIFENBAUM, J., KOHN, C., VOBLOVA, N., DUBROVSKA, G., ZAVARIRSKAYA, O., GLOE, T., CREAN, C. S., LUFT, F. C., HUANG, Y., SCHUBERT, R. & GOLLASCH, M. 2010. Systemic peripheral artery relaxation by KCNQ channel openers and hydrogen sulfide. *J Hypertens,* 28**,** 1875-82.

SCHLETT, C. L., MASSARO, J. M., LEHMAN, S. J., BAMBERG, F., O'DONNELL, C. J., FOX, C. S. & HOFFMANN, U. 2009. Novel measurements of periaortic adipose tissue in comparison to anthropometric measures of obesity, and abdominal adipose tissue. *Int J Obes (Lond),* 33**,** 226-32.

SCHLING, P. & LOFFLER, G. 2002. Cross talk between adipose tissue cells: impact on pathophysiology. *News Physiol Sci,* 17**,** 99-104.

SCHLING, P., MALLOW, H., TRINDL, A. & LOFFLER, G. 1999. Evidence for a local renin angiotensin system in primary cultured human preadipocytes. *Int J Obes Relat Metab Disord,* 23**,** 336-41.

SCHUSTER, V. L. 2002. Prostaglandin transport. *Prostaglandins Other Lipid Mediat,* 68-69**,** 633-47.

SELL, H., DIVOUX, A., POITOU, C., BASDEVANT, A., BOUILLOT, J. L., BEDOSSA, P., TORDJMAN, J., ECKEL, J. & CLEMENT, K. 2010. Chemerin correlates with markers for fatty liver in morbidly obese patients and strongly decreases after weight loss induced by bariatric surgery. *J Clin Endocrinol Metab,* 95**,** 2892-6.

SHEN, W., TIAN, C., CHEN, H., YANG, Y., ZHU, D., GAO, P. & LIU, J. 2013. Oxidative stress mediates chemerin-induced autophagy in endothelial cells. *Free Radic Biol Med,* 55**,** 73-82.

SHIBATA, R., SATO, K., PIMENTEL, D. R., TAKEMURA, Y., KIHARA, S., OHASHI, K., FUNAHASHI, T., OUCHI, N. & WALSH, K. 2005. Adiponectin protects against

myocardial ischemia-reperfusion injury through AMPK- and COX-2-dependent mechanisms. *Nat Med,* 11**,** 1096-103.

SHYU, K. G., LIEN, L. M., WANG, B. W., KUAN, P. & CHANG, H. 2016. Retraction: Resistin contributes to neointimal formation via oxidative stress after vascular injury. *Clin Sci (Lond),* 130**,** 1842.

SIDOSSIS, L. & KAJIMURA, S. 2015. Brown and beige fat in humans: thermogenic adipocytes that control energy and glucose homeostasis. *J Clin Invest,* 125**,** 478-86.

SIMMONS, D. L., BOTTING, R. M. & HLA, T. 2004. Cyclooxygenase isozymes: the biology of prostaglandin synthesis and inhibition. *Pharmacol Rev,* 56**,** 387-437.

SNETKOV, V. A., SMIRNOV, S. V., KUA, J., AARONSON, P. I., WARD, J. P. & KNOCK, G. A. 2011. Superoxide differentially controls pulmonary and systemic vascular tone through multiple signalling pathways. *Cardiovasc Res,* 89**,** 214-24.

SOLTIS, E. E. & CASSIS, L. A. 1991. Influence of perivascular adipose tissue on rat aortic smooth muscle responsiveness. *Clin Exp Hypertens A,* 13**,** 277-96.

SPIROGLOU, S. G., KOSTOPOULOS, C. G., VARAKIS, J. N. & PAPADAKI, H. H. 2010. Adipokines in periaortic and epicardial adipose tissue: differential expression and relation to atherosclerosis. *J Atheroscler Thromb,* 17**,** 115-30.

STANLEY, C. P. & O'SULLIVAN, S. E. 2014. Cyclooxygenase metabolism mediates vasorelaxation to 2-arachidonoylglycerol (2-AG) in human mesenteric arteries. *Pharmacol Res,* 81**,** 74-82.

STEJSKAL, D., KARPISEK, M., HANULOVA, Z. & SVESTAK, M. 2008. Chemerin is an independent marker of the metabolic syndrome in a Caucasian population--a pilot study. *Biomed Pap Med Fac Univ Palacky Olomouc Czech Repub,* 152**,** 217-21.

STELMANSKA, E., KMIEC, Z. & SWIERCZYNSKI, J. 2012. The gender- and fat depot-specific regulation of leptin, resistin and adiponectin genes expression by progesterone in rat. *J Steroid Biochem Mol Biol,* 132**,** 160-7.

STEMME, V., SWEDENBORG, J., CLAESSON, H. & HANSSON, G. K. 2000. Expression of cyclo-oxygenase-2 in human atherosclerotic carotid arteries. *Eur J Vasc Endovasc Surg,* 20**,** 146-52.

STEPAN, H., PHILIPP, A., ROTH, I., KRALISCH, S., JANK, A., SCHAARSCHMIDT, W., LOSSNER, U., KRATZSCH, J., BLUHER, M., STUMVOLL, M. & FASSHAUER, M. 2011. Serum levels of the adipokine chemerin are increased in preeclampsia during and 6 months after pregnancy. *Regul Pept,* 168**,** 69-72.

STREETER, J., THIEL, W., BRIEGER, K. & MILLER, F. J., JR. 2013. Opportunity nox: the future of NADPH oxidases as therapeutic targets in cardiovascular disease. *Cardiovasc Ther,* 31**,** 125-37.

SZASZ, T., BOMFIM, G. F. & WEBB, R. C. 2013. The influence of perivascular adipose tissue on vascular homeostasis. *Vasc Health Risk Manag,* 9**,** 105-16.

SZASZ, T. & WEBB, R. C. 2012. Perivascular adipose tissue: more than just structural support. *Clin Sci (Lond),* 122**,** 1-12.

TAKAOKA, M., SUZUKI, H., SHIODA, S., SEKIKAWA, K., SAITO, Y., NAGAI, R. & SATA, M. 2010. Endovascular injury induces rapid phenotypic changes in perivascular adipose tissue. *Arterioscler Thromb Vasc Biol,* 30**,** 1576-82.

TAN, K. C., XU, A., CHOW, W. S., LAM, M. C., AI, V. H., TAM, S. C. & LAM, K. S. 2004. Hypoadiponectinemia is associated with impaired endothelium-dependent vasodilation. *J Clin Endocrinol Metab,* 89**,** 765-9.

TANG, S. Y., MONSLOW, J., TODD, L., LAWSON, J., PURE, E. & FITZGERALD, G. A. 2014. Cyclooxygenase-2 in endothelial and vascular smooth muscle cells restrains atherogenesis in hyperlipidemic mice. *Circulation,* 129**,** 1761-9.

TANKO, L. B., BAGGER, Y. Z., QIN, G., ALEXANDERSEN, P., LARSEN, P. J. & CHRISTIANSEN, C. 2005. Enlarged waist combined with elevated triglycerides is a strong predictor of accelerated atherogenesis and related cardiovascular mortality in postmenopausal women. *Circulation,* 111**,** 1883-90.

TAYLOR, R. W., GRANT, A. M., WILLIAMS, S. M. & GOULDING, A. 2010. Sex differences in regional body fat distribution from pre- to postpuberty. *Obesity (Silver Spring),* 18**,** 1410-6.

THALMANN, S. & MEIER, C. A. 2007. Local adipose tissue depots as cardiovascular risk factors. *Cardiovasc Res,* 75**,** 690-701.

THANNICKAL, V. J. & FANBURG, B. L. 2000. Reactive oxygen species in cell signaling. *Am J Physiol Lung Cell Mol Physiol,* 279**,** L1005-28.

THOMAS, D. W., MANNON, R. B., MANNON, P. J., LATOUR, A., OLIVER, J. A., HOFFMAN, M., SMITHIES, O., KOLLER, B. H. & COFFMAN, T. M. 1998. Coagulation defects and altered hemodynamic responses in mice lacking receptors for thromboxane A2. *J Clin Invest,* 102**,** 1994-2001.

TILG, H. & MOSCHEN, A. R. 2006. Adipocytokines: mediators linking adipose tissue, inflammation and immunity. *Nat Rev Immunol,* 6**,** 772-83.

TOMITA, M., HOLMAN, B. J., SANTORO, C. P. & SANTORO, T. J. 2005. Astrocyte production of the chemokine macrophage inflammatory protein-2 is inhibited by the spice principle curcumin at the level of gene transcription. *J Neuroinflammation,* 2**,** 8.

TONG, Y. A., ZHAO, H. F., LABRIE, F. & PELLETIER, G. 1989. Ontogeny of prolactin mRNA in the rat pituitary gland as evaluated by in situ hybridization. *Mol Cell Endocrinol,* 67**,** 11-6.

TRAUPE, T., D'USCIO, L. V., MUENTER, K., MORAWIETZ, H., VETTER, W. & BARTON, M. 2002a. Effects of obesity on endothelium-dependent reactivity during acute nitric oxide synthase inhibition: modulatory role of endothelin. *Clin Sci (Lond),* 103 Suppl 48**,** 13S-15S.

TRAUPE, T., LANG, M., GOETTSCH, W., MUNTER, K., MORAWIETZ, H., VETTER, W. & BARTON, M. 2002b. Obesity increases prostanoid-mediated vasoconstriction and vascular thromboxane receptor gene expression. *J Hypertens,* 20**,** 2239-45.

TRAYHURN, P. 2005. Endocrine and signalling role of adipose tissue: new perspectives on fat. *Acta Physiol Scand,* 184**,** 285-93.

TRAYHURN, P. & WOOD, I. S. 2005. Signalling role of adipose tissue: adipokines and inflammation in obesity. *Biochem Soc Trans,* 33**,** 1078-81.

VAN STIJN, C. M., KIM, J., BARISH, G. D., TIETGE, U. J. & TANGIRALA, R. K. 2014. Adiponectin expression protects against angiotensin II-mediated inflammation and accelerated atherosclerosis. *PLoS One,* 9**,** e86404.

VARLAMOV, O., WHITE, A. E., CARROLL, J. M., BETHEA, C. L., REDDY, A., SLAYDEN, O., O'ROURKE, R. W. & ROBERTS, C. T., JR. 2012. Androgen effects on adipose tissue architecture and function in nonhuman primates. *Endocrinology,* 153**,** 3100-10.

VERHAGEN, S. N. & VISSEREN, F. L. 2011. Perivascular adipose tissue as a cause of atherosclerosis. *Atherosclerosis,* 214**,** 3-10.

VERLOHREN, S., DUBROVSKA, G., TSANG, S. Y., ESSIN, K., LUFT, F. C., HUANG, Y. & GOLLASCH, M. 2004. Visceral periadventitial adipose tissue regulates arterial tone of mesenteric arteries. *Hypertension,* 44**,** 271-6.

VILLAR, I. C., FRANCIS, S., WEBB, A., HOBBS, A. J. & AHLUWALIA, A. 2006. Novel aspects of endothelium-dependent regulation of vascular tone. *Kidney Int,* 70**,** 840-53.

VILLAR, I. C., HOBBS, A. J. & AHLUWALIA, A. 2008. Sex differences in vascular function: implication of endothelium-derived hyperpolarizing factor. *J Endocrinol,* 197**,** 447-62.

VIRTANEN, K. A., LIDELL, M. E., ORAVA, J., HEGLIND, M., WESTERGREN, R., NIEMI, T., TAITTONEN, M., LAINE, J., SAVISTO, N. J., ENERBACK, S. & NUUTILA, P. 2009. Functional brown adipose tissue in healthy adults. *N Engl J Med,* 360**,** 1518-25.

VITALI, A., MURANO, I., ZINGARETTI, M. C., FRONTINI, A., RICQUIER, D. & CINTI, S. 2012. The adipose organ of obesity-prone C57BL/6J mice is composed of mixed white and brown adipocytes. *J Lipid Res,* 53**,** 619-29.

VOULGARI, P. V., ALAMANOS, Y., PAPAZISI, D., CHRISTOU, K., PAPANIKOLAOU, C. & DROSOS, A. A. 2000. Prevalence of Raynaud's phenomenon in a healthy Greek population. *Ann Rheum Dis,* 59**,** 206-10.

WAGNER, E. M. 2000. TNF-alpha induced bronchial vasoconstriction. *Am J Physiol Heart Circ Physiol,* 279**,** H946-51.

WANG, G. R., ZHU, Y., HALUSHKA, P. V., LINCOLN, T. M. & MENDELSOHN, M. E. 1998. Mechanism of platelet inhibition by nitric oxide: in vivo phosphorylation of thromboxane receptor by cyclic GMP-dependent protein kinase. *Proc Natl Acad Sci U S A,* 95**,** 4888-93.

WANG, P., XU, T. Y., GUAN, Y. F., SU, D. F., FAN, G. R. & MIAO, C. Y. 2009. Perivascular adipose tissue-derived visfatin is a vascular smooth muscle cell growth factor: role of nicotinamide mononucleotide. *Cardiovasc Res,* 81**,** 370-80.

WANKHADE, U. D., SHEN, M., YADAV, H. & THAKALI, K. M. 2016. Novel Browning Agents, Mechanisms, and Therapeutic Potentials of Brown Adipose Tissue. *Biomed Res Int,* 2016**,** 2365609.

WATTS, S. W., DORRANCE, A. M., PENFOLD, M. E., ROURKE, J. L., SINAL, C. J., SEITZ, B., SULLIVAN, T. J., CHARVAT, T. T., THOMPSON, J. M., BURNETT, R. & FINK, G. D. 2013. Chemerin connects fat to arterial contraction. *Arterioscler Thromb Vasc Biol,* 33**,** 1320-8.

WEISBERG, S. P., MCCANN, D., DESAI, M., ROSENBAUM, M., LEIBEL, R. L. & FERRANTE, A. W., JR. 2003. Obesity is associated with macrophage accumulation in adipose tissue. *J Clin Invest,* 112**,** 1796-808.

WHITE, R. E., HAN, G., DIMITROPOULOU, C., ZHU, S., MIYAKE, K., FULTON, D., DAVE, S. & BARMAN, S. A. 2005. Estrogen-induced contraction of coronary arteries is mediated by superoxide generated in vascular smooth muscle. *Am J Physiol Heart Circ Physiol,* 289**,** H1468-75.

WHITE, U. A. & TCHOUKALOVA, Y. D. 2014. Sex dimorphism and depot differences in adipose tissue function. *Biochim Biophys Acta,* 1842**,** 377-92.

WIMALASUNDERA, R., FEXBY, S., REGAN, L., THOM, S. A. & HUGHES, A. D. 2003. Effect of tumour necrosis factor-alpha and interleukin 1beta on endothelium-dependent relaxation in rat mesenteric resistance arteries in vitro. *Br J Pharmacol,* 138**,** 1285-94.

WIND, S., BEUERLEIN, K., ARMITAGE, M. E., TAYE, A., KUMAR, A. H., JANOWITZ, D., NEFF, C., SHAH, A. M., WINGLER, K. & SCHMIDT, H. H. 2010. Oxidative stress and endothelial dysfunction in aortas of aged spontaneously hypertensive rats by NOX1/2 is reversed by NADPH oxidase inhibition. *Hypertension,* 56**,** 490-7.

WITHERS, S. B., AGABITI-ROSEI, C., LIVINGSTONE, D. M., LITTLE, M. C., ASLAM, R., MALIK, R. A. & HEAGERTY, A. M. 2011. Macrophage activation is responsible for loss of anticontractile function in inflamed perivascular fat. *Arterioscler Thromb Vasc Biol,* 31**,** 908-13.

WITTAMER, V., FRANSSEN, J. D., VULCANO, M., MIRJOLET, J. F., LE POUL, E., MIGEOTTE, I., BREZILLON, S., TYLDESLEY, R., BLANPAIN, C., DETHEUX, M., MANTOVANI, A., SOZZANI, S., VASSART, G., PARMENTIER, M. & COMMUNI, D. 2003. Specific

recruitment of antigen-presenting cells by chemerin, a novel processed ligand from human inflammatory fluids. *J Exp Med,* 198**,** 977-85.

WITTAMER, V., GREGOIRE, F., ROBBERECHT, P., VASSART, G., COMMUNI, D. & PARMENTIER, M. 2004. The C-terminal nonapeptide of mature chemerin activates the chemerin receptor with low nanomolar potency. *J Biol Chem,* 279**,** 9956-62.

WOJCICKA, G., JAMROZ-WISNIEWSKA, A., ATANASOVA, P., CHALDAKOV, G. N., CHYLINSKA-KULA, B. & BELTOWSKI, J. 2011. Differential effects of statins on endogenous H2S formation in perivascular adipose tissue. *Pharmacol Res,* 63**,** 68-76.

WONG, P. S., GARLE, M. J., ALEXANDER, S. P., RANDALL, M. D. & ROBERTS, R. E. 2014a. A role for the sodium pump in H2O2-induced vasorelaxation in porcine isolated coronary arteries. *Pharmacol Res,* 90**,** 25-35.

WONG, P. S., RANDALL, M. D. & ROBERTS, R. E. 2015a. Sex differences in the role of NADPH oxidases in endothelium-dependent vasorelaxation in porcine isolated coronary arteries. *Vascul Pharmacol,* 72**,** 83-92.

WONG, P. S., ROBERTS, R. E. & RANDALL, M. D. 2014b. Sex differences in endothelial function in porcine coronary arteries: a role for H2O2 and gap junctions? *Br J Pharmacol,* 171**,** 2751-66.

WONG, P. S., ROBERTS, R. E. & RANDALL, M. D. 2015b. Sex differences in the role of transient receptor potential (TRP) channels in endothelium-dependent vasorelaxation in porcine isolated coronary arteries. *Eur J Pharmacol,* 750**,** 108-17.

WRIGHT, D. H., ABRAN, D., BHATTACHARYA, M., HOU, X., BERNIER, S. G., BOUAYAD, A., FOURON, J. C., VAZQUEZ-TELLO, A., BEAUCHAMP, M. H., CLYMAN, R. I., PERI, K., VARMA, D. R. & CHEMTOB, S. 2001. Prostanoid receptors: ontogeny and implications in vascular physiology. *Am J Physiol Regul Integr Comp Physiol,* 281**,** R1343-60.

WU, J., COHEN, P. & SPIEGELMAN, B. M. 2013. Adaptive thermogenesis in adipocytes: is beige the new brown? *Genes Dev,* 27**,** 234-50.

XIA, N., HORKE, S., HABERMEIER, A., CLOSS, E. I., REIFENBERG, G., GERICKE, A., MIKHED, Y., MUNZEL, T., DAIBER, A., FORSTERMANN, U. & LI, H. 2016. Uncoupling of Endothelial Nitric Oxide Synthase in Perivascular Adipose Tissue of Diet-Induced Obese Mice. *Arterioscler Thromb Vasc Biol,* 36**,** 78-85.

XU, L., MIYOSHI, H., NISHIMURA, K., JISAKA, M., NAGAYA, T. & YOKOTA, K. 2007. Gene expression of isoformic enzymes in arachidonate cyclooxygenase pathway and the regulation by tumor necrosis factor alpha during life cycle of adipocytes. *Prostaglandins Other Lipid Mediat,* 83**,** 213-8.

YAMAGUCHI, Y., DU, X. Y., ZHAO, L., MORSER, J. & LEUNG, L. L. 2011. Proteolytic cleavage of chemerin protein is necessary for activation to the active form, Chem157S, which functions as a signaling molecule in glioblastoma. *J Biol Chem,* 286**,** 39510-9.

YAMAUCHI, T., KAMON, J., ITO, Y., TSUCHIDA, A., YOKOMIZO, T., KITA, S., SUGIYAMA, T., MIYAGISHI, M., HARA, K., TSUNODA, M., MURAKAMI, K., OHTEKI, T., UCHIDA, S., TAKEKAWA, S., WAKI, H., TSUNO, N. H., SHIBATA, Y., TERAUCHI, Y., FROGUEL, P., TOBE, K., KOYASU, S., TAIRA, K., KITAMURA, T., SHIMIZU, T., NAGAI, R. & KADOWAKI, T. 2003. Cloning of adiponectin receptors that mediate antidiabetic metabolic effects. *Nature,* 423**,** 762-9.

YAMAWAKI, H., TSUBAKI, N., MUKOHDA, M., OKADA, M. & HARA, Y. 2010. Omentin, a novel adipokine, induces vasodilation in rat isolated blood vessels. *Biochem Biophys Res Commun,* 393**,** 668-72.

YAMAZAKI, T., KAWAI, C., YAMAUCHI, A. & KURIBAYASHI, F. 2011. A highly sensitive chemiluminescence assay for superoxide detection and chronic granulomatous disease diagnosis. *Trop Med Health,* 39**,** 41-5.

YAN, H., DU, J. & TANG, C. 2004. The possible role of hydrogen sulfide on the pathogenesis of spontaneous hypertension in rats. *Biochem Biophys Res Commun,* 313**,** 22-7.

YANG, D., ELNER, S. G., BIAN, Z. M., TILL, G. O., PETTY, H. R. & ELNER, V. M. 2007. Pro-inflammatory cytokines increase reactive oxygen species through mitochondria and NADPH oxidase in cultured RPE cells. *Exp Eye Res,* 85**,** 462-72.

YANG, G., WU, L., JIANG, B., YANG, W., QI, J., CAO, K., MENG, Q., MUSTAFA, A. K., MU, W., ZHANG, S., SNYDER, S. H. & WANG, R. 2008. H2S as a physiologic vasorelaxant: hypertension in mice with deletion of cystathionine gamma-lyase. *Science,* 322**,** 587-90.

YANG, J., PARK, Y., ZHANG, H., XU, X., LAINE, G. A., DELLSPERGER, K. C. & ZHANG, C. 2009. Feed-forward signaling of TNF-alpha and NF-kappaB via IKK-beta pathway contributes to insulin resistance and coronary arteriolar dysfunction in type 2 diabetic mice. *Am J Physiol Heart Circ Physiol,* 296**,** H1850-8.

YIANNIKOURIS, F., GUPTE, M., PUTNAM, K. & CASSIS, L. 2010. Adipokines and blood pressure control. *Curr Opin Nephrol Hypertens,* 19**,** 195-200.

YOSHIMURA, T. & OPPENHEIM, J. J. 2008. Chemerin reveals its chimeric nature. *J Exp Med,* 205**,** 2187-90.

YUDKIN, J. S., ERINGA, E. & STEHOUWER, C. D. 2005. "Vasocrine" signalling from perivascular fat: a mechanism linking insulin resistance to vascular disease. *Lancet,* 365**,** 1817-20.

YUE, R., XIA, X., JIANG, J., YANG, D., HAN, Y., CHEN, X., CAI, Y., LI, L., WANG, W. E. & ZENG, C. 2015. Mitochondrial DNA oxidative damage contributes to cardiomyocyte ischemia/reperfusion-injury in rats: cardioprotective role of lycopene. *J Cell Physiol,* 230**,** 2128-41.

ZABEL, B. A., ALLEN, S. J., KULIG, P., ALLEN, J. A., CICHY, J., HANDEL, T. M. & BUTCHER, E. C. 2005. Chemerin activation by serine proteases of the coagulation, fibrinolytic, and inflammatory cascades. *J Biol Chem,* 280**,** 34661-6.

ZABEL, B. A., NAKAE, S., ZUNIGA, L., KIM, J. Y., OHYAMA, T., ALT, C., PAN, J., SUTO, H., SOLER, D., ALLEN, S. J., HANDEL, T. M., SONG, C. H., GALLI, S. J. & BUTCHER, E. C. 2008. Mast cell-expressed orphan receptor CCRL2 binds chemerin and is required for optimal induction of IgE-mediated passive cutaneous anaphylaxis. *J Exp Med,* 205**,** 2207-20.

ZHANG, D. X., YI, F. X., ZOU, A. P. & LI, P. L. 2002. Role of ceramide in TNF-alpha-induced impairment of endothelium-dependent vasorelaxation in coronary arteries. *Am J Physiol Heart Circ Physiol,* 283**,** H1785-94.

ZHANG, M., SONG, P., XU, J. & ZOU, M. H. 2011. Activation of NAD(P)H oxidases by thromboxane A2 receptor uncouples endothelial nitric oxide synthase. *Arterioscler Thromb Vasc Biol,* 31**,** 125-32.

ZHANG, R., LIU, S., GUO, B., CHANG, L. & LI, Y. 2014. Chemerin induces insulin resistance in rat cardiomyocytes in part through the ERK1/2 signaling pathway. *Pharmacology,* 94**,** 259-64.

ZHAO, L., YAMAGUCHI, Y., SHARIF, S., DU, X. Y., SONG, J. J., LEE, D. M., RECHT, L. D., ROBINSON, W. H., MORSER, J. & LEUNG, L. L. 2011. Chemerin158K protein is the dominant chemerin isoform in synovial and cerebrospinal fluids but not in plasma. *J Biol Chem,* 286**,** 39520-7.

ZHOU, J. X., LIAO, D., ZHANG, S., CHENG, N., HE, H. Q. & YE, R. D. 2014. Chemerin C9 peptide induces receptor internalization through a clathrin-independent pathway. *Acta Pharmacol Sin,* 35**,** 653-63.

ZHU, M., LIU, P. Y., KASAHARA, D. I., WILLIAMS, A. S., VERBOUT, N. G., HALAYKO, A. J., FEDULOV, A., SHOJI, T., WILLIAMS, E. S., NOMA, K., SHORE, S. A. & LIAO, J. K. 2011. Role of Rho kinase isoforms in murine allergic airway responses. *Eur Respir J,* 38**,** 841-50.

ZOU, L., WANG, W., LIU, S., ZHAO, X., LYV, Y., DU, C., SU, X., GENG, B. & XU, G. 2016. Spontaneous hypertension occurs with adipose tissue dysfunction in perilipin-1 null mice. *Biochim Biophys Acta,* 1862**,** 182-91.